Decrypting the Vibrio cholerae crtS site and its role on the coordinated replication of the two chromosomes

Francisco de Lemos Martins

Sorbonne Université

Complexité du Vivant

Institut Pasteur – Unité Plasticité du Génome Bactérien

Decrypting the *Vibrio cholerae crtS* site and its role on the coordinated replication of the two chromosomes

Par Francisco de Lemos Martins

Thèse de doctorat de Microbiologie et Génétique

Dirigée par Didier Mazel

Présentée et soutenue publiquement le 26 juin 2018

Devant un jury composé de :

Pr. Guennadi SEZONOV	Professeur	Président du jury
Pr. Justine COLLIER	Directeur de Recherche	Rapporteur
Dr. Franck PASTA	Enseignant/Chercheur	Rapporteur
Dr. Christophe POSSOZ	Chargé de Recherche	Examinateur
Dr. Stéphane DUIGOU	Chargé de Recherche	Examinateur
Pr. Didier MAZEL	Professeur	Directeur de thèse
Dr. Marie-Eve VAL	Chargé de Recherche	Co-Encadrant de thèse

ABSTRACT

Bacterial genomes are mainly composed of two types of replicons: chromosomes, which are essential, and plasmids. Although most bacteria have only one chromosome, bacteria with secondary chromosomes have arisen independently in several taxa and represent approximately 10% of all bacterial species. Secondary chromosomes originate from plasmids and possess plasmid-type replication systems. While chromosomes replicate once and during a defined period of the cell cycle, plasmids generally replicate randomly. *Vibrio cholerae* has its genome divided in two chromosomes (Chr1 and Chr2) that use distinct initiators for replication. Chr1 replication depends on the ubiquitous initiator DnaA, while Chr2 replication is initiated by a *Vibrio* specific factor, RctB. Despite its plasmid origins, Chr2 replication is tightly controlled and occurs once per cell cycle. Both chromosomes communicate with each other to coordinate their replication through an RctB-binding locus on Chr1, called *crtS*. We have shown that *crtS* replication is crucial to trigger Chr2 replication initiation. However, the molecular mechanism by which *crtS* controls the initiation of Chr2 replication was still obscure. Here we combined *in vivo* and *in vitro* approaches to shed light on this question. We have shown that *crtS* activity is driven by RctB binding in a methylation-independent manner. Furthermore, functional analysis of *crtS* mutants suggests that its single stranded form may adopt a hairpin conformation upon passage of the replication fork, which somehow activates Chr2 replication. This mechanism appears to be an effective way to integrate the Chr2 replication in the cell cycle.

ACKNOWLEDGEMENTS

This thesis reflects the support of many people who influenced my work in different ways and to whom I would like to thank.

First, I would like to thank the jury members for having accepted to judge this thesis, either as reviewers, Dr. Justine Collier and Dr. Franck Pasta, or as examiners, Dr. Christophe Possoz and Dr. Stéphane Duigou. I would also like to express my gratitude to Prof. Guennadi Sezonov for having accepted to be the president of the jury.

I am very grateful to my supervisor Didier Mazel who kindly accepted me in his lab and for the trust he has put on me to conduct this project. Thank you for all your support throughout these years. Your constant optimism and good mood certainly helped me to be more motivated during this thesis.
I would like to express my gratitude to Marie-Eve Val, for being an extraordinary supervisor and for the continuous support during my thesis. Thank you for your patience, your motivation and for your precious guidance. Thank you for sharing your wisdom and for allowing me to learn with your experience. Without your supervision and constant help this thesis would not have been possible.
I want to thank all the present and previous lab members with whom I had the opportunity to work with. Aleks, Alfonso, Céline, Christophe, Claire, Evelyne, Jakub, José, Julia, Magaly, Rocio, Sebastian and Zeynep: thank you for your helpful advice and for having always created a good environment in the lab. It was a great pleasure to work with you! Jason, thank you for having guided me during my first days in the lab when I was starting the PhD adventure. Thank you Florian for all the help and support, and for your precious contribution to this work. And also for the famous “pause cigarette”! Veronica, thank you for your true friendship and for all the great moments that we spent together during this journey. I will never forget how snapchat made our days more joyful!

Even if I kept on escaping from the Portuguese lunches, I would like to thank the Portuguese community in Pasteur, especially Sofia, Jorge, Marisa, Carolina and André! Obrigado por me fazerem falar português de vez em quando e de não me fazerem esquecer a “língua de Camões”!

I would like to thank the PPU program and all the people involved for the effort you put in the organization of this great program for international PhD students. I also would like to thank my PPU fellows for the great moments we spent together, especially during the retreats.

I could not have survived these last three years and half without the support of my friends, even if some are a bit far. Thank you Carlota, Catarina S., Joana F., Joana M., Mafalda, Rafael, Sofia and Vera. Thank you for your visits, your friendship and for being always by my side since our university times!

I also would like to thank the friends I made since my arrival in France, especially Maria-Vittoria and Benedetta. This adventure wouldn't have been the same without you!

I am profoundly grateful to Marco for all the support and immense patience during the last months. I know it has been a though journey and I am very thankful to have you by my side. Thank you for your constant motivating words, always encouraging me to move forward.

A very special acknowledgment to my parents, my brother and my sister-in-law for always supporting my decisions and for being there for me whenever I needed. Thank you for your regular visits and for making the physical distance between us feel a little bit shorter than what it actually is. Muito obrigado pelo vosso apoio incondicional e por estarem sempre disponíveis. Obrigado pelas vossas visitas frequentes e por me fazerem sentir a distância um bocadinho mais curta do que aquela que na realidade nos separa.

TABLE OF CONTENTS

INTRODUCTION

I. Bacterial genome organization

The organization of prokaryotic genomes is not stochastic. It is even quite the opposite, as their organization reflects a compromise between functional and regulatory purposes (Junier, 2014; Lawrence, 2003; Rocha, 2008). For instance, enzymes for each step of a biosynthetic or catabolic pathway are generally encoded by a single operon and are often co-localized on the chromosome with the cognate regulator (Rocha, 2008). The chromosomal location of a gene can influence its expression level (Bryant et al., 2014; Soler-Bistué et al., 2015) and, in the case of fast-replicating species, the copy number of the gene (Dryselius et al., 2008). It is also possible to observe a general bias for bacterial genes orientation to be enriched in the leading strand to avoid head-on collisions between the transcriptional and DNA replicative machineries (Rocha, 2004). The large majority of bacteria possess a single circular chromosome, but approximately 10% of the species have a genome split on two or more chromosomes. Given the fact that the structured nature of prokaryotic genomes mirrors functional purposes, it is unlikely that the multipartite genome structure simply represents an evolutionary peculiarity. Instead, this genomic architecture must be the result of selective pressures acting on these genomes throughout the course of the evolution. Understanding the organization of these genomes may shed light on the advantages of having this genomic architecture, as well as on the selective constraints that were on the basis of their origin. Many important bacteria harbour a divided genome. These bacteria include plant symbionts such as many of the rhizobia (Galibert et al., 2001), plant pathogens such as *Agrobacterium* (Goodner et al., 2001), and animal and human pathogens, including *Brucella* (DelVecchio et al., 2002), *Vibrio* (Heidelberg et al., 2000), and *Burkholderia* (Chain et al., 2006).

Depending on their characteristics, there are several terms that describe the different types of DNA molecules that are present within a multipartite genome. The term replicon is generic and refers to any replicative DNA molecule regardless of its specific nature. In its strictest sense, it should be used only in reference to DNA molecules with a single origin of replication. This definition excludes the chromosomes of some archea that have multiple origins of replication (Barry and Bell, 2006; Wu et al., 2014). Based on its specific characteristics each replicon can be classified in four different groups: chromosomes, secondary chromosomes or chromids, megaplasmids and plasmids.

1.1. Chromosomes

Chromosome refers to the primary replicon of the cell. The chromosome is always the largest replicon in the genome and contains the majority of the core/essential genes (Harrison et al., 2010). There is approximately a 100-fold range in the sizes of fully sequenced and assembled bacterial chromosomes, with average and median sizes of ~3.65 Mb and ~3.46 Mb, respectively. The average and median bacterial genome sizes, *senso lato* (including all replicons), are ~3.87 Mb and ~3.65 Mb, respectively. This demonstrates that the chromosome accounts for almost all of the genetic material of most prokaryotic organisms. However, this is not always the case. The chromosomes of *Sinorhizobium meliloti* 1021 and *Burkholderia xenovorans* LB400 account for only 54,6% and 50,3% of their genomes, respectively (Chain et al., 2006; Galibert et al., 2001). From the 1708 bacterial species with a complete genome available in the NCBI database (March 2016), 1017 (~59,5%) contain a chromosome but no secondary replicon (chromid, megaplasmid or plasmid), while only 192 (~11%) have a chromid and/or megaplasmid. The major features the different replicon classes are summarized in Table 1 (Harrison et al., 2010).

1.2. Plasmids and Megaplasmids

Many of the secondary replicons in bacterial genomes do not possess core and essential genes, being dispensable for cell viability in the majority of the environments. The genes carried on these replicons generally have genomic signatures, such as GC content and dinucleotide composition, which differ considerably from the chromosome. This indicates that most of them were acquired through recent horizontal gene transfer (HGT) (Harrison et al., 2010). These types of replicons, lacking core genes, are referred to as plasmids and megaplasmids. The difference between the two resides solely on size. There is no established size boundary between plasmids and megaplasmids, meaning that any size limitation is purely arbitrary. It has been suggested a lower cut-off of 350 kb for megaplasmid status since this value equals roughly to 10% of the median bacterial genome size. Any nonessential replicon of <350 kb is therefore classified as a plasmid (diCenzo and Finan, 2017).

The term megaplasmid was first used to designate the large *S. meliloti* plasmid (Rosenberg et al., 1981). Since then, the term has been used simply as a way of referring to a large plasmid. Possibly there is a more functional way, not relying solely on size, to distinguish plasmids from megaplasmids but this has yet to be elucidated. For instance, megaplasmids often have a copy number equal or similar to that of the chromosome, they often encode their own partitioning systems, and the replication and partitioning of megaplasmids may be integrated into the cell cycle.

Characteristic	Chromosome	Chromid	Plasmid
Size	Always the largest replicon	Largest secondary replicons[a]	Smallest replicons[a]
G + C	Varies	Usually within 1% of chromosome	Often >1% lower than chromosome
Maintenance and replication systems	Chromosome-type	Plasmid-type	Plasmid-type
Core genes	280 universal, 75 uniquely on chromosomes	Some core genes, none universal, none unique	Few genes shared at any phylogenetic level
Phylogenetic distribution of genes	Wide conservation of genes and synteny between genera	Gene conservation and shared synteny only within genus	Genes specific to strain or species

Table 1. Differences between chromosomes, chromids and plasmids (Adapted from Harrison et al., 2010). [a]Except in *Deinococcus deserti* VCD115 where the chromid is smaller than either of the two accompanying plasmids.

1.3. Chromids or secondary chromosomes

Secondary chromosomes or chromids refer to large secondary replicons that carry essential genes. Since these replicons carry plasmid-type maintenance and replication systems, in 2010 Harrison et al. proposed the term chromid to define them. According to these authors the term chromid refers to a replicon that is an intermediate between a chromosome and a plasmid (Harrison et al., 2010) and the term secondary chromosome should no longer be used. In 2017 diCenzo and Finan argue that the term secondary chromosome should be used to describe a secondary replicon formed through the split of an ancestral chromosome into two replicons. So far there is only a single case of such an event described in the literature (Ausiannikava et al., 2018). It is very likely that almost all secondary replicons carrying essential core genes evolved from plasmids. For this reason, from now on the terms chromid and secondary chromosome will be used indiscriminately.

There are essentially three fundamental criteria that clearly distinguish chromids from chromosomes and plasmids. Chromids have plasmid-type maintenance and replication systems; a nucleotide composition similar to that of the chromosome, and carry several core genes that are found on the chromosome in other species (Harrison et al., 2010). All chromids described so far encode their own initiator molecules that control replication independently from the chromosome and may have

additional regulatory controls that integrate their replication into the cell cycle (Orlova et al., 2016; Ramachandran et al., 2017; Rasmussen et al., 2007; Venkova-Canova and Chattoraj, 2011). The majority of chromids are within 1% of the G + C composition of their host chromosomes. Within a given genome, chromosomes and chromids have core regions that are highly similar in composition. The number or the nature of the core genes is not important to define the chromids. What is important is the fact that these genes are widely distributed, located on the chromosome in most other species. The possession of these genes renders the chromid indispensable and stabilizes other genes present on the replicon. In addition to these principal characteristics, the majority of the chromids identified so far share other properties. They are normally larger than the accompanying plasmids but smaller than the chromosome (Ochman, 2002), and carry many genes with a restricted or sporadic phylogenetic distribution.

1.4. Phylogenetic Distribution of Multipartite Genomes

Approximately 11% of all complete bacterial genomes (1708 genomes) contain a megaplasmid and/or chromid (diCenzo and Finan, 2017). From the bacterial species examined, 7,4% included at least one strain with at least one putative chromid and 6,4% included at least one strain with at least one megaplasmid (Fig. 1). It seems that there is an affinity for putative chromids to co-occur with megaplasmids, as ~2,5% of all the species examined had both a chromid and a megaplasmid (not necessarily in the same strain). This may reflect an intrinsic evolutionary property of these bacteria to select for promiscuous replicons or the difficulty in distinguishing clearly between them. The majority of species that have both putative chromids and megaplasmids belong to the genus *Burkholderia* and to the order *Rhizobiales*, which are known to carry both elements. The higher prevalence of putative chromids than of megaplasmids in the bacterial phylogeny may reflect a greater instability or more dynamic nature of the latter.

Multipartite genomes are dispersed throughout the bacterial phylogeny. Though, it is possible to distinguish clear clusters of species with multipartite genomes (Fig. 1). Megaplasmids seem to be common in genera that contain numerous soil and marine bacteria that interact with eukaryotic species in either a symbiotic or a pathogenic relationship. Examples include members of the genera *Bacillus*, *Burkholderia*, *Sinorhizobium*, *Rhizobium*, *Mesorhizobium*, *Agrobacterium*, and *Methylobacterium*. Megaplasmids are also found in the genera *Rhodococcus* and *Novosphingobium*, which contain soil and marine organisms capable of inhabiting polluted environments and catabolizing the pollutants. Putative chromids are similarly found to be prevalent in several genera with species that enter into symbiotic or pathogenic relationships with eukaryotic organisms. These include members of *Sinorhizobium*, *Rhizobium*, *Agrobacterium*, *Burkholderia*, *Cupriavidus*, *Vibrio*,

Pseudoalteromonas, *Azospirillum*, *Ralstonia*, and *Prevotella*. Putative chromids are also prevalent in a few genera containing species that are able to survive in extreme environments, such as *Ralstonia*, *Deinococcus*, and *Cupriavidus*. Sequencing biases and underrepresentation of genome sequences from certain taxa may explain the absence of additional clusters in the phylogeny.

As described below, chromids appear to contain genus-specific genes, and the presence of a chromid may correspond to the emerge of a new genus (Harrison et al., 2010). In contrast, megaplasmids are rarely conserved at the genus level. It is possible to find multiple species in a genus containing a megaplasmid, however in these cases the different species may have unique megaplasmids, carrying replication and partitioning proteins that do not share a common ancestry (Österman et al., 2014).

Figure 1. Distribution of multipartite genomes throughout the bacterial phylogeny based on the analysis of 1708 bacterial species. The taxon names are colored based on the genome structure. Red corresponds to species with no megaplasmid or chromid; green to species with megaplasmids but no chromid; blue to species with chromids but no megaplasmid; and purple to species with both megaplasmids and chromids. Genera enriched for megaplamids and/or chromids are labeled. From diCenzo and Finan, 2017.

1.5. Mechanisms of Chromid Formation

There essentially are two hypotheses explaining the process of an essential secondary replicon formation: the schism hypothesis and the plasmid hypothesis (Choudhary et al., 2012; Egan et al., 2005; Fricke et al., 2009; Moreno, 1998; Prozorov, 2008). Though, the plasmid hypothesis represents the mechanism accounting for the formation of essential secondary replicons in most, if not essentially all, species examined to date.

1.5.1. The Schism Hypothesis

The schism hypothesis claims that a second essential replicon is formed as a result of a split of an ancestral chromosome into two replicons, a chromosome and a secondary chromsome. The schism hypothesis is the older of the two ideas and was first proposed to describe the chromid formation of *Brucella suis* (Jumas-Bilak et al., 1998) and *Rhodobacter sphaeroides* (Choudhary et al., 1997). According to this hypothesis the properties of the two resulting replicons would be highly similar, with an equal distribution of core genes between both replicons. The construction of viable *E. coli* or *Bacillus subtilis* strains with their single chromosome artificially split into two self-replicating chromosomes provides support to this idea (Itaya and Tanaka, 1997; Liang et al., 2013). However, the strong enrichment of essential genes on the chromosomes of species with multiple replicons is inconsistent with this model (Harrison et al., 2010). Additionally, evidence now indicates that the chromids of *B. suis* and *R. sphaeroides* did not result from a schism event.

The fact that *B. suis* biovar 3 has a single chromosome with a size corresponding to the sum of the chromosome and chromid sizes of biovars 1, 2 and 4 led to the idea that the single-replicon structure was ancestral (Jumas-Bilak et al., 1998). However, phylogenetic analysis subsequently showed this was not true and that the single chromosome of biovar 3 resulted from a fusion of the chromosome and chromid in this lineage (Moreno, 1998).

In *R. sphaeroides*, the many highly similar genomic features between the 3.2-Mb chromosome and the 0.94-Mb chromid (Choudhary et al., 1997) together with the large number of gene duplications between these replicons (Choudhary et al., 2004), and the large number of predicted essential genes on the chromid (Choudhary et al., 1994; Mackenzie et al., 2001) suggested that the secondary chromosome resulted from a split of an ancestral chromosome. However, the lower coding density of the chromid than of the chromosome (Kontur et al., 2012; Mackenzie et al., 2001), gene functional biases as determined by Cluster of Orthologous Genes (COG) analyses (Mackenzie et al., 2001), differences in evolutionary rates (Choudhary et al., 2007), and variations in gene content and size (Choudhary et al., 2007; Nereng and Kaplan, 1999) are inconsistent with this hypothesis. So far, there

is little evidence for the formation of a secondary essential replicon through the schism hypothesis. However, a recent study of the halophilic archeon *Haloferax volcanii* describes for the first time a genome rearrangement event that led to the formation of two chromosomes through a chromosomal schism (Ausiannikava et al., 2018). In this organism the main chromosome appears to have split into two elements via homologous recombination between two near-identical *sod* (superoxide dismutase) genes. The newly-generated replicons are *bona fide* chromosomes since each bears chromosomal replication origins, rRNA loci and essential genes (Ausiannikava et al., 2018). This is the first case of the evolution of a new chromosome without interspecies HGT in prokaryotes.

1.5.2. The Plasmid Hypothesis

Contrary to the schism hypothesis claiming that a secondary essential replicon evolves from a chromosome, the plasmid hypothesis proposes that it evolves from a megaplasmid. In this case, the coevolution of a megaplasmid with a chromosome will result in a regression of the genomic signature of the megaplasmid to that of the chromosome and the acquisition of essential genes potentially through transfer from the chromosome.

The fact that the replication and partitioning machinery of chromids resembles that of megaplasmids (Harrison et al., 2010) supports the plasmid hypothesis. For instance, replicons of the *repABC* family carrying essential genes, and considered chromids, have *repABC* replication/partitioning genes that have a codon usage more similar to that of the chromosome than do *repABC* family members that do not carry essential genes (Castillo-Ramírez et al., 2009). Additionally, data from phylogenetic analysis of the plasmid partitioning protein RepA is consistent with chromids evolving from pre-existing megaplasmids in the Alphaproteobacteria (Harrison et al., 2010).

It is the main chromosome that carries the majority of the conserved genes at all phylogenetic levels (Fig. 2). Despite the fact that chromids carry housekeeping genes essential for growth, there are no genes that are universally chromid-encoded. There are a large number of genes that are conserved on all chromids within a genus, and the vast majority of genes on the chromid are conserved among strains within a species. Chromid genes shared between genera within a family are only 40% of the number shared by species within a genus, whereas the corresponding number of shared choromosomal genes is 70%. At higher phylogenetic levels than the genus, the ortholog of a given chromid gene is more than likely to be found on the chromosome (Fig. 2, red). These are conserved genes that are usually chromosomal in location but have become chromid-borne within a particular genus. Another case can happen when a few or no orthologs are found at higher phylogenetic levels than the genus. In this case, those genes are characteristic of the genus and they are likely to confer phenotypes that are diagnostic at this level. Contrary to chromosomes and chromids, plasmids do

not have a conserved set of core genes across all species or a consistent gene phylogeny (Harrison et al., 2010).

The fact that essential genes are strongly underrepresented on chromids (Harrison et al., 2010) is expected if the chromid originated from a megaplasmid that subsequently gained a few core genes. There is also a consistently observed bias in the functional annotation of genes present on chromids versus genes on chromosomes (Chain et al., 2006; Goodner et al., 2001; Heidelberg et al., 2000; Mackenzie et al., 2001), which is not shocking if the chromid and chromosome originated independently. In contrast, equal distributions of core genes and of functional annotations would be expected if the chromid formed as a result of a chromosomal split. Overall, it seems that the plasmid hypothesis is likely to explain the formation of most, if not all, chromids studied so far.

Figure 2. Gene conservation between pairs of genomes at different phylogenetic levels. Comparison between 70 chromid-containing genomes. From Harrison et al., 2010.

1.5.3. Megaplasmid Domestication

The transition from megaplasmid to chromid requires two main conversions: the improvement of the genomic signatures to that of the chromosome and the acquisition of core/essential genes. Genomic signatures, such as codon usage and dinucleotide composition, are influenced by a variety of factors

and can have adaptive advantages (Carbone et al., 2003; Wong et al., 2002). Evolutionary forces selecting for optimized genome function may drive the similarity of the genomic signatures between chromosomes and chromids. This can be caused, for example, by selection for improved translational efficiency or mutational biases of the cellular machinery (Carbone et al., 2003; Wong et al., 2002).

Individual genomes and replicons have distinct codon usage signatures (Grantham et al., 1980). Chromids are much more similar to chromosomes than to plasmids that are found in the same organisms. For instance, the chromosome and the chromid of *Agrobacterium tumefaciens* C58 are very similar in average codon usage but rather distinct from the two plasmids (Fig. 3). Plasmids have a lower G + C content than chromosomes and chromids in most of all available genomes (Daubin et al., 2003; van Passel et al., 2006; Rocha and Danchin, 2002). It seems that plasmids have an intrinsically different equilibrium base composition from the chromosomal genome and that plasmid genes never ameliorate fully (Lawrence and Ochman, 1997) to the chromosomal composition of their hosts. Still, plasmids do reflect the bias of their respective chromosomes to some degree. The codon usage of each plasmid is closer to that of the chromosome in its current genome than to those in other genomes (Fig. 3) (Campbell et al., 1999; van Passel et al., 2006). In contrast chromids are much closer in codon usage to chromosomes than to plasmids. This implies that they have spent a long period in the same cellular environment as the chromosomes they are associated with (Wong et al., 2002). Nevertheless, chromid codon usage deviates from that of chromosomes in a consistent direction that is towards that of plasmids.

Figure 3. Relative synonymous codon usage (RSCU) in the genes of *Agrobacterium tumefaciens* C58 and *Burkholderia ambifaria* MC40-6. (a). Principal components plot of RSCU for every protein-coding gene, classified by replicon. (b) Centroids corresponding to averages of the genes on each replicon. From Harrison et al., 2010.

The occurrence of essential genes on a chromid is more difficult to explain because before their acquisition, the cell was fully capable of surviving. There are two possible mechanisms to explain it. The primary process is through interreplicon translocations resulting in the transfer of essential

genes from the chromosome to the secondary replicon. On the *S. meliloti* pSymB chromid there are two essential genes, *engA* and an unique arginine tRNA, $^{ARG}tRNA_{CCG}$ (diCenzo et al., 2013). Computational analysis of the surrounding region demonstrated that their presence on pSymB is the result of the translocation of a contiguous 69-kb fragment, including *engA* and the tRNA, from the chromosome to the pSymB precursor in a recent *S. meliloti* ancestor (diCenzo et al., 2013, 2016). In *V. cholerae*, five putatively essential genes (*dsdA*, *infC*, *thrS*, L20, and L35) are present in two clusters on the chromid, while in related *Vibrio* species these genes are chromosomally situated (Egan et al., 2005). Numerous other clusters of genes in the *Vibrio* and *Burkholderia* genera and the order Rhizobiales are predicted to have moved from the chromosome to a secondary replicon (Slater et al., 2009). Similarly, 25 to 30% of genes on the *S. meliloti* chromid have orthologs on the *Agrobacterium tumefaciens* chromosome (Wong and Golding, 2003), suggesting significant amounts of interreplicon gene flow. This is supported by the results of a genealogy study that are suggestive of recombination between the *S. meliloti* replicons in nature (Sun et al., 2006). In addition, in *Bacillus cereus* strains there seems to be frequent transfer of genes between chromosomes and plasmids (Zheng et al., 2015). The exact mechanism through which gene transfer from the chromosome to a secondary replicon occurs has not been studied. However, the fact that the multiple replicons of a multipartite genome can naturally form cointegrants (Guo et al., 2003; Val et al., 2014a) raises the hypothesis that the integration of the replicons can be followed by an imprecise excision event resulting in interreplicon translocations (Ng et al., 1998). Another possibility relies on a recombination event, mediated, for example, by insertion sequence (IS) elements (Val et al., 2014a). This may result in the excision of a chromosomal gene region that is subsequently captured by the secondary replicon.

The second putative mechanism that explains the presence of core genes in secondary replicons is genetic redundancy. It was shown that 10% of chromosomal genes in *S. meliloti* may have a functionally redundant copy on one of the secondary replicons (diCenzo and Finan, 2015). Also in *R. sphaeroides* (Bavishi et al., 2010; Choudhary et al., 2004), *V. cholerae* (Heidelberg et al., 2000), *B. cereus* (Zheng et al., 2015), and *Burkholderia vietnamiensis* (Maida et al., 2014) there seems to be some gene duplications between the chromosome and the secondary replicons. This genetic redundancy could be the result of an interreplication duplication of a chromosome gene or the acquisition of an orthologous gene through horizontal gene transfer. As long as the gene on the secondary replicon fully complements the disruption of the chromosomal version, the degeneration of the chromosomal copy would be fitness neutral. This way, the second copy of the gene would become the only functional copy, illustrating the transference of a core gene to a secondary replicon (diCenzo and Finan, 2017).

II. Replication of bacterial replicons

In most bacteria, there is typically a single circular chromosome, and initiation is triggered at a single origin of replication. Replication then proceeds bidirectionally along the two chromosome arms until reaching the replication terminus, where the process stops. However, not all replication is bidirectional. Some plasmids undergo unidirectional vegetative replication, while conjugative replication occurs by a rolling-circle mechanism.

In bacteria with a multipartite genome, secondary chromosomes or chromids encode their own initiator proteins which resemble plasmid initiators. However, contrary to most plasmids, whose replication can occur multiple times and at any point in the cell cycle, all chromids and megaplasmids, that have been studied so far, are replicated in a cell cycle dependent manner. This raises some important questions regarding the mechanisms ensuring their stability and how these replicons overcome the lack of timing of the original plasmids and link replication to the cell cycle. Understanding the processes of replication initiation and the formation of the replisome is crucial for understanding the replication control systems.

2.1. Chromosome replication: the *E. coli* model

2.1.1. Initiation of chromosome replication

The majority of bacterial chromosomes carry a single origin distinguished by two classes of sequence elements: conserved repeats that are important for initiator recognition and an AT-rich DNA-unwinding element (DUE) where the replication bubble originates (Bramhill and Kornberg, 1988; Gille and Messer, 1991; Kowalski and Eddy, 1989) (Fig. 4). The ~260 bp origin of *Escherichia coli*, *oriC*, is by far the most well characterized system for replication initiation. *E. coli oriC* bears a complex array of conserved sequence motifs. Most of these are recognized by the ubiquitous prokaryotic replication initiator, DnaA (Fuller et al., 1984; McGarry et al., 2004; Speck et al., 1999), whereas others are recognized by factors that modulate initiator/origin interactions (Fig. 4).

One predominant motif is the DnaA box (sites R1–R5) (15, 16), which is recognized by DnaA, a member of the AAA+ ATPase family (ATPases associated with diverse activities). In the cell, DnaA exists in both ATP- and ADP-bound forms. DnaA–ATP is considered to be the active form of the protein as this is required for oligomerisation at the origin (Nishida et al., 2002; Sekimizu et al., 1987), an event which triggers DNA unwinding and ultimately, assembly of the replisome. DnaA boxes are recognized either by ATP-bound or ADP-bound DnaA (ATP-DnaA and ADP-DnaA,

respectively), with regions R1, R2, and R4 bound most tightly (Fig. 4) (Leonard and Grimwade, 2011; Margulies and Kaguni, 1996; Schaper and Messer, 1995; Sekimizu et al., 1987). I-sites and τ-sites constitute two other classes of DnaA binding sites that associate more weakly with the initiator and are preferentially recognized by ATP-DnaA (Kawakami et al., 2005; Leonard and Grimwade, 2011; McGarry et al., 2004). In order for the helical DnaA oligomer to form at the origin and induce DNA unwinding, both strong and weak DnaA-binding sites need to bind DnaA (McGarry et al., 2004; Rozgaja et al., 2011).

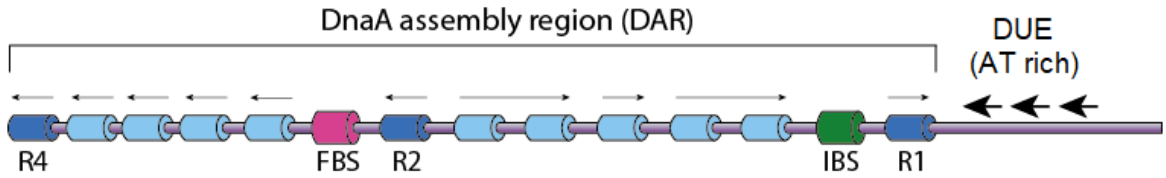

Figure 4. Organization of the chromosomal origin of replication (*oriC*) in *E. coli*. *E. coli oriC* consists of the AT-rich DNA-unwinding element (DUE) and DnaA assembly region. DnaA binding motifs and its directionality are indicated by the thin black arrows. The dark blue cylinders correspond to high- (R1 and R4) and moderate-affinity (R2) DnaA boxes while the light blue cylinders represent the low-affinity DnaA boxes. IBS – IHF binding site; FBS – FIS binding site; Black arrows with large heads indicate the AT-rich DUE.

The DUE contains several copies of a fourth type of DnaA binding element termed an ATP-DnaA box. These sites reside within three 13-bp AT-rich repeats historically designated as L, M, and R (Bramhill and Kornberg, 1988; Gille and Messer, 1991). Similar to I-sites and τ-sites, ATP-DnaA boxes are bound preferentially by ATP-DnaA (Speck and Messer, 2001; Speck et al., 1999). ATP-DnaA box recognition requires the cooperative assembly of multiple ATP-DnaA protomers and depends on initiator binding to the adjacent R1 element (Speck and Messer, 2001).

In *E. coli*, DnaA-ATP binding to DNA is facilitated by the DnaA initiator-associated protein (DiaA) (Bell and Kaguni, 2013; Leonard and Mechali, 2013). This protein forms homotetramers and each protomer contains a specific site for binding to DnaA (Keyamura et al., 2007, 2009; Natrajan et al., 2009; Zawilak-Pawlik et al., 2011). This allows the binding of a single tetramer to multiple DnaA molecules, which can stimulate cooperative binding of DnaA to *oriC* and the unwinding reaction (Fig. 5). The binding of other factors to *oriC* such as IHF, HU and Fis also affect the formation of the initiation complex (Fig. 5) (Cassler et al., 1995; Gille et al., 1991; Grimwade et al., 2000; Hiasa and Marians, 1994; Hwang and Kornberg, 1992; Leonard and Grimwade, 2004; Margulies and Kaguni, 1998; Ozaki and Katayama, 2012; Ryan et al., 2002, 2004; Wold et al., 1996). For instance, the binding of IHF induces a 180 degree bend in the DNA (Dillon and Dorman, 2010) that positively regulates replication initiation. The formation of the DnaA-oligomer introduces positive writhe in the bound DNA (Zorman et al., 2012), which is responsible for the localized strand opening at the DUE

(Fig. 5) (Duderstadt et al., 2011). In addition, transcription by RNA polymerase in or around *oriC* is also thought to facilitate strand opening (Baker and Kornberg, 1988; Bates et al., 1997; Skarstad et al., 1990). The unwound DNA is then stabilized by binding to the ssDNA binding site of DnaA located in the ATPase domain (Fig. 5) (Duderstadt et al., 2011; Speck and Messer, 2001).

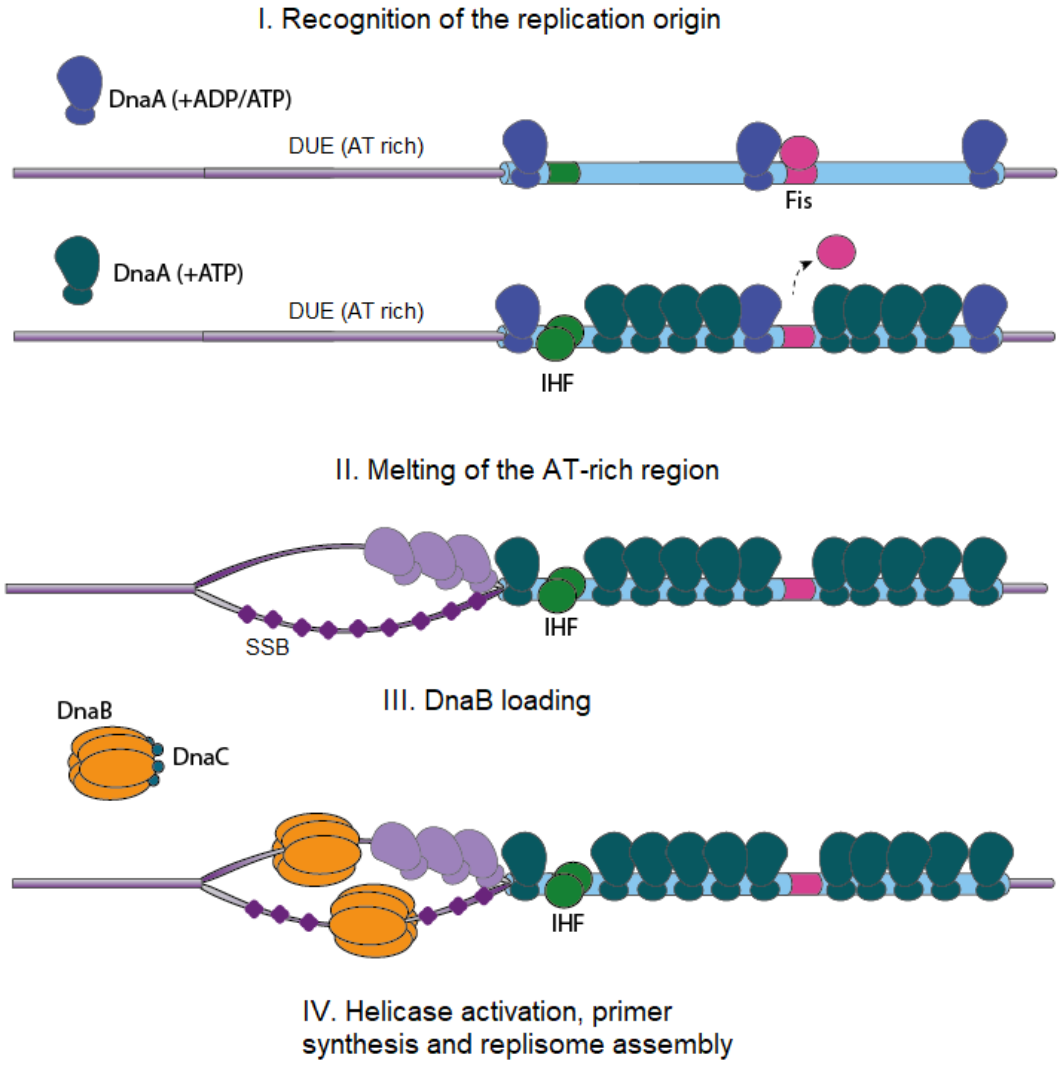

Figure 5. Sequence of events during chromosomal replication initiation. For a certain period before replication initiation, DnaA-ADP predominates and binds only high- and moderate-affinity DnaA boxes. When the level of DnaA-ATP increases and becomes predominant, DnaA-ATP cooperatively binds to the low-affinity sites. The binding of IHF induces DNA bending between the AT-rich DUE and DnaA box R1 that is crucial for stimulation of DUE unwinding. In addition, DUE unwinding requires the binding of DnaA to ssDNA. The DnaB helicase delivery requires the DnaC accessory protein. After its loading, the helicase unwinds the DNA double helix and a polymerase complex is assembled after the synthesis of a short RNA fragment by a primase. Single-stranded DNA binding protein (SSB) aids the formation and stabilization of the origin of replication.

2.1.2. Helicase loading in bacteria/Replisome formation

Following the unwinding of the DUE, the formation of the replisome involves the recruitment of other proteins to the replication process. A homohexameric DNA helicase is loaded onto ssDNA at the replication origin by the concerted action of both DnaA and a dedicated loading factor. In *E. coli*, the helicase, DnaB, is loaded onto the ssDNA by the helicase loader DnaC (Fig. 5) (Abe et al., 2007; Marszalek and Kaguni, 1994; Marszalek et al., 1996). The primase, DnaG, is next recruited via an interaction with the N-terminal domain of DnaB. DnaG mediates synthesis of primer RNA, as DNA polymerases need a pre-existing nucleic acid fragment from which to begin DNA synthesis. Active primer formation appears to induce the dissociation of DnaC, in a step which is necessary for DnaB to begin to function as an active helicase. The loading of the helicase is important for the recruitment of the DNA polymerase clamp, DnaN. The clamp is a ring-shaped DNA-binding protein that wraps around the DNA and keeps Pol III* attached to it in order to proceed the primer elongation (Georgescu et al., 2008; O'Donnell, 2006). After the synthesis of Okazaki fragments, the clamp remains loaded on the nascent DNA while Pol III* mediates the synthesis of the next Okazaki fragment (O'Donnell, 2006). This has an important role in the replication initiation control by regulating DnaA activity. This process is described in more detail below (section 2.1.4.2).

2.1.3. Chromosome Replication Termination

The termination of chromosomal replication involves several events that occur as the replication forks meet in the terminus region of the circular bacterial chromosome. One process involves the action of a directional system, such as the *E. coli* Tus-*Ter* system. This helps to maintain the directionality of the replication fork and it is crucial to assure that converging forks not pass each other and continue replication, resulting in over-replication.

In many chromosomes and plasmids replication termination is directed towards dedicated termination regions (*Ter*). This assures that the replichores are of similar size and that the last replicated regions are accessible to the cellular machinery for the final stages of the chromosome processing, such as decatenation and chromosome dimer resolution (Lesterlin et al., 2004). However, contrary to the proteins involved in the initiation of DNA replication, the terminator proteins and their cognate DNA sequence elements that comprise the replication fork trap (the *Ter* sites) are not broadly conserved. Note that some bacteria don't seem to harbour an active dedicated termination replication system (such as *V. cholerae*). In this case, termination of replication seems to occur by the fusion of the two converging replication forks.

2.1.3.1. *E.coli* Tus-*Ter* system

In *E. coli*, most of the termination events seem to occur within the ~200kb of the *ter* region. Within this region the replication forks meet at random positions. The Tus-*Ter* system controls replication fork directionality by recognition and binding of chromosomal *Ter* sites by the Tus protein. This protein binds in a directional manner, and does not allow replication fork passage in the case of *Ter* site inversion (Hill et al., 1987). If progress of one of the forks is delayed, the other fork is likely to encounter a *Ter* site bound by the terminator protein, Tus. When this occurs, fork replication stops until the second fork arrives (Duggin and Bell, 2009).

2.1.3.2. *B. subtilis* RTP-*Ter* system

In *B. subtilis* replication termination is mediated by the binding of the replication terminator protein (RTP) to the *Ter* sites. Despite having the same biological function, the RTP terminator protein of *B. subtilis* does not share any sequence or structural homology to the *E. coli* Tus protein. In addition, the *Ter* sites in *B. subtilis* are more clustered towards the centre of the terminus region. Similarly to *E. coli*, the termination complex blocks DNA replication in a polar manner. Replication forks that encounter the *B. subtilis* RTP-*Ter* complex from the core side are blocked, although those that encounter RTP-*Ter* from the auxiliary side are not (Wake, 1997).

2.1.4. Regulation of chromosome replication

Chromosome replication must be coordinated with other cell cycle events. The transmission of genetic material to the cellular offspring is a fundamental challenge for all organisms and is crucial for their survival. The regulation of chromosome replication initiation not only determines the overall rate of DNA synthesis, but helps to coordinate DNA replication with other cell cycle events, such as chromosome segregation, cell growth and division. This coordination is essential since it assures that at each origin, replication initiates once and only once per division cycle; and at least one round of replication is completed and the nucleoids have segregated before the completion of cell division (Fig. 6).

Figure 6. The bacterial cell cycle. The bacterial cell cycle is traditionally divided into three stages: the period between division (cell "birth") and the initiation of chromosome replication (known as the B period); the period required for replication (known as the C period); and the time between the end of replication and completion of division (known as the D period). From Wang and Levin, 2009.

Nutrient availability and metabolic status seems to affect every step, from initiation, through elongation to chromosome segregation (Wang and Levin, 2009). There seems to be an extensive regulatory network that ensures that replication is coordinated with growth, which allows the cells to maintain genome integrity in different environmental conditions.

In bacteria under fast-growing conditions the different processes, such as cell growth, chromosome replication, chromosome segregation and the assembly of the division machinery at the division site, occur simultaneously (Fig. 7). The chromosome begins a subsequent round of replication prior to the completion of the first, although only one round is initiated per cell division. In these conditions at least one round of replication is finished before cytokinesis, ensuring that each daughter cell receives at least one complete genome. This phenomenon, termed multifork replication, was first discovered in *B. subtilis* (Yoshikawa et al., 1964), however it is not a universal feature of the bacterial life cycle. During multifork replication cells can have four or more copies of the region proximal to *oriC* and one copy of the region proximal to *terC* (Fig. 7). This imbalance has implications for gene expression levels as well as for the activity of the initiator protein DnaA (Wang and Levin, 2009).

Figure 7. Chromosome replication during slow- and fast-growth conditions. (a) In slow-growing bacterial cells there is a single round of replication per division cycle. During replication each cell has only two copies of the origin region (*oriC*) and one copy of the terminus (*terC*). (b) Multifork replication in fast-growing conditions leads to a copy number imbalance between *oriC* and *terC*. This phenomenon has an impact on gene dosage and consequently on gene expression levels. From Wang and Levin, 2009.

DNA replication is regulated in a way that over-initiation events are prevented and sufficient initiation must be ensured so that one initiation event occurs per generation per origin. The frequency of replication must match the growth rate, otherwise the cellular DNA concentration will be altered. The cellular concentration of DnaA protein was found to be constant irrespective of the growth media (Hansen et al., 1991) and a theoretical model has suggested that the production of DnaA couples growth rate to replication frequency (Hansen et al., 1991). The ratio of ATP-DnaA to ADP-DnaA varies throughout the cell cycle and peaks right before replication initiation (Kurokawa et al., 1999). It has therefore been suggested that the frequency of initiation is determined by the accumulation of ATP-DnaA at *oriC* during steady-state growth (Donachie and Blakely, 2003). The

control of initiation relies on a reduction of the availability and/or activity of both the DnaA protein and the *oriC* region at the various steps after initiation, for example before unwinding and/or immediately after the establishment of replication forks.

2.1.4.1. Regulation at the origin sequence in *E. coli*

a) Origin Sequestration

In *E. coli*, origin usage is prevented by a process called origin sequestration. This process depends on the Dam (DNA adenine methyltransferase) and SeqA proteins (Waldminghaus and Skarstad, 2009). SeqA discriminates between new and old origins by the methylation status of GATC sequences, which are present at high frequency in the *oriC* DNA sequence. In turn, Dam methylates the adenines present in these sequences. As these sequences are palindromic, both A residues in the duplex DNA sequence are methylated, resulting in a fully methylated state. When this sequence is replicated, a hemi-methylated state (where the nascent strand is not yet methylated) exists before further action of Dam. The hemi-methylated GATC sites are the binding targets of SeqA (Lu et al., 1994; Slater et al., 1995). SeqA binding is maintained for about 10 min after initiation in cells with a doubling time of 30 min (Lu et al., 1994). During this time the origin is bound by SeqA which prevents GATC methylation by Dam methylase (Boye et al., 1996; Fujikawa et al., 2004; Guarné et al., 2002; Lu et al., 1994). Additionally, the binding of SeqA multimers to the supercoiled DNA causes DNA topological changes (Kang et al., 2003; Torheim and Skarstad, 1999), and within *oriC* it inhibits DnaA binding to the low-affinity boxes, thereby inhibiting initiation (Nievera et al., 2006).

b) Regulation by transcription at and near the origin

Transcription around and at *oriC* can affect replication initiation and may also contribute to regulation of initiation frequency. *oriC* is flanked by two genes, *gidA* and *mioC*. *gidA* encondes a protein involved in modification of specific tRNA molecules (Bregeon et al., 2001; Moukadiri et al., 2009), while *mioC* encodes a protein that has been implicated in biotin synthesis *in vitro* (Birch et al., 2000). Both genes are transcribed in the same direction and *oriC* is located downstream of *mioC*. Consequently, the *mioC* transcripts read through *oriC* (Messer and Weigel, 1997), while *gidA* gene is transcribed away from *oriC*. The *mioC* promoter region harbours a DnaA box cluster and DnaA binding downregulates *mioC* gene transcription (Hansen et al., 2007; Messer and Weigel, 1997). Transcription of *mioC* is repressed before replication initiation and is derepressed after it. The pattern of *gidA* transcription is opposite to that of *mioC* (Bogan and Helmstetter, 1997; Ogawa and Okazaki, 1994; Theisen et al., 1993). Although the deletion of the promoters of these genes does not

affect initiation regulation in wild-type cells during steady-state growth, their transcription can stimulate initiation in cells bearing a mutation impeding initiation (Bates et al., 1997). However, constitutive transcription of *mioC* impedes initiation (Su'etsugu et al., 2003).

c) Regulation of DnaA Gene Transcription

The cellular DnaA concentration was found to be constant irrespective of growth medium and the cell cycle (Hansen et al., 1991). However, the transcription of the *dnaA* gene is regulated in a cell cycle-specific manner; it increases before initiation and decreases after initiation (Theisen et al., 1993). The main reason for the oscillation resides on Dam and SeqA (Bogan and Helmstetter, 1997) and is important to sustain timely initiation (Riber and Lobner-Olesen, 2005). The *dnaA* gene promoter is sequestered by SeqA for almost the same duration as the origin (Campbell and Kleckner, 1990; Lu et al., 1994; Riber and Lobner-Olesen, 2005) being unavailable to the transcription machinery. Since the *dnaA* gene is situated near *oriC*, this decreases DnaA production and therefore the initiation potential soon after new replication forks have been launched (Riber and Lobner-Olesen, 2005). In addition, *dnaA* gene transcription is autoregulated by the presence of DnaA boxes in the *dnaA* promoter region (Speck et al., 1999).

2.1.4.2. Control outside the origin

a) The Specific DNA Element (*datA*)-Dependent Timely Inactivation of DnaA

There are about 300 high-affinity DnaA binding sites and a very large number of low-affinity sites around the chromosome (Hansen et al., 2007; Kitagawa et al., 1996; Roth and Messer, 1998). As the chromosome is replicated, the DnaA binding sites are duplicated and contribute to titration of DnaA away from *oriC*. The main titration site, *datA*, is situated near *oriC* and is duplicated soon after replication initiation (Kitagawa et al., 1996, 1998, Morigen et al., 2003, 2005; Ogawa et al., 2002) (Fig. 8). The *datA* site binds on average 60 DnaA molecules (Hansen et al., 2007) which represses the occurrence of extra initiations/reduces the initiation potential at *oriC* when *oriC* is still in sequestration (Kitagawa et al., 1998). The *datA* site is about 1 kb in size and contains 5 high-affinity DnaA binding sites and about 25 low-affinity sites (Hansen et al., 2007; Kitagawa et al., 1996, 1998). High-affinity DnaA boxes 2 and 3 are essential for efficient binding of DnaA to *datA*. DnaA bound to these sites works as a core for further cooperative DnaA binding (Ogawa et al., 2002).

In addition, this locus contains a IHF-binding site, which is essential for *datA* function (Nozaki et al., 2009). The IHF-*datA* complex promotes DnaA-ATP hydrolysis, yielding DnaA-ADP (Kasho and

Katayama, 2013). The supercoiled structure of the *datA* region stimulates assembly of DnaA and IHF, which enhances this process (Kasho et al., 2017). The binding of IHF to *datA* is cell cycle specific, taking place immediately after initiation. This provides a mechanism for the timing of *datA* mediated DnaA-ATP hydrolysis (Kasho and Katayama, 2013).

b) Regulation of the DnaA Nucleotide Form by DARS

The *E. coli* chromosome contains two sites which specifically interact with DnaA-ADP and reactivate it by exchanging ADP to ATP and producing DnaA-ATP (Fujimitsu et al., 2009). These DnaA-reactivating sequence sites are termed DARS1 and DARS2 and are located halfway within the intergenic region between *oriC* and *terC*, to the right and left of *oriC*, respectively (Fig. 8) (Fujimitsu et al., 2009). These sites both include a cluster of three DnaA boxes, so multiple ADP-DnaA molecules can form complexes with DARS, facilitating the release of ADP from DnaA. The resultant apo-DnaA molecules are likely released from DARS because of reduced complex formation activity, which allows the binding of ATP and DnaA reactivation. *De novo*-synthesized DnaA binds ATP, providing cells with a basal level of ATP-DnaA. However, this alone is not enough to assure replication initiation in a timely manner. Both DARS1 and DARS2 are required for timely initiation during the cell cycle (Fujimitsu et al., 2009). Each DARS contains a regulatory region in addition to the common sequence containing the DnaA box cluster (Fujimitsu et al., 2009; Leonard and Grimwade, 2009). However, the mechanisms by which the regulatory regions stimulate the DnaA-reactivating function are not completely understood.

The regulatory region of DARS2 contains specific binding sites for the DNA bending proteins IHF and Fis, which are required for DARS2 function/activation (Kasho et al., 2014). The simultaneous binding of IHF and Fis to DARS2 facilitates DnaA-ATP regeneration *in vivo* (Kasho et al., 2014), providing a mechanism for the timing of DnaA reactivation. The binding of IHF to DARS2 appears to be cell-cycle regulated and independent of DNA replication, while the binding of Fis is linked to the growth phase: occurring during exponential growth but not on stationary phase (Kasho et al., 2014).

The chromosomal positioning of DnaA binding sequences such as *datA*, DARS1 and particularly DARS2 relative to *oriC* has been shown to be important for the proper timing of DNA replication initiation (Fig. 8) (Frimodt-Møller et al., 2016; Inoue et al., 2016). Relocation of *datA* and DARS1 to the replication terminus or origin, respectively, perturbs replication initiation. These effects may be attributed to a gene dosage effect, or decreased/increased proximity to DnaA (Frimodt-Møller et al., 2016). In turn, the relocation of DARS2 has a more significant impact. Translocation of this site close to the terminus causes decreased initiation events and asynchronous replication. This suggests that

the chromosomal location of DARS2 is important for regulating DNA replication synchrony (Frimodt-Møller et al., 2016; Inoue et al., 2016).

Figure 8. Effect of DARS1 and *datA* chromosomal positioning. (A) In the WT, *oriC* and the *dnaA* gene are sequestered by the SeqA/Dam system following initiation of replication. The period of sequestration allows RIDA and the early duplication of *datA* to decrease the DnaA-ATP/DnaA-ADP ratio to a level inhibiting new rounds of initiation. (B) When *datA* is relocated close to *terC*, only RIDA and the single copy of *datA* next to *terC* act to lower the DnaA-ATP/DnaA-ADP ratio during the sequestration period, resulting in higher concentration of DnaA-ATP compared to the WT and earlier re-initiation. (C) When DARS1 is relocated close to *oriC*, RIDA and *datA* act to lower the DnaA-ATP/DnaA-ADP ratio similar to the WT. However, the early duplication of DARS1 results in an earlier rejuvenation of DnaA-ATP from DnaA-ADP. Thus, the DnaA-ATP level increases faster than for WT cells, leading to the following initiation at a reduced mass. (D) DARS2 requires the binding of IHF to be active, which occurs only prior to initiation. Thus, moving DARS2 close to *oriC* does not alter the origin concentration because IHF availability does not change. In contrast, when DARS2 is relocated close to *terC* its gene dosage decreases, which may be insufficient to generate the pre-initiation burst in DnaA-ATP required for initiation at all cellular origins. The red circle and green circles correspond to Dna-ADP and DnaA-ATP, respectively. The size of the circles is proportional to the cellular amounts of each DnaA form. From Frimodt-Møller et al., 2016.

c) Regulation of the DnaA nucleotide form by RIDA

After promoting replication initiation, ATP-DnaA is hydrolysed in a manner dependent on a complex consisting of ADP-Hda protein and the DNA-bound polymerase β-clamp, DnaN (Katayama et al., 1998; Kato and Katayama, 2001; Kurokawa et al., 1999; Su'etsugu et al., 2008). The resultant ADP-DnaA is inactive in initiation. This system is termed RIDA (regulatory inactivation of DnaA) and is crucial for DnaA inactivation, supporting the once-per-generation initiation (Camara et al., 2005; Kurokawa et al., 1999; Riber et al., 2009). Hda protein consists of a short N-terminal region containing the clamp-binding motif and an AAA+ domain (Dalrymple et al., 2001; Kato and Katayama, 2001; Kurz et al., 2004; Su'etsugu et al., 2005; Xu et al., 2009). The Hda AAA+ domain specifically binds ADP, but not ATP (Su'etsugu et al., 2008). ADP-Hda is monomeric and active in RIDA, whereas apo-Hda is multimeric and inactive in RIDA (Su'etsugu et al., 2008).

During replication elongation, the clamps remain on the lagging strand after Okazaki fragments are synthesized and the DNA polymerase III core is released (Balakrishnan and Bambara, 2013; Goodman and Woodgate, 2013; Hedglin et al., 2013; MacAlpine and Almouzni, 2013; Yuzhakov et al., 1996). These DNA-bound clamps interact with ADP-Hda protein, and the resultant complex subsequently interacts with ATP-DnaA, promoting ATP hydrolysis (Su'etsugu et al., 2004, 2008). Although DNA-free clamps can bind Hda, they are inactive in RIDA, meaning this system is activated upon replication initiation and loading of DNA polymerase III holoenzyme. This ensures the timely and replication-coupled activation of RIDA and makes a link between initiation regulation and DNA replication

elongation, as ATP hydrolysis only becomes activated following the start of DNA synthesis (Camara et al., 2005; Kasho and Katayama, 2013; Kato and Katayama, 2001).

2.1.4.3. Coordination of regulation for *oriC* and DnaA

Immediately after replication initiation SeqA binds to hemimethylated *oriC*. This binding lasts approximately one third of the doubling time (10 min in a culture with a doubling time of 30 min) and depends on the balance between Dam methylase and SeqA activities (Bach et al., 2003). The ratio of ATP-DnaA to ADP-DnaA peaks at initiation, and then decreases gradually due to RIDA activity. It takes approximately 15 minutes to decrease this ratio to the lowest levels, and very likely less than 10 min to decrease the ratio enough to prevent initiation from occurring when the origins are released from SeqA sequestration. The coordination between *oriC* sequestration by SeqA and DnaA inactivation by RIDA is crucial for repressing untimely initiation events (Katayama et al., 2010; Keyamura et al., 2009; Kurokawa et al., 1999; Lu et al., 1994; Skarstad and Løbner-Olesen, 2003).

The regulation of replication initiation in *E. coli* does not involve control over the concentration of origins. All origins present in the cell are initiated at the same time once per generation irrespective of how many there are (Helmstetter and Leonard, 1987; Lobner-Olesen, 1999). This means that all origins are initiated during a short time interval and all new origins are sequestered until initiation is no longer possible.

2.2. Chromids and Megaplasmid replication: The RepABC model

As mentioned in the previous chapter many alphaproteobacteria have a multipartite genome, carrying secondary chromosomes. Generally, these replicons have one or more genes that are essential for core physiology, as well as a GC content similar to that of the primary chromosome. However, they possess plasmid-like replication and partitioning systems similar to that of the plasmids found in these organisms. RepABC family plasmids are found exclusively in alphaproteobacteria and their long-term survival requires faithful vertical transmission from the mother cell to daughter cells. Most of the larger alphaproteobacterial plasmids replicate their DNA and distribute it to daughter cells via proteins encoded by the *repABC* cassette.

Contrary to the well-studied replication and partitioning systems found in enterobacteria, *repABC* cassettes are only starting to be the focus of detailed studies. The best characterized *repABC* cassettes are found on the symbiosis plasmids p42d of *Rhizobium etli* and pSymA from *Sinorhizobium meliloti*, on two different Ti plasmids from *A. tumefaciens* and on plasmid pTAV1 from *Paracoccus versutus* (Fig. 9a) (Bartosik et al., 1997, 1998, Cevallos et al., 2002, 2008; Chai and Winans, 2005a; MacLellan et al., 2004; Pappas, 2008; Venkova-Canova et al., 2004).

2.2.1. Genetic structure of *repABC*-type cassettes

The *repABC* operons encode three proteins, *repA*, *repB* and *repC*, that are expressed as an operon from promoters that lie upstream of *repA* (Fig. 9a) (Pappas and Winans, 2003a; Ramírez-Romero et al., 2001). RepC is sufficient for replication, while RepA and RepB direct the partitioning of daughter plasmids. The RepA and RepB proteins of these cassettes generally resemble the larger family of ParA and ParB proteins and are likely to have similar general properties. The origin of replication and partitioning (*par*) sites are also localized within or near the *repABC* operon. All *repABC* cassettes contain a gene between *repB* and *repC* that encodes a short, non-translated counter-transcribed RNA called *repE* in pTiR10. This small RNA downregulates the expression of *repC* (Fig. 9a) (Chai and Winans, 2005a; MacLellan et al., 2004; Venkova-Canova et al., 2004), thereby controlling plasmid copy number and incompatibility.

In some cases there is a fourth gene, *repD*, spanning the gap between *repA* and *repB* (Chai and Winans, 2005b). This is the case of plasmids pTiR10 and pTiC58 (Fig. 9a), however the *repD* sequence is completely divergent between the two plasmids. Possibly the expression of *repD* has no function other than to ensure the expression of downstream genes. Within the *repD* gene of pTiR10 and pTiC58 there are two RepB-binding *par* sites that are required for plasmid partitioning (Fig. 9a) (Chai

and Winans, 2005b). When *repD* is not present, as it is the case of p42d, pSymA and pTAV1 plasmids, the *par* sites lie directly upstream or downstream of the corresponding *repABC* operons (Fig. 9a).

Figure 9. Genetic organization of representative *repABC* cassettes. The partitioning sites are shown in orange, and the AT-rich regions that are believed to contain the plasmid origin of replication are represented in blue. Arrows immediately upstream of *repC* represent counter-transcribed RNAs (*repE* in the case of pTiR10). The *repD* gene of pTiC58 is provisional and based solely on DNA sequence analysis. B) The *repE-repC* region of pTiR10, showing the highly represented GANTC sites near the *repE* promoter and in the AT-rich region. The GANTC sites at these locations are a common feature of *repABC* operons. From Pinto et al., 2012.

There are two other notable features of these operons. First, each has an evident AT-rich region within *repC* that seems to contain the origin of plasmid replication (Fig. 9b). Second, the DNA sequence GANTC is over-represented in the putative replication origin and in the promoter of the couter-transcribed RNA (Fig. 9b). These sequences are substrates for a DNA methylase that modifies the A residues, and the motifs might play a part in the timing of various events in the cell cycle (Brilli et al., 2010). Even though methylation does not seem to affect the binding affinity of RepC for DNA (Pinto et al., 2011) it might influence the binding of other replication factors or enhance origin melting (Bae et al., 2003; Collins and Myers, 1987; Guo et al., 1995). Alphaproteobacteria do not have a protein homologous to SeqA, but another protein might play an analogous role in origin sequestration. In addition, methylation of *repE* promoter might as well influence the production of the small RNA, affecting RepC synthesis.

2.2.2. RepC and the origin of replication

RepC-type proteins have been found exclusively in alphaproteobacteria (Bartosik et al., 1997; Burgos et al., 1996; Castillo-Ramírez et al., 2009; Palmer et al., 2000; Petersen et al., 2009), and they do not show apparent homology to any other replication initiator proteins. Most of the *repC* are essential and sufficient for plasmid replication in the respective hosts (Bartosik et al., 1997; Cervantes-Rivera

et al., 2011; Chai and Winans, 2005a; Izquierdo et al., 2005; Mercado-Blanco and Olivares, 1994; Pinto et al., 2011), indicating that the origin of replication is located inside this gene (Bartosik et al., 1997; Cervantes-Rivera et al., 2011; Cevallos et al., 2008; Pinto et al., 2011). All *repC* genes contain an AT-righ sequence of 150 nucleotides near the middle of the protein-coding sequence. This AT-rich sequence is a common feature of diverse replication origins.

In pTiR10 RepC transcription and translation seem to be inhibited by a counter-transcribed RNA, known as RepE (Chai and Winans, 2005a) (Fig. 9a). RepE is a non-translated RNA of approximately 50 nucleotides in length enconded by a gene liying between *repB* and *repC*. This small RNA includes a predicted stem-loop that is thought to function through base pairing with complementary mRNA sequences (Cervantes-Rivera et al., 2010; Chai and Winans, 2005a). (RepC expression is also affected by autoregulation mediated by RepA and RepB (Pappas and Winans, 2003b; Ramírez-Romero et al., 2001). In pTiR10 RepA binds to one of the four promoters that provides a basal expression of the operon (Pappas and Winans, 2003b), which ultimately affects replication frequency and plasmid copy number.)

In the iteron-type plasmids (described below) the replication initiator binds to directly repeated DNA sequences at the origin of replication called iterons (Francia et al., 2004; Gering et al., 1996; Kwong et al., 2004; Rajewska et al., 2012; Ravin et al., 2003; Tanaka et al., 2005) and recruit DnaA, causing the melting of the AT-rich region at the origin. The DNA-DnaA complexes then recruit the replicative DNA helicase bound to the loading factor (DnaB and DnaC, respectively, in *E. coli*) and finally the DNA polymerase. Contrary to these plasmids, origins that require RepC for activity lack iterons (Rajewska et al., 2012). In addition, there are no apparent DnaA-binding motifs matching the consensus sequence for alpha-proteobacteria anywhere within *repC* (Brilli et al., 2010). Possibly RepC recruits DnaA, which would then recruit DnaB-DnaC (Messer, 2002). Another possibility is that RepC recruits DnaB-DnaC directly.

2.3. Plasmid replication: the Iteron model

Iteron plasmids are extrachromosomal genetic elements that can be found in all Gram-negative bacteria. Besides carrying antibiotic resistance genes, they can bring other features to their hosts, such as genes for degradation of specific compounds or toxin production. Plasmids such as P1, F, RK2, R6K, pSC101 and pPS10 are well-characterized members of the interon-based replication family (Fig. 10A) (Paulsson and Chattoraj, 2006). These plasmids are characterized by the presence of directed repeats located within the origin of replication that are called iterons. Their number and length can vary depending on the plasmid. These motifs play a crucial role during DNA replication initiation and are also critical for plasmid copy number control. Adjacent to the iterons lies the gene encoding the replication initation protein, generally called Rep protein. The binding of the Rep protein to the iterons has a dual role. It is responsible for initiating the process of plasmid DNA synthesis and at the same time for inhibiting the replication initiation process.

2.3.1. Replication Initiation of iteron-based plasmids

The first step of replication initiation at the plasmid origin is the formation of an initial complex facilitated by the specific interaction of Rep proteins with iterons (Fig. 10B). Rep proteins exist in cells mostly as dimers (Kawasaki et al., 1990; Toukdarian et al., 1996). However, it is its monomeric form that is replication active (Ishiai et al., 1994; Toukdarian et al., 1996; Wickner et al., 1991). The dissociation of dimers into monomers is achieved by the action of chaperones DnaJ and DnaK, which results in conformational changes in the Rep structure (Díaz-López et al., 2003). The cooperative interaction of Rep monomers with iterons results in local destabilization of the DNA duplex at the level of the AT-rich region (Fig. 10B) (Bowers et al., 2007; Perri and Helinski, 1993). This region is considered to be a DUE where single-stranded DNA (ssDNA) is created. Rep protein is very often accompanied in its action by host initiator DnaA protein that binds DnaA-boxes located in the plasmid origin (Fig. 10B). In addition, in some plasmid origins, such as the plasmid P1 origin pSC101 and R6K, a binding site for the integration host factor (IHF) can also be identified (Fekete et al., 2006). The binding of IHF induces a binding of the DNA, which is required for the activity of the origin (Fekete et al., 2006). DnaA is mainly needed for the enhancement or stabilization of the Rep plasmid induced open complex formation and for the helicase delivery and loading. During the RK2 plasmid replication initiation, the host-encoded DnaBC helicase complex is delivered to the DnaA-box sequence through interaction with DnaA (Fig. 10B). Subsequently the plasmid initiator translocates the helicase to the opened plasmid origin. The helicase unwinds the DNA double helix, and after a short RNA fragment is synthesized by a primase, a polymerase complex is assembled. Similarly to the

chromosomal DNA replication, single stranded DNA binding protein (SSB) is required for replication initiation of iteron-containing plasmid DNA.

Other motifs that can be found within some plasmid origins are the GATC sites, however they are not directly involved in the replication process. They are usually overlapped with AT-rich repeated sequences (Brendler et al., 1991; Rajewska et al., 2008) or located adjacent to these repeats (Brendler et al., 1991). During replication, hemimethylated GATC sites are subjected to sequestration by SeqA (Brendler et al., 1995; Slater et al., 1995), which prevents replication proteins from binding to the origin. For the proper activity of the origin of interon-containing plasmid not only the presence and the sequence of essential motifs, such iterons, DnaA-boxes and AT-rich repeats is important. The proper location of these motifs relative to each other has a great impact on replication activity. In particular, changes in proper helical phasing have a negative influence on plasmid replication (Doran et al., 1998).

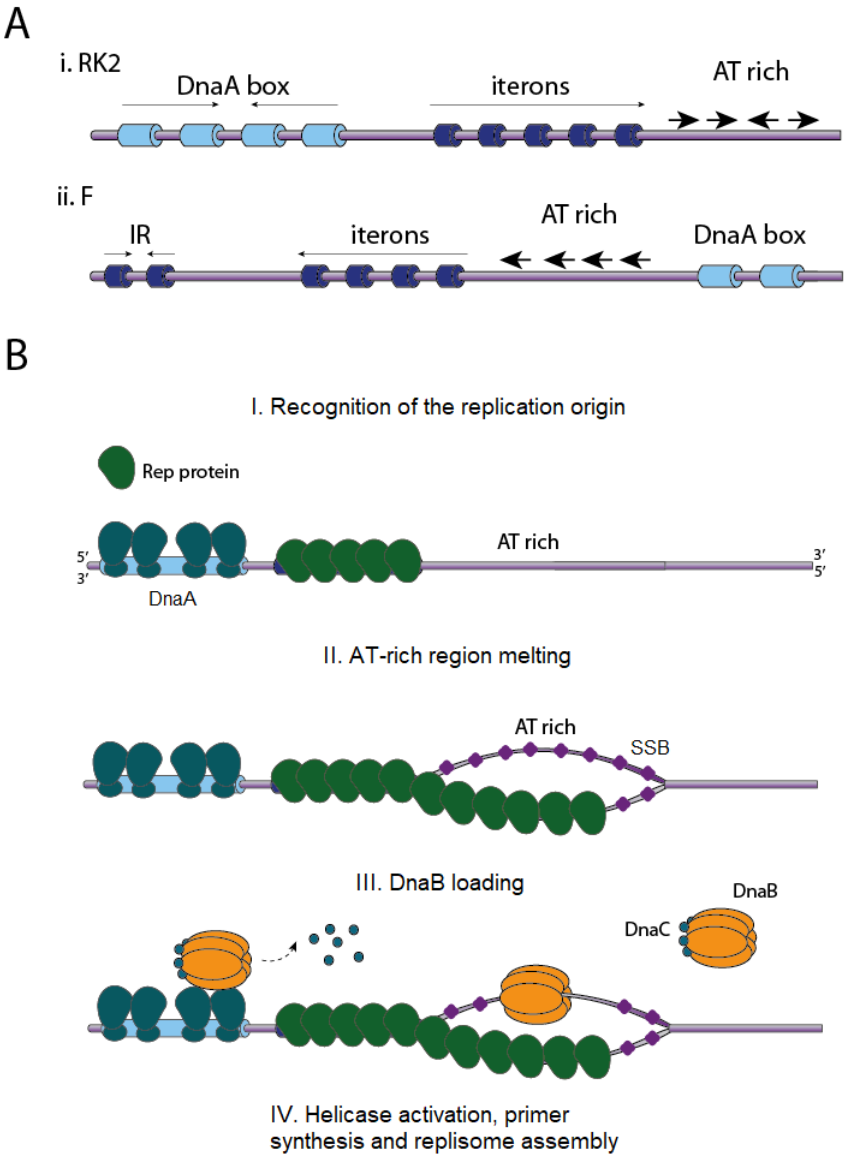

Figure 10. Origin structure and replication initiation model of the iteron-bearing plasmids. The iteron-containing plasmid origin is recognized by the plasmid-encoded initator (Rep), which binds cooperatively to the iterons. The interaction of Rep with iterons results in the formation of an open complex and destabilization of the AT-rich region, which creates ssDNA. In some plasmids, such RK2, pPS10, F, R6K, P1 and pSC101 the formation of the open complex requires cooperation of the plasmid Rep and host DnaA proteins. During the RK2 replication initiation, the host-encoded DnaBC helicase complex is delivered to the DnaA-box sequence through interaction with DnaA, and subsequently the plasmid initiator translocates the helicase to the opened plasmid origin. The helicase unwinds the DNA double helix, and after a short RNA fragment is synthesized by a primase, a polymerase complex is assembled. Single-stranded DNA binding protein (SSB) is required for replication initiation of iteron-plasmids. The black arrows in the AT rich region indicate the orientation of the repeated sequences, which is important for origin opening.

2.3.2. Copy number control of iteron-based plasmids

The iteron-bearing plasmids occur in a low-copy number per bacterial cell; therefore they evolved a number of strategies to ensure their hereditary stability and maintenance. The copy number control is such that the initiation rate per plasmid copy is a decreasing function of plasmid concentration (autoregulation or negative feedback regulation). This requires a tight regulation of replication and the main elements involved are the iterons.

Although essential for replication initiation, iterons also play a role as replication inhibitors. Upon replication, when the number of iterons increases, the sister origins compete for the initator binding, making it a limiting factor for initiation. This mechanism of initiator retention is referred to as “initiator titration” (Fig. 11) (Chattoraj et al., 1984; Tolun and Helinski, 1981; Tsutsui et al., 1983). However, titration per se is not sufficient for the copy number control. When the plasmid replicates the gene dosage for the initiator also increases and more initiator is made as well.

Initiator synthesis is controlled by transcriptional autorepression (Fig. 11). Transcriptional auto-repression is a well-known mechanism for maintaining levels of gene product within narrow limits (Becskei and Serrano, 2000; Simpson et al., 2003).The initiator promoters are sometimes buried within the array of origin iterons, and initiator binding to origin iterons also serves to repress the promoter (Chattoraj et al., 1984). More commonly, initiator promoters have adjacent inverted repeats of half-iterons (García de Viedma et al., 1995; Ingmer and Cohen, 1993; Ishiai et al., 1994; York and Filutowicz, 1993), which serve as dedicated operators of transcription of the initiator gene. Similarly to initiator titration, transcription autorepression is relieved once the initiator molecules are titrated away on newly-replicated plasmids reducing their cytoplasmic concentration.

Another mechanism used to reduce the increase in initiator monomers levels upon plasmid replication is initiator dimerization (Fig. 11). As mentioned above, the chaperones DnaJ and DnaK actively convert dimers to monomers, the replication initiator active form. Dimerization lowers the

monomer concentration so there is not enough to saturate the origin and initiate replication. In addition dimers of Rep participate in transcription auto-repression by binding to the inverted repeats located close to the *rep* gene promoter.

Initiator dimers have also been postulated to participate in another key mechanism that restricts initiation referred to as “handcuffing” (Fig. 11). In handcuffing, sister origins on different plasmid molecules are inactivated by coupling them through initiator bridges that require the participation of dimeric initiators (McEachern et al., 1989; Pal and Chattoraj, 1988). This bridging is believed to cause steric hindrance to the origin activity. In theory, this could create a stable system on its own, since at higher plasmid concentrations, each plasmid copy would be more likely to be handcuffed, ensuring less initiation of replication per copy when there are many copies per cell.

In handcuffing the initiator proteins couple two origin regions located on separate plasmid molecules, inactivating them. The *ori* coupling requires the participation of dimeric initiators (McEachern et al., 1989; Pal and Chattoraj, 1988) and occurs via binding of the Rep protein to the iterons. The resulting bridging is believed to cause steric hindrance to the origin activity, which prevents new rounds of replication (Park et al., 2001) by inhibiting origin melting (Zzaman and Bastia, 2005). This system appears to be a major mechanism that controls iteron-plasmid copy number. At higher plasmid concentrations, each plasmid copy would be more likely to be handcuffed, ensuring less initiation of replication per copy when there are many copies per cell. In addition, this process takes advantage of the dynamic of initiator dimers: when a plasmid replicates, initiator synthesis increases, which increases the concentration of dimer initiators. This lowers the replication probability following a round of replication and could also provide a sharp downshift in replication when the desired copy number is reached.

Figure 11. Replication control in the iteron-based plasmid P1. The initiator is controlled negatively by three mechanisms: auto-repression (1), inactivation by dimerization (2), and limiting availability by titration (3). Upon initiation, the number of iterons increases, which titrates the limiting amount of monomers, preventing the saturation of the iteron arrays and consequently a new round of replication. Initiator dimers do not bind iterons but participate in handcuffing (4), serving as replication inhibitors. Additionally, the handcuffing reaction strengthens transcriptional repression. The chaperones DnaK/J actively convert dimers to monomers. The increase in the level of monomers over dimers reduces handcuffing and helps to saturate the origin with monomers, allowing replication initiation. The inhibitory interactions are shown in red. From Ramachandran et al., 2017.

III. The *Vibrio cholerae* paradigm

Vibrio cholerae is a halophilic Gram-negative bacteria belonging to the γ-proteobacteria class. It is found in aquatic fresh water and marine environments, either as a free-living organism or associated with shellfish and other marine organisms. *V. cholerae* is of particular public health interest, since it is the causative agent of the severe diarrhoeal disease cholera, which kills approximately 120000 people every year (Clemens et al., 2017). Cholera is contracted by ingestion of contaminated water or food and is therefore associated with inadequate sanitation and poverty. As a result, cholera is endemic mainly in the developing world, despite the fact that *V. cholerae* is found in temperate zones around the planet. Although there are at least 200 known serogroups of *V. cholerae*, the disease has generally been associated with the O1 and O129 serogroups (Sack et al., 2004). The O1 serogroup is divided into two major serotypes, Inaba and Ogawa, and these can be further divided into two biotypes, classical and El Tor.

In marine environments, the chitinous exoskeleton of many animals represents an abundant surface where bacterial communities form. *V. cholerae* is commonly found forming biofilms on theses surfaces (Huq et al., 1983; Tamplin et al., 1990). This association with zooplankton has a strong impact on its lifestyle, since chitin is the major carbon and nitrogen source for *V. cholerae*. In addition, chitin constitutes the signal that triggers a state of natural competence, enabling extensive horizontal gene transfer (HGT) events (Meibom et al., 2005). HGT events are a key point in the evolvability of *V. cholerae* (Blokesch, 2016), which is mainly illustrated by the fact that the cholera toxin is encoded in a phage (Waldor and Mekalanos, 1996). The response to chitin has an ecological meaning for a free-living marine bacterium. In marine environments phosphate is limiting and *V. cholerae* can use extracellular DNA as a phosphate source (McDonough et al., 2016; Pratt et al., 2010). Thus, it is only worth paying the cost of expressing the natural competence machinery when living in community, where potentially interesting DNA is available to be captured. The fact that *V. cholerae* uses a type 6 secretion system as a weapon to kill non-kin surrounding bacteria to steal their DNA strongly supports this idea (Borgeaud et al., 2015). The development of such sophisticated genetic machineries to exploit HGT extensively is a proof of a high degree of genetic plasticity, and is certainly a powerful source of innovative functions.

3.1. *Vibrio cholerae* genome organization

The genome of *V. cholerae* is organized on two different replicons (Fig. 12) (Trucksis et al., 1998). It harbours a large primary chromosome (Chr1) of 2,96 Mbp and a chromid (Chr2) of 1,07 Mbp, with an average G+C content of 46,9% and 47,7%, respectively (Heidelberg et al., 2000). Chr1 is closely

related to other bacterial chromosomes while Chr2 has distinctly plasmid-like features. This two replicon organization is conserved among vibrios. While the size of Chr1 is relatively constant, the size of Chr2 is more variable. This indicates a higher plasticity of the chromid that could help in the adaptation of vibrio species to the various environmental niches in which they are found (Reen et al., 2006).

The genetic information is asymmetrically distributed between the two replicons. Most of the genes encoding essential functions and pathogenicity are found on Chr1. These include the essential genes for DNA replication and repair, transcription, translation and synthesis of the cell wall. Upon sequencing of *V. cholerae* genome it was found that 42% of the genes on Chr1 had no known function or homologue, while 59% of the genes on Chr2 were found to be hypothetical or with unknown function (Heidelberg et al., 2000). A large part of these unknown genes are found in the superintegron, located on Chr2 (Mazel et al., 1998). A high number of genes specific to *Vibrio* are also found on Chr2. There are also essential genes located on Chr2, including *rpmL* and *rplT*, which encode ribosomal proteins L22 and L35, a translation initiation factor, *infC*, and *thrS*, an aminoacyl tRNA synthetase (Egan and Waldor, 2003; Heidelberg et al., 2000). Regulatory genes for processes including energy metabolism, starvation survival, quorum sensing, and expression of the entertoxigenic haemolysin HlyA are split between the two replicons. A large proportion of genes involved in the regulation of DNA repair are found on Chr2.

Figure 12. The two chromosomes of *V. cholerae.* From Heidelberg et al., 2000.

As mentioned above, Chr2 harbours a genetic element called superintegron, which makes up approximately 3% of the genome. Like most bacterial integron systems, the *V. cholerae* superintegron acts as a reservoir of silent open reading frames (ORFs). These ORFs may be excised from the integron and inserted downstream of a promoter, which renders them functional (Stokes and Hall, 1989). There are 179 gene cassettes containing at least 215 ORFs within the structure, however most of these ORFs remain unidentified (Rowe-Magnus et al., 2003). The superintegron is known to accommodate genes homologous to antibiotic resistance genes, genes involved in virulence, and other similarly adapted functions. It is likely that these genes are captured and integrated into the superintegron following HGT events. This gives *V. cholerae* additional resources for adaptation to rapidly changing environments (Rowe-Magnus et al., 2001, 2002).

Due to *V. cholerae* genome architecture, the two chromosomes are differentially subjected to gene dosage effects in rapid growth conditions that allow multifork replication. The late replication of Chr2 relative to Chr1 means that there are always a greater number of Chr1 origins than Chr2 origins within a cell (Srivastava and Chattoraj, 2007). Chr1 gene expression levels are generally higher and show an influence from gene dosage. Indeed, Chr1 encodes most of the growth essential and growth related genes, many of which located near the origin of replication. On the other hand, Chr2 gene expression levels are lower and appear to be independent of gene dosage (Dryselius et al., 2008). In addition, a recent study has shown that the position of a locus harbouring ribosomal protein genes (S10) relative to the origin of replication correlates with a reduction of its dosage, mRNA abundance and growth rate (Soler-Bistué et al., 2015). These effects were also followed by a significant reduction in the host-invasion capacity (Soler-Bistué et al., 2015). This illustrates that the genomic position of genes involved in the flux of genetic information conditions global growth and bacterial physiology. The distinct genetic distribution between the two chromosomes and the differential gene dosage may both contribute and be enhanced by an improved adaptive capacity.

3.2. Chr1 and Chr2 cellular arrangement and segregation

V. cholerae Chr1 and Chr2 are longitudinally arranged in the cell (Fig. 13). In this type of arrangement, the origin and terminus of replication are located at opposite poles and the two chromosome arms reside beside each other along the long axis of newborn cells creating an *ori-ter* pattern. Chr1 covers the entirety of the cell, with *ori1* at the old pole and *ter1* at the new pole. In turn, Chr2 only resides in the younger half of the cell, with *ori2* at mid-cell and *ter2* towards the new pole (Fig. 13)(David et al., 2014).

The localization of specific chromosomal regions such as the origin and terminus of replication is often determined by dedicated systems that control their segregation timing and positioning. In

bacteria displaying an *ori-ter* arrangement, the origin regions are segregated to opposite cell halves and maintained in proximity of the old poles by an origin-specific partition system (Reyes-Lamothe et al., 2012; Wang and Rudner, 2014). Most bacteria carry *parAB* genes in their chromosome that participate in chromosome partition. In *V. cholerae*, two distinct ParAB-*parS* systems, ParAB1-*parS1* and ParAB2-*parS2*, drive the localization and segregation patterns of *ori1* and *ori2*, respectively (Fig. 13) (Fogel and Waldor, 2006; Yamaichi et al., 2007).

The location of *ori1* at the old pole has been found to be mainly mediated by an interaction between ParA1 and a specific anchor protein, HubP (Yamaichi et al., 2012). HubP interacts directly with ParA1, which in turn recruits the ParB1-*parS1* complexes. While ParAB2-*parS2* system is essential for Chr2 segregation, disruption of the ParAB1-*parS1* system does not impact Chr1 partitioning. In addition, in the absence of ParA1, *ori1* is still kept in the old pole region, though in a less precise manner. In this case, replication was shown to drive the longitudinal organization of Chr1 (David et al., 2014; Yamaichi et al., 2012). After duplication at the centre of the cell, the two *ori2* copies follow a symmetric segregation moving to the future cell centres of the two daughter cells. The ParAB2-*parS2* partitioning system is essential for this process (Yamaichi et al., 2007). While replication and segregation of Chr1 and Chr2 origins occurs at different spatial and temporal points, replication and segregation of their termini are synchronous and occur at midcell (David et al., 2014; Rasmussen et al., 2007). Similarly to *E. coli*, the organization, positioning and segregation dynamics of *V. cholerae* chromosomes *ter* depends on the MatP macrodomain protein. *V. cholerae* encodes an ortholog of *E. coli* MatP and *ter1* and *ter2* both harbour MatP binding motifs (*matS*) with a density similar to *E. coli ter* (Demarre et al., 2014; Mercier et al., 2008). MatP helps to maintain the terminus region of the two chromosomes at mid-cell until the onset of septation (Demarre et al., 2014).

Figure 13. *V. cholerae* Chr1 and Chr2 arrangement and segregation. Left panel: In newborn cells, *ori1* is anchored to the old pole by HubP and the ParAB1-*parS1* system, while MatP helps to keep *ter1* close to the old pole. During the cell cycle HubP is the first factor moving towards the opposite, followed by ParAB1 and one

sister copy of the newly replicated *ori1*. In turn, the *ter1* region bound by MatP relocates to mid-cell where the newly duplicated *ter1* regions remain together until the end of the cell cycle. Right panel: In newborn cells, Chr2 lies on the younger half of the cell. *ori2* is kept at the mid-cell by the ParAB2-*parS2* system and the *ter2* region close to the new cell pole by MatP. In pre-divisional cells, after replication, the *ori2* sister copies are segregated at the quarter positions by the parAB2-*parS2* system, while the *ter2* sister copies are restricted to the area around the division site by MatP. From Espinosa et al., 2017.

Before cell division any chromosome dimers formed by homologous recombination between sister-chromatids must be resolved (Lesterlin et al., 2004). As it happens in *E. coli*, dimers of Chr1 and Chr2 in *V. cholerae* are resolved by the action of the XerCD site-specific recombinase at the *dif* sites, *dif1* and *dif2*, located on the *ter* regions of Chr1 and Chr2, respectively (Val et al., 2008). As *E. coli*, the recombination event is controlled by FtsK, which links the resolution of dimeric chromosomes to the cell division. In addition, FtsK facilitates the segregation of a specific region of sister chromosomes across the division septum (Demarre et al., 2014).

3.3. Cell division control

V. cholerae carries homologues of most of the *E. coli* cell division proteins. However, their cell cycle choreography is significantly different. At the beginning of the cell cycle all of the divisome components are specifically located at the new pole. It is only at about 50% of the cell cycle that FtsZ molecules relocate to mid-cell to form a loose pre-divisional Z-ring. The remaining divisome components leave the new pole and join the early divisome complex at midcell at about 80% of the cell cycle. At this point, the pre-divisional FtsZ structures merge into a compact Z-ring. Finally, at 90% of the cell cycle, cell wall constriction initiates, leaving a short time to complete cell division (Fig. 14A) (Galli et al., 2016, 2017).

In *E. coli*, the combined action of two FtsZ-polymerization inhibitory systems, Min and nucleoid occlusion (NO), specifically licenses cell division at mid-cell at the end of each round of replication/segregation cycle (Bernhardt and de Boer, 2005; de Boer et al., 1991; Lutkenhaus, 2007; Yu and Margolin, 1999). The Min system, composed of the proteins MinC, MinD and MinE, prevents the Z ring from forming at the cell poles, directing it to mid-cell (Lutkenhaus, 2007). This is achieved through the regulated oscillation of the Min proteins between the two cell poles. The continuous shuttling of MinCD between the poles creates a concentration grandient of MinC with a minimum at mid-cell (Lutkenhaus, 2007). On the other hand, NO prevents closure of the Z ring over the bulk of the nucleoid (Bernhardt and de Boer, 2005; Wu and Errington, 2004). Binding sites for SlmA, a protein that inhibits FtsZ polymerization, are scattered around the *E. coli* chromosome and essentially absent from the terminus region. As a result, cell division can only initiate at the very end

of the chromosome duplication/segregation cycle, when sister *ter*, devoid of SlmA binding sites (SBS), are the only chromosomal regions left at mid-cell (Cho et al., 2011; Tonthat et al., 2011).

Figure 14. Divisome assembly and regulation of the Z-ring positioning in *V. cholerae*. (A) In newborn cells all the division proteins are located at the new pole. Around 50% of the cell cycle FtsZ and the early cell division proteins leave the cell pole and relocate to mid-cell where they form a pre-divisional structure. At about 80% of the cell cycle, the Z-ring merges into a compact structure, which coincindes with the arrival of the late cell division proteins at mid-cell. Finally, at approximately 90% of the cell cycle the cell constriction starts. (B) Spatial regulation of the division site placement by the Min system. The oscillation of MinCD between the cells poles creates a gradient of MinC (inhibitor of FtsZ polymerization), being lowest at the mid-cell and highest at the poles. This phenomenon is responsible for positioning the Z-ring formation at the mid-cell. (C) Spatiotemporal regulation of the division site placement by the NO system. The inhibitor of Z-ring assembly, SlmA, binds to specific DNA sequences distributed all over the Chr1 and Chr2 with the exception of *ter1* and *ter2* regions. During the cell cycle the spatial arrangement and segregation timing of Chr1 and Chr2 direct FtsZ molecules and assembly of divisional Z-rings to the SlmA-free zones. It is only at 80% of the cell cycle that both *ter1* and *ter2* regions co-localize at mid-cell, allowing the assembly of divisional Z-rings at the future division site. From Espinosa et al., 2017.

In *V. cholerae* similar mechanisms seem to exist, since it carries orthologues of both the Min and NO effectors, MinCDE and SlmA, respectively (Fig. 14 B and C) (Galli et al., 2016). Indeed, *V. cholerae* MinD was shown to shuttle between poles similarly to what happens in *E. coli* (Galli et al., 2016). However, while in *E. coli* Min is the major regulator of division site placement, in *V. cholerae* NO seems to play a major role (Galli et al., 2016). Both Chr1 and Chr2 carry SBS sites and their distribution was shown to drive the choreography of the cell division proteins as well as the timing of assembly and maturation of the divisome (Fig. 14C) (Galli et al., 2016).

3.4. Replication control in *Vibrio cholerae*

Both Chr1 and Chr2 carry a single origin of replication, *ori1* and *ori2*, respectively. However, the factors responsible for controlling replication initiation of the two chromosomes of *V. cholerae* are distinct (Fig. 15) (Duigou et al., 2006). Replication of Chr1 is initiated by the bacterial universal

initiator DnaA while Chr2 replication is initiated by a Vibrio-specific factor, called RctB (Pal et al., 2005).

Figure 15. Common principles that control P1 plasmid, *E. coli* chromosome, and *V. cholerae* Chr2 replication. The targets of control are the initiator and the origin. The initiators are controlled by autorepression, titration, and inactivation, and the origins are controlled by sequestration and handcuffing. From Ramachandran et al., 2017.

3.4.1. Replication initiation of Chr1

The structure of *ori1* is very similar to the *E. coli oriC* (Egan and Waldor, 2003). *ori1* contains an AT rich region flanked by five putative high affinity DnaA boxes that allow DnaA binding. It also carries an IHF binding site and several GATC sites that are substrates for Dam methylation. *ori1* methylation plays an important role in the timing of re-initiation through sequestration of hemimethylated sites by SeqA (Fig. 19A) (Demarre and Chattoraj, 2010). The fact that *ori1* is able to functionally replace *oriC* in *E. coli* (Demarre and Chattoraj, 2010; Koch et al., 2010) suggests that *V. cholerae* Chr1 replication initiation is subjected to similar regulatory processes (Fig. 15). Indeed, DARS1 and DARS2 are conserved among *E. coli*-related species. In *V. cholerae* the DnaA box clusters upstream of *uvrB* and *mutH* are highly conserved (Fig. 16) (Fujimitsu et al., 2009). This suggests that *V. cholerae* DnaA is subjected to the same reactivation process by DARS, where DnaA-ADP is converted to DnaA-ATP by nucleotide exchange.

Despite the similarities between *E. coli* and *V. cholerae* there is a notable difference at the level of the helicase loading upon replication initiation. *V. cholerae* Chr1 carries a gene encoding for DciA, the primordial loader/activity regulator of the replication helicase, while in *E. coli* it was replaced by DnaC. DciA is likely to control the loading and release of the replicative helicase, DnaB, on either side of the origins of Chr1 and Chr2, to start bidirectional replication (Brézellec et al., 2016).

Figure 16. Bacterial DnaA box-clusters similar to DARS of *E. coli*. DnaA boxes are marked with rectangles and the arrows indicate its direction. Sequences that differ from the consensus DnaA box (TTATNCACA) are in lowercase. From Fujimitsu et al., 2009.

3.4.2. Replication initiation and regulation of Chr2

Contrary to *ori1*, the structure of *ori2* is similar to the iteron-based replication origin of large low copy number plasmids, such as F and P1. *ori2* harbours a single DnaA binding site and unwinding of its AT-rich region results from the binding of a specific initiator, RctB, to short 11-12 mers motifs (Fig. 17). RctB is a four-domain protein of 658 amino acids conserved within the Vibrionaceae family. It shares no sequence homology with any other replication initiators (Egan and Waldor, 2003) but its structure resembles some plasmid initiators. More precisely, the structure of its two central domains (domains 2 and 3) bears significant structural similarity to several well-characterized iteron-plasmid initiators, such as RepE (F-plasmid), RepA (pPS10 plasmid) and π (R6K plasmid) (Orlova et al., 2016). However, RctB is considerably larger, and contains at least 2 additional domains (domains 1 and 4). Domains 1, 2 and 3 contain winged-helix-turn-helix DNA binding motifs, all of which implicated in binding to *ori2*, and in the initiator's capacity to mediate *ori2*-based replication. In solution, RctB adopts a head-to-head dimeric configuration, mediated by interactions between residues in domain 2 (Orlova et al., 2016).

As it occurs with Chr1, the homeostatic system that regulates Chr2 replication relies on a negative-feedback control of the availability of its active initiator. For Chr2, *V. cholerae* has integrated complex regulatory mechanisms that appear to be a combination of those found in iteron-like plasmids to

control the level and activity of RctB. These include initiator autoregulation, initiator titration, initiator dimerization and origin handcuffing (Fig. 19B) (del Solar et al., 1998).

The origin region of Chr2 is divided into three functional units: *rctB*, encoding the initiator of replication; *ori2*, the minimal origin of replication; and *incII*, a negative regulatory region which contains a transcribed but non-translated ORF, *rctA* (Egan and Waldor, 2003). The organization of *ori2* is similar to the iteron-bearing plasmid origins. It contains six iterons, which are 12-mer repeated initiator binding sites. RctB binding to iterons promotes the unwinding of *ori2* for initiation (Duigou et al., 2008). The adjacent *incII* region negatively regulates Chr2 replication. It contains five regulatory iterons (11- and 12-mers) and two 39-mer motifs, one of which in *rctA* (Venkova-Canova and Chattoraj, 2011). The binding of RctB to the 39-mer motifs acts as a negative regulator of *ori2* initiation and helps in the regulation of the timing of Chr2 replication. The high inhibitory activity of the 39-mers is mainly achieved by two mechanisms: initator titration and origin handcuffing (Fig. 19B) (Jha et al., 2012; Venkova-Canova and Chattoraj, 2011; Venkova-Canova et al., 2006). The iterons located on the *incII* region have a regulatory function serving as titration sites for RctB. In addition, their precise arrangement and orientation help to restrain the strong inhibitory activity of the 39-mer motifs. The 39-mers, in contrast, enhance handcuffing of the regulatory iterons with themselves (Venkova-Canova and Chattoraj, 2011).

rctA brings another important mechanism for the regulation of Chr2 replication (Venkova-Canova et al., 2006). Transcription of *rctA* attenuates its own 39-mer inhibitory activity, probably by interfering with RctB binding. In turn, RctB binds to regulatory iterons located in the *rctA* promoter region, repressing *rctA* transcription (Egan et al., 2006; Venkova-Canova et al., 2006). This mechanism of transcriptional interference participates in adjusting the level of available RctB. RctB also auto-regulates its own expression through binding at another RctB binding motif called the 29-mer in the promoter region of *rctB* (Venkova-Canova et al., 2012). The 29-mer functions as a transcription operator, from which RctB exerts a negative feedback regulation on its own transcription (Egan et al., 2006). The 29-mer also participates in the control of *ori2* initiation through handcuffing with *ori2* iterons (Venkova-Canova et al., 2012). The 39- and 29-mer motifs are closely related. Indeed, the 29-mer is a truncated version of the 39-mer and can be functionally replaced by a 39-mer (Jha et al., 2012; Venkova-Canova et al., 2012). The difference between the two sequences resides on the central AT-rich region. While this region is 19-bp long in the 39-mer, in the 29-mer motif it is only 9-bp long (Venkova-Canova and Chattoraj, 2011).

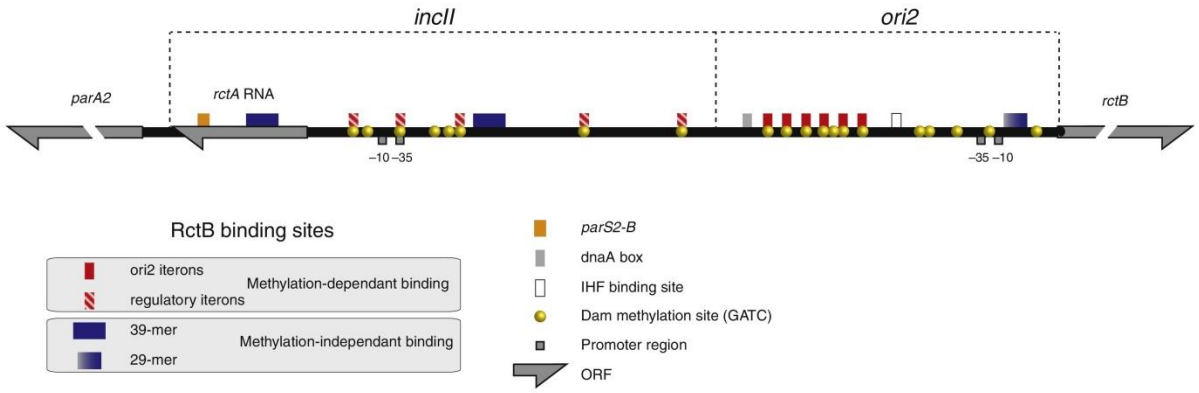

Figure 17. Map of the *V. cholerae* Chr2 origin region. It is divided in three units: *rctB* (gene enconding for the initiator of replication), *ori2* (the minimal function origin), and *incII* (a negative regulatory region). The RctB binding to the iterons requires full methylation of these sites (red boxes), while the binding to the 39-mers/29-mer is methylation independent (blue boxes). From Val et al., 2014b.

The head-to-head dimeric configuration of RctB in solution is structurally incompatible with binding to the head-to-tail array of 12-mer iterons in *ori2* (Fig. 18A)(Orlova et al., 2016). This implies that a structural reorganization must take place prior to formation of the initiator complex on origin DNA. In iteron-plasmids, DnaKJ chaperones remodel the dimerization domain of the initiator, which results in reduced dimerization and increased monomer binding and initiator function (Giraldo et al., 2003; Nakamura et al., 2007; Wickner et al., 1991). A similar mechanism is likely to operate on RctB to promote 12-mer binding and initiator function (Fig. 18B). Indeed, the RctB dimerization domain is folded similarly to the dimerization domains of plasmid initiators and chaperones increase RctB monomer binding (Jha et al., 2017). In addition, RctB dimerization defective mutants do not bypass the chaperone requirement for DNA binding. This indicates that RctB dimerization is an inhibitory mechanism and remodelling of monomers is an obligatory role of chaperones (Jha et al., 2017). In contrast, RctB binding to the 39-mers does not seem to require remodelling. Instead, a distinct mechanism dependent on DnaK appears to occur. The DnaK interaction site of RctB (K-I site) is inhibitory for 39-mer binding and this inhibitory activity is restrained by DnaK binding (Jha et al., 2017).

Figure 18. The head-to-head dimer structure of RctB is incompatible with *ori2* binding and implies structural reorganization by chaperones. (A) The RctB head-to-head dimeric configuration is not structurally compatible with binding to the 12-mer direct repeats in *ori2*. RctB domain 2 is coloured in different shades of orange, while domain 3 is coloured in different shades of purple. The bottom monomer is modelled to be bound to its site on the origin, according to the residues involved in the DNA binding (red sticks) and structural alignments. When one of the monomers is bound to DNA, the DNA binding residues of the second monomer do not face the same DNA molecule, and they cannot interact with the following binding side on the DNA. (B) DnaK remodels RctB promoting its monomerization and binding to the 12-mer sites in *ori2*. From Jha et al., 2017 and Orlova et al., 2016.

In addition to effect of mediated by the DnaKJ chaperones, RctB activity seems to be dependent on ATP. RctB was shown to bind and hydrolyze ATP but, in contrast to DnaA, its ATP-bound form is inactive (Duigou et al., 2008). However, the role of ATP on RctB activity is still subject of disussion (personal communication from Dhruba Chattoraj). Indeed, RctB lacks any apparent ATP-binding motifs and its plasmid counterparts, the Rep initiators, do not have ATPase activity.

Beyond the origin region of Chr2, RctB was shown to bind other locus on Chr2 and Chr1. On Chr2, 40 kb away from *ori2*, it binds to a 74 kb DNA region containing five iterons and one 39-mer, which has an inhibitory role on *ori2* replication (Baek and Chattoraj, 2014). In contrast, RctB binds to a Chr1 locus sharing no homology with either iterons or 39-mers (Baek and Chattoraj, 2014). The role of this locus is detailed below.

Figure 19. Control of *V. cholerae* Chr1 and Chr2 replication initiation. (A) Chromosome-like regulatory mechanisms. The left panel illustrates *ori1* and the mechanisms controlling its unwinding (Dam/SeqA, RIDA, *datA*, ATP and phospholipid synthesis, DARS). The involvement of Dam and SeqA in Chr1 replication initiation was experimentally demonstrated, while the controls exerted by RIDA, *datA*, ATP and phospholipid synthesis and DARS are represented based on the fact that *V. cholerae ori1* is able to functionally replace *oriC* in *E. coli*. *V. cholerae ori2* is depicted on the right panel. Dam methylation directly affects RctB binding to the iterons. (B) Plasmid-like regulatory mechanisms of Chr2 replication (right panel) compared to the mechanisms regulating P1 origin of replication unwinding (left panel). Black arrow-head and T-head lines: initiation activating mechanisms; red arrow-head and T-head lines: initiation inhibitory mechanisms; grey circles: DnaA; grey pentagons: DnaA boxes; black circles: methylated GATC sites; red rectangles with curved angles: SeqA; jelly-fish shapes: phospholipids; yellow circles: IHF; yellow squares: IHF binding site; pink circle: ParB2; pink square: *parS2*; orange circles: RctB (top and bottom right panels) or RepA (bottom left panel); small orange arrow box: *rctA*; large orange arrow box: *rctB* or *repA*; cyan arrow boxes: iterons; dark blue diamond boxes: 29-39-mers. From Espinosa et al., 2017.

3.4.3. Cell-cycle-dependent regulation and replication coordination of Chr1 and Chr2

Despite the similarities between Chr2 and the iteron-based plasmids, Chr2, like Chr1, replicate only once per cell cycle. Chr1 initates replication at the beginning of the replication period of the cell cycle (C period), while Chr2 initiation is delayed, starting approximately at two-thirds of the replication period (Rasmussen et al., 2007). As Chr2 size corresponds to one-third of Chr1, both chromosomes terminate their replication at the same time, which marks the end of the C period (Fig. 20). Even if the two chromosomes have independent replication initiation machineries, it appears that Chr1 and Chr2 communicate to coordinate their replication. This is reinforced by the presence of an RctB-binding site on Chr1 (Baek and Chattoraj, 2014).

Figure 20. *V. cholerae* Chr1 and Chr2 terminate replication synchronously. From Rasmussen et al., 2007.

3.4.3.1. Dam regulated processes

As mentioned above, Chr1 *ori1* displays several GATC sites that are substrates for methylation by Dam. This regulates the timing of subsequent initiation/re-initiation through sequestration of hemi-methylated sites by SeqA. Chr2 also has an overrepresentation of Dam methylation sites on its origin region. Similarly to what happens on *ori1*, the hemi-methylated state of *ori2* is extended, allowing *ori2* sequestration by SeqA to prevent immediate re-initiation (Fig. 19A) (Demarre and Chattoraj, 2010). While *ori1* methylation is only required for once-per-cell-cycle replication, in *ori2* it is essential for Chr2 initiation (Demarre and Chattoraj, 2010; Val et al., 2012). All iterons on the origin of Chr2 have GATC sites that need to be fully methylated to bind RctB (Demarre and Chattoraj, 2010). Thus, RctB binding to iterons functions in a cell-cycle dependent manner. In contrast, the 29- and 39-mer motifs do not need to be methylated to bind RctB (Venkova-Canova et al., 2012). This demonstrates that there is interplay between methylation-dependent and independent processes that results in an equilibrium of RctB, allowing the correct timing of Chr2 replication initiation. Chr2 seems to have integrated a very sophisticated plasmid-derived initiation regulation system and improved it to behave in the cell like a chromosome, replicating only once per cell cycle.

3.4.3.2. ParAB2-RctB crosstalk

In addition to its involvement in Chr2 segregation, ParB2 contributes to Chr2 replication regulation, establishing a link between replication and segregation. ParB2 binding to *parS2* within the *rctA* ORF nearby the 39-mer RctB-binding motif interferes with *rctA* replication inhibitory activity (Yamaichi et al., 2011). ParB2 spreads from *parS2* into the *rctA* 39-mer which likely interferes with RctB binding (Venkova-Canova et al., 2013). ParB2 was also reported to promote replication by direct binding to a more distant 39-mer contained in *incII*, without spreading from *parS2*. On this 39-mer, ParB2 competes with RctB to restrain its activity (Venkova-Canova et al., 2013). Alternatively, binding of RctB to *rctA* activates *parAB2* expression (Yamaichi et al., 2011). These binding fluctuations underlie

a regulatory network controlling both replication and partitioning of Chr1 and Chr2, demonstrating how chromosome replication and origin segregation are intimately intertwined.

3.4.3.3. Chr2 replication control in *trans* by a Chr1 site

As mentioned above, RctB binds a locus on Chr1 that shares no homology with the already known RctB binding sites, such as iterons or 39-mers. This Chr1 site was shown to act as a replication enhancer of *ori2* by increasing RctB affinity for iterons and decreasing its affinity for 39-mers. The presence of plasmids carrying this RctB-binding site in *E. coli* abolished the requirement for the DnaK/J chaperones, which are normally required to promote initiation at *ori2* in *E. coli* (Baek and Chattoraj, 2014). It was suggested this locus may function as a DNA chaperone, remodelling RctB and altering its binding to both iterons and 39-mers. However, this remodelling would act differently from the DnaKJ which increases binding to both iterons and 39-mers. In the same study the authors demonstrated that the RctB-binding site on Chr1 could be narrowed down to a 70-bp long region keeping its replication-enhancing activity of *ori2*-driven plasmids. However, a larger region of 150-bp was more efficient in enhancing replication at *ori2* (Baek and Chattoraj, 2014). This site is AT-rich, contains a putative DnaA box and several conserved GATC sites. The presence of such site on Chr1 reveals a novel check-point control mechanism in *V. cholerae*, where Chr1 communicates with Chr2 to coordinate their replication. However, the exact role of this locus on the replication coordination of Chr1 and Chr2 is still largely unknown and has been the subject of my thesis (see Results).

3.5. Replication coordination between multiple replicons in other species

V. cholerae is the model of bacteria with a split-genome where replication and segregation of the two chromosomes has been extensively explored. However, recent studies have shown that there are a few other examples where replication of the secondary replicons appears to be coordinated with the main chromosome. For instance, in other species of the *Vibrionaceae* family, the two chromosomes terminate replication in synchrony, while Chr2-initiation timing relative to Chr1 is variable. In these species, the sequence and function of the RctB-binding site on Chr1 found in *V. cholerae* seems to be conserved (Kemter et al., 2018).

Outside the *Vibrionaceae* family there are also other examples that have been reported. This is the case of the intracellular pathogen *B. abortus* whose genome is similarly distributed between two replicons of unequal sizes. This bacterium harbours a large chromosome (chrI) of 2,1 Mb and a small chromosome (chrII) of 1,2 Mb (Chain et al., 2005) that shares chromosomic and plasmidic features. chrII belongs to the alphaproteobacterial chromids carrying a *repABC* cassette. In this organism, both chromosomes are oriented along the cell length axis and replication of chrII is initiated after origin

duplication of chrI (Deghelt et al., 2014). In addition, the segregation of *terII* occurs well before cell septation, while *terI* segregation is observed in constricting cells. This suggests a spatio-temporal organization of the *B. abortus* multipartite genome and the existence of a mechanism coordinating these events in time (Deghelt et al., 2014).

Similarly, in *S. meliloti*, duplication of chromosomal and megaplasmid origins of replication are spatially and temporally separated (Frage et al., 2016). This bacterium possesses a tripartite genome composed of one chromosome and two megaplasmids, pSymA and pSymB, belonging to the RepABC family (Galibert et al., 2001). The replication initiation control of the megaplasmids does not seem to be dependent on the ubiquitous replication initiator DnaA, however they replicate only once per cell cycle. In addition, there is a strict temporal order of segregation of the origins of the 3 replicons, starting with the chromosome followed by pSymA and then by pSymB (Frage et al., 2016).

Another example where replication and segregation of the different replicons seems to occur in a well-coordinated manner is illustrated by the opportunistic pathogen *B. cenocepacia* J2315 (Du et al., 2016). This bacterium carries a main chromosome of 3,87 Mb (c1), two secondary chromosomes of 3,21 Mb (C2) and 0,87 Mb (c3) and a plasmid of 0,09 Mb. Similarly to above-mentioned main chromosomes, the replication origin of c1 is typically chromosomal, while those of c2 and c3 are plasmid-like. However, all initiate replication at mid-cell and segregate towards the cell quarter positions sequentially, c1-c2-p1/c3 (Fig. 21) (Du et al., 2016). c2 segregation is as well-phased with the cell cycle as c1, implying that its plasmid-like origin has become subject to regulation not typical of plasmids. In contrast, c3 segregates more randomly through the cycle (Du et al., 2016). Despite the positioning of each chromosome being specified solely by the respective partition proteins, the partition system of the largest chromosome appears to play a global role in the cell cycle. The absence of c1 ParA protein alters replication of all three chromosomes, suggesting that the partition system of the main chromosome is a major participant in the choreography of the cell cycle (Du et al., 2016).

Figure 21. Segregation and positioning of replication origin regions during *B. cenocepacia* cell cycle. The sequential partition of c1-c2-c3-p1 is illustrated. All origins are shown as gravitating to the centre of cell halves before division. From Du et al., 2016.

IV. Thesis project

During my thesis I focused my attention on the Chr1 RctB-binding locus, renamed *crtS* for Chr2 replication triggering site. In a recent publication, that was part of this thesis, we have demonstrated that *crtS* replication is crucial for Chr2 replication initiation. Indeed, moving *crtS* to other positions on Chr1 leads to a corresponding shift in Chr2 initiation, meaning that replication of *crtS* triggers Chr2 replication.

Despite having clarified the role of this locus in the replication coordination of Chr1 and Chr2, the molecular basis behind *crtS* function remains a subject of speculation. During my PhD project I have tried to elucidate the *crtS*-RctB mediated mechanism that triggers Chr2 replication. I have characterized the *crtS* role on *ori2* replication regulation and I have dissected its primary sequence to identify the genetic determinants required for Chr2 replication activation. The study of this system sheds light on the management of multiple chromosomes by bacteria, particularly in *V. cholerae*, and can help us to better understand the plasmid domestication mechanisms leading to the formation of *bona fide* chromosomes, whose replication is cell-cycle coordinated.

RESULTS

I. "A checkpoint control orchestrates the replication of the two chromosomes of *Vibrio cholerae*"

1.1. Summary of the publication

Replication of the two *V. cholerae* chromosomes is coordinated with the cell cycle, however their replication initiation is not synchronous. Chr2 initiates replication when two-thirds of Chr1 has already been replicated. Despite the delay in Chr2 initiation, both chromosomes terminate replication at the same time, which suggests that their replication is coordinated.

Here we show that Chr2 monitors the replication status of Chr1 to time its own replication. By constructing *V. cholerae* strains with altered chromosome sizes we observed that Chr2 systematically initiates replication when the same region on Chr1 is replicated and termination synchrony is not a prerequisite. This indicated that the coordination is not mediated at the level of replication termination but instead through a region on Chr1 localized within the first two-thirds of either or both replichores (acting as a "checkpoint" in replication of Chr2). Rearrangements on Chr1 affecting the symmetry of the replichores led us to conclude that this region is located on the Chr1 right replichore. Within this region, a locus had just been identified in a ChIP-chip experiment of RctB (Baek and Chattoraj, 2014). This locus shares no homology to the previously described RctB-binding sites (iterons and 39-mers) and surprisingly the binding of RctB *in vitro* could not be obtained (Baek and Chattoraj, 2014). At the time, the authors suggested that this novel site acts as a DNA chaperone to enhance *ori2* replication by increasing RctB affinity for iterons and decreasing RctB affinity for 39-mers. Nevertheless, Baek et al. also reported that the deletion of this locus only had a mild effect on the bacteria fitness and physiology (Baek and Chattoraj, 2014). The presence of such site on Chr1 suggests that the two chromosomes communicate with each other during replication. However, the role of this locus in the replication coordination of Chr1 and Chr2 was unclear. On this study, we investigated the mechanism coordinating the replication of both chromosomes.

We have shown that the distance between *ori1* and the Chr1 RctB-binding locus plays a role in the regulation of Chr2 replication, suggesting that the timing of its replication exerts a control on Chr2 replication initiation. To test the role of this locus in the coordination of the timing of replication between Chr1 and Chr2 we relocated this site to different positions on Chr1 at varying distances from ori1. Repositioning it closer to or farther from the *ori1* caused Chr2 initiation to be initiated earlier or

later, respectively, in the cell cycle. This revealed that replication of the Chr1 RctB binding locus triggers Chr2 replication. We renamed this locus *crtS* for Chr2 replication triggering site. Further analyses by chromosome conformation capture (3C) have unveiled trans contacts between the two chromosomes. *ori2* exhibits preferential contacts with the right replichore of Chr1. More precisely, the contact maps show that *crtS* and *ori2* display enhanced physical contacts, suggesting that the regulatory mechanisms may involve a mechanistic interaction between the two chromosomes. Unlike reported by Baek et al. (Baek and Chattoraj, 2014), we observed that *crtS* is very important in the control of Chr2 replication. In our hands, *crtS* deletion led to strong fitness defects and was associated with cell filamentation and DNA damage. In addition, *crtS* mutants displayed an imbalance in the copy number of Chr1 and Chr2, revealing improper regulation/activation of Chr2 replication. My contribution to this work has been to characterize these *crtS* mutants. We demonstrated that *ΔcrtS* mutants are highly unstable and rapidly acquire mutations that up-regulate *ori2* initiation to compensate the lack of *crtS* activation.

Overall, the results presented on this publication demonstrate that *crtS* is crucial for the activation of Chr2 replication. Indeed, the replication of *crtS* is responsible to trigger Chr2 replication initiation (Fig. 22). This reveals a novel check-point control mechanism in this bacterium, in which Chr1 communicates with Chr2 to coordinate their replication.

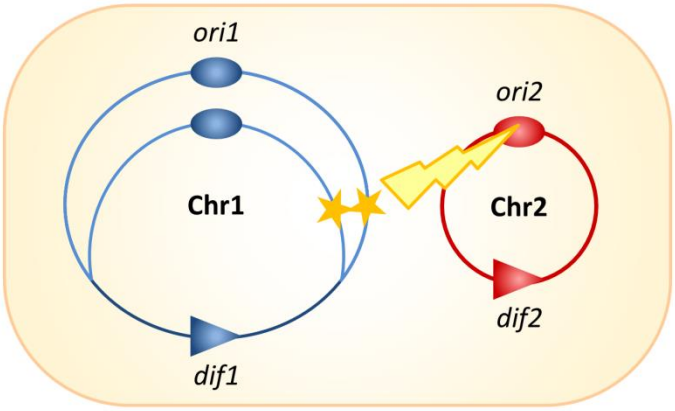

Figure 22. Model for the coordinated replication of the two chromosomes of *V. cholerae*. *crtS* replication triggers Chr2 replication initiation. This can be either caused by duplication of the *crtS* site, increasing its gene dosage, or DNA conformational changes due to the passage of the replication fork. *crtS* is indicated by the yellow stars and the thunder shape indicates the signal triggering Chr2 replication whose mechanism remains to be elucidated.

1.2. Science Advances publication

MICROBIOLOGY

A checkpoint control orchestrates the replication of the two chromosomes of *Vibrio cholerae*

10.1126/sciadv.1501914

Marie-Eve Val,[1,2] Martial Marbouty,[2,3] Francisco de Lemos Martins,[1,2] Sean P. Kennedy,[4] Harry Kemble,[1,2] Michael J. Bland,[1,2] Christophe Possoz,[5] Romain Koszul,[2,3] Ole Skovgaard,[6]* Didier Mazel[1,2]*

Bacteria with multiple chromosomes represent up to 10% of all bacterial species. Unlike eukaryotes, these bacteria use chromosome-specific initiators for their replication. In all cases investigated, the machineries for secondary chromosome replication initiation are of plasmid origin. One of the important differences between plasmids and chromosomes is that the latter replicate during a defined period of the cell cycle, ensuring a single round of replication per cell. *Vibrio cholerae* carries two circular chromosomes, Chr1 and Chr2, which are replicated in a well-orchestrated manner with the cell cycle and coordinated in such a way that replication termination occurs at the same time. However, the mechanism coordinating this synchrony remains speculative. We investigated this mechanism and revealed that initiation of Chr2 replication is triggered by the replication of a 150-bp locus positioned on Chr1, called *crtS*. This *crtS* replication–mediated Chr2 replication initiation mechanism explains how the two chromosomes communicate to coordinate their replication. Our study reveals a new checkpoint control mechanism in bacteria, and highlights possible functional interactions mediated by contacts between two chromosomes, an unprecedented observation in bacteria.

INTRODUCTION

Bacteria with secondary chromosomes are frequent and have arisen independently in several taxa (*1*). This is the case for pathogens such as *Vibrio* or *Burkholderia*, symbionts such as *Rhizobia*, and others. Domestication of large plasmids, after transfer of essential genes, appears to explain the origin of secondary chromosomes (*2*). Evidence supporting this hypothesis includes the fact that all secondary chromosomes carry plasmid-like replication systems (*2*). Replication of bacterial chromosomes is regulated at initiation from a single well-conserved origin of replication (*oriC*) under the control of DnaA, the universal initiator of chromosome replication in bacteria (*3*), whereas plasmids have various types of replication origins. Usually, their replication is controlled by an initiator binding to directly repeated sequences (iterons) or by an antisense RNA (*4*).

All reported members of the Vibrionaceae family (*Vibrio*, *Listonella*, *Aliivibrio*, and *Photobacterium*) have two chromosomes of uneven size (*5*). Most of our knowledge on the replication control of secondary chromosomes comes from studies of *Vibrio cholerae*, the causative agent of cholera in humans. *V. cholerae* has two circular chromosomes, a main chromosome (Chr1) of 3 Mbp and a secondary chromosome (Chr2) of 1 Mbp (*6*). Chr1 replication is initiated at an *oriC*-like origin, *ori1*, by DnaA. Chr2 has a plasmid-like origin, *ori2*, where replication is regulated by a *Vibrio*-specific factor, RctB (*7*). RctB is a large protein [658 amino acids (AA)] that binds to DNA as a monomer or as a dimer (*8*). RctB binds and hydrolyzes adenosine 5′-triphosphate (ATP), but unlike DnaA, the ATP-bound form of RctB is inactive (*9*). Various regulatory mechanisms, such as initiator autoregulation, initiator titration, and origin handcuffing, control the level and activity of RctB [for review, see the study by Val *et al.* (*10*)]. RctB binds to iterons (12-mer sites) in *ori2*, which promotes replication initiation. Additionally, RctB binds other regulatory sites. Within *ori2*, RctB binds to 39-mer regulatory sites, which strongly inhibit *ori2* initiation (*11*). Beyond the origin region of Chr2, chromatin immunoprecipitation with DNA microarray (ChIP-chip) analysis revealed that RctB binds to a locus on Chr2 (coordinates 956828-1030773) containing five iterons and one 39-mer, which inhibits the replication of an *ori2*-driven plasmid (mini-chr2) in *Escherichia coli* (*12*). RctB was also found to bind a locus on Chr1 sharing no homology with either iterons or 39-mers. This site was shown to act as a replication enhancer of *ori2* by increasing RctB affinity for iterons and decreasing RctB affinity for 39-mers (*12*). Serial deletions of a DNA fragment containing the Chr1 RctB ChIP-chip binding peak (fragments chrI-2 to chrI-10) showed that the replication-enhancing activity of a mini-chr2 in *E. coli* could be narrowed down to a 70-bp chrI-9 fragment (coordinates 818000-818069). However, the larger (150 bp) chrI-4 fragment (coordinates 817947-818099) was more efficient in enhancing mini-chr2 replication in *E. coli*. The presence of such a site on Chr1 suggested that the two chromosomes communicate with each other during replication. However, the role of this locus in the replication coordination of Chr1 and Chr2 remains a subject of speculation.

Chromosomes replicate during a defined period of the cell cycle, ensuring a single round of replication per cell. Plasmids generally have no such constraint, replicating randomly during the bacterial cell cycle (*13*). Despite its plasmid origin, Chr2 replication occurs only once per cell cycle (*14*). Initiation of Chr2 replication is also delayed so that the two chromosomes terminate replication at nearly the same time (*15*). The mechanism responsible for triggering Chr2 replication at a specific time of the cell cycle remains unknown. Here, we provide new insights into this regulatory process, and we explain how Chr2 monitors the replication status of Chr1 to time its own replication. We show that the Chr1 RctB binding site (*12*), renamed *crtS* for Chr2 replication triggering site, is crucial for the activation of Chr2 replication. We demonstrate that the replication of *crtS* triggers the replication of Chr2. We also show that the *crtS* locus and *ori2* localize to the same region of the cell during the entire cell cycle and display enhanced physical contacts, suggesting that

[1]Bacterial Genome Plasticity, Department of Genomes and Genetics, Institut Pasteur, Paris 75015, France. [2]CNRS UMR 3525, Paris 75015, France. [3]Spatial Regulation of Genomes, Department of Genomes and Genetics, Institut Pasteur, Paris 75015, France. [4]Biomics Pole, CITECH, Institut Pasteur, Paris 75015, France. [5]Department of Genome Biology, Institute of Integrative Biology of the Cell (I2BC), Paris-Sud University, CEA, CNRS, Gif-sur-Yvette 91190, France. [6]Department of Science, Systems and Models, Roskilde University, Roskilde DK-4000, Denmark.
*Corresponding author. E-mail: mazel@pasteur.fr (D.M.); olesk@ruc.dk (O.S.)

the regulatory mechanisms may involve a structural interplay. This study reveals a new checkpoint control mechanism in bacteria.

RESULTS

Marker frequency analysis reveals the relative replication pattern of the two chromosomes of *V. cholerae*

Replication of bacterial chromosomes occurs bidirectionally and terminates in the region opposite to the origin, in the vicinity of the dimer resolution site (*dif*), forming two replicated halves called replichores (Fig. 1A, top) (*16*). Assuming that Chr1 and Chr2 replicate at the same speed, replication of Chr2 must be delayed so that replication termination of the two chromosomes can be synchronous (*15*). Control of Chr2 replication initiation might be linked to cell mass or some "timer" on Chr1 that, when replicated, signals initiation on Chr2. We used marker frequency analysis (MFA) to precisely analyze the replication pattern of the two chromosomes of a culture of wild-type *V. cholerae* El Tor N16961 strain (WT) grown under steady-state conditions. MFA provides an unprecedented resolution of the replication timing and the replication fork speed, can pinpoint the origin and the terminus of chromosome replication, and can detect chromosomal rearrangements (*17*). Indeed, the MFA plot of WT compared to the reference genome sequence (AE003852) registered a discrepancy in Chr1 organization (fig. S1). Rectification of the Chr1 reference sequence corrected the deviation. MFA of WT confirmed that both chromosomes are replicated bidirectionally, with each chromosome having one origin (*ori1* and *ori2*) and one terminus (*ter1* and *ter2*) of replication. The linearity and the slopes of the graphs for the four replichores indicate that replication speed is constant for both chromosomes (Fig. 1A, bottom). This analysis confirmed that Chr1 and Chr2 terminate replication concomitantly and that Chr2 is initiated when about two-thirds of Chr1 is replicated, as hypothesized.

Chr2 replication initiation depends on the location of a timer region on Chr1

Chr2 replication initiation, after two-thirds of Chr1 has been replicated, could be linked to an unknown mechanism for coordination of replication termination of the two chromosomes, consistent with their relative sizes, 3 and 1 Mbp. To evaluate the impact of the chromosome sizes on their relative timing of replication, we generated two mutants with altered chromosome sizes using a dual site-specific recombination tool to transfer DNA from one chromosome to the other (*18*). In the CSV2 mutant, Chr1 and Chr2 sizes remained unbalanced at 2.5 and 1.5 Mb, respectively, whereas in the ESC2 strain, the two chromosomes are each at 2 Mb (Fig. 1, B and C). Increasing the size of Chr2 abolished synchronous termination in both ESC2 and CSV2 mutants, with the now larger Chr2 terminating replication after Chr1 (Fig. 1, B and C). MFA also revealed that Chr2 systematically initiates replication when a discrete position along one (or both) Chr1 replichore(s) is being replicated (Fig. 1, B and C). This finding suggested that a region located on Chr1 may trigger Chr2 replication initiation, and should be localized within the first two-thirds of either or both replichores and act as a "checkpoint" in replication of Chr2.

The relative timing of initiation of Chr1 and Chr2 can be followed by qPCR analysis of the *ori1*/*ori2* ratio. We reasoned that a change in this ratio in isogenic mutants, where Chr1 size was unaltered but replichores were rearranged, would yield a signal for the region of interest. This was performed by inversion between a fixed intergenic locus (downstream of ORF VC018, that is, near *ori1* on the left replichore) and other intergenic loci located at increasing distances from *ori1* along the right replichore (Fig. 1D). Such inversions either caused no fitness cost (JB392) or were similarly affected (JB590, JB659, JB771, and JB963) compared to WT (fig. S2). We monitored the impact of each inversion on the *ori1*/*ori2* ratio in exponentially growing cultures (Fig. 1E). In WT, the *ori1*/*ori2* ratio is around 2, matching the observations of fast-growing *V. cholerae* (*15*). In mutants JB392, JB590, and JB659, *ori1*/*ori2* ratios decreased, indicating that the region triggering Chr2 replication may be closer to *ori1*, causing earlier Chr2 replication initiation. In mutant JB771 and JB963, the *ori1*/*ori2* ratio remains ~2, indicating the wild type–like timing of replication and that the locus triggering Chr2 initiation must be at the same distance from *ori1* as in wild type. These results indicate that a locus located between VC659 and VC771 and its distance from *ori1* play a role in the regulation of Chr2 replication. This region contains the Chr1 RctB binding locus, located in a noncoding region upstream of VC765 (*12*). Strikingly, the $\log_2$(*ori1*/*ori2*) ratio increases linearly with the distance between *ori1* and the Chr1 RctB binding locus (Fig. 1F). This observation indicates that the timing of replication of the Chr1 RctB binding locus exerts a control on Chr2 replication initiation.

Replication of the Chr1 RctB binding locus (*crtS*) triggers Chr2 replication initiation

We tested the Chr1 RctB binding locus for its role in the coordination of the timing of replication between Chr1 and Chr2. Hereafter, we will refer to the Chr1 RctB binding locus as *crtS*. *crtS* was relocated to four intergenic loci on Chr1 at varying distances from *ori1* (Fig. 2A). *crtS*-positional mutants display wild type–like fitness and phenotype (fig. S3). Therefore, all the determinants for *crtS* proper function appeared contained within its sequence. MFA showed that in $crtS_{VC23}$ and $crtS_{VC392}$, where *crtS* is closer to *ori1*, Chr2 initiates earlier than in WT (Fig. 2B). In $crtS_{VC2238}$, where *crtS* is positioned at the same distance from *ori1* but on the other replicore, Chr2 initiates roughly at the same time as in WT (Fig. 2B). In $crtS_{VC963}$, with *crtS* farther from *ori1*, Chr2 initiates later than in WT (Fig. 2B). We calculated the *ori1*/*ori2* and *ori2*/*crtS* ratios from the MFA (Fig. 2C). The $\log_2$ of *ori1*/*ori2* ratio is linearly correlated with the *ori1*-*crtS* distance (R^2 = 0.9988), suggesting that the timing of replication of *crtS* controls the timing of Chr2 replication initiation. The *crtS*/*ori2* ratio remains constant (~0.8), indicating that there is a constant delay between *crtS* replication and Chr2 replication initiation.

To confirm these observations, we tracked pairwise combinations of fluorescently labeled chromosomal positions using epifluorescence microscopy (*19*). We compared the distribution of *ori1* with *ori2* foci, VC783 (near *crtS*) with *ori2* foci, and *ter1* with *ter2* foci in both WT and $crtS_{VC23}$ strains (Fig. 3 and figs. S4 and S5). Images of exponentially growing cells were acquired, and cell length, along with the position of each tagged loci, was followed. WT cells ranged in size from 2 μm (newborn cells) to 4.5 μm (dividing cells), with two *ori1* foci appearing in cells from 2.5 to 3 μm and two *ori2* foci from 3 to 3.5 μm (Fig. 3, A, C, and E, and fig. S6, left). This observation indicates that *ori1* is replicated and segregated before *ori2*, as previously observed (*19*). In $crtS_{VC23}$, cells with two *ori1* and two *ori2* foci appeared in the same cell size range from 2.5 to 3 μm (Fig. 3, B, D, and F, and fig. S6, right), consistent with the MFA results showing that *ori2* is replicated shortly after *ori1* (Fig. 2B). In WT, duplication of VC783 foci

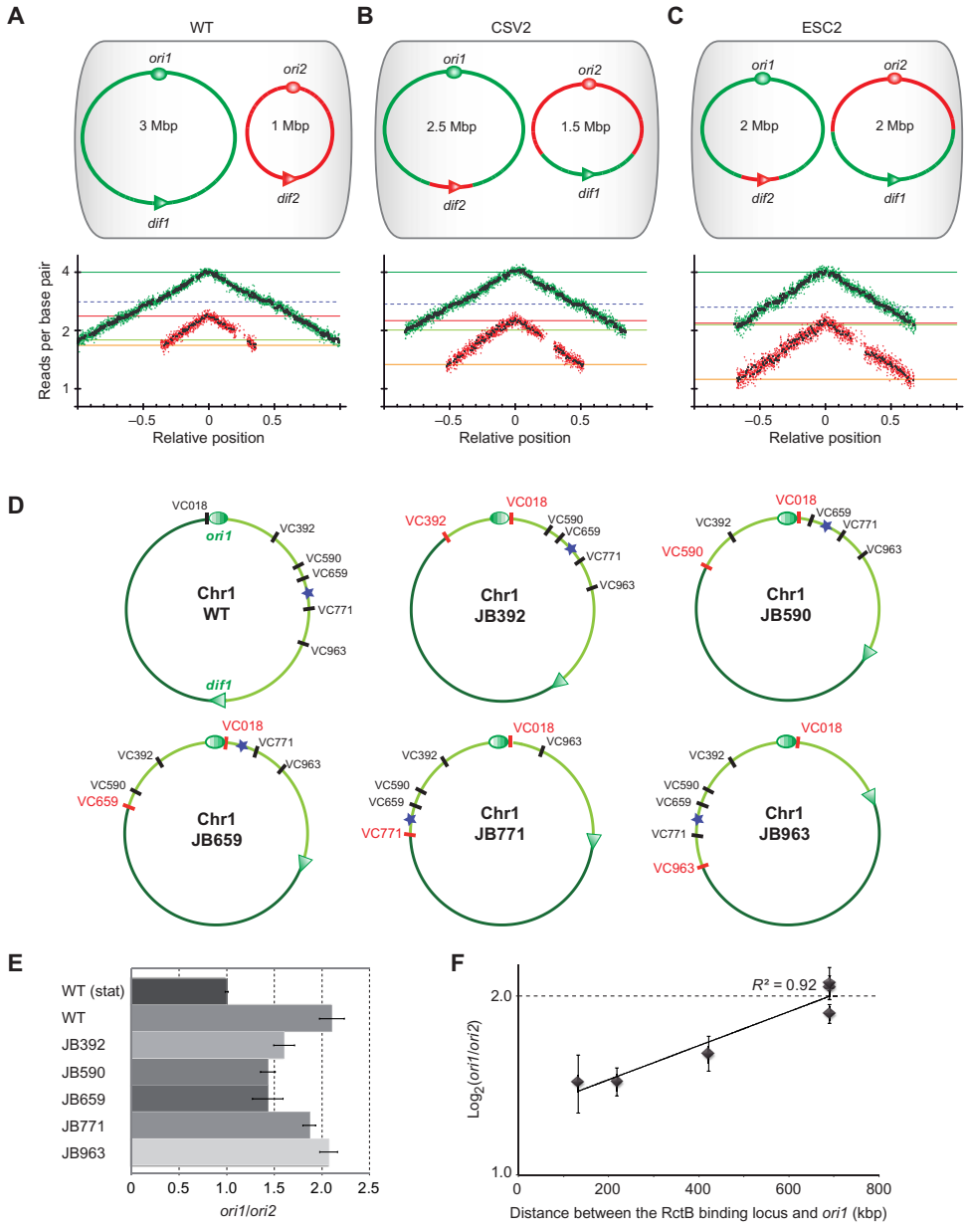

Fig. 1. Chr1 and Chr2 replication coordination is promoted by the presence of a timer on Chr1 and not by the requirement to terminate their replication synchronously. (**A**) Top: Genome structure of wild-type (WT) *V. cholerae*. Ovals indicate the origins of replication (*ori1* and *ori2*) and triangles show *dif* sites (*dif1* and *dif2*) on Chr1 (green) and Chr2 (red). Bottom: MFA of exponentially growing WT cultures using a corrected reference sequence of Chr1 (fig. S1). Log_2 of number of reads starting at each base (normalized against reads from a stationary phase WT control) is plotted against their relative position on Chr1 and Chr2. Positions of *ori1* and *ori2* are set to 0 for a better visualization of the bidirectional replication. Any window containing repeated sequences is omitted; thus, the large gap observed in the right arm of Chr2 consists of filtered repeated sequences within the superintegron (*28*). Green (Chr1) and red (Chr2) dots indicate the average of 1000-bp windows; black dots indicate the average of 10,000-bp windows. Dark green, light green, red, and orange lines indicate *ori1*, *ter1*, *ori2*, and *ter2* number of reads, respectively; dashed blue lines indicate the Chr1 RctB binding locus (*12*). The same color code is used for all MFA figures. (**B** and **C**) Genomic variants CSV2 (Chr1 = 2.5 Mbp and Chr2 = 1.5 Mbp) (B) and ESC2 (Chr1 = 2 Mbp, Chr2 = 2 Mbp) (C) are the same as in (A). The genetic exchanges made between Chr1 and Chr2 are shown in green and red. (**D**) Chr1 map of WT and genomic variants (JB392, JB590, JB659, JB771, and JB963) with large chromosomal inversions around a fixed locus (VC018) and other loci located at increasing distances from *ori1* (VC392, VC590, VC659, VC771, and VC963), respectively. For each genomic mutant, the loci flanking the DNA inversion are shown in red. The left (dark green) and right (light green) replichores are separated by *ori1* (oval) and *dif1* (triangle). The position of the Chr1 RctB binding locus is indicated by a blue star. (**E**) Histogram representing quantitative PCR–measured *ori1*/*ori2* ratios from relative gDNA quantification of exponentially fast-growing strains (gDNA from WT stationary culture was used for normalization). Bars display means (±SD) of at least three experiments. (**F**) Log_2(*ori1*/*ori2*) plotted as a function of the distance between *ori1* and the RctB binding locus displays a linear relationship (R^2 = 0.92). Dots show means (±SD) of three experiments.

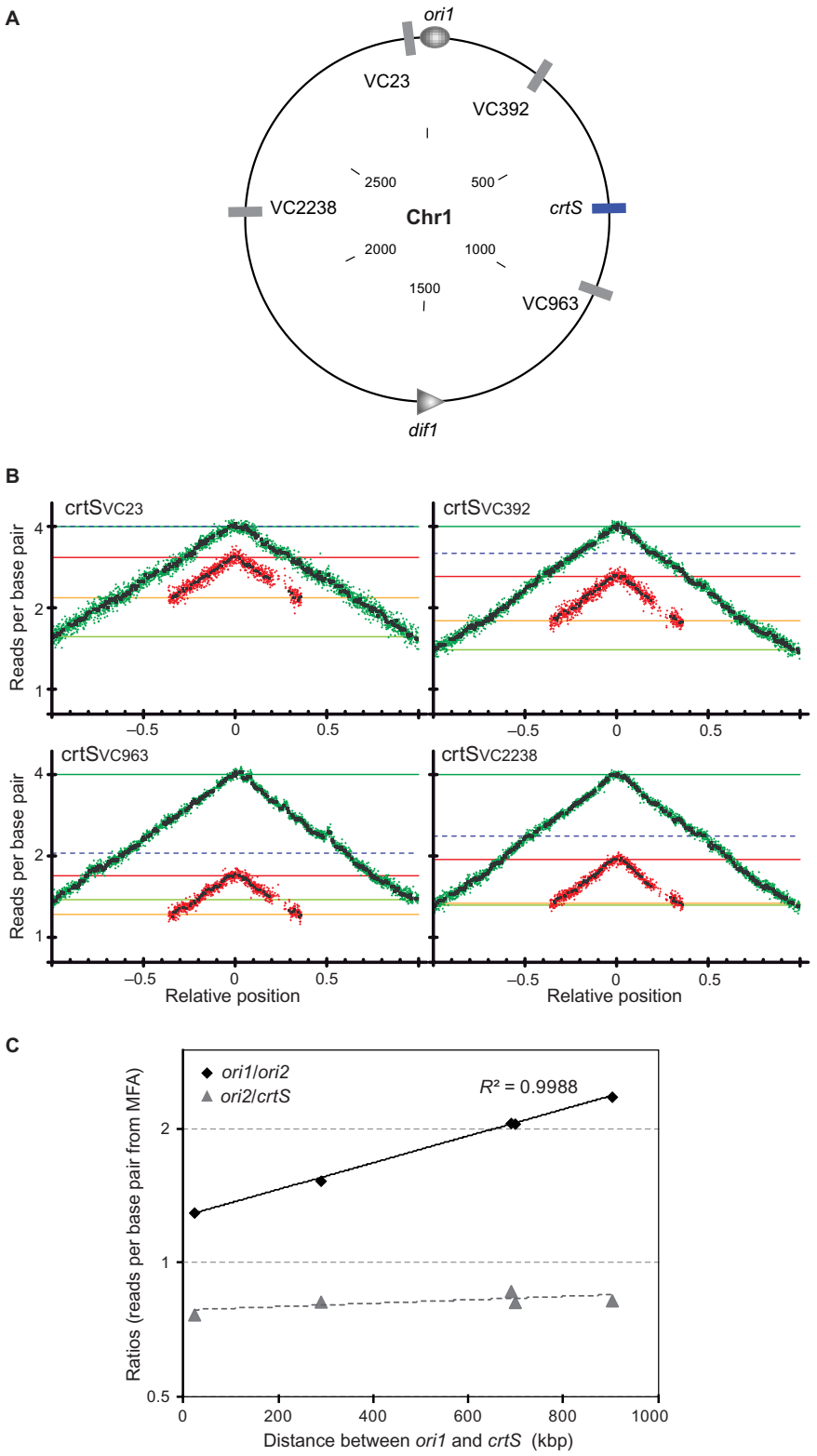

Fig. 2. Timing of replication of the Chr1 RctB binding locus (*crtS*) controls the timing of initiation of Chr2. (**A**) Circular map of WT Chr1 showing the native location of *crtS* (blue bar) and the various loci where *crtS* was relocated (gray bars) with respect to *ori1* (oval) and *dif1* (triangle). The inside scale designates DNA size in kilobase pair. (**B**) MFA of relocated *crtS* mutants ($crtS_{VC23}$, $crtS_{VC392}$, $crtS_{VC963}$, and $crtS_{VC2238}$). The dashed blue lines indicate the number of reads of the loci where *crtS* has been relocated. (**C**) Log_2(*ori1*/*ori2*) and log_2(*ori2*/*crtS*) plotted as a function of the distance between *crtS* and *ori1* in kilobase pair. The ratios were calculated as the ratios of the number of reads per base pair (from MFA) for each designated loci.

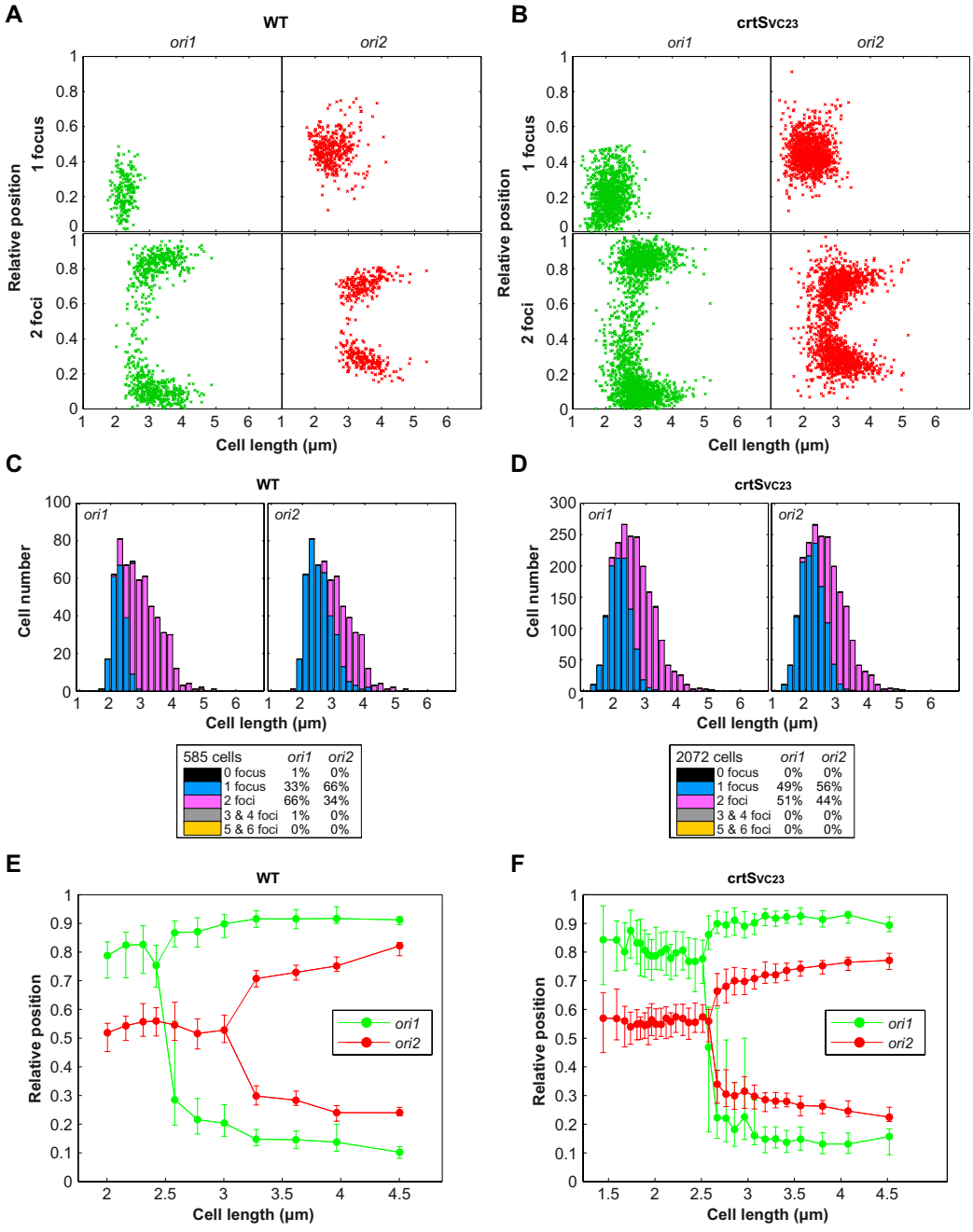

Fig. 3. Segregation of *ori2* (but not *ter2*) occurs earlier when *crtS* is transposed near *ori1*. (**A** and **B**) Plot showing the position of *ori1* (left panel) and *ori2* (right panel) foci inside WT (A) and mutant $crtS_{VC23}$ (B) cells. Foci are oriented longitudinally relative to the old pole of the cell as a function of cell length. The old pole of the cells was defined as the closest pole to an *ori1* focus. The *x* axis represents the cell length (in micrometers). The *y* axis represents the relative position of the focus in bacterial cells, 0 being the old pole and 1 the new pole. Snapshot images of 585 WT and 2072 $crtS_{VC23}$ mutant cells were analyzed. (**C** and **D**) Histograms displaying the amount of cells that exhibit zero, one, two, three, four, or five and six fluorescent foci according to cell size (in micrometers) in WT (C) and mutant $crtS_{VC23}$ (D) cells. (**E** and **F**) By correlating the longitudinal position of *ori1* and *ori2* foci as a function of cell length, the segregation choreographies of the *ori1* and *ori2* were reconstituted throughout the cell cycle of WT (E) and mutant $crtS_{VC23}$ (F) bacterial cells. Cells were classified according to their size and grouped by 30 to define each size interval. For most loci and cell length intervals, there were cells with either a single focus or two separated foci, the relative proportions of each type varying as a function of cell length. Only the position of the foci corresponding to the dominant cell type in each cell length interval was plotted. The median positions of the observed foci (filled circles), along with the 25th to 75th percentiles (error bars), were plotted for each cell size bin. The *x* axis represents the cell length (in micrometers). The *y* axis represents the relative position of the focus in bacterial cells (0, new pole and 1, old pole).

(near *crtS*) occurs shortly before *ori2* foci duplication (fig. S4, C and E), which is in accordance with MFA, showing a delay between *crtS* replication and *ori2* replication (Fig. 1A). In $crtS_{VC23}$, when *crtS* is no longer near VC783, *ori2* foci duplicate before VC783 foci (fig. S4, D and F), consistent with MFA results (Fig. 2B). Duplications of the *ter1* and *ter2* foci in WT were only visible at the end of the cell cycle in dividing cells (fig. S5, A, C, and E, and fig. S6, left). Surprisingly, most $crtS_{VC23}$ cells with two *ter1* and two *ter2* foci appeared in the same cell size range as WT (fig. S5, B, D, and F, and fig. S6, right). Because MFA studies showed that *ter2* is replicated long before *ter1* in $crtS_{VC23}$ mutant (Fig. 2B), this result indicates that duplicated *ter1* and *ter2* remain colocalized at mid-cell until cell division occurs.

To further probe the influence of *crtS* doubling on the initiation of Chr2 replication, we analyzed two mutant strains, $crtS_{WT/VC23}$ and $crtS_{WT/VC2238}$, carrying two chromosomal copies of *crtS*. The $crtS_{WT/VC23}$ mutant carries the native *crtS* site, as well as an extra copy near *ori1* (VC23), so that one *crtS* is replicated before the other. The two *crtS* copies of the $crtS_{WT/VC2238}$ mutant are located at equal distances from *ori1* on each replichore; thus, the two *crtS* are replicated at the same time. Both mutants displayed a significant loss of fitness compared to WT, with $crtS_{WT/VC2238}$ being the least affected (fig. S7). Both $crtS_{WT/VC23}$ and $crtS_{WT/VC2238}$ mutants displayed a wider cell size range, from 2 μm (newborn cells) to 5.5 μm (dividing cells) (Fig. 4 and fig. S8), indicating a flaw in the cell cycle control. Tracking of fluorescently labeled *ori1* and *ori2* loci reveals that most $crtS_{WT/VC23}$ newborn cells exhibit two *ori2* foci but only one *ori1* focus (Fig. 4, A and B) compared to WT (Fig. 3A). Most $crtS_{WT/VC23}$ dividing cells present two *ori1* foci and four *ori2* foci (Fig. 4, A to C), suggesting that whereas Chr1 goes from one to two copies, Chr2 goes from two to four copies per cell cycle. Similar results were obtained with the $crtS_{WT/VC2238}$ mutant (fig. S8). In both mutants, daughter cells usually receive one copy of *ori1* and two copies of *ori2*, whereas WT daughter cells normally receive a single copy of both *ori1* and *ori2* (Fig. 4, C to E). Sporadically, in both mutant strains, we observed that cell division occurs asymmetrically, leading to uneven chromosome partitioning. The proportion of cells with three *ori2* foci in $crtS_{WT/VC2238}$ (15%) is equivalent to the proportion of cells with one *ori2* foci (14%) (Fig. 4E), suggesting that these cells could have arisen from the asymmetric cell division of four *ori2* foci cells. However, $crtS_{WT/VC23}$ cells display a larger fraction of cells containing three *ori2* foci (30%) and a smaller fraction of cells with only one ori2 foci (7%) (Fig. 4D), meaning that uneven chromosome partitioning alone does not explain the existence of three ori2 foci cells. We speculate that in $crtS_{WT/VC23}$, one of the two *ori2* duplicates before the other. These differences between $crtS_{WT/VC23}$ and $crtS_{WT/VC2238}$ suggest that the difference in location and/or timing of replication of the extra *crtS* site alters the synchrony of initiation of multiple origins. These observations are puzzling because they do not fit with the *E. coli* paradigm where multiple origins initiate in synchrony (*20*). To explain that one *ori2* is duplicated before the other in $crtS_{WT/VC23}$, we hypothesized that the duplication of one *crtS* 3triggers the firing of only one *ori2*. This may require a direct contact between the replicated *crtS* and *ori2*.

Chromosome conformation capture reveals a preferential contact between Chr1 and Chr2

To test for the possibility that Chr1-located *crtS* site regulation of Chr2 replication initiation involves physical contacts between the two chromosomes, we applied chromosome conformation capture [3C; (*21*)] to exponentially growing cultures in rapid (LB) and slow [minimal medium (MM)] growth conditions (Fig. 5A and fig. S9). As expected, the two chromosomes in the resulting contact map turned out as two well-individualized entities, each exhibiting a strong diagonal signal reflecting frequent contacts between adjacent loci (Fig. 5A) (*22*). These chromosomes presented local domains of increased contact frequencies, separated by barriers (fig. S10), similar to the chromatin interaction domains (CIDs) previously described in *Bacillus subtilis* (*23*, *24*) and *Caulobacter crescentus* (*25*). The intrachromosomal contact maps of Chr1 and Chr2 differ with respect to the presence of a secondary perpendicular diagonal that reflects the bridging of left and right replichores by cohesin complexes in other bacteria (*23*–*25*). Whereas Chr1 did not present such a signal, Chr2 displayed a secondary diagonal revealing radically different folding of the two chromosomes (Fig. 5A). The conversion of contact maps into three-dimensional (3D) structures (fig. S9C and movies S1 and S2) (*26*) shows that whereas Chr1 adopts a largely open structure, Chr2 folds into a helicoidally shape with its two replichores tightly interlaced. It appears from this matrix that Chr2 folds into a structure similar to that of *B. subtilis* (*23*, *24*) or *C. crescentus* (*27*), whereas Chr1 adopts a structure closer to the one observed for *E. coli* chromosome (*22*). The superintegron, a large gene capture and excision system localized on Chr2 (*28*), defines a clear CID surrounded by two highly transcribed genes (fig. S10). This observation suggests a specific topological structure, which can reflect the generally low transcription in this DNA element.

Overall, the chromosomes of *V. cholerae* present known features of chromosome organization in bacteria, as well as new ones. Indeed, the contact maps unveiled trans contacts between the two chromosomes at an unprecedented resolution. The two replichores of Chr2 present enrichment in contact with the bottom third of Chr1 replichore, as indicated by the cross-shaped trans contacts (Fig. 5B). These contacts initiate at *dif* sites and extend along the length of the chromosome up to *ori2* for Chr2 and midway to Chr1. The spatial proximity of the terminus regions (*ter*), surrounding *dif1* and *dif2*, is a striking driver of organization, with strong contacts between the *ter* regions, visible in both growth conditions (fig. S9A). The circos representation of the strongest interactions of 100 kbp surrounding *dif2* (Fig. 5C) illustrates the enrichment of contacts between the *ter* regions. This is also visible in the 3D contact maps (fig. S9C and movies S1 and S2). These results are consistent with the imaging of the *ter1* and *ter2* showing a colocalization of the regions to the mid-cell at the end of the cell cycle (fig. S5E). The circos representation of the contacts made by a 50-kbp window centered on *ori2* reveals preferential contacts with the right replichore of Chr1 (Fig. 5D). These contacts initiate at *crtS* and become stronger immediately after. More precisely, the contacts involve a region on the Chr2 left replichore adjacent to *ori2*, pointing toward a mechanical interplay that would drive this interaction.

crtS is crucial for Chr2 replication initiation at *ori2*

To assess the importance of *crtS* on Chr2 replication, we deleted a 150-bp sequence (coordinates 817950-818100), which closely corresponds to the chrI-4 sequence (coordinates 817947-818099) deleted by Baek and Chattoraj (*12*). Baek and Chattoraj (*12*) reported that chrI-4–deleted mutants showed minimal phenotypic changes and no growth defects, indicating that its action was probably modest. In contrast, our Δ*crtS* mutants exhibited strong fitness defects and suffered marked physiological changes, with a large proportion of filamentous cells (Fig. 6A, top, and fig. S11). To corroborate the marked phenotype of Δ*crtS* mutants with a problem in *ori2* replication initiation, we deleted

crtS in a *V. cholerae* strain where *ori2* was replaced by a second *ori1* locus and is thus no longer dependent on RctB (ICO1) (*18*). ICO1Δ*crtS* mutants displayed no marked filamentous phenotypes and no additional growth defects compared to ICO1 (Fig. 6A, bottom, and fig. S11), confirming that the Δ*crtS* phenotype is linked to a deficiency in replication initiation of Chr2 at *ori2*. By performing MFA on mutant Δ*crtS* #7 (with two separate chromosomes), we could detect the location of *ori2* by the overrepresentation of sequences (sharp peak), indicating that replication initiation still occurs at *ori2*. However, the MFA also highlighted an imbalance in the copy number of Chr1

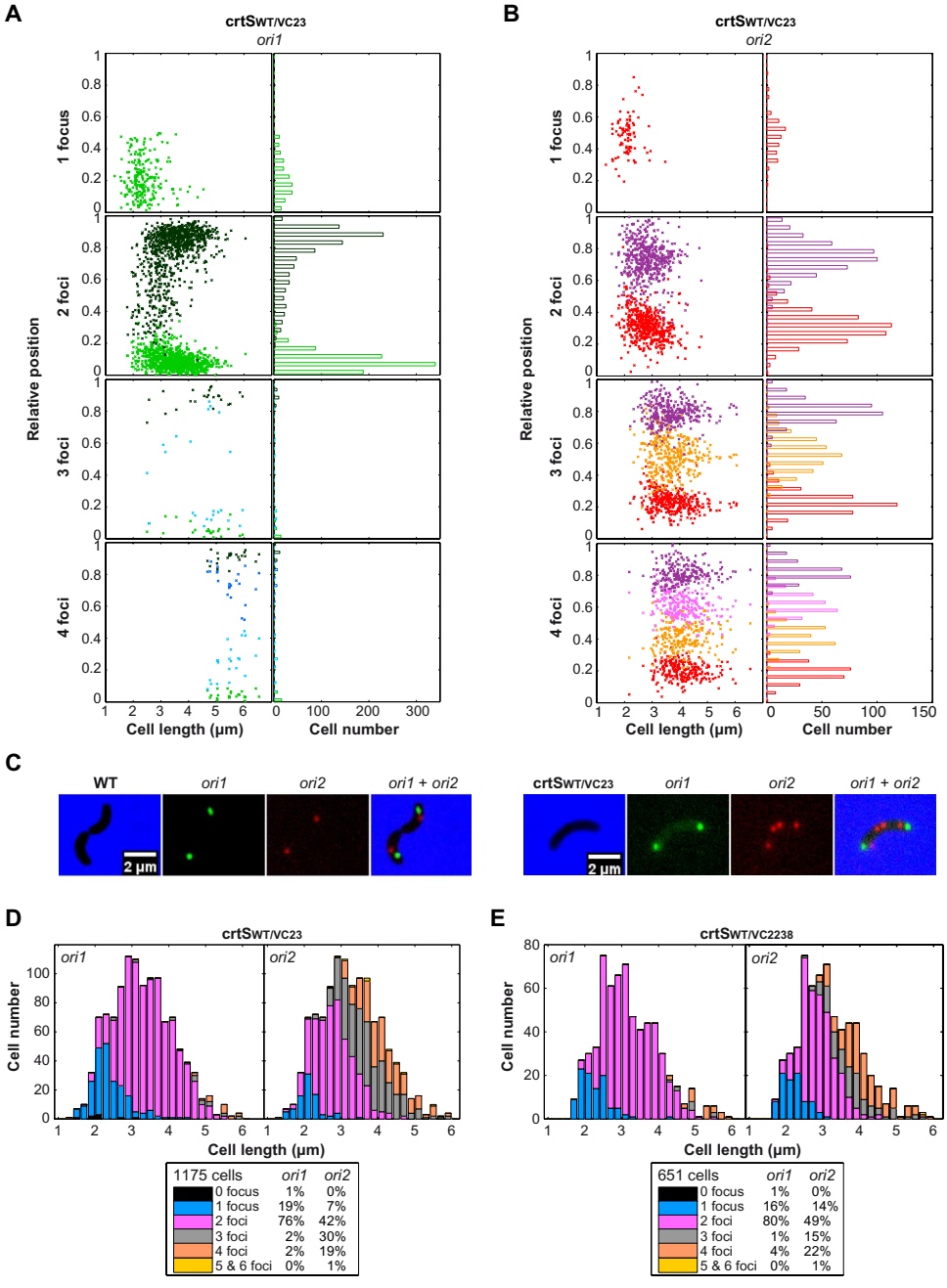

Fig. 4. Two chromosomal copies of *crtS* doubles Chr2 copy number. (**A** and **B**) Position of *ori1* (A) and *ori2* (B) foci inside $crtS_{WT/VC23}$ cells. Foci are oriented longitudinally relative to the old pole of the cell as a function of cell length. The old pole of the cell was defined as the closest pole to an *ori1* focus. On the left panel, the *x* axis represents the cell length (in micrometers). On the right panel, the *x* axis indicates cell number. The *y* axis represents the relative position of the focus in bacterial cells, 0 being the old pole and 1 the new pole. (**C**) Representative pictures of dividing cells (WT and $crtS_{WT/VC23}$) observed by fluorescence microscopy. Cells were fluorescently labeled near *ori1* and *ori2*. Merged pictures of *ori1* (green) and *ori2* (red) and phase-contrast (blue) micrographs show 2× more red spots than green spots in mutant $crtS_{WT/VC23}$. (**D** and **E**) Amount of $crtS_{WT/VC23}$ (D) and $crtS_{WT/VC2238}$ (E) cells exhibiting zero, one, two, three, four, or five and six *ori1* foci (left panel) and *ori2* foci (right panel) according to cell size (in micrometers).

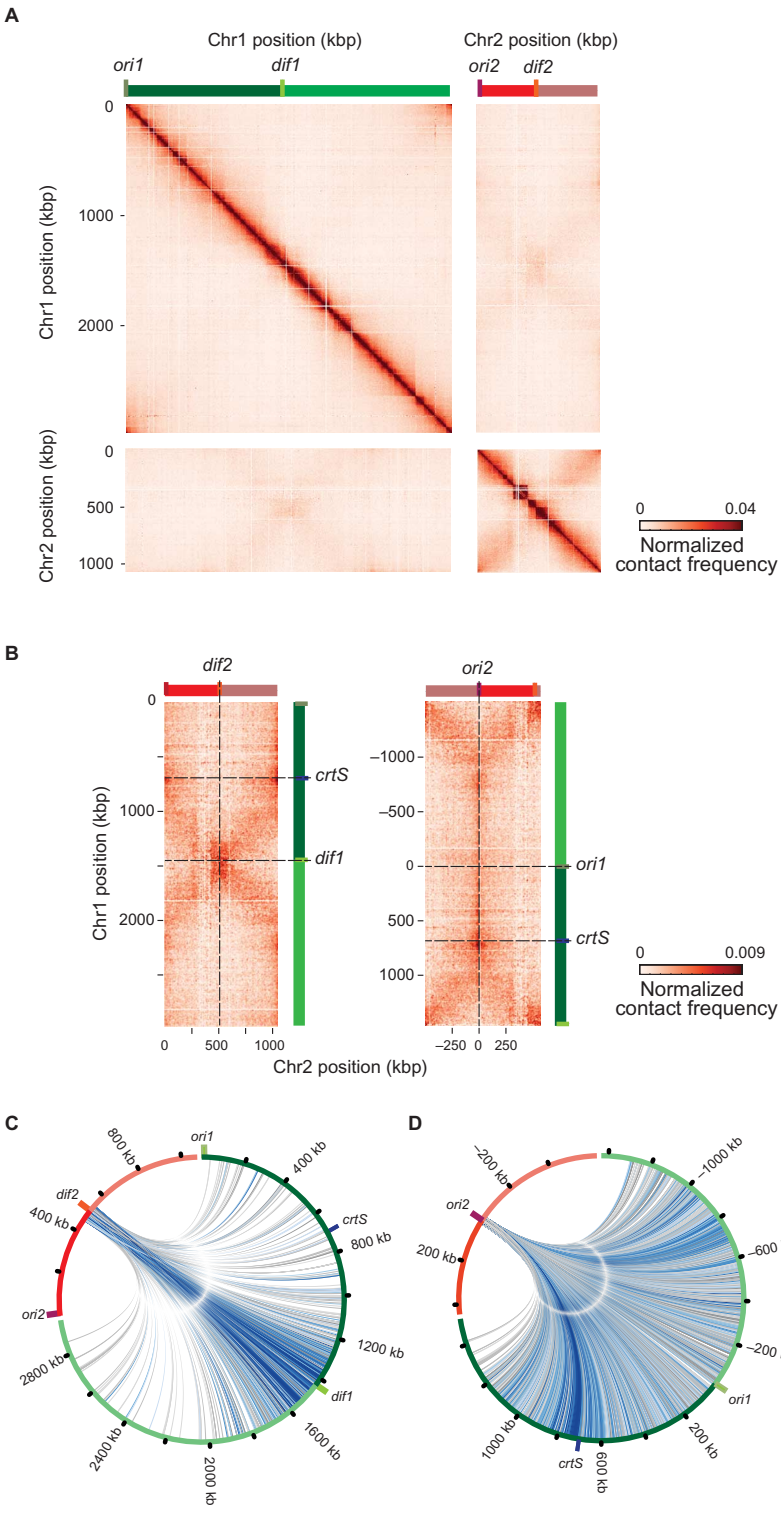

Fig. 5. Intra- and interchromosomal interactions in *V. cholerae*. (**A**) Normalized and filtrated genomic contact map obtained from an asynchronous population of WT cells growing exponentially in LB. *x* and *y* axes represent genomic coordinates of each chromosome centered on *dif* sites (light green bar, *dif1*; orange bar, *dif2*). Origins of replication are shown as a dark green bar (*ori1*) and a dark red bar (*ori2*). Chr1 and Chr2 are represented by dark green (right arm) or light green (left arm) and dark red (right arm) or light red (left arm). The color scale reflects the frequency of contacts between two regions of the genome (arbitrary units), from white (rare contacts) to dark red (frequent contacts), and is conserved across all panels of all figures. (**B**) Interchromosomal contact map centered on *dif* (left panel) or *ori* sites (right panel). The *crtS* site is indicated as a blue bar. (**C** and **D**) Circos representation of interactions of 100 kbp (20 bin) around *dif2* with Chr1 (C) and circos representation of interactions of 50 kbp (10 bin) around *ori2* with Chr1 (D).

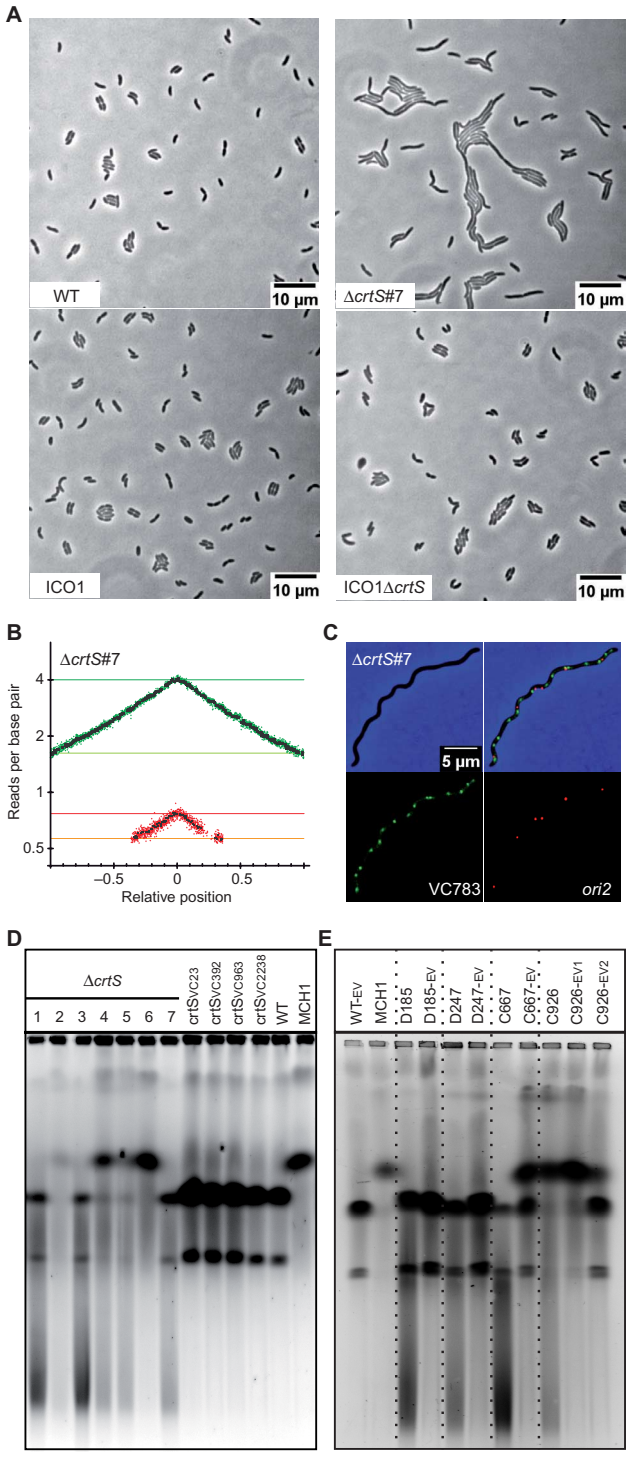

Fig. 6. *crtS* is crucial for Chr2 replication initiation at *ori2*. (**A**) Phenotype of *crtS*-deleted mutants in WT and ICO1. Representative pictures of phase-contrast microscopy of live cells growing on LB agar pads: WT, Δ*crtS* #7 (with two separate chromosomes), ICO1, and ICO1Δ*crtS*. (**B**) MFA of WTΔ*crtS* #7. (**C**) Representative picture of a filamentous Δ*crtS* cell observed with fluorescence microscopy. Loci near *crtS* (VC783) and *ori2* were fluorescently labeled. Merged pictures of VC783 (green) and *ori2* (red) and phase-contrast (blue) micrographs show a higher number of green spots than red spots. (**D**) Ethidium bromide–stained pulsed-field gel electrophoresis (PFGE) of native gDNA. From left to right: Independent clones of *crtS*-deleted mutants (WTΔ*crtS* #1 to #7), mutants with relocated *crtS* ($crtS_{VC23}$, $crtS_{VC392}$, $crtS_{VC963}$, and $crtS_{VC2238}$), and WT (two chromosomes) and MCH1 (one synthetic fused chromosome), which are used as size reference (*18*). (**E**) Same as (D). From left to right: $WT\text{-}_{EV}$ (control), MCH1 (one synthetic fused chromosome), and independent clones of Δ*crtS* mutants before (D185, D247, C667, and C926) and after a 200-generation evolution (-_{EV}). For C926, samples were harvested after 100 (-_{EV1}) and 200 generations (-_{EV2}) to track the tendency of the fused chromosome to revert to two separate chromosomes.

and Chr2 with an *ori1*/*ori2* ratio of 5.2 and a *ter1*/*ter2* ratio of 2.9 (Fig. 6B). This imbalance was also observed by imaging fluorescently labeled Chr1 and Chr2 loci in a Δ*crtS* mutant strain. Figure 6C shows a typical Δ*crtS* filamentous cell with more VC783 foci than *ori2* foci, whereas in WT, the two loci duplicate around the same time (fig. S4E), and most cells display the same number of VC783 and *ori2* foci (fig. S4C). Time-lapse fluorescence microscopy of Δ*crtS* cells shows that filaments grow and accumulate many Chr1 foci (movie S3). These filaments divide irregularly and occasionally give rise to a Chr2-less cell, which does not grow (movie S4).

PFGE revealed a high instability in the genome structure of Δ*crtS* mutants. In many instances, the two chromosomes had spontaneously fused (Fig. 6D; Δ*crtS* #2 and #4 to #6), and in all Δ*crtS* mutants, a smear was clearly visible in the PFGE (Fig. 6D; Δ*crtS*), indicating either genomic DNA (gDNA) degradation or a high level of genomic instability. *crtS*-positional mutants, however, did not display gDNA degradation/instability, thus evidencing the proper activity of *crtS* when transposed to ectopic chromosomal positions (Fig. 6D; $crtS_{VC23}$, $crtS_{VC392}$, $crtS_{VC963}$, and $crtS_{VC2238}$). The high instability observed in the genome of Δ*crtS* mutants suggested a positive selection toward chromosome fusion. To test for this constraint, we grew four independent cultures of Δ*crtS* mutants for 200 generations to investigate spontaneous fusion and other potential suppressors. PFGE analysis was performed on samples collected at the beginning and at the end of the experiment. At generation 0, three mutants (D185, D247, and C667) carried two chromosomes, whereas the fourth (C926) had already undergone a fusion. After 200 generations, both C926 and C667 displayed a mixed population of cells with fused and separate chromosomes, whereas D185 and D247 showed no sign of chromosome fusion (Fig. 6E). Evolved mutants significantly improved their fitness over 200 generations (fig. S12). Moreover, the DNA smear trademark of a Δ*crtS* deletion was no longer detectable in any of the evolved mutants ($D185\text{-}_{EV}$, $D247\text{-}_{EV}$, $C667\text{-}_{EV}$, and $C926\text{-}_{EV2}$) (Fig. 6E). Microscopy and flow cytometry showed that $D185\text{-}_{EV}$ recovered a wild-type morphology with less than 1% of aberrantly sized cells (fig. S13). However, $D247\text{-}_{EV}$, $C667\text{-}_{EV}$, and $C926\text{-}_{EV2}$ populations still displayed some filamentation. MFA of D247, before experimental evolution, is very similar to the MFA of Δ*crtS* #7 and shows that no genome rearrangement had yet occurred (fig. S14). However, MFA of D185 shows that gene amplification (triplication) had occurred before experimental evolution and reverted in the evolved mutant $D185\text{-}_{EV}$ (fig. S14). Stress-induced gene amplification has been observed in *E. coli* and may confer a selective advantage to cells under stress (*29*). After 200 generations, MFA of $D185\text{-}_{EV}$ and of $D247\text{-}_{EV}$ reveals an up-regulation of *ori2* initiation, presumably compensating for the lack of *crtS* activation, as shown by the increase in the Chr2/Chr1 copy number ratio compared to their parental strains (fig. S14). Such a remarkable rescue of phenotype of all Δ*crtS* mutants over 200 generations suggested that compensatory mutations were required to restore, even partially, the growth defects. $D185\text{-}_{EV}$ whole-genome sequencing revealed a single mutation, leading to a F230S substitution in RctB, not present in D185. $D247\text{-}_{EV}$ genome sequence also revealed a single mutation (C to A transversion), 25 nucleotides upstream of the *rctB* start codon within the 29-mer RctB binding site, which is important for autorepression of RctB expression and *ori2* initiation negative regulation via handcuffing with iterons (*30*). Further analysis of the *ori2* regions of $C667\text{-}_{EV}$ and $C926\text{-}_{EV2}$ revealed two new single mutations in RctB, which were absent from their parental strain (table S1). In all four mutants, Δ*crtS* phenotype was partially rescued by *rctB*-related mutations, further supporting the direct connection between *crtS* and RctB.

DISCUSSION

Approximately 10% of bacterial species have genomes split over multiple chromosomes. The machineries controlling replication initiation of secondary chromosomes are always of plasmid origin (*2*). An important difference between plasmids and chromosomes is that the latter replicate once, and only once, per cell cycle. In *V. cholerae*, the two chromosomes satisfy this rule; furthermore, they are known to have a synchronous termination of replication. However, it remains unclear how this is coordinated. Here, we show that the timing of Chr2 replication initiation directly depends on the position of a short intergenic sequence (*crtS*) on Chr1. Our results provide strong evidence that the replication of *crtS* triggers initiation of Chr2 replication. Additionally, we reveal preferential contacts between Chr1 and Chr2, suggesting the existence of mechanistic functional interactions between these two chromosomes. This study unravels a novel checkpoint control mechanism allowing the replication coordination of multiple chromosomes in bacteria.

crtS is crucial for Chr2 replication

Here, deletion of *crtS* severely impairs growth and is associated with filamentation and DNA damage (Fig. 6A, top, and fig. S11). The large cell size heterogeneity in Δ*crtS* mutants prevented statistically robust analysis based on fluorescence microscopy data. Nevertheless, filaments containing fewer Chr2 than Chr1 were consistent with MFA analysis showing Chr2 underrepresentation in Δ*crtS* mutants (Fig. 6, B and C). In Δ*crtS* filaments, we observed more VC783 foci than *ori2* foci, suggesting that failure of proper regulation/activation of Chr2 replication is responsible for the observed filamentation. It was reported that deletion of the chrI-4 sequence (ΔchrI-4) led only to mild phenotypic changes (*12*). ΔchrI-4 mutants were also characterized by a delay in *ori2* foci duplication (*12*). Why Δ*crtS* differs from ΔchrI-4 phenotype previously characterized could be explained by some differences in the way these sequences were deleted (see the Supplementary Materials). We further show that *crtS* is directly involved in the regulation of replication initiation at *ori2* through an RctB-associated mechanism because its deletion does not affect the physiology of the ICO1 mutant, in which Chr2 replication is no longer dependent on RctB at *ori2* (Fig. 6A, bottom). Strains with *crtS* relocated to different positions along Chr1 did not show any of the Δ*crtS* phenotypes, indicating that the 150-bp *crtS* DNA sequence is both necessary and sufficient to trigger Chr2 replication initiation, independently of its genetic context (Fig. 6D and fig. S3).

Replication of *crtS* orchestrates the replication of Chr1 and Chr2

The replication pattern of WT and mutant strains was investigated by MFA. WT MFA results show that the copy number of *ori1* is higher than that of *ori2*, whereas the copy numbers of *ter1* and *ter2* are similar (Fig. 1A), in agreement with former hypotheses and results, suggesting a synchronized termination (*15*). Displacing the *crtS* locus to different positions on Chr1 modified Chr1 and Chr2 replication synchronization (Fig. 2, A and B). The *ori1*/*ori2* ratio is perfectly correlated with the distance between *ori1* and *crtS* (Fig. 2C), demonstrating that Chr2 replication initiation timing is dependent on this parameter, with *crtS* replication triggering Chr2 replication. According to MFA, there is a

constant delay between *crtS* replication and the firing at *ori2* (Fig. 2C), which roughly corresponds to the replication of 200 kbp, suggesting that the transfer of information to *ori2* is not immediate. This delay may correspond to the time needed to activate RctB and the *ori2* initiation system. Therefore, both the position of *crtS* and this delay account for the Chr1 and Chr2 termination synchrony. The *crtS* position may have been selected throughout evolution by the constraint imposed by this activation delay.

Transient genome remodeling suppresses *crtS* deletion

Spontaneous chromosome fusions are common suppressor events of *crtS* deletion, but these marked rearrangements are transient and can revert back to a two-chromosomal genomic configuration over time (Fig. 6, D and E). We previously showed that recombination-induced chromosome fusions occur spontaneously within wild-type populations of *V. cholerae* (*31*). These rearrangements are quickly reversed or outcompeted, probably as a result of slower growth linked to an increase in replication duration due to the larger chromosome size and/or metabolic cost due to gene dosage imbalance. Fused chromosomes can be stabilized upon depletion of Dam methylase, which is essential for Chr2 replication initiation (*31*). Here, we hypothesize that chromosome fusions are a transient and conveniently accessible suppressor step when confronted with *crtS* deletion, ensuring replication of Chr2 through piggybacking of the Chr1 replication machinery. The higher cost of this genome state would subsequently favor the acquisition and maintenance of compensatory mutations, permitting the restoration of the wild type–like two-chromosome structure. This was observed in mutant C926-$_{EV2}$, which acquired a compensatory mutation in RctB (R195C) and resolved the chromosome fusion (Fig. 6E and table S1).

RctB-associated mutations compensate Δ*crtS* by altering Chr2 initiation regulation

Our 200-generation evolution experiment results showed that the phenotype of Δ*crtS* mutants was largely rescued by the selection of spontaneous mutations in the origin region of Chr2. Although the phenotypes of the evolved Δ*crtS* mutants vary, they all involve an increase in fitness, a decrease in cell filamentation, and an absence of gDNA degradation compared to their parental strain (figs. S12 and S13). MFA of the evolved *crtS* mutants showed a higher Chr2/Chr1 copy number ratio, suggesting an up-regulation of *ori2* initiation (fig. S14). This rapid acquisition of suppressor mutations can explain why our observations on Δ*crtS* mutants differ from those of Baek and Chattoraj (*12*). Considering the rapid genome remodeling and acquisition of compensatory mutations in *ori2* of Δ*crtS* mutants, we speculate that the ΔchrI-4 mutant previously characterized (*12*) has acquired compensatory mutations to overcome the marked effect of *crtS* deletion. All Δ*crtS* compensatory mutations were directly related to RctB (table S1), including three in the coding sequence (R195C, F230S, and L357I). RctB is a large, relatively poorly characterized protein that presents a 70-AA C-terminal region (451 to 521) involved in both iterons and 39-mer binding, as well as in dimerization (*8*). Previous *rctB* mutants were selected in the *E. coli* heterologous host for causing replication overinitiation of mini-Chr2 (*9*, *32*–*34*). These "copy-up" mutants of RctB show reduced dimer binding to iterons (*32*), reduced dimerization (*33*), or reduced 39-mer binding (*32*) or fail to bind ATP (*9*), all consistently preventing RctB to repress replication. Most of these mutations were found outside the 70-AA C-terminal region (*34*), implying that important functions for *ori2* replication control remains to be identified in RctB. One of our Δ*crtS* suppressor mutants (R195C) was already documented as a copy-up mutant (*34*). An additional mutation was found in the promoter region of RctB within the 29-mer RctB binding site, possibly impairing binding. Up-regulation of Chr2 replication initiation could result from the suppression of RctB autorepression leading to an increase in RctB expression, or from the abolition of the 29-mer negative regulatory function by handcuffing with iterons (*30*). The mutations obtained in our study were selected directly in *V. cholerae* on Chr2, therefore taking into account the native physiological levels of all partners interacting to regulate Chr2 replication initiation. The experimental evolution screening of *crtS* mutants provides a promising approach to unravel new regulatory factors involved in *V. cholerae* Chr2 replication.

Chr1 and Chr2 termini cohesion before cell division

MFA shows that *V. cholerae* Chr1 and Chr2 finish replication at *ter1* (around *dif1*) and *ter2* (around *dif2*), respectively, in a nearly synchronous manner (Fig. 1A). In WT, both *ter1* and *ter2* are recruited early to mid-cell and remain together until the end of the cell cycle (fig. S5E), and 3C analysis shows strong interactions between the two *ter* regions (Fig. 5C). When Chr2 replication completes before Chr1 in crtS$_{VC23}$ mutant (Fig. 2B), *ter2* foci relocate earlier to mid-cell but remain at mid-cell until cell division, and segregate roughly at the same time as *ter1* foci, like in WT (fig. S5, E and F, and fig. S6). These results suggest that *ter1* and *ter2* localization at mid-cell, where septum formation occurs at the end of the cell cycle, is important to coordinate their proper segregation before cell division.

In bacteria, chromosome replication, segregation, and cell division are precisely orchestrated mechanisms. In *E. coli*, the Ter domain relocates to mid-cell as replication completes and becomes accessible to the divisome machinery for the final steps of cell division, including chromosome compaction, dimer resolution, and decatenation (*35*–*38*). MatP, a DNA binding protein, bridges distant *matS* sites within the Ter domain to organize it into a compact structure (*39*, *40*) that interacts with the divisome to coordinate segregation and cell division (*38*). Chromosome dimer resolution at *dif* is mediated by the XerCD site-specific recombinases and the DNA translocase FtsK, which is anchored at the septum (*36*). In *V. cholerae*, MatP is known to play a role in Ter confinement of the two chromosomes at mid-cell after replication (*41*) and both Chr1 and Chr2 require the septal protein FtsK to resolve their dimers (*42*). Therefore, *ter1* and *ter2* cohesion at mid-cell may be important for their proper segregation, which may be coordinated by MatP or another mechanism that remains to be found.

Proposed mechanisms that mediate the signal between *crtS* replication and *ori2* initiation

Our study shows that Chr2 initiation requires *crtS* replication (Fig. 2C), meaning that either DNA conformational changes caused by the passage of the replication fork across *crtS*, or the doubling in copy number of *crtS* after duplication triggers Chr2 replication. The binding activity of RctB to chrI-4 (*crtS*) was observed by ChIP-chip (*12*). It was reported that RctB binding could only be observed in vitro by DNase I footprinting when chrI-4 was carried by a supercoiled plasmid (*12*). Mutations of the protected bases abolished the enhancer activity of chrI-4, suggesting a direct interaction between chrI-4 and RctB (*12*). Baek and Chattoraj (*12*) suggested that chrI-4 could act as a DNA chaperone to remodel RctB to an active form with altered DNA binding activities. Indeed, by using a mini-Chr2 in *E. coli*, they show that addition of chrI-4 in trans abolishes the requirement for DnaK/J chaperones, which

are normally important to promote RctB-dependent initiation at *ori2* (*12*, *32*). Initiator remodeling upon interaction with their cognate DNA binding sites has been observed for iteron-bearing plasmids (*43*), as well as for *E. coli* DnaA (*44*). RctB could form a bidentate protein simultaneously using two DNA binding domains to contact two DNA loci (for example, *crtS* and *ori2*). In mutants with two chromosomal copies of *crtS*, we observed that most of newborn cells have two *ori2* and only one *ori1* (Fig. 4 and fig. S8), suggesting that it is the duplication of the *crtS* sequence itself that triggers Chr2 replication initiation, and that the duplication of the single-copy *crtS* sequence in wild type is limiting initiation at *ori2*. Once *crtS* is duplicated, dimers of RctB could simultaneously contact two *crtS* sites, allowing a higher DNA binding affinity to iterons. In mutants with two chromosomal copies of *crtS*, a large proportion of cells divide with two *ori1* and four *ori2* foci, giving rise to newborn cells already having one *ori1* and two *ori2* foci (Fig. 4, C to E). Hence, passage of the replication fork across *crtS* might still be an option for triggering Chr2 replication if the signal had been sent in the mother cell. *crtS* contains two GATC sites that are substrates for Dam methylase. RctB binding is sensitive to the methylation state of iterons sites, which need to be fully methylated (*45*). The passage of the replication fork across *crtS* would generate transiently hemimethylated GATC sites that may affect RctB binding. However, mutation of the two GATC sites had no impact on *crtS* function. Passage of the replication fork also generates single-stranded DNA on the template for lagging-strand synthesis. RctB could recognize a DNA hairpin structure formed by the single-stranded state of *crtS*, thereby modifying its binding affinities for iterons and/or 39-mers. A better understanding of the genetic determinants enclosed within the *crtS* sequence will provide new clues to decipher the *crtS*-RctB–mediated mechanism that triggers Chr2 replication, and perhaps a better understanding of the mechanisms controlling the activation/deactivation of RctB.

A large fraction of $crtS_{WT/VC23}$ cells display three *ori2* foci, suggesting that one of the two *ori2* duplicates before the other (Fig. 4D). These observations are different from *E. coli*, where multiple origins initiate in synchrony (*20*). To accommodate for a generation time shorter than the replication time in fast-growing cells, overlapping rounds of replication occur with multiple origins of replication. In *E. coli*, multiple origins fire synchronously, such that either 2, 4, or 8 (that is, 2^n) origins of replication are present at the same time (*20*). In *E. coli*, several mechanisms are responsible for the coordinated initiation of multiple origins (DnaA titration, regulatory inactivation of DnaA, origin sequestration, and DnaA reactivation sequences) (*46*). All these mechanisms control the availability of the active form of DnaA for initiating replication from *oriC*. If the control of *ori2* initiation by *crtS* was done only by controlling the availability of the RctB active form, we would expect a similar synchrony in the firing of multiple *ori2*, and this would be observed by cells containing only 2^n *ori2* foci (for example, 2 or 4). Because a large portion of $crtS_{WT/VC23}$ cells have three *ori2* foci, we hypothesize that the duplication of one *crtS* triggers the firing of only one *ori2*. This reinforces the hypothesis that firing could necessitate a contact between *crtS* and *ori2*. Fluorescence microscopy of WT fluorescently labeled near *crtS* (VC783) and *ori2* loci shows that the two loci localize to the same region throughout the cell cycle (fig. S4E). The contacts between *ori2* and Chr1 revealed by 3C may be caused by the simultaneous binding of RctB to *ori2* and *crtS*. The most frequent contacts between *ori2* and Chr1 occur downstream of *crtS* (Fig. 5D). A possible explanation is that, following the duplication of the *crtS* locus, the replication machineries of Chr1 and Chr2 are in the vicinity of each other until the end of replication of the two chromosomes. Nonreplicating cells (that is, stationary phase) lose the cross-shape contacts observed between Chr1 and Chr2 replichores during exponential growth (Fig. 5B, right), suggesting that replication is indeed responsible for the contacts of the two chromosomes along their chromosomal arms. Overall, the 3C analysis of the *V. cholerae* chromosomes points to a direct interplay between 3D organization and replication regulation. How trans topological contacts would drive a functional interaction between the two chromosomes remains unknown.

Concluding remarks

Bacteria can be subjected to sudden environmental changes and must adapt their replication rate to their growth rate. Fast-growing bacteria often initiate multiple overlapping rounds of DNA replication. Interrelated mechanisms control the availability of the active form of DnaA to regulate chromosome initiation, some of which are modulated by growth rate (*46*). *V. cholerae* is a fast-growing bacterium that encounters a broad spectrum of habitats (for example, aquatic environments and human beings). Here, we describe a system for the replication control of multiple chromosomes. We demonstrate that Chr2 surveys the replication of Chr1 via the *crtS* locus and only initiates replication when this site has been replicated. Repositioning *crtS* closer to or further from the *ori1* causes Chr2 initiation to be initiated earlier or later, respectively, in the cell cycle. If the signal is not received (for example, Δ*crtS* mutant), initiation of Chr2 will be impaired and the cell will filament, accumulating many copies of Chr1. We suggest this mechanism to be an example of a bacterial cell cycle checkpoint; coordination of passage from early cell cycle, with only Chr1 replicating, into the late part of the cell cycle, with both chromosomes replicating. The location of *crtS* on Chr1 dictates the timing of replication initiation at *ori2* so that replication of the two chromosomes terminate simultaneously. This, in turn, ensures coordinated and faithful segregation of the chromosomes in line with cell division. The *crtS*-RctB–mediated checkpoint control of Chr2 initiation is a simple and flexible mechanism to ensure a cell cycle–specific time setting of Chr2 replication relative to Chr1 replication. This novel mechanism is an elegant and cost-effective way for secondary chromosomes to benefit from the already well-adapted replication regulatory system of the host main chromosome.

Replication of eukaryotic genomes is initiated from multiple origins located on each chromosome, enabling the complete genomic replication within the S phase of the cell cycle (*47*). Thus, bacteria with multiple replicons may share similarities with eukaryotes in the control of their genomic replication. However, it is observed in eukaryotes that (i) not all origins are activated within a single replication round and (ii) activated origins do not start replication simultaneously (*48*). The observed tight control of initiation at *ori2* is different from the stochastic nature of initiation at eukaryotic origins (*49*). Nevertheless, we envisage that replication-dependent controls, such as the checkpoint described here, may contribute to the orchestration of the complex eukaryotic DNA replication.

MATERIALS AND METHODS

Experimental design

Our objective was to determine the regulatory pathway responsible for triggering Chr2 replication at a specific point of the cell cycle, so that the two chromosomes terminate replication at nearly the same time. To

achieve this, we created several *V. cholerae* derivatives with altered chromosome organization and monitored their replication pattern to determine whether this synchronization was directly linked to the replication of a specific region in Chr1. We used genome engineering, MFA, microscopy, and chromosome conformation capture to identify the elements involved in this regulatory pathway.

Bacterial strains and plasmids

The bacterial strains and plasmids used in this study are listed in table S2. Large genome rearrangements were performed following the procedures described by Val *et al.* (*18*). Details are given in the Supplementary Materials.

Quantitative PCR

qPCR was performed on the gDNA of cells growing exponentially in LB at 37°C [OD_{450} (optical density at 450 nm), ~0.15]. Primers used to determine *ori1/ori2* ratios are listed in table S3. Details are given in the Supplementary Materials.

Marker frequency analysis

MFA was performed on the gDNA of cells growing exponentially in LB (glucose) at 30°C (OD_{450}, ~0.15). Libraries were sequenced using an Ion Proton sequencer (Life Technologies). MFA was performed essentially as described by Skovgaard *et al.* (*17*). Details are given in the Supplementary Materials.

Pulsed-field gel electrophoresis

PFGE was done following the procedure described by Val *et al.* (*10*). Details are given in the Supplementary Materials.

Fluorescence microscopy

All Chr1 loci were labeled with a $parS_{pMT1}$ site, and Chr2 loci were labeled with a *lacO* array. The genes encoding for yGFP-Δ30$ParB_{pMT1}$ and LacI-mCherry protein fusions were inserted in the *lacZ* gene using plasmid pAD19 (table S2) (*19*). Cultures for microscopy were grown in minimal fructose medium to limit replication rounds to once per cell cycle. Microscopy observations and data analysis were performed following procedures and using MATLAB scripts already described by David *et al.* (*19*). Details are given in the Supplementary Materials.

Chromosome conformation capture

3C libraries were built, sequenced, and analyzed as previously described (*23*). For all the data, we generated matrices with bins of 5 kbp using a four-base cutter (Hpa II). Both matrices (LB and MM) showed a strong correlation together using Spearman's rank correlation coefficient (ρ = 0.488, $P < 10$ to 64). Experimental details are given in the Supplementary Materials.

SUPPLEMENTARY MATERIALS

Supplementary material for this article is available at http://advances.sciencemag.org/cgi/content/full/2/4/e1501914/DC1

Materials and Methods

fig. S1. Chromosomal inversion detected around ori1 when WT sequences are mapped against the National Center for Biotechnology Information (NCBI) reference genome AE003852.

fig. S2. Large DNA inversions either caused no fitness cost (JB392) or were similarly affected (JB590, JB659, JB771, and JB963).

fig. S3. Complementation of Δ*crtS* filamentous phenotype by addition of an ectopic chromosomal copy of crtS.

fig. S4. Duplication and segregation of VC783 and ori2 foci in WT and mutant crtSVC23 throughout the cell cycle.

fig. S5. Duplication and segregation of ter1 and ter2 foci in WT and mutant crtSVC23 throughout the cell cycle.

fig. S6. ori2 foci duplicate earlier when crtS is located near ori1.

fig. S7. The addition of an extra copy of crtS affects the growth of *V. cholerae*.

fig. S8. Doubling in ori2 copy number in mutant with two chromosomal copies of crtS.

fig. S9. Comparison of global chromosome organization of *V. cholerae* in different growth conditions.

fig. S10. Comparison of directional index analysis at a 100-kbp scale with transcription and GC content for fast-growing cells.

fig. S11. Δ*crtS* mutants have a fitness defect, whereas ICO1Δ*crtS* shows no additional growth defect.

fig. S12. Fitness improvement of Δ*crtS* mutants by the acquisition of compensatory mutations.

fig. S13. Loss of filamentation phenotype of Δ*crtS* mutants by the acquisition of compensatory mutations.

fig. S14. MFA of crtS mutants before and after acquisition of compensatory mutations.

fig. S15. The effect of MFA normalizations.

table S1. Compensatory mutations obtained after evolution of Δ*crtS* mutants.

table S2. List of plasmids and bacterial strains.

table S3. Primers used in qPCR.

movie S1. 3D representations of the contact map from fig. S9 (exponential growth of the WT in LB).

movie S2. 3D representations of the contact map from fig. S9 (exponential growth of the WT in MM).

movie S3. Time-lapse fluorescence microscopy of Δ*crtS* filamentous cells, tagged at VC783 (Chr1) and near ori2 (Chr2), growing on an M9 MM agar pad supplemented with fructose and thiamine.

movie S4. Time-lapse fluorescence microscopy of Δ*crtS* filamentous cells, tagged at VC783 (Chr1) and near ori2 (Chr2), growing on an M9 MM agar pad supplemented with fructose and thiamine.

References (*50*–*64*)

REFERENCES AND NOTES

1. C. Mackenzie, S. Kaplan, M. Choudhary, *Microbial Evolution: Gene Establishment, Survival, and Exchange*, R. V. Miller, M. J. Day, Eds. (ASM Press, Washington, DC, 2004).
2. P. W. Harrison, R. P. J. Lower, N. K. D. Kim, J. P. W. Young, Introducing the bacterial 'chromid': Not a chromosome, not a plasmid. *Trends Microbiol.* **18**, 141–148 2010).
3. T. Katayama, S. Ozaki, K. Keyamura, K. Fujimitsu, Regulation of the replication cycle: Conserved and diverse regulatory systems for DnaA and oriC. *Nat. Rev. Microbiol.* **8**, 163–170 (2010).
4. G. del Solar, M. Espinosa, Plasmid copy number control: An ever-growing story. *Mol. Microbiol.* **37**, 492–500 (2000).
5. K. Okada, T. Iida, K. Kita-Tsukamoto, T. Honda, Vibrios commonly possess two chromosomes. *J. Bacteriol.* **187**, 752–727 (2005).
6. J. F. Heidelberg, J. A. Eisen, W. C. Nelson, R. A. Clayton, M. L. Gwinn, R. J. Dodson, D. H. Haft, E. K. Hickey, J. D. Peterson, L. Umayam, S. R. Gill, K. E. Nelson, T. D. Read, H. Tettelin, D. Richardson, M. D. Ermolaeva, J. Vamathevan, S. Bass, H. Qin, I. Dragoi, P. Sellers, L. McDonald, T. Utterback, R. D. Fleishmann, W. C. Nierman, O. White, S. L. Salzberg, H. O. Smith, R. R. Colwell, J. J. Mekalanos, J. C. Venter, C. M. Fraser, DNA sequence of both chromosomes of the cholera pathogen *Vibrio cholerae*. *Nature* **406**, 477–483 (2000).
7. S. Duigou, K. G. Knudsen, O. Skovgaard, E. S. Egan, A. Løbner-Olesen, M. K. Waldor, Independent control of replication initiation of the two *Vibrio cholerae* chromosomes by DnaA and RctB. *J. Bacteriol.* **188**, 6419–6424 (2006).
8. J. K. Jha, R. Ghirlando, D. K. Chattoraj, Initiator protein dimerization plays a key role in replication control of *Vibrio cholerae* chromosome 2. *Nucleic Acids Res.* **42**, 10538–10549 2014).
9. S. Duigou, Y. Yamaichi, M. K. Waldor, ATP negatively regulates the initiator protein of *Vibrio cholerae* chromosome II replication. *Proc. Natl. Acad. Sci. U.S.A.* **105**, 10577–10582 (2008).
10. M.-E. Val, A. Soler-Bistué, M. J. Bland, D. Mazel, Management of multipartite genomes: The *Vibrio cholerae* model. *Curr. Opin. Microbiol.* **22**, 120–126 (2014).
11. T. Venkova-Canova, D. K. Chattoraj, Transition from a plasmid to a chromosomal mode of replication entails additional regulators. *Proc. Natl. Acad. Sci. U.S.A.* **108**, 6199–6204 (2011).
12. J. H. Baek, D. K. Chattoraj, Chromosome I controls chromosome II replication in *Vibrio cholerae*. *PLOS Genet.* **10**, e1004184 (2014).
13. K. Nordström, S. Dasgupta, Copy-number control of the *Escherichia coli* chromosome: A plasmidologist's view. *EMBO Rep.* **7**, 484–489 (2006).
14. E. S. Egan, A. Løbner-Olesen, M. K. Waldor, Synchronous replication initiation of the two *Vibrio cholerae* chromosomes. *Curr. Biol.* **14**, R501–R502 (2004).
15. T. Rasmussen, R. B. Jensen, O. Skovgaard, The two chromosomes of *Vibrio cholerae* are initiated at different time points in the cell cycle. *EMBO J.* **26**, 3124–3131 (2007).
16. E. P. Rocha, The organization of the bacterial genome. *Annu. Rev. Genet.* **42**, 211–233 (2008).
17. O. Skovgaard, M. Bak, A. Løbner-Olesen, N. Tommerup, Genome-wide detection of chromosomal rearrangements, indels, and mutations in circular chromosomes by short read sequencing. *Genome Res.* **21**, 1388–1393 (2011).

18. M.-E. Val, O. Skovgaard, M. Ducos-Galand, M. J. Bland, D. Mazel, Genome engineering in *Vibrio cholerae*: A feasible approach to address biological issues. *PLOS Genet.* **8**, e1002472 (2012).
19. A. David, G. Demarre, L. Muresan, E. Paly, F.-X. Barre, C. Possoz, The two cis-acting sites, *parS1* and *oriC1*, contribute to the longitudinal organisation of *Vibrio cholerae* chromosome I. *PLOS Genet.* **10**, e1004448 (2014).
20. K. Skarstad, E. Boye, H. B. Steen, Timing of initiation of chromosome replication in individual *Escherichia coli* cells. *EMBO J.* **5**, 1711–1717 (1986).
21. J. Dekker, K. Rippe, M. Dekker, N. Kleckner, Capturing chromosome conformation. *Science* **295**, 1306–1311 (2002).
22. M. Marbouty, A. Cournac, J.-F. Flot, H. Marie-Nelly, J. Mozziconacci, R. Koszul, Metagenomic chromosome conformation capture (meta3C) unveils the diversity of chromosome organization in microorganisms. *ELife* **3**, e03318 (2014).
23. M. Marbouty, A. Le Gall, D. I. Cattoni, A. Cournac, A. Koh, J.-B. Fiche, J. Mozziconacci, H. Murray, R. Koszul, M. Nollmann, Condensin- and replication-mediated bacterial chromosome folding and origin condensation revealed by Hi-C and super-resolution imaging. *Mol. Cell* **59**, 588–602 (2015).
24. X. Wang, T. B. K. Le, B. R. Lajoie, J. Dekker, M. T. Laub, D. Z. Rudner, Condensin promotes the juxtaposition of DNA flanking its loading site in *Bacillus subtilis*. *Genes Dev.* **29**, 1661–1675 (2015).
25. T. B. K. Le, M. V. Imakaev, L. A. Mirny, M. T. Laub, High-resolution mapping of the spatial organization of a bacterial chromosome. *Science* **342**, 731–734 (2013).
26. A. Lesne, J. Riposo, P. Roger, A. Cournac, J. Mozziconacci, 3D genome reconstruction from chromosomal contacts. *Nat. Methods* **11**, 1141–1143 (2014).
27. M. A. Umbarger, E. Toro, M. A. Wright, G. J. Porreca, D. Baù, S.-H. Hong, M. J. Fero, L. J. Zhu, M. A. Marti-Renom, H. H. McAdams, L. Shapiro, J. Dekker, G. M. Church, The three-dimensional architecture of a bacterial genome and its alteration by genetic perturbation. *Mol. Cell* **44**, 252–264 (2011).
28. D. Mazel, B. Dychinco, V. A. Webb, J. Davies, A distinctive class of integron in the *Vibrio cholerae* genome. *Science* **280**, 605–608 (1998).
29. A. Slack, P. C. Thornton, D. B. Magner, S. M. Rosenberg, P. J. Hastings, On the mechanism of gene amplification induced under stress in *Escherichia coli*. *PLOS Genet.* **2**, e48 (2006).
30. T. Venkova-Canova, A. Saha, D. K. Chattoraj, A 29-mer site regulates transcription of the initiator gene as well as function of the replication origin of *Vibrio cholerae* chromosome II. *Plasmid* **67**, 102–110 (2012).
31. M.-E. Val, S. P. Kennedy, A. J. Soler-Bistué, V. Barbe, C. Bouchier, M. Ducos-Galand, O. Skovgaard, D. Mazel, Fuse or die: How to survive the loss of Dam in *Vibrio cholerae*. *Mol. Microbiol.* **91**, 665–678 (2014).
32. J. K. Jha, G. Demarre, T. Venkova-Canova, D. K. Chattoraj, Replication regulation of *Vibrio cholerae* chromosome II involves initiator binding to the origin both as monomer and as dimer. *Nucleic Acids Res.* **40**, 6026–6038 (2012).
33. B. Koch, X. Ma, A. Løbner-Olesen, *rctB* mutations that increase copy number of *Vibrio cholerae oriCII* in *Escherichia coli*. *Plasmid* **68**, 159–169 (2012).
34. Y. Yamaichi, M. A. Gerding, B. M. Davis, M. K. Waldor, Regulatory cross-talk links *Vibrio cholerae* chromosome II replication and segregation. *PLOS Genet.* **7**, e1002189 (2011).
35. M. Stouf, J.-C. Meile, F. Cornet, FtsK actively segregates sister chromosomes in *Escherichia coli*. *Proc. Natl. Acad. Sci. U.S.A.* **110**, 11157–11162 (2013).
36. S. P. Kennedy, F. Chevalier, F.-X. Barre, Delayed activation of Xer recombination at *dif* by FtsK during septum assembly in *Escherichia coli*. *Mol. Microbiol.* **68**, 1018–1028 (2008).
37. O. Espeli, C. Lee, K. J. Marians, A physical and functional interaction between *Escherichia coli* FtsK and topoisomerase IV. *J. Biol. Chem.* **278**, 44639–44644 (2003).
38. O. Espéli, R. Borne, P. Dupaigne, A. Thiel, E. Gigant, R. Mercier, F. Boccard, A MatP-divisome interaction coordinates chromosome segregation with cell division in *E. coli*. *EMBO J.* **31**, 3198–3211 (2012).
39. R. Mercier, M.-A. Petit, S. Schbath, S. Robin, M. El Karoui, F. Boccard, O. Espéli, The MatP/*matS* site-specific system organizes the terminus region of the *E. coli* chromosome into a macrodomain. *Cell* **135**, 475–485 (2008).
40. P. Dupaigne, N. K. Tonthat, O. Espéli, T. Whitfill, F. Boccard, M. A. Schumacher, Molecular basis for a protein-mediated DNA-bridging mechanism that functions in condensation of the *E. coli* chromosome. *Mol. Cell* **48**, 560–571 (2012).
41. G. Demarre, E. Galli, L. Muresan, E. Paly, A. David, C. Possoz, F.-X. Barre, Differential management of the replication terminus regions of the two *Vibrio cholerae* chromosomes during cell division. *PLOS Genet.* **10**, e1004557 (2014).
42. M.-E. Val, S. P. Kennedy, M. El Karoui, L. Bonné, F. Chevalier, F.-X. Barre, FtsK-dependent dimer resolution on multiple chromosomes in the pathogen *Vibrio cholerae*. *PLOS Genet.* **4**, e1000201 (2008).
43. T. Díaz-López, M. Lages-Gonzalo, A. Serrano-López, C. Alfonso, G. Rivas, R. Díaz-Orejas, R. Giraldo, Structural changes in RepA, a plasmid replication initiator, upon binding to origin DNA. *J. Biol. Chem.* **278**, 18606–18616 (2003).
44. K. Fujimitsu, T. Senriuchi, T. Katayama, Specific genomic sequences of *E. coli* promote replicational initiation by directly reactivating ADP-DnaA. *Genes Dev.* **23**, 1221–1233 (2009).
45. G. Demarre, D. K. Chattoraj, DNA adenine methylation is required to replicate both *Vibrio cholerae* chromosomes once per cell cycle. *PLOS Genet.* **6**, e1000939 (2010).
46. A. C. Leonard, J. E. Grimwade, Regulation of DnaA assembly and activity: Taking directions from the genome. *Annu. Rev. Microbiol.* **65**, 19–35 (2011).
47. N. Rhind, D. M. Gilbert, DNA replication timing. *Cold Spring Harb. Perspect. Biol.* **5**, a010132 (2013).
48. N. Agier, O. M. Romano, F. Touzain, M. Cosentino Lagomarsino, G. Fischer, The spatiotemporal program of replication in the genome of *Lachancea kluyveri*. *Genome Biol. Evol.* **5**, 370–388 (2013).
49. M. Hawkins, R. Retkute, C. A. Müller, N. Saner, T. U. Tanaka, A. P. S. de Moura, C. A. Nieduszynski, High-resolution replication profiles define the stochastic nature of genome replication initiation and termination. *Cell Rep.* **5**, 1132–1141 (2013).
50. F. Le Roux, J. Binesse, D. Saulnier, D. Mazel, Construction of a *Vibrio splendidus* mutant lacking the metalloprotease gene *vsm* by use of a novel counterselectable suicide vector. *Appl. Environ. Microbiol.* **73**, 777–784 (2007).
51. R. L. Marvig, M. Blokesch, Natural transformation of *Vibrio cholerae* as a tool - Optimizing the procedure. *BMC Microbiol.* **10**, 155 (2010).
52. A. Soler-Bistué, J. A. Mondotte, M. J. Bland, M.-E. Val, M.-C. Saleh, D. Mazel, Genomic location of the major ribosomal protein gene locus determines *Vibrio cholerae* global growth and infectivity. *PLOS Genet.* **11**, e1005156 (2015).
53. H. Bremer, G. Churchward, An examination of the Cooper-Helmstetter theory of DNA replication in bacteria and its underlying assumptions. *J. Theor. Biol.* **69**, 645–654 (1977).
54. S. Cooper, C. E. Helmstetter, Chromosome replication and the division cycle of *Escherichia coli*$_{B/r}$. *J. Mol. Biol.* **31**, 519–540 (1968).
55. O. Sliusarenko, J. Heinritz, T. Emonet, C. Jacobs-Wagner, High-throughput, subpixel precision analysis of bacterial morphogenesis and intracellular spatio-temporal dynamics. *Mol. Microbiol.* **80**, 612–627 (2011).
56. B. Langmead, S. L. Salzberg, Fast gapped-read alignment with Bowtie 2. *Nat. Methods* **9**, 357–359 (2012).
57. M. Imakaev, G. Fudenberg, R. P. McCord, N. Naumova, A. Goloborodko, B. R. Lajoie, J. Dekker, L. A. Mirny, Iterative correction of Hi-C data reveals hallmarks of chromosome organization. *Nat. Methods* **9**, 999–1003 (2012).
58. A. Cournac, H. Marie-Nelly, M. Marbouty, R. Koszul, J. Mozziconacci, Normalization of a chromosomal contact map. *BMC Genomics* **13**, 436 (2012).
59. K. Papenfort, K. U. Förstner, J.-P. Cong, C. M. Sharma, B. L. Bassler, Differential RNA-seq of *Vibrio cholerae* identifies the VqmR small RNA as a regulator of biofilm formation. *Proc. Natl. Acad. Sci. U.S.A.* **112**, E766–E775 (2015).
60. M. Krzywinski, J. Schein, İ. Birol, J. Connors, R. Gascoyne, D. Horsman, S. J. Jones, Circos: An information aesthetic for comparative genomics. *Genome Res.* **19**, 1639–1645 (2009).
61. L. Feng, P. R. Reeves, R. Lan, Y. Ren, C. Gao, Z. Zhou, Y. Ren, J. Cheng, W. Wang, J. Wang, W. Qian, D. Li, L. Wang, A recalibrated molecular clock and independent origins for the cholera pandemic clones. *PLOS One* **3**, e4053 (2008).
62. R. Lan, P. R. Reeves, Recombination between rRNA operons created most of the ribotype variation observed in the seventh pandemic clone of *Vibrio cholerae*. *Microbiology* **144**, 1213–1221 (1998).
63. J. R. Dixon, S. Selvaraj, F. Yue, A. Kim, Y. Li, Y. Shen, M. Hu, J. S. Liu, B. Ren, Topological domains in mammalian genomes identified by analysis of chromatin interactions. *Nature* **485**, 376–380 (2012).
64. K. L. Meibom, M. Blokesch, N. A. Dolganov, C.-Y. Wu, G. K. Schoolnik, Chitin induces natural competence in *Vibrio cholerae*. *Science* **310**, 1824–1827 (2005).

Acknowledgments: We thank S. Aguilar Pierlé and A. Soler Bistué for useful discussion and I. Vallet-Gely and F.-X. Barre for sharing MATLAB functions. **Funding:** This research was funded by the Institut Pasteur, INSERM, and CNRS. This work was supported by a grant from the French National Research Agency (ANR-10-BLAN-131301). R.K. was funded by the European Research Council (FP7/2007-2013; ERC grant agreement 260822). M.M. was funded by the Association pour la Recherche sur le Cancer fellowship (20100600373). F.d.L.M. and M.J.B. were supported by the Pasteur-Paris University Program. **Author contributions:** Conceived and designed the experiments: M.-E.V., M.M., R.K., O.S., and D.M. Performed the experiments: M.-E.V., M.M., S.P.K., F.d.L.M., M.J.B., C.P., and H.K. Analyzed the data: M.-E.V., M.M., R.K., O.S., and D.M. Wrote the paper: M.-E.V., S.P.K., R.K., O.S., and D.M. **Competing interests:** The authors declare that they have no competing interests. **Data and materials availability:** All data needed to evaluate the conclusions in the paper are present in the paper and/or the Supplementary Materials. Additional data related to this paper may be requested from the authors. Sequence reads used for MFA and 3C experiments have been submitted to NCBI Sequence Read Archive under accession number SRP070634.

Submitted 30 December 2015
Accepted 28 March 2016
Published 22 April 2016
10.1126/sciadv.1501914

Citation: M.-E. Val, M. Marbouty, F. de Lemos Martins, S. P. Kennedy, H. Kemble, M. J. Bland, C. Possoz, R. Koszul, O. Skovgaard, D. Mazel, A checkpoint control orchestrates the replication of the two chromosomes of *Vibrio cholerae*. *Sci. Adv.* **2**, e1501914 (2016).

Science Advances

A checkpoint control orchestrates the replication of the two chromosomes of *Vibrio cholerae*

Marie-Eve Val, Martial Marbouty, Francisco de Lemos Martins, Sean P. Kennedy, Harry Kemble, Michael J. Bland, Christophe Possoz, Romain Koszul, Ole Skovgaard and Didier Mazel

Sci Adv **2** (4), e1501914.
DOI: 10.1126/sciadv.1501914

1.3. Complementary results: RctB-associated mutations compensate Δ*crtS* deleterious mutation by altering Chr2 initiation regulation

In the previous publication we have shown that *crtS* is crucial for Chr2 replication. *crtS* deletion severely impairs cells fitness, which is directly linked to improper regulation/activation of Chr2 replication. PFGE analysis of *ΔcrtS* mutants revealed that, in some cases, transient genome remodelling suppresses *crtS* deletion. In the absence of *crtS*, Chr2 seems to temporarily benefit from Chr1 replication machinery which is shown by chromosome fusion events. However, this situation does not seem sustainable since after a 200-generation experimental evolution these strains acquired mutations affecting *ori2* and revert to the two chromosome configuration. At the time of the publication we had only performed extensive analysis by whole-genome sequencing and subsequently MFA on two of these mutants. Here we present additional data concerning strains C667 and C926 before and after the evolution experiment. The –EV suffix refers to the clones isolated after the 200-generation experimental evolution.

Microscopy and flow cytometry revealed that after 200 generations filamentation was no longer detectable for strain C926-EV, compared to the 5,6% filamentous cells observed in the parental strain C926 (Fig. 23). However, the phenotype of *crtS* deletion mutants is quite diverse and filamentation is not always evident. For strain C667 cell filamentation was not apparent before the evolution experiment (Fig. 23). In turn, genomic instability characterized by Chr2 replication downregulation seems to be a hallmark of *crtS* deletion mutants.

MFA of C667 before the experiment is very similar to the *ΔcrtS* MFA pattern, showing Chr2 downregulation and no genome rearrangement (Fig. 23). In contrast, MFA of strain C926 does not show the typical triangular form with a sharp peak corresponding to *ori2*. Indeed, C926 MFA pattern reveals a chromosome fusion event between Chr1 and Chr2, which is consistent with the already published PFGE data on this mutant (Fig. 23). After 200 generations, this genomic arrangement is reversed back to a two-chromosomal genomic configuration. MFA of C667-EV and C926-EV reveals an up-regulation of *ori2* initiation compared to the respective parental strains (Fig. 23). The increase in the Chr2/Chr1 copy number ratio is explained by the acquisition of mutations on *ori2* that compensate the lack of *crtS* activation.

Previous *rctB* mutants causing replication overinitiation of *ori2*-based plasmids have already been selected in *E. coli* (Duigou et al., 2008; Jha et al., 2012; Koch et al., 2012; Yamaichi et al., 2011). These “copy-up” mutants of RctB were shown to consistently prevent RctB to repress replication by causing reduced dimer binding to iterons (Jha et al., 2012), reduced dimerization (Koch et al., 2012), or

reduced 39-mer binding (Jha et al., 2012) or fail to bind ATP (Duigou et al., 2008). Indeed, mutations at the same position as two of the *ΔcrtS* suppressor mutations identified in our study (R195C and L357I) have already been documented as copy-up mutants (Yamaichi et al., 2011).

With the exception of strain D247-EV carrying a mutation on the 29-mer region, the remaining evolved mutants carry mutations affecting RctB domain 2 (Fig. 24). Domain 2 harbours the RctB dimerization interface (Orlova et al., 2016). RctB binds to 12-mers on *ori2* in both monomer and dimer forms, however the monomers are the active initiators for Chr2 (Jha et al., 2012). Dimers appear to serve as direct competitors of monomers for 12-mer binding (Jha et al., 2012) and are involved in handcuffing by bridging the 12-mers (Venkova-Canova and Chattoraj, 2011), which functions as an inhibitory mechanism for Chr2 replication. We have not further investigated the impact of our mutations on RctB structure or on how it affects its binding to the different sites, such as iterons, 39-mers and *crtS*. However, the fact that three of the mutations lie within the domain 2 led us to speculate that they may inhibit the formation of RctB dimers, and consequently favour Chr2 replication activation. This is merely speculative, since additional experiments are required to effectively prove that Chr2 up-regulation is linked to the impossibility of RctB dimer formation.

The acquisition of RctB-associated mutations suggests a direct interplay between *crtS* and RctB to coordinate chromosome replication. On the next chapter, we provide additional evidence supporting this direct interaction.

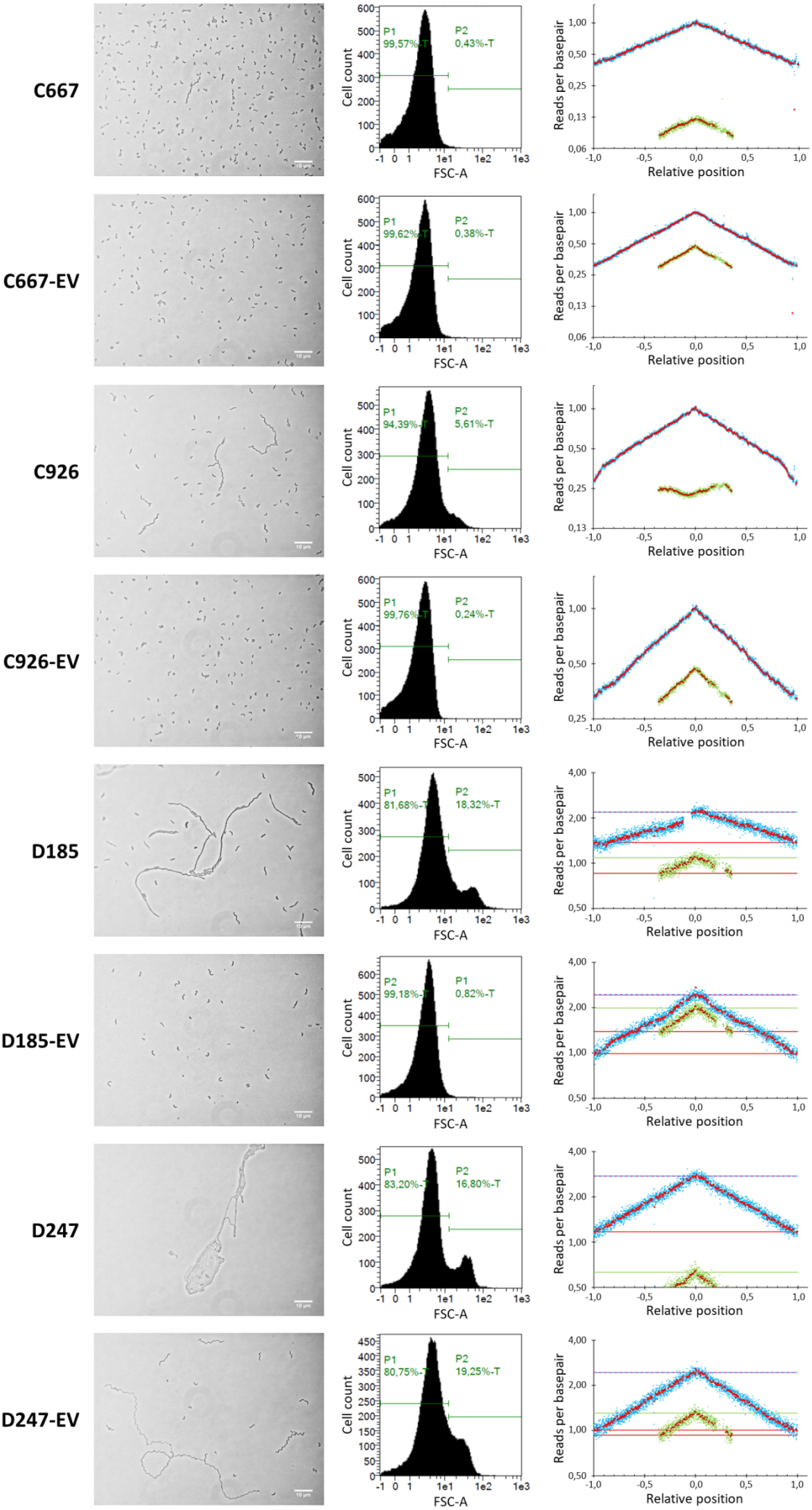
C667
P1
99,57%-T
P2
0,43%-T
C667-EV
P1
99,62%-T
P2
0,38%-T
C926
P1
94,39%-T
P2
5,61%-T
C926-EV
P1
99,76%-T
P2
0,24%-T
D185
P1
81,68%-T
P2
18,32%-T
D185-EV
P2
99,18%-T
P1
0,82%-T
D247
P1
83,20%-T
P2
16,80%-T
D247-EV
P1
80,75%-T
P2
19,25%-T
Cell count
FSC-A
Reads per basepair
Relative position

Figure 23. Characterization of *ΔcrtS* mutants before and after experimental evolution. (A) *ΔcrtS* mutants are frequently characterized by cell filamentation and downregulation of Chr2 replication, which is restored after 200 generations. (Left panel) Representative picture of *ΔcrtS* mutants observed by phase-contrast microscopy. The white bar corresponds to 10 µm. (Central panel) Cell size distribution determined by flow cytometry of cells grown in M9 (fructose, thiamine) using MACSQUANT Analyzer (Miltenyi Biotec). The x-axis and y-axis represent Forward Scatter Area and cell count, respectively. The proportion of normal size cells (P1) was calibrated on a WT population. P2 represents the proportion of abnormally longer cells. P1 and P2 regions are indicated by green lines. (Right panel) MFA of exponentially growing *crtS* mutants. Positions of *ori1* and *ori2* are set to 0. Blue and green dots correspond to Chr1 and Chr2 reads, respectively.

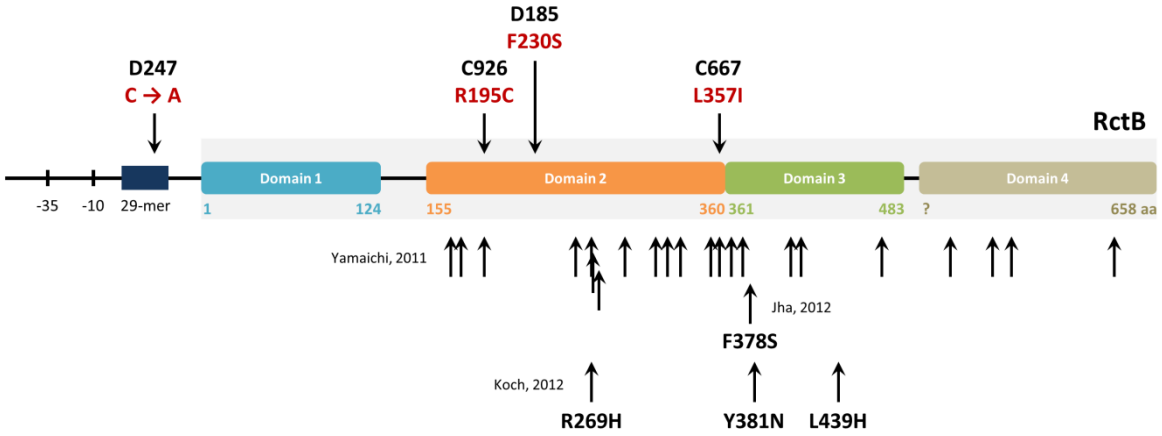

Figure 24. Map showing the *ori2* compensatory mutations acquired after 200 generations. The arrows above the map correspond to the mutations identified in our study, while the arrows below indicate the copy-up mutants previously documented (Jha et al., 2012; Koch et al., 2012; Yamaichi et al., 2011). Mutations at the amino acid positions 195 and 357 have already been described in the literature, however with different amino acid substitutions. RctB coding region is depicted in light grey. The different domains composing RctB are indicated with different colours.

II. Research Article in preparation:

RctB monomers binding to *crtS* controls the *V. cholerae* Chr2 copy number

de Lemos Martins, F.*, Fournes, F.*, *et al.* (in preparation).

* These authors contributed equally to this work

Introduction

Nearly 10% of bacteria harbor large secondary replicons being classified either as chromids or as megaplasmids (1,2). Chromids (also called secondary chromosomes) encode essential core genes and have nucleotide and codon compositions close to the chromosome, suggesting that they have evolved together for hundreds of millions of years to become domesticated (2,3). Chromids replicate using plasmid-like mechanisms indicating that they originated from plasmids or megaplasmids (2). Since plasmids are frequently maladapted to a new genetic background, their stabilization in the genome must require adaptation to the host cell cycle and physiology. Replication is primarily regulated at the initiation step (4) and plasmid eventually become domesticated as *bona fide* secondary chromosomes through cell-cycle synchronized replication controls. As of today, most of our knowledge on the conjoint management of chromosomes and chromids comes from the bacterial model *Vibrio cholerae*, which has a genome divided over a main chromosome (Chr1) of 3 Mbp and a chromid (Chr2) of 1 Mbp (5-7).

Each of the two replicons encodes for its own initiator protein to start replication at unalike replication origins (8). Chr1 replication initiation is performed by DnaA the ubiquitous chromosome replication initiator in bacteria (9), and the replication origin of *V. cholerae* Chr1 (*ori1*) is fairly similar to the canonical *Escherichia coli* chromosomal origin (*oriC*) (8,10). *ori1* contains five DnaA binding sites (DnaA boxes), an IHF binding site and an AT-rich region for replication initiation. In addition, Chr1 *ori1* contains several GATC sites for methylation by DNA adenine methyltransferase (Dam) which regulates the timing of subsequent re-initiation through sequestration of hemi-methylated sites by SeqA (11,12). On the other hand, Chr2 replication initiation is triggered by a *Vibrio*-specific factor called RctB, and Chr2 replication origin (ori2) is closely related to the one of iteron-type plasmids (8). *ori2* can be divided in two regions: a minimal origin of replication (Figure 1A, (+)) and a region of regulation of Chr2 replication (Figure 1A, (-)). The minimal origin of replication contains the *rctB* encoding gene and six repeated 12-mers (iterons) onto which RctB binds to promote replication initiation with the unwinding of a contiguous AT-rich sequence (13). It also contains putative IHF and DnaA binding sites, the latter being required for replication at *ori2* (14,15). ori2 regulatory regions contains a transcribed but non-translated ORF (*rctA)* and two types of RctB binding sites: five regulatory iterons and two 39-mer motifs one of which is found in *rctA (16).* RctB binds efficiently to the 39-mer motifs where it serves as a negative regulator of *ori2* initiation (16,17). This inhibitory

activity is mainly achieved by origin handcuffing which consists in bridging 39-mers with iterons via RctB (7,16-18). ori2 handcuffing is a strong inhibitor and to counterweigh it other mechanisms will interfere, such as the out-competition of RctB binding to 39-mer by ParB2 (19), the redirection of 39-mer handcuffing with other regulatory iterons (16) or *rctA* transcriptional interference of RctB binding to 39-mer (18). In addition to the *ori2* binding regions, RctB binds to a 74 kb DNA stretch containing five iterons and one 39-mer motif, located 40 kb away from *ori2* (20). This locus appears to be reminiscent of the *E. coli datA* titration locus and negatively regulates *ori2* replication (21,22).

RctB is a 658 AA protein with four domains. Its central region (domains 2 and 3) is structurally homologous to iteron plasmid initiators while its outer domains (domains 1 and 4) are unique (23). RctB has three identified DNA binding surfaces in domains 1, 2 and 3 and the protein can adopt a monomeric or a dimeric form (23). Its dimer interface is mediated by domains 2 and 3 and mutations impairing its dimerization such as $RctB_{D314P}$, have been identified (23). RctB was reported to bind as a monomer or as a dimer onto iterons but only as a monomer on 39-mers (17,24). RctB is remodeled by chaperones DnaJ and DnaK which promote the binding of RctB to both iterons and 39-mers (17). DnaK specifically interacts with RctB to promote its monomerization but also to remodel RctB monomers (25).

Analogous to that of eukaryotes, the bacterial cell cycle is divided into three stages: cell birth to chromosome replication initiation (B), chromosome replication (C) and termination of replication to cell division (D). Chromosomes ensure a single round of replication per cell cycle (26). This is not the case for iteron-type plasmids, which replicate several times per cell cycle (7). In *V. cholerae,* Chr2 has integrated a more sophisticated replication regulation system. Despite its plasmid-like vestiges, Chr2 replication is restricted to only once per cell cycle. Dam methylation is essential for *ori2* replication initiation while it is not for *ori1* (27). All iterons in *ori2* have a GATC site that needs to be fully methylated in order to bind RctB (28). Therefore, RctB binding to iterons functions in a cell-cycle dependent manner. In contrast, RctB binding to the 39-mer motifs do not require methylation (29). Dam regulation of Chr2 replication offered some clues as to how Chr2 replication is limited to once per cell cycle (29). In *V. cholerae*, the timing of Chr1 and Chr2 initiations is coordinated in such a way that they terminate replicating at the same time (30). Chr1 initiates at the onset of the C period while initiation of Chr2 is delayed and occurs when 2/3rds of the C period has completed (30). In fact, Chr2 monitors the replication status of Chr1 to time its own replication via a non-coding locus on Chr1, called *crtS* (Chr2 replication triggering site) (31). This locus was originally found by the ChIP-chip of RctB on *V. cholerae* genome (20) and its critical role in the coordinated timing of Chr1 and Chr2 replication was only revealed later (31). Indeed, Chr2 initiates replication only when *crtS* has been replicated (31).

crtS is a intergenic sequence located ~690 Kb downstream of *ori1* on Chr1 (between VC0764 and VC0765 genes), conserved in the *Vibrionaceae* family (20,32). Its sequence shows no homology to previously described RctB binding sites, *i.e.* iteron or 39-mer. *crtS* contains an AT-rich stretch, a putative DnaA box and several conserved GATC sites. Deletion of *crtS* severely impairs growth and is associated with cell filamentation and Chr2 loss (31). This phenotype was shown to be directly linked

to improper regulation/activation of Chr2 replication (31). The presence of *crtS* in *E. coli* enhances the replication of an *ori2*-driven plasmid (mini-chr2) (15,20). Serial deletions of a DNA fragment containing *crtS* in a plasmid showed that the replication-enhancing activity of a mini-chr2 in *E. coli* could be narrowed down to a 70-mer site (chrI-9) (20). Baek et al. reported that *in vitro*, *crtS* only has a visible effect if present on a supercoiled plasmid (20). Indeed, the binding of purified RctB on *crtS* could never be directly observed by electrophoretic mobile shift assay (EMSA) using linear DNA (20). RctB binding site on *crtS* was inferred by primer extension mapping of a DnaseI footprinting with *crtS* contained on plasmid. Seven protected bases were found within the 70-mer to have an important role in *crtS* activity (20). It was shown that *crtS*-containing plasmids increased RctB affinity to iterons, decreased RctB affinity to 39-mers and also abolished the requirement for the DnaK/J chaperones, which are normally required to promote initiation at *ori2* in *E. coli* (20). Baek et al. suggested that *crtS* may act like a DNA chaperone to remodel RctB which would alter its binding to both iterons and 39-mers. However this remodeling would act differently than DnaK/J which increase RctB binding to both iterons and 39-mers.

The molecular mechanism by which *crtS* controls the initiation of Chr2 replication is still largely unknown. Chr2 initiation requires *crtS* replication, meaning that either DNA alterations caused by the passage of the replication fork across *crtS* or the doubling in copy number of *crtS* after duplication triggers Chr2 replication (31). In a previous work, we showed that in mutants with two chromosomal copies of *crtS*, the majority of newborn cells display an unbalanced chromosome ratio with two ori2 and only one ori1 (31). This suggested that having two copies of *crtS* is enough to trigger Chr2 replication initiation. On the other hand, the replication of *crtS* generates transiently hemi-methylated GATC sites that could affect RctB binding and send a signal to trigger Chr2 replication. In this work, we combined *in silico*, *in vivo and in vitro* approaches to study the genetic determintants enclosed within the *crtS* sequence, to characterize the binding parameters of RctB on *crtS* and to inspect the involvement of other factors (Dam methylation, ParAB2, DnaA, DnaK/J) in the *crtS*-RctB-ori2 replication system. We show that *crtS* regulates not only the timing of Chr2 initiation but also its copy number. We defined the minimal *crtS* functional sequence in *V. cholerae* and found out that it significantly differs from the 70-mer previously found in *E. coli*. We show that RctB *in vitro* binds to a linear 54-bp *crtS* site. This binding is dependent on DnaK/J and independent of Dam. We show that DnaA binds to ori2 but not *crtS*, rejecting the existence of DnaA box in *crtS*. We show that RctB binds to *crtS* under its monomeric form and further promote the binding of additional RctB monomers. We propose that RctB molecules oligomerize on Chr1 from *crtS* (the nucleation site), and that upon the passage of the replication fork, RctB is somehow activated to trigger Chr2 replication.

Results

1. *crtS* regulates Chr2 copy number

To better characterize the molecular function of *crtS* on Chr2 maintenance, we reconstituted an artificial replication system in Escherichia coli based on *ori2*, RctB and *crtS*. We constructed a set of strains derived from *E. coli* MG1655 carrying up to four chromosomal *crtS* sites (Table S1) and generated a plasmid, pORI2, which replication in MG1655 solely depends on *ori2*. We performed a plasmid stability assay over 60 generations to follow the loss of pORI2 in function of *crtS* copy number (Figure S1). In absence of *crtS*, pORI2 is lost at a high rate of ~15% per generation while in the presence of only 1 *crtS*, the loss of pORI2 dropped to 5% per generation (Figure 1B). pORI2 stability increased exponentially as a function of *crtS* copy number (Figure 1C) and was only loss at a rate of 1% per generation when MG1655 contained 4 *crtS* sites. To understand how *crtS* stabilizes pORI2, we measured the impact of *crtS* on pORI2 copy number. We used multiplex digital PCR (dPCR) to monitor copy number variation between chromosome and pORI2 in MG1655 with various *crtS* site number (33). We observed an exponential increase of pORI2 copy number as a function of *crtS* number (Figure 1D, S2A). These results explains the concomitant exponential increase in pORI2 stability since the higher the copy number is, the more likely the two daughter cells will contain the plasmid. In absence of an active partition system if plasmid segregate randomly, the probability of having a plasmid-less daughter cell is $2^{(1-CN)}$, where CN is the plasmid copy number. In *E. coli*, *crtS* stabilizes pORI2 by stimulating its replication which increases its copy number. In *V. cholerae*, we have previously shown that 2 chromosomal copies of *crtS* double *ori2* number of replicating cells leading cells dividing with 1 *ori1* and 2 *ori2*. Using dPCR, we measured the copy number variation between Chr1 and Chr2 of non-replicating *V. cholerae* carrying 1, 2 or 3 *crtS* sites. As expected, Chr2 copy number increased with the number of *crtS* sites (Figure 1E). In WT (VC0764), the ori2/ori1 ratio equaled 1 meaning that non-replicating cells have the same number of Chr1 and Chr2. When a second *crtS* site was added near ori1 (VC0023) or near the terminus of Chr1 (VC0963), Chr2 copy number relative to Chr1 increased similarly (*ori2*/*ori1* ~1.7). When a third *crtS* site was added in the *attTn7* site (VC0487), Chr2 copy number relative to Chr1 increased up to 2. Unlike in *E. coli*, Chr2 copy number increased logarithmically as a function of *crtS* number suggesting that Chr2 copy number is restricted in *V. cholerae* (Figure S2B).

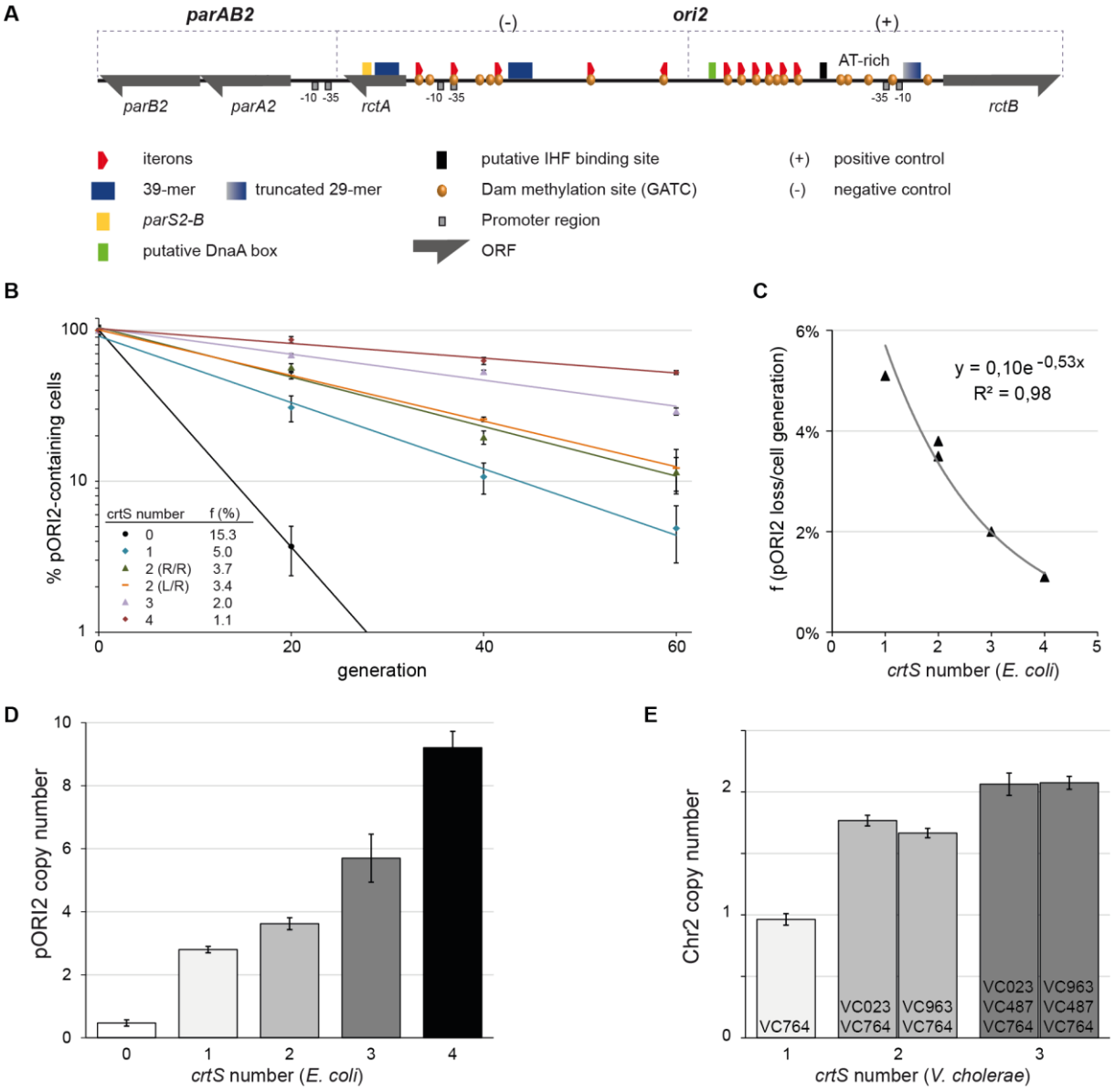

Figure 1. *crtS* controls Chr2 copy number

(A) Schematic map of ori2, the origin region of *V. cholerae* Chr2 and the contiguous parAB2 genes. ori2 is divided in two. (+) the minimal functional origin includes an array of six regular spaced iterons oriented in a head-to-tail manner each containing a GATC Dam methylation site, a contiguous AT-rich region, putative binding sites for IHF and DnaA, the rctB gene encoding for the initiator. RctB auto-regulates its own expression through binding to a 29-mer (truncated 39-mer) located in its promoter region (29). (-) the negative regulatory region includes two 39-mers, five iterons and the *rctA* non-translated ORF which harbors an iteron in its promoter and a 39-mer and a parS2(-B) site within its coding sequence **(B)** pORI2 plasmid loss in *E. coli* strains carrying up to four chromosomal *crtS* sites. f : frequency of pORI2 loss at each cell generation. 2(R/R), the two crtS sites are located on the same chromosomal arm. 2(L/R), the two crtS sites are located on different arms **(C)** Exponential increase of pORI2 stability (experimental values from B) as a function of *crtS* copy number in E. coli. **(D)** Histograms representing pORI2 copy number relative to the chromosome (pORI2/oriC) in E. coli strains carrying up to four chromosomal crtS sites. pORI2 and oriC copy number were measured by dPCR on genomic DNA from non-replicating cells (stationary phase) after 16hours growth with antibiotic selection for the plasmid. (E) Histograms representing Chr2 copy number relative to Chr1 (ori1/ori2) in V. cholerae strains carrying up to three chromosomal crtS sites. ori1 and ori2 copy number were measured by dPCR on genomic DNA from non-replicating cells (stationary phase) after

16hours growth. All the data represent the mean of three independent experiments (+/- standard deviation).

2. *crtS* and parAB2 have an additive effect on the control of *ori2* replication

Adjacent to *ori2* are found ParA2 and ParB2 encoding genes that are related to plasmid partitioning systems and which are crucial for Chr2 maintenance (34). Plasmid partitioning systems consist of two proteins, ParA and ParB, and cis-acting centromere-like sites, *parS*. One parB2 binding sites is located within *ori2*, in *rctA* (Figure 1A, parS2-B). ParB2 spreads from *parS2*-B into the *rctA* 39-mer and interferes with RctB 39-mer-binding replication inhibitory activity (19). ParB2 also binds directly to a 39-mer motif outside rctA without requiring initial binding to a parS2 site and out-compete RctB binding (19). On the other hand, binding of RctB to *rctA* activates *parAB2* expression (35). These binding fluctuations show how chromosome replication and origin segregation can be intimately intertwined. It was previously shown that *crtS* decreases the binding of RctB to 39-mer (20). This would enhance replication initiation at *ori2* by precluding 39-mer inhibitory effect. Similarly, ParB2 promotes replication at *ori2* by restraining RctB binding to 39-mer (19). We investigated the contribution of both *crtS* and parAB2 on *ori2* replication to look for potential genetic interactions that would provide us new insights into *crtS* mechanism of action. We compared the maintenance of two *ori2*-plasmids, pORI2 and pORI2-parAB2 which includes the *ori2* neighbouring parA2 and parB2 genes (Figure 1A). We first measured their stability over 80 generations in MG1655 in presence and absence of one chromosomal copy of *crtS* (Figure 2A). Both *crtS* and parAB2 independently stabilized the plasmid at similar rates (5% and 5.4% plasmid loss per generation, respectively). When both *crtS* and parAB2 are present, plasmid loss dropped to 0.9% per generation. Because ParAB2 is active in both segregation and replication of Chr2, we measured the copy number of the *ori2*-plasmids to discern the impact of ParAB2 on replication only. Figure 2B shows that *crtS* and *parAB2* independently increase pori2 copy number. Actually, pori2 copy number is higher in the presence of *crtS* than in the presence of parAB2. The difference between the sum of the individual values obtained with *crtS* and parAB2 only (2.8 and 1.8, respectively) and the value obtained in the presence of both *crtS* and parAB2 (4.7) is not significant (P = 0,4596 by Student's t test), suggesting that the contribution of *crtS* and parAB2 to pORI2 replication control constitutes an additive effect.

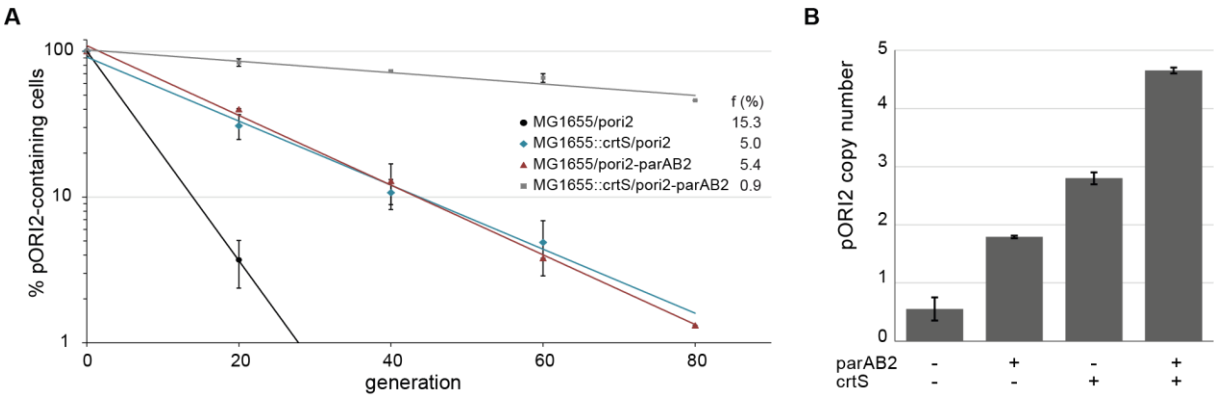

Figure 2. crtS and parAB2 have an additive effect on the control of ori2 copy number

(A) Loss of pORI2 (with or without parAB2) in *E. coli* strains (with or without a *crtS* site). f : frequency of plasmid loss at each cell generation. **(B)** Copy-number of pORI2 (with or without parAB2) relative to the chromosome (pORI2 /oriC) in *E. coli* strains (with or without a *crtS* site).

3. RctB binds to linear *crtS* independently of its methylation state

We characterized the binding of RctB to *crtS* by EMSA. We first checked the binding properties of our purified RctB protein onto iterons and 39-mer containing linear DNA to see if the protein behaved as reported (17). As expected, RctB binding to iterons is Dam-methylation dependent and the binding of RctB to the 39-mer is Dam-methylation independent (Figure S3). From previous ChIP-chip of RctB, it was expected that RctB would bind to *crtS*. However, Baek et al. reported that no binding of RctB could be directly detected on a 153bp *crtS*-containing linear DNA (Figure S4, ChrI-4) (20). Here, we characterized the binding of RctB on a crtS-linear DNA of 114bp encompassing the 70bp minimal functional *crtS* site reported in *E. coli* (Figure S4, ChrI-9) (20). In our conditions, RctB formed a complex with crtS radiolabeled linear DNA (Figure 3A, 114bp *crtS*). Since RctB preferentially binds to Dam methylated iterons (12) and the larger *crtS*-containing fragments contains two very conserved GATC sites than can be Dam methylated, we compared the binding of RctB on *in vitro* methylated and unmethylated DNA substrates (Figure 3A, 114bp *crtS* vs. 114bp $crtS^{Me}$). We observed that RctB could bind indistinguishably to both methylated and unmethylated *crtS*-containing DNA fragments with no apparent different efficiencies (Figure 3B, 114bp *crtS* vs. 114bp $crtS^{Me}$). These results were confirmed *in vivo* in *V. cholerae* mutants with point mutations in the native *crtS* (GATC to GAAC) (Figure S5). These results allowed us to conclude that the methylation state of *crtS* has no impact on either RctB binding nor its control on the *ori2* replication initiation.

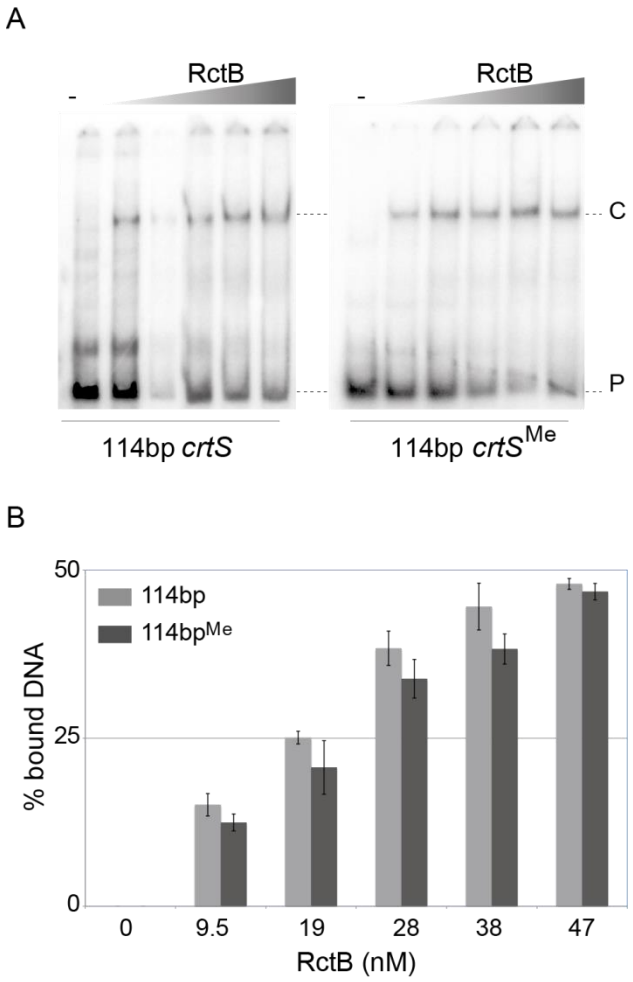

Figure 3. RctB binding to *crtS* is methylation independent

(A) EMSA experiment showing the interaction between increasing concentrations of RctB and *crtS*. Two different probes carrying *crtS* are compared: the methylated (^{Me}) or unmethylated 114bp *crtS*. The unbound DNA (P) and complexed with RctB (C) are represented. **(B)** Quantification of three independent experiments presented in (A), the concentrations in Nano-molar of RctB are presented in the X-axis. Percent of bound DNA (% bound DNA) are equal to [intensity of the shifted band/combined intensities of shifted and unbound DNA band]x100. The grey bars correspond to the unmethylated 114bp *crtS* and the dark grey bars correspond to the methylated *crtS*.

4. The *crtS* 62bp minimal site overlaps with DNase I footprinting of RctB

We next determined the minimal functional sequence of *crtS* by testing its activity on Chr2 replication in *V. cholerae*. To do so, we used a *crtS*-containing DNA fragment of 164bp and reduced it from either side down to 58bp (Figure 4A - left panel). These fragments were inserted specifically in the Tn7 insertion site (*attTn7*) located on Chr1 of *V. cholerae*, prior excision of its own native site (Figure S6). Using dPCR, we measured the copy number variation between Chr1 and Chr2 of non-replicating *V. cholerae* carrying the various *crtS* sizes (Figure 4A - right panel). If *crtS* is active in triggering Chr2 replication, we expect an *ori1*/*ori2* ratio ~1 (e.g. WT). If the active length of *crtS* is disrupted, Chr2 will be lost which will translate into a high *ori1*/ori2 ratio (e.g. 58-bp fragment). Our results show that a 62-bp sequence is sufficient to keep an equal copy number of Chr1 and Chr2 in *V. cholerae* suggesting that the 62-bp sequence is the minimal *crtS* site. The minimal *crtS* site doesn't contain any GATC sites which corroborates with the fact that RctB doesn't require Dam methylation to bind to *crtS*. Moreover, the minimal *crtS* site doesn't contain the putative DnaA binding site (Figure S7A) (20). We compared the binding of *V. cholerae* $DnaA_{Vc}$ to both *ori2* and *crtS* in the presence of ATP and observed that $DnaA_{Vc}$ binds to *ori2* but not to *crtS* (Figure S7B). These results were confirmed *in vivo* in *V. cholerae* mutants with point mutations in the putative DnaA binding site of *crtS* (Figure S7C). We conclude that the DnaA box-like motif on *crtS* is too degenerated (three mismatches to the consensus sequence) to bind DnaA (even in the presence of ATP) and should no longer be referred to as a DnaA box.

We verified that the active 62-bp *crtS* overlap with the localization of the RctB binding site within *crtS* by performing a DNase I footprinting experiment were RctB-bound DNA is protected from DNase I cleavage. Using a non-methylated *crtS*-containing 270-bp linear DNA substrate, we were able to detect a window of RctB protected DNA against the DNase I digestion, (Figure 4B). With increasing amounts of RctB, we only observed two hypersensitive DNase I cleavage sites (RctB, I & II). Upon addition of $DnaK_{Vc}$ and $DnaJ_{Vc}$ chaperones, a region of protection extended from one cleavage site (RctB+DnaK/J, II) in both directions and unraveled a new DNase I hypersensitive cleavage site (RctB+DnaK/J, III). This result suggests that DnaK/J promote RctB binding to *crtS* and that the DNA bound by RctB is distorted. We further used a monomeric mutant of RctB where aspartate 314 is substituted by proline residue (D314P) that disrupts the dimerization process (23). With $RctB_{D314P}$ mutant, the protected region was more discernable and flanked by additional DNase I hypersensitive cleavage sites ($RctB_{D314P}$, IV), and correctly correspond to the results observed with RctB+DnaK/J. The protected window obtained with RctB+DnaK/J and $RctB_{D314P}$ largely overlaps with the 62-bp minimal *crtS* site (Figure S4). These footprint results suggest that RctB preferentially binds to *crtS* as monomers. Note that two hypersensitive cleavage sites (RctB+DnaK/J, I & II) disappear in $RctB_{D314P}$ footprint suggesting that RctB and $RctB_{D314P}$ binding on *crtS* are slightly different. Altogether, these results may suggest that DnaK/J by enhancing RctB monomerization, promote the binding of RctB to *crtS*.

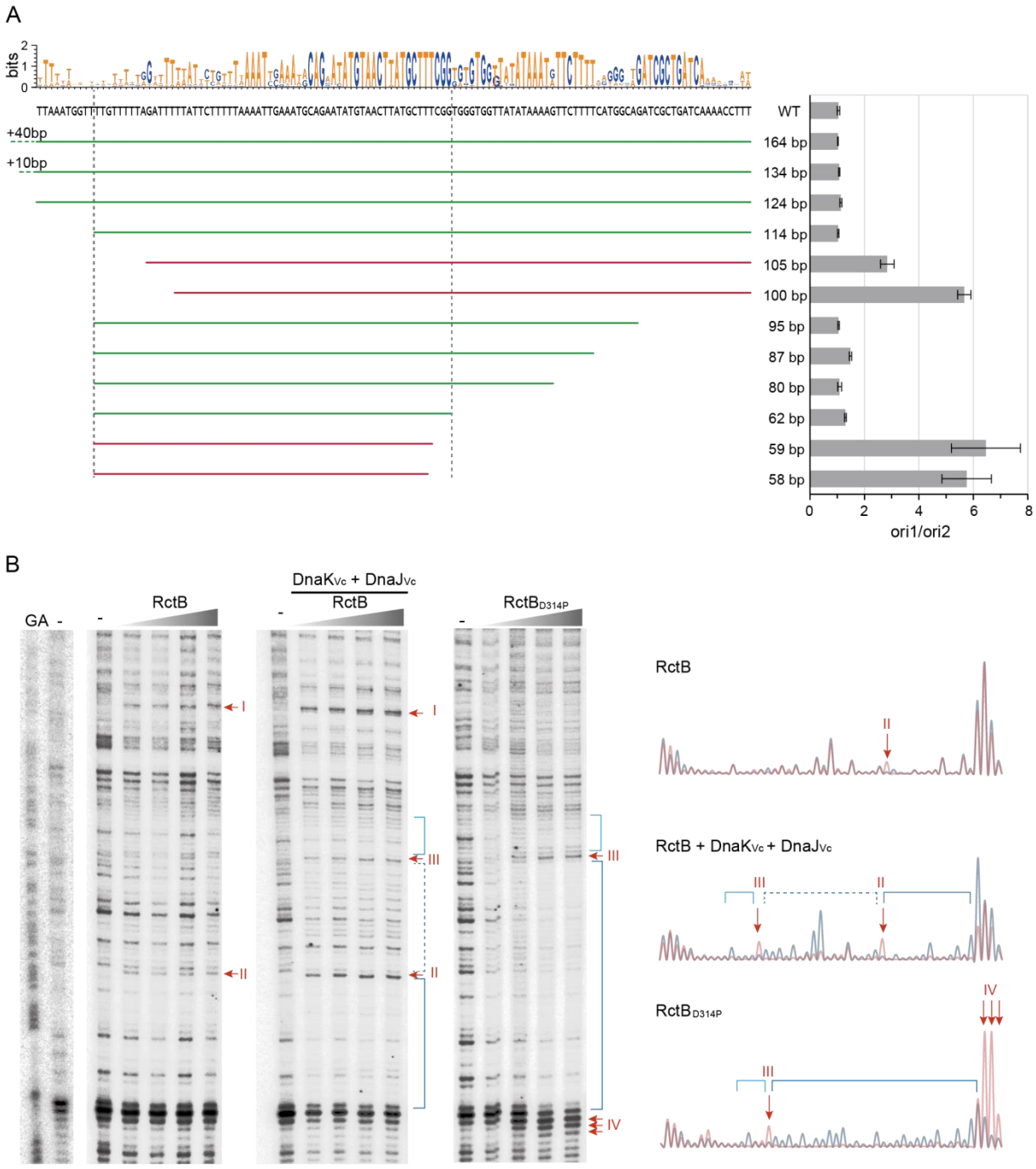

Figure 4. *crtS* minimal functional site in *V. cholerae* largely overlaps its binding site

(A) WebLogo illustration of the 124bp consensus sequence surrounding *crtS* from 28 Vibrionaceae species published with complete assembled genomes on NCBI (Figure S7). The heights of letters within the stack indicates the relative frequency of each base at that position. The sequence under the WebLogo corresponds to V. cholerae N16961 (WT). Histograms representing ori1/ori2 ratios measured by dPCR on the gDNA from non-replicating *V. cholerae* strains carrying various *crtS* sizes (from 164bp down to 58bp). Various length of *crtS* were inserted in *V. cholerae attTn7* site prior deleting the native *crtS* site (Figure S6). Active *crtS* sites (ori1/ori2 ~1) are represented by green lines. Inactive *crtS* sites (ori1/ori2 > 1.5) are represented by red lines. ori1 and ori2 copy number were measured by dPCR on genomic DNA from non-replicating cells (stationary phase) after 16hours growth. All the data represent the mean of three independent experiments (+/- standard deviation). The two vertical grey dash lines indicate the limits of the minimal 62bp functional *crtS* site. **(B)** The DNase I footprinting experiment was performed with an identical increasing concentration of RctB and $RctB_{D314P}$ (from 20nM to 100nM), in the presence of absence of 5nM of $DnaK_{Vc}$ and 5nM of $DnaJ_{Vc}$.

From the left to the right: the G+A chemical sequencing ladder is presented near a digested sequence without protein, the footprint with RctB, RctB+DnaK/J_{Vc} and $RctB_{D314P}$ and the right panel correspond to the quantification of the last lines of each presented gel. The hypersensitive cleavage sites (I, II, III, IV) and the protected windows are indicated on the gels and the quantifications.

5. RctB binds to *crtS* as a monomer

To characterize the binding of RctB on a 54bp *crtS* site inferred from the previous footprint results (Figure 4B), we used EMSA (Figure 5). In the presence of RctB alone, RctB with DnaK/J_{Vc} or $RctB_{D314P}$ and at increasing protein concentration, we observed at least two complexes: C2 and C3 (Figure 5A). We compared the migration of these complexes with RctB and $RctB_{D314P}$ bound to 54bp linear DNA fragments containing a 39-mer motif. This allowed us to conclude that C2 corresponds to the binding of two RctB molecules on *crtS* and that the complex C3 is formed by the binding of a third RctB molecule (Figure 5A, S9). At higher concentration of RctB (+DnaKJ_{Vc}) and $RctB_{D314P}$ an additional complex appeared, C4, which is probably due to the binding of a fourth RctB molecule. Note that C2 complexes formed by RctB and $RctB_{D314P}$ harbor a slight shift of migration, possibly due to the different conformations of the complex, also observed in footprinting experiments (Figure 4B, 5A). The quantification of the EMSA experiments showed that RctB binding to *crtS* was more efficient in presence of DnaK/J_{Vc} or when RctB is present only as a monomer ($RctB_{D314P}$) (Figure 5A). These results, in agreement with the results obtained from the footprint (Figure 4B), allowed us to conclude that RctB binds to *crtS* as a monomer. In presence of $DnaK_{Vc}$ and $DnaJ_{Vc}$ and with increasing concentration of RctB, the C2 and C3 complexes appeared earlier and the C4 is also observed (Figure 5A). This result suggests that the chaperones, in addition to monomerization of RctB, enhance the oligomerization of RctB onto the DNA. We next verified this activity on the methylated iteron and 39-mer. In presence of RctB or $RctB_{D314P}$, the shifted bands of the probes carrying one iteron or one 39-mer corresponding to C1 and C2 showed an identical migration, as described above. Furthermore, $RctB_{D314P}$ showed a higher efficiency to bind the two different sites. These results suggest that RctB binds to the iterons and the 39-mer only as a monomer. At the higher $RctB_{D314P}$ concentration a third band: C3 can be observed. When DnaK/J_{Vc} are added to the reaction with either RctB or $RctB_{D314P}$, the C3 complex is observed at all concentrations and has become majoritarian, suggesting an activation of the RctB oligomerization by DnaK/J_{Vc}. Taken together these results allowed us to conclude that the chaperones DnaK and DnaJ are involved in two-step of RctB modification. First DnaK/J_{Vc} permit the transfer of RctB from its dimeric to its monomeric form and then modify the RctB monomer to enhance its oligomerization onto the DNA.

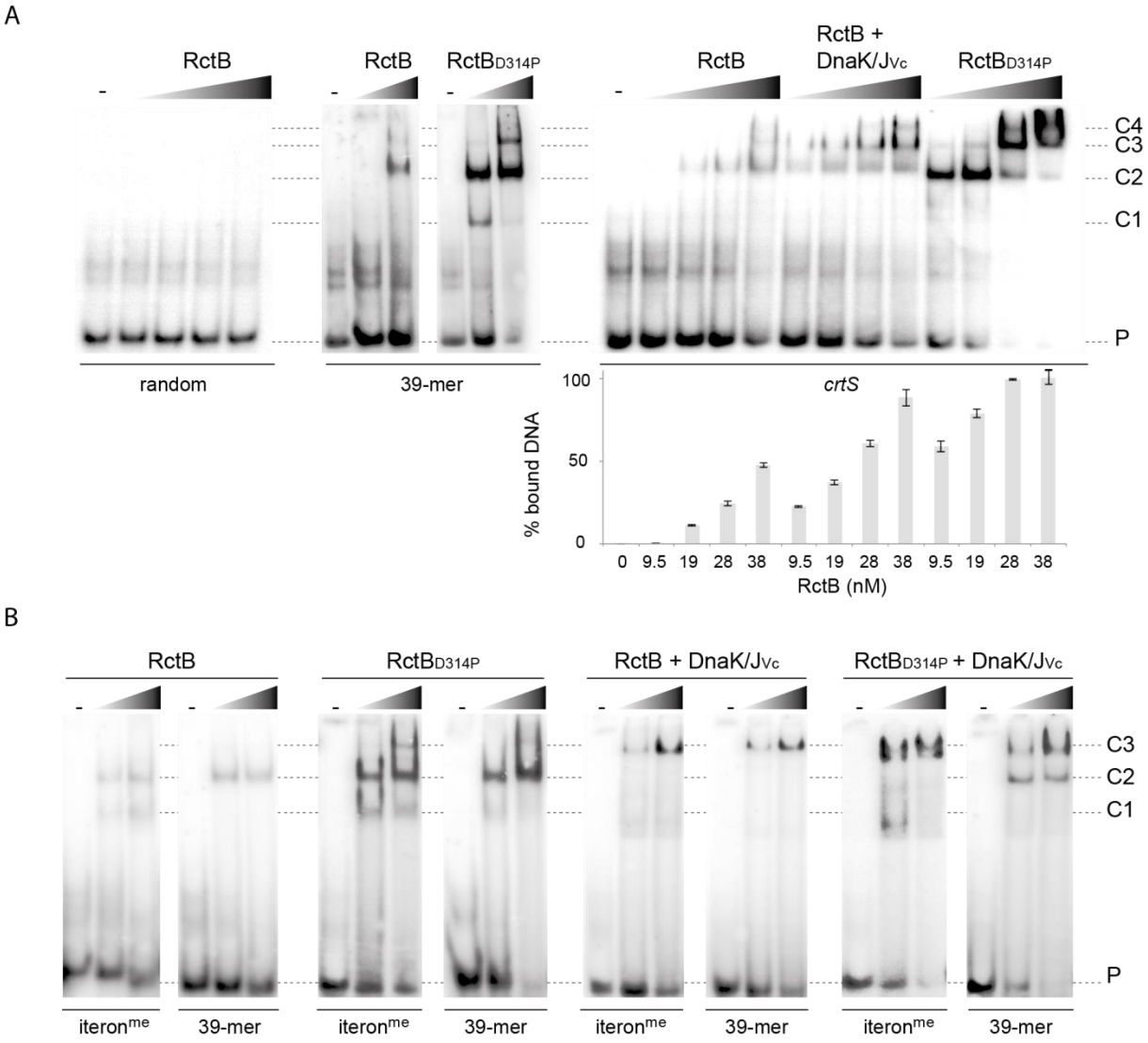

Figure 5. DnaK/J_{Vc} promote the monomerization and the oligomerization of RctB

(A) EMSA experiments with a 54bp DNA probe carrying either a negative control, or the 39-mer, or *crtS*. The unbound DNA (P) and the bound DNA (C1, C2, C3 and C4) are represented. The C1, C2, C3 and C4 complexes correspond to the binding of 1, 2, 3 and 4 RctB molecules, respectively. The histograms corresponds to the quantification of three independent experiments with the 54bp-crtS, the RctB concentration are presented in the x-axis and the DnaK/J_{Vc} concentration were the same as in Figure 4B. **(B)** Comparison of results obtained by EMSA experiments using 40bp probes carrying one methylated iteron (12-mer) or one 39-mer. The RctB and $RctB_{D314P}$ concentration were 19nM and 38 nM. Remaining details are the same as those described in A.

Discussion

crtS controls Chr2 copy number

In our previous study, we looked at the role of *crtS* in replicating cells (31). We observed that the timing of replication of *crtS* determines the timing of initiation of Chr2. Hence the location of *crtS* compared to *ori1* was important in controlling the timing of Chr2 replication. However, we didn't look at the role of *crtS* on Chr2 copy number control. In this study, we measured *ori1*:*ori2* ratios in non-replicating cells to infer the number of Chr2 relative to Chr1. In wild-type *V. cholerae* with a unique *crtS* site, non-replicating cells have an equal number of Chr1 and Chr2 (Figure 4A, WT). When *crtS* is moved closer to *ori1* in the *attTn7* site (VC0487), we observed an equal number of Chr1 and Chr2 like in WT (Figure 4A, 164bp). Therefore the location of *crtS* compared to *ori1* has no impact on Chr2 copy number. When we increase the number of *crtS* sites, this balance is altered and Chr2 number exceed Chr1 number (Figure 1). However, whether we added a second site near the origin or the terminus of Chr1, the effect was the same (Figure 1E, VC0023 vs. VC0963). This confirms that *crtS* location has no effect on Chr2 copy number. In absence of a functional *crtS*, Chr2 copy number relative to Chr1 dramatically drops (Figure 4, 58bp) which is coherent with Chr2 loss already observed in a population of *crtS* deleted mutants (31). Having a unique copy of *crtS* is important to maintain an equal ratio of Chr1 and Chr2 suggesting that *crtS* limits Chr2 replication to one round per cell generation. This study demonstrates that *crtS* not only controls the timing of initiation of Chr2 but also regulates its copy number.

We also observed in *E. coli*, that by adding up to four chromosomal copies of *crtS*, we gradually increased the copy number of an *ori2*-driven plasmid (pORI2). This demonstrates that just by providing *crtS* and ori2 in *E. coli*, we can reconstitute a controlled replication system where the copy number of an *ori2*-driven plasmid will depend on the number of *crtS* chromosomal sites. We further observed that *crtS* and parAB2 have an additive effect on the control of pORI2 copy number (Figure 2B). Indeed in the presence of single *crtS* site, an *ori2*-driven plasmid with a partition system (ParAB2, parS2) is very stable in absence of antibiotic selection with less than 1% loss per cell generation (Figure 2A). The cumulative stabilisation effect of *crtS* and parAB2 is higher than the cumulative effect of 4 *crtS* sites in absence of parAB2 (Figure 1B, 2A). This ability of *crtS* to regulate pORI2 copy number displays obvious interesting potentials for biotechnological applications such as controlling the dosage of genes of interest encoded on an *ori2*-driven plasmid by simply modifying the *E. coli* host (carrying various number of *crtS*) or keeping an artificial plasmid stable without requiring antibiotic selection.

Furthermore, we saw an important difference between *E. coli* and *V. cholerae* in the *crtS*-mediated control of *ori2* copy number. While we observed an exponential increase of pORI2 copy number as a function of *crtS* number in *E. coli*, Chr2 copy number slowly increased in a logarithmically manner in *V. cholerae* (Figure S2B). In strains with 3 *crtS*, pORI2 reached a copy number of ~6 in *E. coli* while Chr2 only displayed a copy number of ~2 in *V. cholerae*. This suggests that Chr2 copy number is restricted in *V. cholerae*. This could be explained by the physiological burden of having multiple Chr2 (e.g.

higher dosage of toxic genes…). However, we didn't see any fitness or morphological defects in *V. cholerae* mutants carrying 2 or 3 *crtS* sites (data not shown). We can also envisage that sister chromatids have to compete for limiting replication factors, such as proteins responsible for replication initiation and/or pools of precursors that are required for DNA synthesis. This is however unlikely, since the same competition should occur for pORI2 and it doesn't appear to be limiting in *E. coli*. Another plausible explanation is the presence on Chr2 of a locus located 40 kb away from *ori2* which negatively regulates replication at *ori2* (20). It would be interesting to see if this locus would restrain pORI2 copy number in *E. coli* as it does in *V. cholerae*.

Another observation is that Chr2 copy number doesn't increase linearly. For example, the ori2/ori1 ratio of non-replicating *V. cholerae* with 2 *crtS* sites equals ~1,7, a decimal number. This suggests the existence of heterogeneity in the population with cells containing more chromosomes than others. We previously observed cell-to-cell variation in the replication dynamics of *V. cholerae* with 2 *crtS* sites (asymmetric cell division resulting in daughter cells that differ in both size and Chr2 copy number) (31). We speculate that this heterogeneity may reflect a relaxation of the replication cell cycle checkpoint.

<u>*crtS* minimal functional site</u>

Since we observed *ori2* replication control discrepancies between *E. coli* and *V. cholerae* or between an *ori2*-driven plasmid and Chr2, we decided to determine the minimal active *crtS* sequence in its native host on the chromosome. We found a minimal chromosomal *crtS* sequence of 62bp in V. cholerae. Surprisingly, some DNA motifs outside the minimal *crtS* site are very conserved (Figure S8) and for this reason these motifs were expected to be important. However, their deletion or mutation have no consequences on *crtS* activity (Figure S4, S5, S7). The minimal 62bp *crtS* site excludes all the conserved GATC methylation sites, suggesting that Dam methylation is not playing a role in the *crtS* mediated activation of *ori2* upon passage of the replication fork (Figure 4). This was confirmed by mutating the GATC sites upstream and downstream of the 62bp (Figure S5). Furthermore, we showed that RctB indifferently binds to methylated and non-methylated *crtS* sequences (Figure 3). The minimal 62bp *crtS* site also excludes the putative DnaA box. We further mutated this box and confirmed that it is not important for *crtS* activity. The *crtS* putative DnaA-box has three mismatches compared to the *ori1* and *ori2* DnaA-boxes. We show that DnaA does not bind to *crtS in vitro* (Figure S7). The putative DnaA-box in *crtS* is probably too degenerated to permit the binding of DnaA. However, we show here the first evidence of DnaA binding to *ori2* (Figure S7). The DnaA box found in ori2 was shown to be essential to initiate the replication initiation of the Chr2 (14). Nevertheless, the exact implication of DnaA in *ori2* replication control is still unknown. From our knowledge on the replication control of iteron-containing plasmids (36), we can hypothesize that DnaA could be implicated in the stabilization of the RctB complex opening the A-T rich region, or could be involved in the recruitment of the other replisome components.

This 62bp minimal sequence is different from the 70bp minimal *crtS* site found in *E. coli* (20). Both sequences only partially overlap (Figure S4). It appears that the 11bp upstream of the 70bp is crucial

for *crtS* proper activity in *V. cholerae* and not important in *E. coli*. On the other hand, the *crtS* putative DnaA box is essential in *E. coli* but is not important in *V. cholerae* for *crtS* activity (Figure 4, S4). Multiple reasons could explain why the *crtS* minimal sequences differ such as the use of different hosts, the use of an artificial plasmid system to test *ori2* replication and the use of a plasmid containing *crtS* in *E. coli* instead of using a chromosomal site. We also observed divergent results when complementing a *crtS* deleted mutant of *V. cholerae* with either *crtS* on the chromosome or on a plasmid (data not shown).

This minimal 62bp *crtS* site largely overlaps with the protected window obtained with RctB+DnaK/J and $RctB_{D314P}$ (Figure 4B, S4). However few bases pairs are protected against the Dnase I outside the 62bp active *crtS* site. These bases pairs are not required to the *in vitro* binding observed with EMSA experiments (Figure 5, S4). Thus, we consider these bases pairs as resulting from a non-specific interaction between RctB and the DNA.

Several monomers of RctB can bind to *iteron, 39-mer and crtS*

The RctB binding activity to *crtS* allowing to correctly characterize this interaction was never shown. In this study, we provide the first characterization of a direct interaction between RctB and *crtS*.

By comparing the binding of RctB and $RctB_{D314P}$ on *crtS*, we clearly observed that RctB preferentially binds to *crtS* as a monomer (Figure 5A). We observed the same for RctB binding to iterons and 39-mer. In Figure 5B, the C1 and C2 complexes formed by RctB and $RctB_{D314P}$ on iterons and 39-mer harbor an identical migration shift. These results together, along with the RctB structural data (23,25), allow us to say that RctB binds to iterons, 39-mers and *crtS* preferentially under its monomeric form. Besides, the region of protection in presence of $RctB_{D314P}$ and RctB+DnaKJ is too large for the binding of one monomer suggesting that more than one RctB binds to *crtS*.

In all cases, the presence of *V. cholerae* DnaK and DnaJ increased the efficiency of RctB binding to its DNA substrates (Figure 5). In iteron-containing plasmids, the chaperones favor monomerisation of plasmid initiators and thereby increase monomer binding to the origin. However, monomers also need to be remodeled to promote iteron binding (37). This could also be the case for RctB. Indeed, the addition of DnaK/J led to the apparition of an additional complex between RctB with either the iterons or the 39-mers (Figure 5B). This was also observed with $RctB_{D314P}$, suggesting the DnaK/J do not only favor RctB monomerization but also remodel RctB to form higher order complexes. We propose the DnaK/J may remodel RctB monomers to further promote the binding of additional RctB monomers. Indeed, we saw that the number of additional DNA/RctB complexes (C1, C2, C3, C4) depends on the length of the DNA containing the RctB-binding site (40bp or 54bp) (Figure 5).

Such observation of RctB was never reported with the addition of DnaK/J. In our experiments we used purified *V. cholerae* DnaK and DnaJ. To our knowledge, previous reported work has always been performed using DnaK and DnaJ from *E. coli*. Comparing the sequences of DnaK from *E. coli* and from *V. cholerae* reveals that the C-terminal extremities of both proteins share only 62% identity. This

observation suggests that species-specific interactions between $DnaK_{Vc}$ and RctB allow for the *in vitro* observation of RctB remodeling that is not observed using the *E. coli* chaperones.

In *V. cholerae*, it appears that the chaperones DnaK and DnaJ are the master regulator of the RctB interaction with its binding sites. Whatever the site, RctB has to be monomerized by DnaK/J to enhance its binding activity. On all its substrates, we show that RctB binds under its monomeric form and further promote the binding of additional RctB monomers. Moreover, DnaK/J could remodel RctB monomers to promote their oligomerization onto DNA after their initial binding. In the case of *crtS*, we propose that RctB monomers oligomerize on Chr1 from *crtS* (the nucleation site) and further trigger Chr2 replication by a replication-dependent mechanism that is still unclear.

Material and Methods

Bacterial strains and plasmids

Bacterial strains, plasmids and primers used in this study are listed in Table S1, S2, S3. Details are given in the Supplementary Material.

Genome editing by co-transformation

Insertions of point mutations in *crtS* were performed according to the MuGENT procedure described in (38). Details are given in the Supplementary Material.

Tn7 transposition

crtS sites of various lengths were transposed into the unique Tn7 attachment site (*attTn7*) of *V. cholerae*, located near VC0487 on Chr1. Briefly, *crtS* sites were inserted between Tn7 recombination sites contained in a shuttle vector (Figure S6, pTn7::*crtS*) (Table S1, pMVM5). *crtS* containing shuttle vectors were then conjugated along with a helper plasmid (Figure S6, pMVM1) in the recipient strain, MV250. pMVM1 encodes for TnsABCD that promote transposition into *attTn7*, at a high frequency (39). The recipient V. cholerae strain, MV250, has its native *crtS* site flanked by frt recombination sites. Once another copy of crtS was inserted in *attTn7*, the native *crtS* was excised using a Flipase encoding plasmid, pMP108 (Table S1).

Digital PCR quantification of DNA loci

The absolute quantification of (*ori1*, *ori2*) and (oriC, pORI2) was performed in multiplex by digital PCR (Stilla Technologies, Villejuif, France) and used to generate ratios (ori2/ori1, pORI2/oriC) (33). Primers and probes are listed in Table S2. Details are given in the Supplementary Material.

Plasmid stability assay

Plasmid stability assays were performed by growing bacteria in MH at 37°C under agitation for 60 or 80 generations. Liquid cultures grown in absence of antibiotic selection were spread every 10 or 20

generations onto MH and MH containing chloramphenicol agar plates to determine the percentage of cells harboring plasmid (Figure S1). Details are given in the Supplementary Material.

Proteins purification

Expression plasmids (pFF066, pFF067, pFF072, pFF078 and pFF079) were used to transform *E.coli* BL2-D3 strain. The resulting strains were grown in LB to an OD600 of 0.6. After 42°C heat chock, protein expression was performed at 16°C and induced with 0.1mM IPTG for at least 8h. Lysis was performed in a buffer-P (50 mM Tris-HCl pH=8, 300 mM Nacl, 10% glycerol) complemented with 0,1mg/ml lysozyme and EDTA free protease inhibitor cocktail (Roche) for 1h30min on ice. After sonication and centrifugation (1h at 20.000 g), the soluble fraction was submitted to chromatography on nickel (1ml His-trap column, GE) using an imidazole gradient in buffer-P. The eluted proteins was then subject to an exclusion dialyze against buffer-S (50 mM Tris HCl pH=8, 500 mM NaCl, 20% glycerol, 1 mM EDTA, 1 mM DTT). After verification on NuPAGE bis-tris protein gel (Invitrogen), proteins were considered as more than 90% pure and store at -80°C (Figure S9).

***In vitro* experiments**

For Electrophoretic Mobile Shift assays (EMSA), the 70-bp and 114-bp *crtS* variant are amplified by PCR and purified by agarose gel electrophoresis. The methylated DNAs are produced *in vitro* using the *E.coli* Dam methylase following the provided protocol (Biolabs).These subtracts, as the other synthetic oligonucleotides carrying the iteron, 39-mer and *54-crtS*, were 5' end labeled with [γ-^{32}P] ATP and T4 DNA polynucleotide kinase. Binding reaction were carried out in a buffer containing 25 mM Tris-HCl pH=8, 250 mM NaCl, 2.5 mM $MgCl_2$, 10% glycerol, 0.5 mM EDTA, 0.5 mM DTT, 0.1 mg/ml BSA, 1 mg of poly(dI-dC) in the presence of 5000 cpm of labeled DNA and the indicated protein concentrations. The reactions were incubated at 30°C for 30min, analyzed by electrophoresis in 5% polyacrylamide native gel run in 1X TBE, then dried and analyzed with the Typhoon FLA 9500 laser scanner.

For the DNAse I footprinting analysis, 20 000 cpm of 270-bp *crtS* carrying-DNAs labeled at the 5' end with [γ-^{32}P] were incubated with various amounts of proteins (RctB, $RctB_{D314P}$, $DnaK_{Vc}$, $DnaJ_{Vc}$). Reaction was performed as for the EMSA. After 30min of incubation at 30°C, the partial digestion of the DNA was initiated by adding DNAse I empirically diluted (1/800). The mixture was incubated 30s at room temperature and stopped by adding the buffer-Stop (0.4M sodium acetate, 10mg/ml ctDNA, 2.5 mM EDTA). DNAs were then ethanol precipitated and re-suspended in 6 µL of loading buffer and separated by electrophoresis in an 8% polyacrylamide denaturing sequencing gel run in 0.6X TBE. Gels were dried and analyzed with the Typhoon FLA 9500 laser scanner.

SUPPLEMENTARY FIGURES

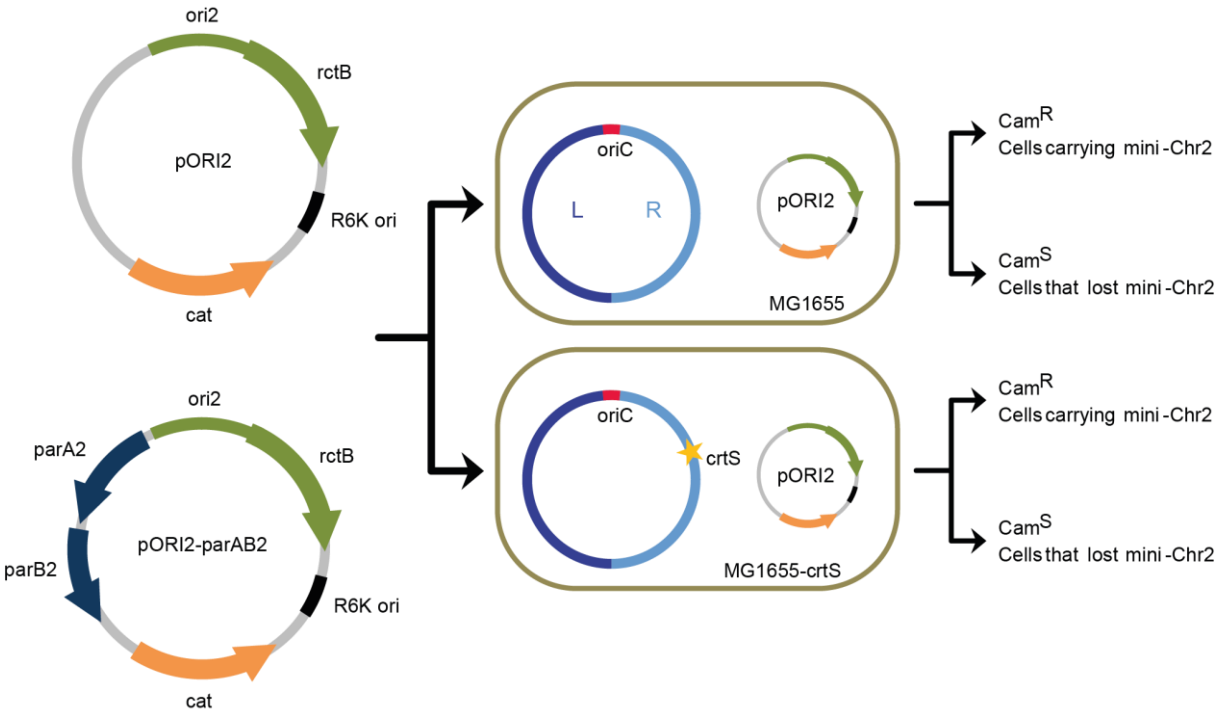

Figure S1. Plasmid stability assay

pORI2 or pORI2-parAB2 are ori2-driven plasmids that can only initiate replication from ori2 in MG1655. Bacteria were grown for 60 to 80 generations without selection for the plasmid. Every 10 or 20 generations, cells were platted on non-selective media and 100 colonies were replica-plated on selective media to check for the presence or absence of the plasmid (see Material and Methods).

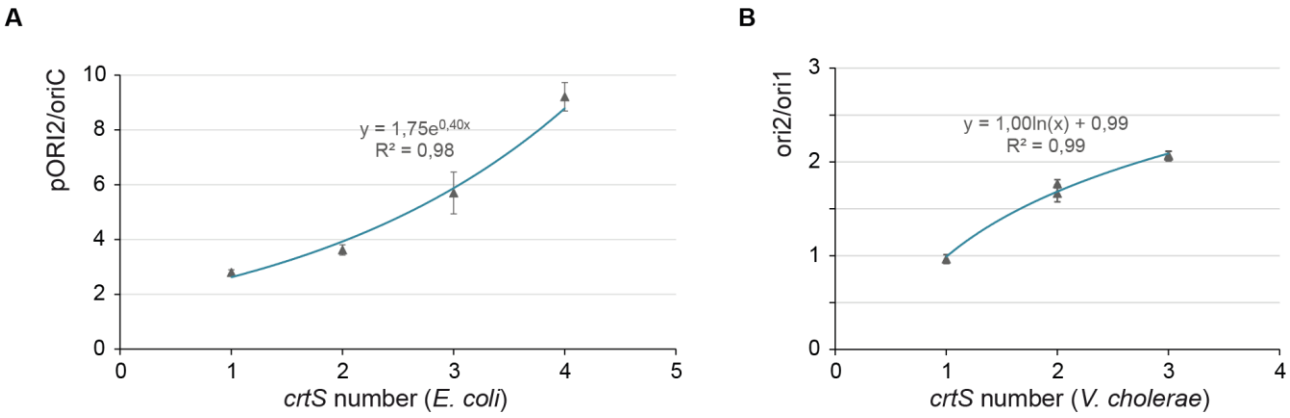

Figure S2. Effect of crtS copy number on ori2 replication in E. coli and V. cholerae

(A) Exponential increase of pORI2 copy number as a function of *crtS* number in *E. coli.* **(B)** Logarithmic increase of Chr2 copy number as a function of *crtS* number in *V. cholerae*.

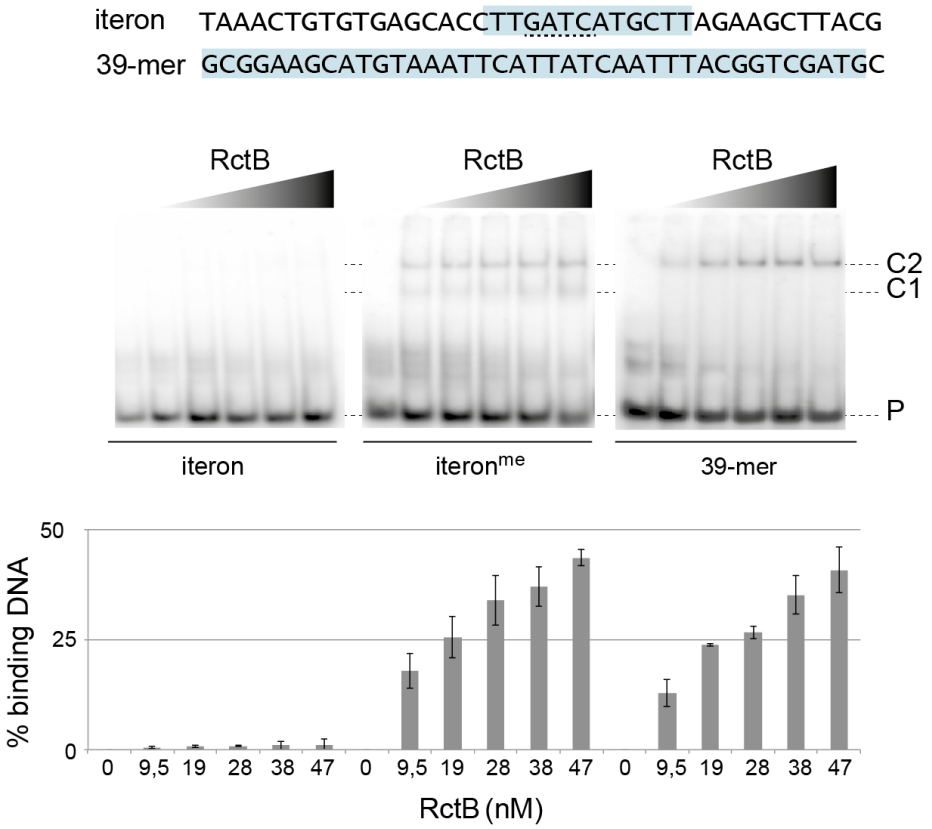

Figure S3. Binding properties of our purified RctB protein onto iterons and 39-mer containing linear DNA

EMSA of RctB using two radiolabeled DNA probes of the same length (40bp) containing either an iteron (unmethylated or methylated ^{me}) or a 39-mer. RctB binding to the iteron is Dam-methylation dependent and the binding of RctB to the 39-mer is Dam-methylation independent. Quantification of three independent experiments, the concentrations in Nano-molar of RctB are presented in the X-axis. Percent of bound DNA (% bound DNA) are equal to [intensity of the shifted band/combined intensities of shifted and unbound DNA band]x100. RctB binding to the iteron forms two complexes (C1 and C2), while the binding of RctB to the 39-mer forms one complex (C2). We observed that the higher complex (C2) formed with the iteron and the 39-mer harbors the same migration shift. This observation could only suggest that the C1 complex corresponds to the binding of one RctB and that the C2 complexes correspond to the binding of two RctB either as monomers or as a dimer. However, we further showed in Figure 5, that C2 corresponds to the binding of two RctB monomers.

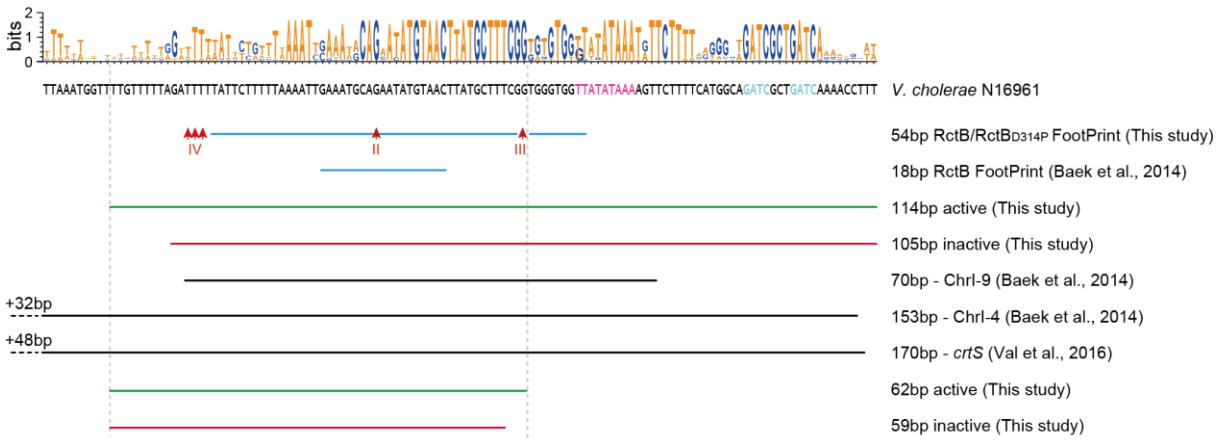

Figure S4. Comparison of *crtS* sequences from this study and previously reported

WebLogo illustration of the 124bp consensus sequence surrounding *crtS* from 28 Vibrionaceae species published with complete assembled genomes on NCBI (Figure S7). The heights of letters within the stack indicates the relative frequency of each base at that position. The sequence under the WebLogo corresponds to V. cholerae N16961 (WT). Active and inactive *crtS* sites (from Figure 4A), are represented by green and red lines, respectively. The hypersensitive cleavage sites (II, III, IV) and the protected windows are indicated in blue (from Figure 4B). Previously reported *crtS* sites are represented in black. The two vertical grey dash lines indicate the limits of the minimal 62bp functional *crtS* site.

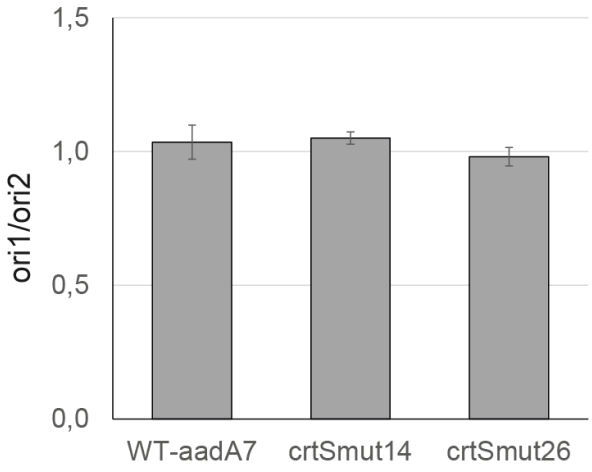

Figure S5. Mutations in *crtS*-flanking GATC sites don't impact Chr2 copy number

Histograms representing ori1/ori2 ratios in V. cholerae strains carrying point mutations in GATC sites flanking *crtS*. WT-addA7 (control strain with aadA7 cassette used for co-transformation of crtS point mutations); crtSmut14 : one GATC site mutated for GAAC upstream of crtS; crtSmut26 : 4 GATC sites mutated for GAAC downstream of crtS.

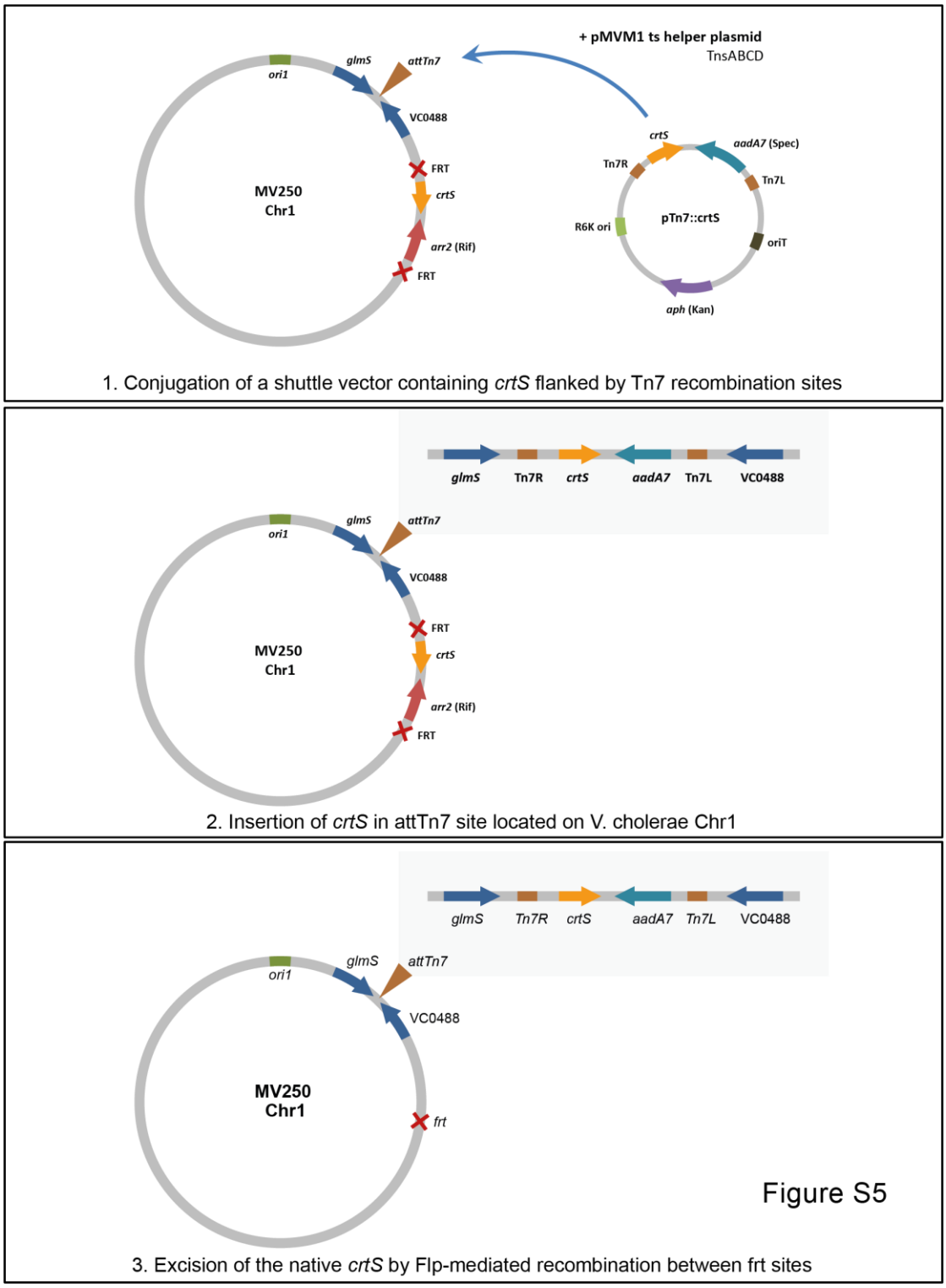

Figure S6. Tn7-mediated insertion of ectopic crtS site in the attTn7 site of V. cholerae Chr1

crtS sites were first cloned between Tn7 recombination sites contained in a shuttle vector (pTn7::*crtS*). *crtS* containing shuttle vectors were then conjugated along with a helper plasmid (pMVM1) in the recipient strain, MV250. pMVM1 encodes for TnsABCD that promote transposition into *attTn7*, at a high frequency. The recipient V. cholerae strain, MV250, has its native *crtS* site flanked by frt recombination sites. Once another copy of crtS was inserted in *attTn7*, the native *crtS* could be excised using a Flipase encoding plasmid. It is important to delete crtS at the end to prevent the rapid acquisition of compensatory mutations previously observed in crtS deleted mutants (31).

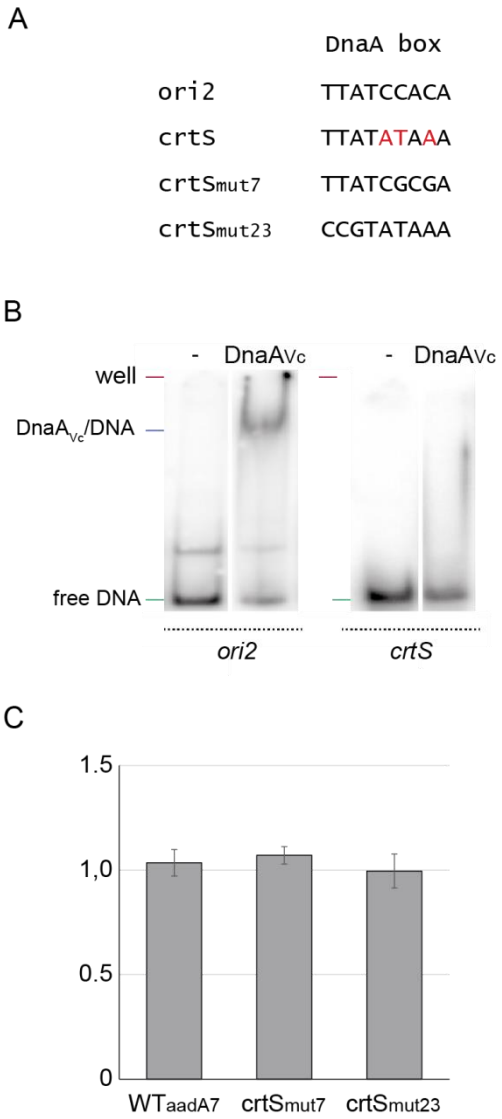

Figure S7. DnaA doesn't bind to crtS and mutations in the conserved formerly called DnaA box don't impact Chr2 copy number

(A) Alignment of *ori2* DnaA box, *crtS* putative DnaA box (three mismatches to the consensus sequence are shown in red) and mutants studied in (C). **(B)** EMSA of *V. cholerae* $DnaA_{Vc}$ to both *ori2* and *crtS* in the presence of ATP. $DnaA_{Vc}$ binds to *ori2* but not to *crtS*. **(C)** Histograms representing ori1/ori2 ratios in V. cholerae strains carrying point mutations in the putative DnaA box. WT-addA7 (control strain with aadA7 cassette used for co-transformation of crtS point mutations); crtSmut7 and crtSmut23 mutations are shown in (A).

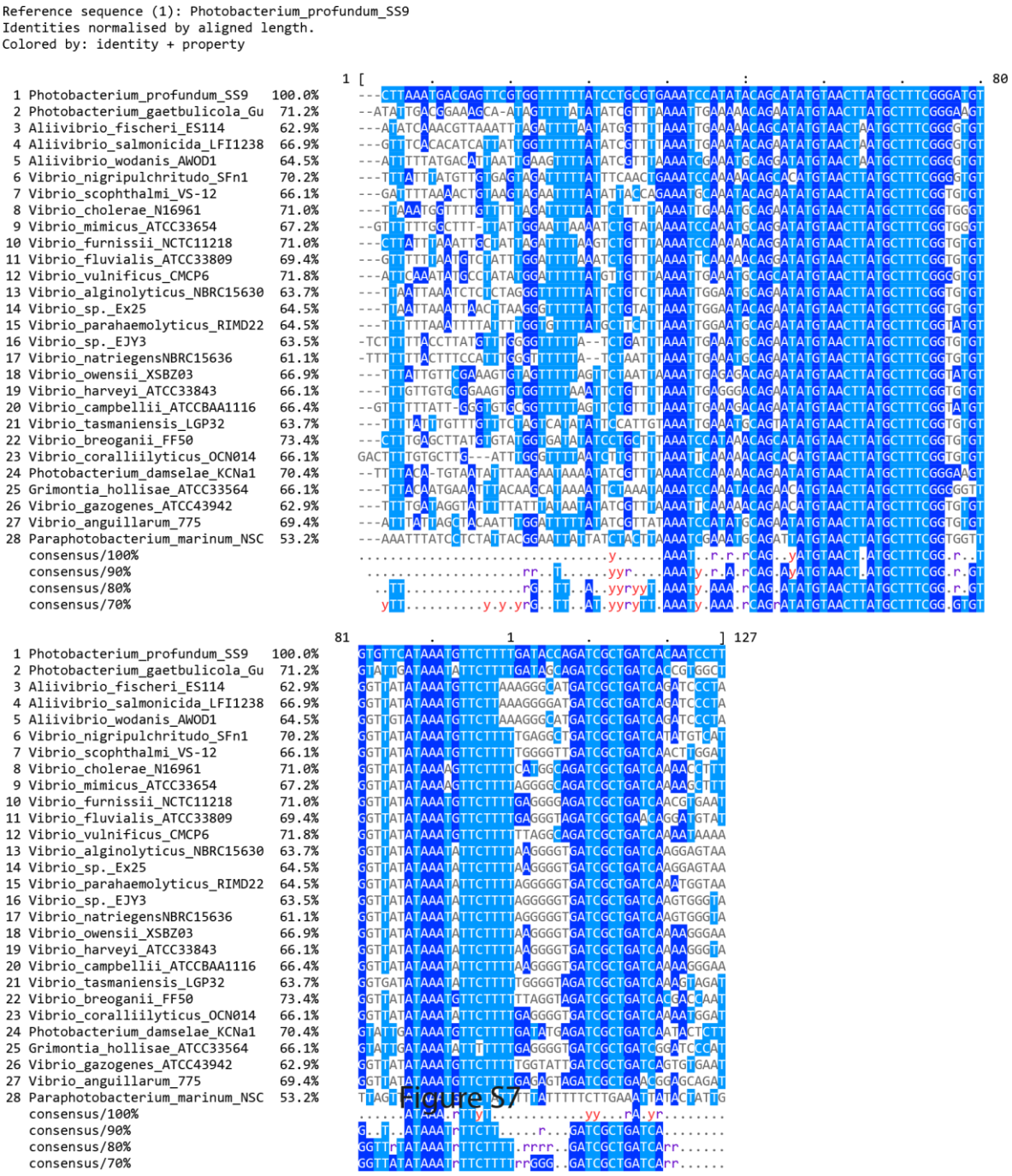

Figure S7

Figure S8. ClustalW alignment of 124bp sequences surrounding crtS taken from 28 complete *Vibrio* genome sequences (NCBI).

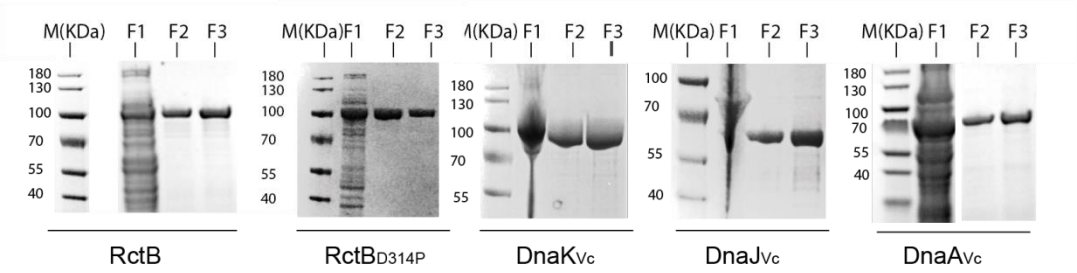

Figure S9. Purified proteins used in this study

SUPPLEMENTARY TABLES

Table S1. List of plasmids and bacterial strains

Name	Relevant genotype or features	Reference
Plasmids		
pSW23T	*oriV*$_{R6K\gamma}$ *oriT*$_{RP4}$; *cat*	(40)
pSW29T	*oriV*$_{R6K\gamma}$ *oriT*$_{RP4}$; *aph*	(40)
pMP7 (pSW7848)	Suicide plasmid for allele exchange - *oriV*$_{R6K\gamma}$ *oriT*$_{RP4}$ *araC* P$_{BAD}$-*ccdB* ; *cat*	(41)
pMVM1	Tn7 helper – *ori*$_{pSCS101}$ *repA*$_{ts}$ *oriT*$_{RP4}$ *araC* P$_{BAD}$-*tnsABCD* ; *bla*	This study
pMVM5	Tn7 shuttle – pSW29T :: [Tn7R-*aadA7*-$_{MCS}$-Tn7L]	This study
pORI2	pSW23T :: *ori2*	This study
pORI2-parAB2	pSW23T :: *ori2-parAB2*	This study
pMVM19	pMVM5 :: *crtS*$_{164}$	This study
pMVM16	pMVM5 :: *crtS*$_{134}$	This study
pMVM14	pMVM5 :: *crtS*$_{124}$	This study
pMVM26	pMVM5 :: *crtS*$_{114}$	This study
pMVM24	pMVM5 :: *crtS*$_{105}$	This study
pMVM3	pMVM5 :: *crtS*$_{100}$	This study
pMP203	pMVM5 :: *crtS*$_{95}$	This study
pMP207	pMVM5 :: *crtS*$_{87}$	This study
pMP205	pMVM5 :: *crtS*$_{80}$	This study
pMP211	pMVM5 :: *crtS*$_{62}$	This study
pMP212	pMVM5 :: *crtS*$_{59}$	This study
pMP222	pMVM5 :: *crtS*$_{58}$	This study
pMP108	*ori*$_{pSCS101}$ *repA oriT*$_{RP4}$ *araC* P$_{BAD}$-*flp* ; *bla*	This study
pFF066	pET-32b :: *dnaA*$_{Vc}$	This study
pFF067	pET-32b:: *rctB*	This study
pFF072	pET-32b :: *rctB*$_{D314P}$	This study
pFF078	pET-32b :: *dnaJ*$_{Vc}$	This study
pFF079	pET-32b :: *dnaK*$_{Vc}$	This study
E. coli		
Π3813	B462 Δ*thyA*::(*erm-pir116*)	(42)
β3914	β2163 *gyrA462 zei-298*::*Tn10*	(42)
MG1655	E. coli K-12 F– λ– *ilvG– rfb*-50 *rph*-1	Lab stock
MG1655-1crtS	MG1655 *lacZ* :: *crtS*$_{170}$	This study
MG1655-2crtS(L/R)	MG1655 *lacZ* :: *crtS*$_{170}$ – [*hycI-crtS-ascB*]	This study
MG1655-2crtS(R/R)	MG1655 *lacZ* :: *crtS*$_{170}$ – [*yaiL-crtS-frmB*]	This study
MG1655-3crtS	MG1655 *lacZ* :: *crtS*$_{170}$ – [*hycI-crtS-ascB*] – [*yaiL-crtS-frmB*]	This study

MG1655-4crtS	MG1655 *lacZ* :: $crtS_{170}$ – [*hycI-crtS-ascB*] – [*yaiL-crtS-frmB*] – [*hypF-crtS-ygbD*]	This study
V. cholerae		
WT (= $crtS_{VC0764}$)	N16961rep *: Vibrio cholerae* serotype O1 biotype El Tor strain N16961 – repaired for hapR	(43)
$crtS_{VC0764\text{-}VC0023}$	WT *with crtS* inserted between VC0023/VC0024	This study
$crtS_{VC0764\text{-}VC0963}$	WT *with crtS* inserted between VC0963/VC0964	This study
$crtS_{VC0764\text{-}VC0023\text{-}VC0487}$	$crtS_{WT/VC0023}$ *with* $crtS_{114}$ inserted in attTn7 (VC0487)	This study
$crtS_{VC0764\text{-}VC0963\text{-}VC0487}$	$crtS_{WT/VC0963}$ *with* $crtS_{114}$ inserted in attTn7 (VC0487)	This study
MV250	N16961rep with crtS site flanked by frt sites (crtS excision using Flippase)	This study
WTΔ*crtS*-$crtS_{164}$	MV250 *with* $crtS_{164}$ inserted in attTn7 and deleted for native crtS	This study
WTΔ*crtS*-$crtS_{134}$	MV250 *with* $crtS_{134}$ inserted in attTn7 and deleted for native crtS	This study
WTΔ*crtS*-$crtS_{124}$	MV250 *with* $crtS_{124}$ inserted in attTn7 and deleted for native crtS	This study
WTΔ*crtS*-$crtS_{114}$	MV250 *with* $crtS_{114}$ inserted in attTn7 and deleted for native crtS	This study
WTΔ*crtS*-$crtS_{105}$	MV250 *with* $crtS_{105}$ inserted in attTn7 and deleted for native crtS	This study
WTΔ*crtS*-$crtS_{100}$	MV250 *with* $crtS_{100}$ inserted in attTn7 and deleted for native crtS	This study
WTΔ*crtS*-$crtS_{95}$	MV250 *with* $crtS_{95}$ inserted in attTn7 and deleted for native crtS	This study
WTΔ*crtS*-$crtS_{87}$	MV250 *with* $crtS_{87}$ inserted in attTn7 and deleted for native crtS	This study
WTΔ*crtS*-$crtS_{80}$	MV250 *with* $crtS_{80}$ inserted in attTn7 and deleted for native crtS	This study
WTΔ*crtS*-$crtS_{62}$	MV250 *with* $crtS_{62}$ inserted in attTn7 and deleted for native crtS	This study
WTΔ*crtS*-$crtS_{59}$	MV250 *with* $crtS_{59}$ inserted in attTn7 and deleted for native crtS	This study
WTΔ*crtS*-$crtS_{58}$	MV250 *with* $crtS_{58}$ inserted in attTn7 and deleted for native crtS	This study
WT-aadA7	WT-aadA7, spectinomycin resistance cassette used for natural co-transformation to co-select for point mutations elsewhere on the genome	This study
$crtS_{mut14}$	Point mutation in a GA**T**C motif to a GA**A**C upstream of crtS by co-transformation with aadA7	This study
$crtS_{mut26}$	Point mutations in four GA**T**C motifs to four GA**A**C downstream of crtS by co-transformation with aadA7	This study
$crtS_{mut7}$	Point mutation in TTATATAAA motif to TTAT**CGCG**A in crtS by co-transformation with aadA7	This study
$crtS_{mut23}$	Point mutation in TTATATAAA motif to **CCGT**ATAAA in crtS by co-transformation with aadA7	This study

Table S2. Primer and probe sequences used in digital PCR reactions.

Assay	**Target**	**Primers** (5 '→ 3')	**Probe** (5 '→ 3')
ori1	VC2774 Chr1 (V. cholerae)	GCTGCTCGACAAATGGAAC	[FAM]-TCCGATGGAAATGTTGGTGAAACACATTCT-[BHQ1]
		AAGATGCGGACTGACCAC	
ori2	VCA002 Chr2 (V. cholerae)	TGTCTCGTCGTCATACCG	[HEX]-ATCTGATCCGCGAACTTCGTCGTCTCT-[BHQ1]
		CTTCACTCCCCTTCCCTTC	
oriC	*atpB* (E. coli)	CCACCGAGAAGAACATGGAG	[FAM]-ATTGTCCAGAAGGTGGCTGGGGGGTTTT-[BHQ1]
		GCCGCAGGATTACATAGGAC	
pORI2	pSW23T (plasmid)	TTATGGTGAAAGTTGGAACCTC	[HEX]-GCCGATCAACGTCTCATTTTCGCCA-[BHQ1]
		GCCGAATAAATACCTGTGACG	

Table S3. Primers used to amplify ori2 and crtS

Plasmid constuct or DNA substrate	**Primer name**	**Primers** (5 '→ 3')
pORI2	FM17	CTATTATTTAAACTCTTTCCTGATACCAAACGAACAAAGTTAAG
	FM18	TACGTAGAATGTATCAGACTAGTCGGGATAGAAAGCACTG
pORI2-parAB2	FM19	CTATTATTTAAACTCTTTCCGCCTAAGAAACCAATAAGGCTAAG
	FM18	TACGTAGAATGTATCAGACTAGTCGGGATAGAAAGCACTG
pSW23T	FM15	GGAAAGAGTTTAAATAATAGGGCCGCTCTAGAACTAGTGG
	FM16	AGTCTGATACATTCTACGTATTCCCATGTCAGCCGTTAAG

SUPPLEMENTARY MATERIAL AND METHODS

Strain constructions

Bacteria were grown in LB broth (Lennox) or Mueller Hinton broth. Antibiotics were used at the following concentrations: carbenicillin, 100 µg/ml; chloramphenicol, 25 µg/ml for *Escherichia coli* and 5 µg/ml for *Vibrio cholerae*; kanamycin, 25 µg/ml; spectinomycin, 100 µg/ml; rifampicin, 1µg/ml. Diaminopimelic acid was used at 0.3 mM, thymidine (dT) at 10µg/ml, glucose at 1% and arabinose at 0.2% (w/v). For cloning purposes in R6K *γ-ori*-based suicide vector, Π3813 was used as a plasmid host (42). For conjugal transfer of plasmids to *V. cholerae* strains, *E. coli* β3914 was used as the donor (42). Natural transformation was performed according to the procedure described in (44).

Genomic DNA was extracted using DNeasy® Tissue Kit (Qiagen). Plasmid DNA was extracted using the GeneJET Plasmid Miniprep Kit (Thermo Scientific, Lafayette, CO, USA). PCR assays were performed using Phusion High-Fidelity PCR Master Mix (Thermo Scientific, Lafayette, CO, USA). DNA concentration was measured on a NanoDrop ND1100 (Thermo Scientific, Lafayette, CO, USA).

Genome editing by co-transformation

Insertions of point mutations in *crtS* were performed according to the MuGENT procedure described in (38). An aadA7 gene cassette conferring resistance to spectinomycin and flanked by 6Kb of DNA sequence homologous to VC1903/1902 intergenic region was co-transformed with 3µg of a 6Kb long DNA fragment containing the point mutation to insert in the genome. Correct genome editing was then confirmed by PCR and sequencing of the mutated loci. Approximately 50% of the spectinomycin resistant clones had also integrated the point mutation.

Digital PCR quantification of DNA loci

Total genomic DNA (gDNA) was prepared with the DNeasy® Tissue Kit (Qiagen) from 1mL of cells in stationary phase (non-replicating). For E. coli [pORI2] assay, gDNA was first digested with DraI. PCR reactions were done with 0.1 ng of gDNA using the PerfeCta Multiplex qPCR ToughMix (Quanta Biosciences, Gaithersburg, MD, USA) within a Sapphire chips. Digital PCR was conducted on a Naica Geode (programmed to perform the sample partitioning step into droplets, followed by the thermal cycling program: 95◦C for 10 minutes, followed by 45 cycles of 95◦C for 10 seconds and 60◦C for 15 seconds) according to the instructions described in (33). Image acquisition was performed using the Naica Prism3 reader. Images were then analyzed using the Crystal Reader (total droplet enumeration and droplet quality control) and the Crystal Miner software (extracted fluorescence values for each droplet).

Plasmid stability assay

Plasmid stability assays were performed by growing bacteria in MH at 37°C under agitation for 60 or 80 generations. For this, each culture was diluted in fresh medium every morning and every evening, allowing the cells to grow for 10 generations between dilutions. Based on the volume of the media in the tubes, we used a 1:1024 dilution factor to obtain growth for 10 generations (as Volume = 2n, with n

= #of generations of bacteria). (We added 39,1 µL from the 10^{-1} dilution of the saturated culture to 4 mL of fresh medium). Every morning, serial dilutions (10^{-4}, 10^{-5}, 10^{-6}) of the saturated cultures were plated on non-selective media (MH). After an overnight incubation at 37ºC, 100 clones were streaked on MH and MH + chloramphenicol to determine the number of plasmid-containing bacteria. The plasmid kinetics was obtained by plotting the percentage of plasmid-containing cells at each time point against the number of generations.

References

1. diCenzo, G.C. and Finan, T.M. (2017) The Divided Bacterial Genome: Structure, Function, and Evolution. *Microbiology and molecular biology reviews : MMBR*, **81**.
2. Harrison, P.W., Lower, R.P., Kim, N.K. and Young, J.P. (2010) Introducing the bacterial 'chromid': not a chromosome, not a plasmid. *Trends in microbiology*, **18**, 141-148.
3. Touchon, M. and Rocha, E.P. (2016) Coevolution of the Organization and Structure of Prokaryotic Genomes. *Cold Spring Harbor perspectives in biology*, **8**, a018168.
4. Nordstrom, K. and Dasgupta, S. (2006) Copy-number control of the Escherichia coli chromosome: a plasmidologist's view. *EMBO reports*, **7**, 484-489.
5. Val, M.E., Soler-Bistue, A., Bland, M.J. and Mazel, D. (2014) Management of multipartite genomes: the Vibrio cholerae model. *Current opinion in microbiology*, **22**, 120-126.
6. Espinosa, E., Barre, F.X. and Galli, E. (2017) Coordination between replication, segregation and cell division in multi-chromosomal bacteria: lessons from Vibrio cholerae. *International microbiology : the official journal of the Spanish Society for Microbiology*, **20**, 121-129.
7. Ramachandran, R., Jha, J., Paulsson, J. and Chattoraj, D. (2017) Random versus Cell Cycle-Regulated Replication Initiation in Bacteria: Insights from Studying Vibrio cholerae Chromosome 2. *Microbiology and molecular biology reviews : MMBR*, **81**.
8. Egan, E.S. and Waldor, M.K. (2003) Distinct replication requirements for the two Vibrio cholerae chromosomes. *Cell*, **114**, 521-530.
9. Hansen, F.G. and Atlung, T. (2018) The DnaA Tale. *Frontiers in microbiology*, **9**, 319.
10. Katayama, T., Ozaki, S., Keyamura, K. and Fujimitsu, K. (2010) Regulation of the replication cycle: conserved and diverse regulatory systems for DnaA and oriC. *Nature reviews. Microbiology*, **8**, 163-170.
11. Boye, E. and Lobner-Olesen, A. (1990) The role of dam methyltransferase in the control of DNA replication in E. coli. *Cell*, **62**, 981-989.
12. Demarre, G. and Chattoraj, D.K. (2010) DNA adenine methylation is required to replicate both Vibrio cholerae chromosomes once per cell cycle. *PLoS genetics*, **6**, e1000939.
13. Duigou, S., Yamaichi, Y. and Waldor, M.K. (2008) ATP negatively regulates the initiator protein of Vibrio cholerae chromosome II replication. *Proceedings of the National Academy of Sciences of the United States of America*, **105**, 10577-10582.
14. Gerding, M.A., Chao, M.C., Davis, B.M. and Waldor, M.K. (2015) Molecular Dissection of the Essential Features of the Origin of Replication of the Second Vibrio cholerae Chromosome. *mBio*, **6**, e00973.
15. Schallopp, N., Milbredt, S., Sperlea, T., Kemter, F.S., Bruhn, M., Schindler, D. and Waldminghaus, T. (2017) Establishing a System for Testing Replication Inhibition of the Vibrio cholerae Secondary Chromosome in Escherichia coli. *Antibiotics*, **7**.
16. Venkova-Canova, T. and Chattoraj, D.K. (2011) Transition from a plasmid to a chromosomal mode of replication entails additional regulators. *Proceedings of the National Academy of Sciences of the United States of America*, **108**, 6199-6204.
17. Jha, J.K., Demarre, G., Venkova-Canova, T. and Chattoraj, D.K. (2012) Replication regulation of Vibrio cholerae chromosome II involves initiator binding to the origin both as monomer and as dimer. *Nucleic acids research*, **40**, 6026-6038.
18. Venkova-Canova, T., Srivastava, P. and Chattoraj, D.K. (2006) Transcriptional inactivation of a regulatory site for replication of Vibrio cholerae chromosome II. *Proceedings of the National Academy of Sciences of the United States of America*, **103**, 12051-12056.
19. Venkova-Canova, T., Baek, J.H., Fitzgerald, P.C., Blokesch, M. and Chattoraj, D.K. (2013) Evidence for two different regulatory mechanisms linking replication and segregation of vibrio cholerae chromosome II. *PLoS genetics*, **9**, e1003579.
20. Baek, J.H. and Chattoraj, D.K. (2014) Chromosome I controls chromosome II replication in Vibrio cholerae. *PLoS genetics*, **10**, e1004184.

21. Kitagawa, R., Ozaki, T., Moriya, S. and Ogawa, T. (1998) Negative control of replication initiation by a novel chromosomal locus exhibiting exceptional affinity for Escherichia coli DnaA protein. *Genes Dev*, **12**, 3032-3043.
22. Kasho, K. and Katayama, T. (2013) DnaA binding locus datA promotes DnaA-ATP hydrolysis to enable cell cycle-coordinated replication initiation. *Proc Natl Acad Sci U S A*, **110**, 936-941.
23. Orlova, N., Gerding, M., Ivashkiv, O., Olinares, P.D., Chait, B.T., Waldor, M.K. and Jeruzalmi, D. (2016) The replication initiator of the cholera pathogen's second chromosome shows structural similarity to plasmid initiators. *Nucleic acids research*.
24. Jha, J.K., Ghirlando, R. and Chattoraj, D.K. (2014) Initiator protein dimerization plays a key role in replication control of Vibrio cholerae chromosome 2. *Nucleic Acids Res*.
25. Jha, J.K., Li, M., Ghirlando, R., Miller Jenkins, L.M., Wlodawer, A. and Chattoraj, D. (2017) The DnaK Chaperone Uses Different Mechanisms To Promote and Inhibit Replication of Vibrio cholerae Chromosome 2. *mBio*, **8**.
26. Boye, E., Lobner-Olesen, A. and Skarstad, K. (2000) Limiting DNA replication to once and only once. *EMBO reports*, **1**, 479-483.
27. Val, M.E., Kennedy, S.P., Soler-Bistue, A.J., Barbe, V., Bouchier, C., Ducos-Galand, M., Skovgaard, O. and Mazel, D. (2014) Fuse or die: how to survive the loss of Dam in Vibrio cholerae. *Molecular microbiology*, **91**, 665-678.
28. Demarre, G. and Chattoraj, D.K. (2010) DNA adenine methylation is required to replicate both Vibrio cholerae chromosomes once per cell cycle. *PLoS Genet*, **6**, e1000939.
29. Venkova-Canova, T., Saha, A. and Chattoraj, D.K. (2012) A 29-mer site regulates transcription of the initiator gene as well as function of the replication origin of Vibrio cholerae chromosome II. *Plasmid*, **67**, 102-110.
30. Rasmussen, T., Jensen, R.B. and Skovgaard, O. (2007) The two chromosomes of Vibrio cholerae are initiated at different time points in the cell cycle. *The EMBO journal*, **26**, 3124-3131.
31. Val, M.E., Marbouty, M., de Lemos Martins, F., Kennedy, S.P., Kemble, H., Bland, M.J., Possoz, C., Koszul, R., Skovgaard, O. and Mazel, D. (2016) A checkpoint control orchestrates the replication of the two chromosomes of Vibrio cholerae. *Science advances*, **2**, e1501914.
32. Kemter, F.S., Messerschmidt, S.J., Schallopp, N., Sobetzko, P., Lang, E., Bunk, B., Sproer, C., Teschler, J.K., Yildiz, F.H., Overmann, J. *et al.* (2018) Synchronous termination of replication of the two chromosomes is an evolutionary selected feature in Vibrionaceae. *PLoS genetics*, **14**, e1007251.
33. Madic, J., Zocevic, A., Senlis, V., Fradet, E., Andre, B., Muller, S., Dangla, R. and Droniou, M.E. (2016) Three-color crystal digital PCR. *Biomolecular detection and quantification*, **10**, 34-46.
34. Yamaichi, Y., Fogel, M.A. and Waldor, M.K. (2007) par genes and the pathology of chromosome loss in Vibrio cholerae. *Proceedings of the National Academy of Sciences of the United States of America*, **104**, 630-635.
35. Yamaichi, Y., Gerding, M.A., Davis, B.M. and Waldor, M.K. (2011) Regulatory cross-talk links Vibrio cholerae chromosome II replication and segregation. *PLoS genetics*, **7**, e1002189.
36. Konieczny, I., Bury, K., Wawrzycka, A. and Wegrzyn, K. (2014) Iteron Plasmids. *Microbiology spectrum*, **2**.
37. Dibbens, J.A., Muraiso, K. and Chattoraj, D.K. (1997) Chaperone-mediated reduction of RepA dimerization is associated with RepA conformational change. *Molecular microbiology*, **26**, 185-195.
38. Dalia, A.B., McDonough, E. and Camilli, A. (2014) Multiplex genome editing by natural transformation. *Proceedings of the National Academy of Sciences of the United States of America*, **111**, 8937-8942.
39. McKenzie, G.J. and Craig, N.L. (2006) Fast, easy and efficient: site-specific insertion of transgenes into enterobacterial chromosomes using Tn7 without need for selection of the insertion event. *BMC microbiology*, **6**, 39.

40. Demarre, G., Guerout, A.M., Matsumoto-Mashimo, C., Rowe-Magnus, D.A., Marliere, P. and Mazel, D. (2005) A new family of mobilizable suicide plasmids based on broad host range R388 plasmid (IncW) and RP4 plasmid (IncPalpha) conjugative machineries and their cognate Escherichia coli host strains. *Research in microbiology*, **156**, 245-255.
41. Val, M.E., Skovgaard, O., Ducos-Galand, M., Bland, M.J. and Mazel, D. (2012) Genome engineering in Vibrio cholerae: a feasible approach to address biological issues. *PLoS genetics*, **8**, e1002472.
42. Le Roux, F., Binesse, J., Saulnier, D. and Mazel, D. (2007) Construction of a Vibrio splendidus mutant lacking the metalloprotease gene vsm by use of a novel counterselectable suicide vector. *Applied and environmental microbiology*, **73**, 777-784.
43. Kuhn, J., Finger, F., Bertuzzo, E., Borgeaud, S., Gatto, M., Rinaldo, A. and Blokesch, M. (2014) Glucose- but not rice-based oral rehydration therapy enhances the production of virulence determinants in the human pathogen Vibrio cholerae. *PLoS neglected tropical diseases*, **8**, e3347.
44. Marvig, R.L. and Blokesch, M. (2010) Natural transformation of Vibrio cholerae as a tool--optimizing the procedure. *BMC microbiology*, **10**, 155.

III: Unpublished results: new insight into *crtS* mechanism of action

As mentioned before, the *crtS* sequence is strongly conserved amongst the *Vibrionaceae*. It is AT-rich, contains conserved GATC sites, which are substrates for Dam methylase, and it was described to harbour a putative DnaA box. In the previous section we have demonstrated that the change in the methylation state of *crtS* upon passage of the replication fork does not impact its function. There are still two possibilities that can explain the requirement of *crtS* replication to trigger Chr2 replication. The first is based on the fact that *crtS* needs to be duplicated and the presence of 2 *crtS* sites would activate Chr2 replication. The second hypothesis relies on the formation of single stranded DNA during replication that could somehow be important to trigger Chr2 replication. DNA secondary structure prediction shows that *crtS* single stranded form may adopt a hairpin conformation upon passage of the replication fork (Fig. 25). To map *crtS* structural features and sequences required for Chr2 replication activation we generated a collection of *crtS* mutants in *V. cholerae* by using a targeted mutagenesis approach.

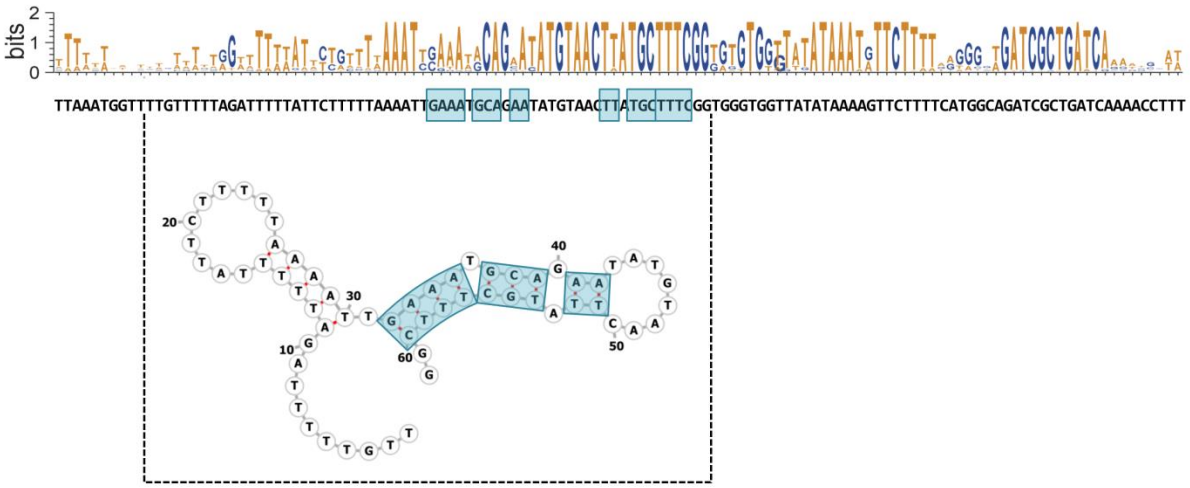

Figure 25. Folding prediction of the *crtS* single-stranded form. The secondary structure of the *crtS* minimal functional site was determined by using the RNAfold webserver. The black dashed lines delimit the 62 bp minimal *crtS* site. The light blue rectangles highlight the bases involved in the formation of a putative hairpin structure.

3.1. *crtS* targeted mutagenesis in *V. cholerae*

We constructed a panel of *V. cholerae* mutants where we perturbed specific features in the *crtS* sequence, such as the bases involved in the formation of a putative hairpin and other highly conserved regions. For this purpose we used two different strategies. The first strategy is based on the recently described natural co-transformation method (see Material & Methods for more details),

which allows scarless genome editing in naturally competent microorganisms such as *V. cholerae* (Dalia et al., 2014). The second approach relies on the chromosomal integration system of the Tn7 transposon (Material & Methods for more details). This is an efficient method that provides site-specific and stable single-copy integration (McKenzie and Craig, 2006). In this case, integration occurs at the single *V. cholerae* natural *attTn7* site, located downstream of the highly conserved *glmS* gene. We used a *V. cholerae* strain carrying its native *crtS* locus flanked by FRT sites. After integration of each mutated *crtS* sequence at the attTn7 site the WT *crtS* is excised by FLP-FRT recombination, leaving a single *crtS* copy on the genome (Fig. 29B in Material & Methods). This strategy avoids the accumulation of compensatory mutations upon deletion of *crtS* since *crtS* deletion mutants are highly unstable and easily accumulate mutations affecting *ori2*, as we previously observed (section 1.3 in the Results chapter).

3.2. Mutations affecting the putative hairpin structure inactivate *crtS*

We performed a functional analysis of the different *crtS* mutants in *V. cholerae* by digital PCR (dPCR). As mentioned previously, *ΔcrtS* mutants show a high genomic instability, which is mainly characterized by the loss of Chr2. For this reason non-replicating cells of these mutants exhibit Chr1/Chr2 ratios greater than 1. For our purposes we established an *ori1*/*ori2* threshold of 1,5 to indicate Chr2 loss, and hence *crtS* inactivation. Based on this assumption, we determined the functionality of the mutated *crtS* sites by measuring the copy number of *ori1*/*ori2* on non-replicating cells. For this purpose, for each strain we collected gDNA from stationary phase cells that was subsequently analysed by dPCR. We found out that all the non-permissive mutations lie within the 62 bp minimal *crtS* site (de Lemos Martins, in preparation). These mutations mostly seem to affect the bases involved in the formation of a putative stem loop (Fig. 26). Surprisingly, one of the non-permissive mutations (Mut28) lies outside the RctB-binding region (Fig. 26). There are two hypotheses that could explain this observation. One possibility relies on the involvement of an additional factor participating in the *crtS*-*ori2* crosstalk. In addition to RctB there might be another factor binding *crtS* that could be essential in the activation of Chr2 replication. Another hypothesis consists on the fact that these sequences (outside RctB-binding region) might impact the proper folding of the putative stem loop structure. Indeed, sequences adjacent to DNA secondary structures might influence their stability. Comparison of the predicted secondary structures for the WT sequence and for the *crtS*-Mut28 (outside RctB-binding site) reveals a drastic change at the level of the DNA conformation (Fig. 27). The stem loop predicted for the WT *crtS* sequence is no longer expected to form from the *crtS*-Mut28. This change in the *crtS* conformation can mask/unmask the bases recognized by RctB and affect its binding, which would ultimately impact *crtS* function as Chr2 replication activator.

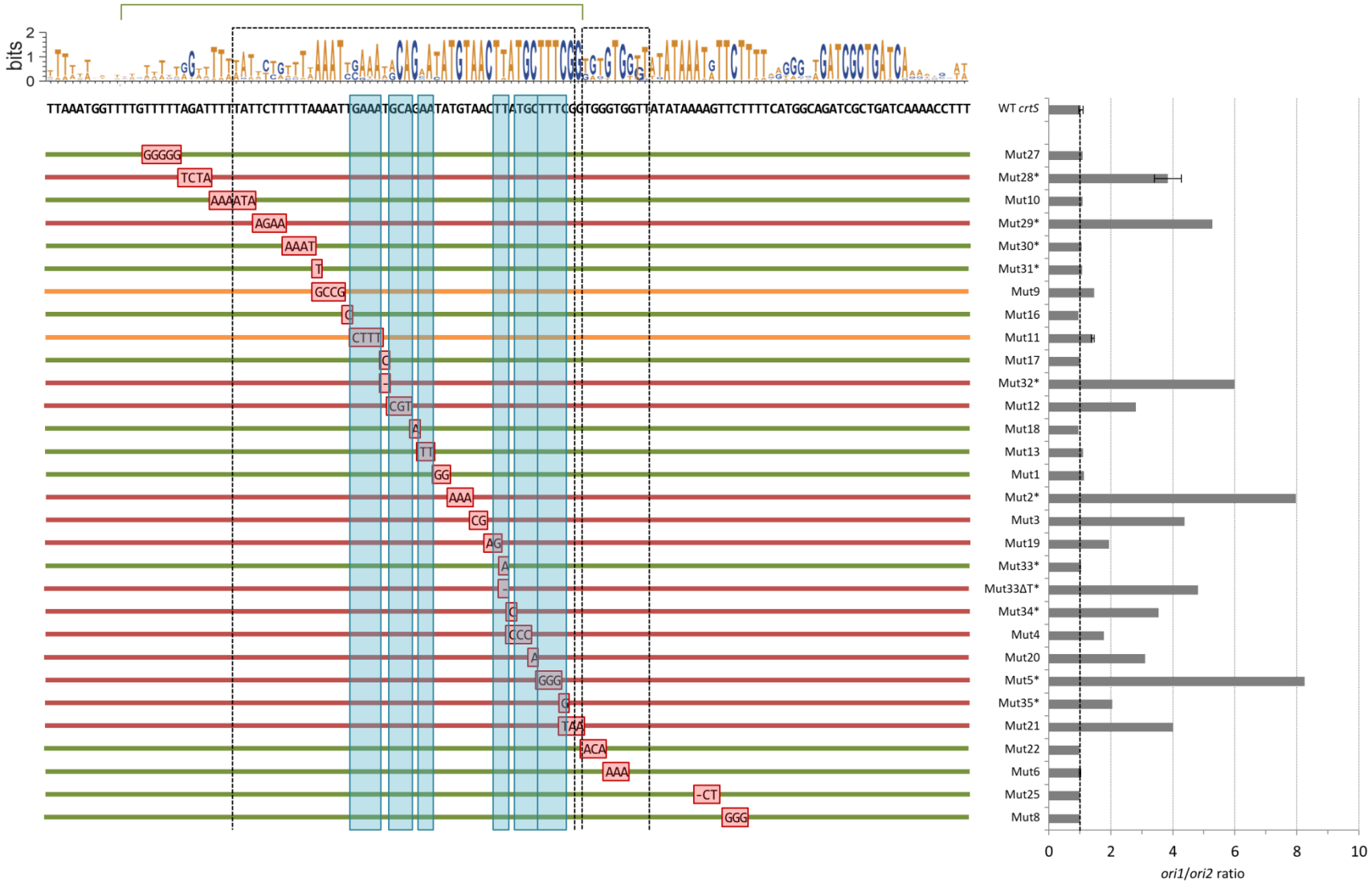

Figure 26. *ori1*/*ori2* ratio on non-replicating *crtS* mutant cells determined by dPCR. gDNA was collected from stationary phase cells and subsequently analysed by dPCR. Chromosome copy number is shown as a ratio between *ori1* and *ori2*. The black dashed line over the graph corresponds to an *ori1*/*ori2* ratio of 1. In our analysis, values above the 1,5 threshold indicate Chr2 loss. The different mutations are highlighted by red rectangles. The green and red lines correspond to the permissive and non-permissive mutations, respectively. Mutants 9 and 11 are indicated by orange lines because the respective *ori1*/*ori2* ratios lie at the limit of the threshold indicating Chr2 loss. The 62-bp minimal *crtS* region is delimited by the green line on the top of the WebLogo; the black dashed lines over the sequence indicate the RctB-binding site; and the blue rectangles highlight the bases involved in the formation of a putative stem loop.

We observed that, at two nucleotide positions, substitution and deletion mutations had different effects (Fig. 27). While a base substitution on Mut17 and Mut33 had a neutral effect, the corresponding deletions (Mut32* and Mut33*ΔT**, respectively) led to an increase in the *ori1*/*ori2* ratio. Indeed, a nucleotide substitution leaves the spacing between the nucleotides composing the *crtS* sequence unaltered. In turn, a deletion changes this spacing. This might negatively affect the formation of an eventual secondary structure or the binding of RctB to *crtS*. Based on DNA secondary structure predictions the hairpin structure of the deletion mutants remains unchanged compared to the respective substitution mutants that are still functional (Fig. 27). In this case, it is likely that the deletions affect the RctB binding, since they lie within the RctB binding region identified by DNase I footprinting (de Lemos Martins, in preparation). On *ori2* it was shown that both the spacing and helical phasing between initiator binding sites, and between these sites and the AT-rich region, are important for replication (Gerding et al., 2015). Mutations perturbing the spacing between these elements reduce or abolish *ori2* replicative function, while concomitantly affecting RctB's binding kinetics (Gerding et al., 2015). Thus, we could imagine a similar situation occurring at the level of the *crtS* site. A simple base substitution might not interfere with its function, while a deletion may negatively impact RctB binding, leading to an improper Chr2 replication activation.

3.3. Conclusions

Overall, these results point out to the formation of a secondary structure as a critical event for the *crtS* function. We hypothesize that upon passage of the replication fork the *crtS* site would adopt a hairpin conformation that ultimately leads to the activation of Chr2 replication. However, additional experiments are essential to confirm this possibility and to understand how such DNA conformation can be on the basis of the *crtS* mechanism of action. Currently, *in vitro* RctB binding to single stranded DNA *crtS* sites and *in vivo* replication slippage assay (Leach, 1994) are performed in the lab to corroborate our hypothesis of *crtS* secondary structure formation upon the passage of the replication fork that would serve as a signal to trigger Chr2 replication.

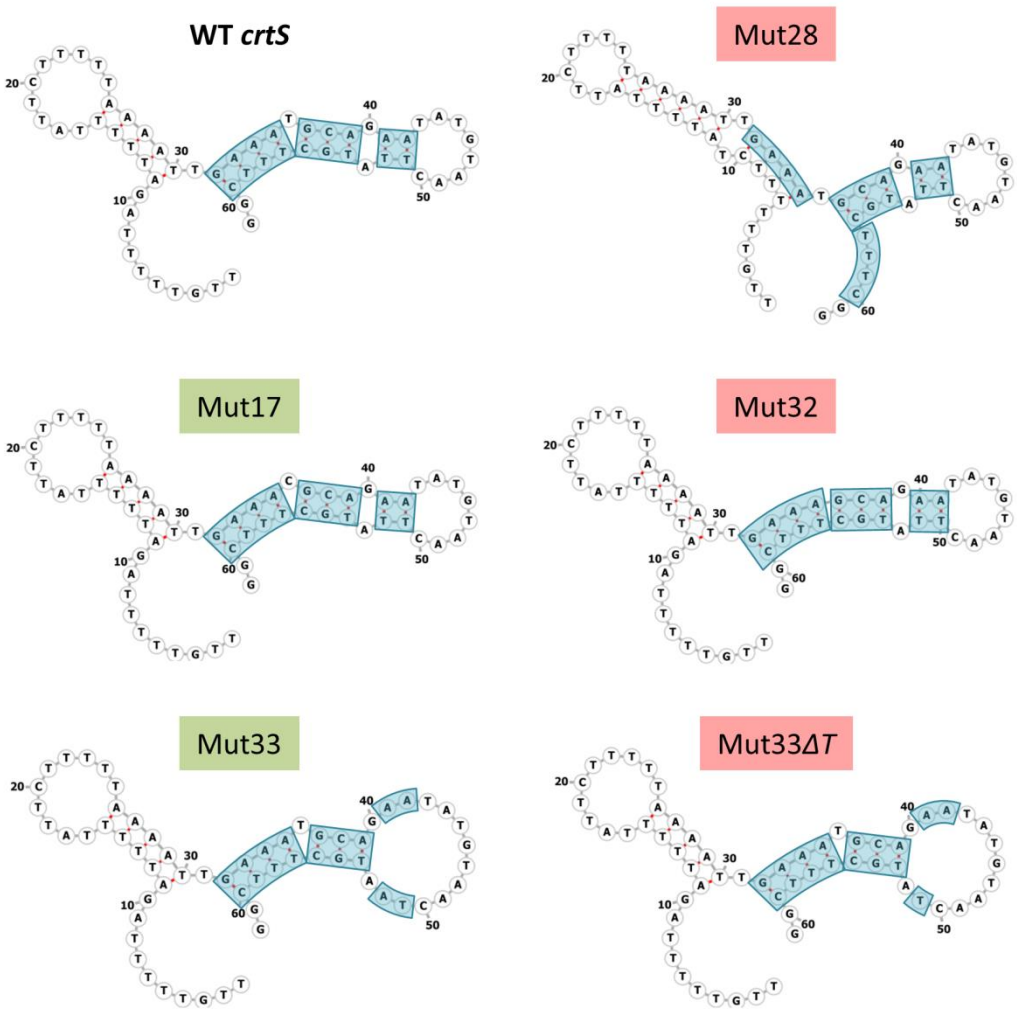

Figure 27. Folding prediction of *crtS* mutated sites. The secondary structure of the different sites was determined with the RNAfold webserver by using the 62 bp minimal *crtS* sequence. The nucleotides highlighted in light blue represent the bases involved in the formation of a stem loop in the WT sequence. The green and red rectangles around the name of the mutations indicate the permissive and non-permissive mutations, respectively.

DISCUSSION

During my PhD I have explored the *crtS*-RctB-mediated mechanism triggering Chr2 replication in *V. cholerae*. We have shown that *crtS* replication is crucial to trigger Chr2 replication, meaning that either DNA alterations caused by the passage of the replication fork across *crtS* or the doubling in *crtS* copy number after duplication triggers Chr2 replication. Here we have used a combination of *in vivo* and *in vitro* approaches to investigate the mechanism behind the *crtS*/*ori2*/RctB *crosstalk.* We have demonstrated that the change in the methylation state of *crtS* during replication is not involved in its function as replication activator of Chr2. Indeed, RctB molecules appear to oligomerize at the level of the *crtS* site in a methylation independent way. Instead, our results point out to the formation of a secondary structure during DNA replication as crucial event for Chr2 replication activation. This would reveal a novel mechanism controlling DNA replication in bacteria. In addition, the existence of a site dependent on the replication of the main chromosome to control the replication of a secondary replicon seems to be an effective way of integrating the later in the cell cycle.

Selective pressure for a 2-chromosome genome arrangement

crtS is crucial for Chr2 replication. We have shown that transient genome remodelling might supress the lack of *crtS* momentarily. This is illustrated by the *crtS* deletion mutant C926. Upon *crtS* deletion this mutant displayed spontaneous fusion of Chr1 and Chr2. We believe this genomic configuration allows Chr2 to benefit from the Chr1 replication machinery in order to compensate the lack of Chr2 replication activation mediated by *crtS*. However, this situation does not seem to be favourable for the cells. After 200 generations C926 mutant acquired mutations affecting Chr2 replication initiator and reverted back to the two-chromosome genome structure. This suggests a strong selective pressure to keep such genomic arrangement.

It has been suggested that the possession of a chromid would enable a bacterium to have a larger genome while keeping the chromosome small, which could allow it to replicate faster (Aiyar et al., 2002; Yamaichi et al., 1999). In fact, the analysis of 70 chromid-bearing genomes shows that the total genome size averages 5,73 ± 1,66 Mb (mean ± standard deviation). While the average for the 729 that do not possess chromids is only 3,38 ± 1,81 Mb. The fact that *V. cholerae* Chr2 replication is initiated later in the cell cycle suggests that the metabolic burden of replication is shifted to a time when cell size is larger and potentially better able to support it. In addition, among root-nodule bacteria, genera possessing secondary chromosomes, such as *Rhizobium* and *Sinorhizobium*, are able to grow faster in culture than those that do not, like *Mesorhizobium* and *Bradyrhizobium* (Harrison et

al., 2010). Probably in *ΔcrtS* mutants the one-chromosome conformation is outcompeted as a result of slower growth linked to an increase in replication duration due to the larger chromosome size resulting from Chr1 and Chr2 fusion.

In fast-growing bacteria it has been shown that having a split genome enables the possibility to differentially coordinate gene expression, through the modulation of gene dosage. As *V. cholerae* Chr1 starts to replicate before Chr2 there is a higher average gene dosage, and, consequent transcription of Chr1 genes (Dryselius et al., 2008; Soler-Bistué et al., 2015). In addition, grouping of genes together on individual replicons may facilitate their coordinated regulation by transcription factors. Indeed, the transcription machinery is not equally distributed throughout the cell (Weng and Xiao, 2014). Multiple transcriptomic studies have demonstrated that particular replicons are enriched in differentially regulated genes during niche adaptation. For example, in the case of *V. cholerae,* it was shown that there are many more Chr2 genes expressed under intestinal growth than under laboratory conditions (Xu et al., 2003). Other examples of replicon-specific patterns of gene expression exist in other bacteria, such as *B. cenocepacia* J2315 (Yoder-Himes et al., 2010), *R. leguminosarum* (Ramachandran et al., 2011), *Rhizobium phaseoli* (López-Guerrero et al., 2012) and *S. meliloti* (Barnett et al., 2004; Becker et al., 2004). Thus, in addition to the possibility of leading to growth defects, this suggests that the single-chromosome arrangement observed in the mutant C926 may provoke an imbalance at the level of gene expression. This is clearly harmful, since *crtS* deletion mutants displaying a fused chromosome rapidly acquire mutations affecting *ori2*, reverting back to the two-chromosme configuration.

Surprisingly, a strain carrying Chr1 and Chr2 artificially fused does not exhibit major fitness defects. Its generation time is only slightly extended compared to the WT strain (Val et al., 2012). However, one major difference between the *Δcrts* mutants carrying a single fused chromosome and the synthetic monochromosomal strain is the fact that the latter was built by respecting known criteria for chromosome organization and maintenance. This synthetic strain contains only a single origin and terminus of replication, which conserves the "*ori-ter*" axial symmetry, gene synteny, strand bias and the polarities of the original replichores. In addition, replication of the fused chromosome initiates at *ori1* of Chr1 and finishes in the terminus of Chr2, near *dif2*. By initiating replication at *ori1*, this synthetic strain conserves the replication-associated gene dosage effects on Chr1. In contrast, chromosome fusion in *ΔcrtS* mutants occurred spontaneously and prokaryotic genomes show intolerance towards various chromosome rearrangements such as inversions or relocations of DNA fragments that alter the chromosome organizational features (Campo et al., 2004; Esnault et al., 2007; Guijo et al., 2001; Hill and Gray, 1988; Lesterlin et al., 2005; Liu et al., 2006; Louarn et al., 1985; Miesel et al., 1994; Segall et al., 1988). Thus, the growth defects observed in the *ΔcrtS* mutants with a

fused chromosome cannot be directly linked to an increase in the chromosome size. Instead, they are likely to be the result of major changes at the level of the chromosome organization patterns.

Requirement for termination synchrony

V. cholerae Chr2 initiates replication when approximately two-thirds of the Chr1 have been replicated. As a consequence, the two chromosomes terminate replication at the same time. We have shown that this pattern can be changed by moving the *crtS* site to other positions, either further away or closer to the terminus, without any deficiencies in cell viability. However, in these rearranged strains, in which Chr2 replication terminates long before Chr1, the two copies of *ter2* remain at midcell until cell division, and segregate approximately at the same time as *ter1*, like in WT cells (Val et al., 2016). This suggests a coordination of events towards the final steps of the cell cycle.

Indeed, termination synchrony seems to be a conserved feature among the Vibrionaceae. The analysis of the *crtS* position on Chr1 of 29 fully sequenced Vibrionaceae species shows that the distance between *crtS* and *ter1* corresponds to the length of the respective Chr2 replichore (Kemter et al., 2018). MFA of eleven different strains from the Vibrionacea group reveals that, in exponentially growing cells, the copy numbers of *ter1* and *ter2* within individual strains is very similar (Kemter et al., 2018). This means that in *Vibrio* species with smaller secondary chromosomes than that of *V. cholerae*, replication of Chr2 starts later. In turn, species with larger secondary chromosomes, replication of Chr2 starts earlier compared to *V. cholerae*. Thus, the delay between the start of Chr1 and Chr2 replication seems to be irrelevant. In contrast, it seems that there is a strong evolutionary pressure to keep Chr1 and Chr2 terminating replication at the same time. This differential timing in Chr2 replication initiation essential to achieve replication termination synchrony between Chr1 and Chr2 is controlled by the position of *crtS* on Chr1 (Val et al., 2016).

The requirement for a synchronous termination can be explained by the coordination of chromosome segregation and cell division. The chromosomal region opposite to the replication origin is the part of the chromosome where dimer resolution occurs at the *dif* site (Kennedy et al., 2008). This is mediated by the XerCD site-specific recombinases and the DNA translocase FtsK, which is anchored at the septum (Val et al., 2008). In addition, chromosome segregation is coordinated with cell division through interactions of the Ter domains with the divisome in *E. coli*, as well as in *V. cholerae* (Demarre et al., 2014; Dupaigne et al., 2012; Espéli et al., 2012). Chr2 harbours binding sites for an inhibitor of Z-ring formation (SBS motifs) that contribute to the regulation of cell division (Galli et al., 2016). The Chr2 SBS motifs help to accurately position the *V. cholerae* divisome at mid-cell and

postpone its assembly to the very end of the cell cycle (Galli et al., 2016). Thus, the cohesion of *ter1* and *ter2* with their respective sister *ter* sequences near the division site observed in *V. cholerae* seems to be important for the final stages of the cell cycle, such as dimer resolution and cell division, and the synchronized termination of the two chromosomes might facilitate the processes involved.

crtS function could be reminiscent of *E. coli* DARS1 and DARS2

Baek et al. suggested that *crtS* may act as a DNA chaperone remodelling RctB. They have shown that *crtS* increases RctB affinity for iterons and decreases it for 39-mers, enhancing *ori2* replication. In addition, *crtS* abolishes the requirement for the DnaK/J chaperones, which are normally required to promote initiation at *ori2* in *E. coli* (Baek and Chattoraj, 2014). Here, we have demonstrated that *crtS* is crucial for Chr2 replication initiation. Relocation of *crtS* to other genomic positions on Chr1 alters the timing of Chr2 replication initiation, meaning that *crtS* replication triggers Chr2 replication.

Similarly to *V. cholerae*, in *E. coli* there are also sequences with a chaperone-like activity. These include *datA*, DARS1 and DARS2. These three elements are all able to modulate DnaA function. While *datA* locus promotes the inactivation of DnaA by converting DnaA-ATP to DnaA-ADP (Kasho and Katayama, 2013), DARS1 and DARS2 are involved on its regeneration, enhancing replication initiation. DARS1 and DARS2 promote the release of the ADP molecule from DnaA, which is necessary for the re-binding of ATP, leading to DnaA reactivation. Yet, DARS1 and DARS2 affect the cell cycle control differently. DARS1 ensures the proper origin concentration by a replication fork-associated gene dosage effect (Frimodt-Møller et al., 2016). This is because DARS1 is always active (Fujimitsu et al., 2009) and *de novo* synthesis of DnaA will along with the constitutive DnaA-ADP rejuvenation at DARS1 ensure a steady DnaA-ATP increase throughout the cell cycle. On the other hand, DARS2 main function is to ensure synchronous initiations between cellular origins, and hence, a reduced gene dosage results in asynchrony (Frimodt-Møller et al., 2016). Rejuvenation at *DARS2* is dependent on the binding of both Fis and IHF (Kasho et al., 2014). The activity at *DARS2* is growth phase regulated by Fis (only active during exponential growth) and cell cycle regulated by IHF (Kasho et al., 2014). Maximal IHF binding to activate *DARS2* occurs immediately before initiation (Kasho et al., 2014). Thus, initiation of all cellular origins in synchrony is explained by a mechanism where DnaA-ATP released from the first origin initiated will trigger initiations on fully methylated not yet initiated origins, by a cascade-like mechanism (Løbner-Olesen et al., 1994). A genotype comparison between 59 *E. coli* species with chromosome sizes ranging between 3,9 Mbp and 5,7 Mbp showed that the relative distances from *oriC* to *datA*, DARS1 and DARS2 are well preserved (Frimodt-Møller et al., 2015). Similarly, among the Vibrionaceae there is a bias on the relative position of *crtS*. Indeed, there is a correlation between *crtS*-*ter1* distance and the length of Chr2 replichores (Kemter et al., 2018).

In the particular case of DARS1 it appears that gene dosage is more important rather than its specific location. In contrast, the genomic location of DARS2 is relevant meaning that the local genomic environment is important for DARS2 function (Frimodt-Møller et al., 2016). In *E. coli*, the correct regulation of initiation at *oriC* relies on the proper position of not only one but all three known sites. The loss or aberrant position of either has a fitness disadvantage, explaining why these regions are conserved with respect to both chromosomal location and sequence. Despite *crtS* relative position conservation, its genetic context does not seem to be important for its function. Relocation of *crtS* to other positions appears to only impact the timing of Chr2 replication initiation, not affecting cell viability or Chr2 copy number (Val et al., 2016). And similarly to DARS1 and DARS2, we have observed that providing the cells with multiple *crtS* sites alters Chr2 copy number. However, it is still not clear if the change in the Chr2 replication pattern is due to a gene dosage effect or to another event occurring during replication, such as the formation of single-stranded DNA.

crtS constitutes another example of a direct link between DNA replication control and genomic initiator binding cluster positions (Frimodt-Møller et al., 2017). Contrary to DARS1 and DARS2 that act in cis, *crtS* is a trans-acting element having an effect on another replicon. In the particular case of *V. cholerae*, the *crtS*-dependent control of Chr2 replication constitutes an effective mechanism to ensure the once per cell cycle replication. Chr2 surveys Chr1 replication status via the *crtS* locus benefiting from the cell-cycle regulated replication of the main chromosome. This system is particularly interesting from the point of view of bacteria with a multipartite genome, where chromids replication should be coordinated with the main chromosome. This might highlight a novel theme in regulation of chromosomal replication initiation.

crtS may adopt a hairpin conformation essential for Chr2 replication activation

V. cholerae Chr2 replication initiation requires *crtS* replication. However, it is still not clear if this is mediated by DNA conformational changes caused by the passage of the replication fork across *crtS* or a gene dosage effect due to its doubling after replication. Baek et al. reported that, in vitro, *crtS* only has a visible effect if present on a supercoiled plasmid (Baek and Chattoraj, 2014). The requirement for supercoiled *crtS* suggests that *crtS* needs to be in a single-stranded state to be active. This is in agreement with the need for *crtS* to be replicated to trigger Chr2 replication, since the passage of the replication fork generates single-stranded DNA on the template for lagging-strand synthesis. So far, our mutational analysis of *crtS* points out to the formation of a single stranded DNA hairpin during replication. When we performed nucleotide substitution at the level of the bases involved in the formation of the putative stem loop, *crtS* was no longer functional in the majority of the cases.

Indeed, the ssDNA formed during replication on the template for lagging-strand synthesis is not simply a transient inert state of DNA. It can fold into secondary structures and interact with proteins, having a role in cellular processes such as site-specific recombination, transcription, and replication (Bikard et al., 2010). Thus the dynamics of the formation of hairpin structures can affect the way proteins interact with DNA. For instance, the DNA-protein interaction can be inhibited if a hairpin overlaps a protein recognition site (Horwitz and Loeb, 1988); and proteins can directly recognize and bind DNA hairpins (Barabas et al., 2008; Gonzalez-Perez et al., 2007; MacDonald et al., 2006; Masai and Arai, 1997; Val et al., 2005). In the particular case of *crtS*, RctB binding might depend on the formation of a secondary structure or instead its formation may mask/unmask the bases recognized by RctB affecting differently Chr2 replication initiation.

From our mutational analysis, not only the *crtS* secondary structure would be recognized but also the sequences uncovered by the hairpin formation. In *V. cholerae* there are several cellular processes mediated by the formation of ssDNA secondary structures. For instance, the *attC* recombinantion sites flanking the gene cassettes in the *V. cholerae* superintegron are recognized and recombined by the integrase only as hairpins folded from the bottom strand of the site (Bouvier et al., 2005; Mazel, 2006). The genetic information required for proper recombination of the *attC* sites is mainly determined by specific features of their secondary structures (Bouvier et al., 2009; MacDonald et al., 2006), such as the extrahelical bases (EHBs), the unpaired central spacer (UCS), and the variable terminal structure (VTS), which ensure strand selectivity and high levels of *attC* recombination (Bouvier et al., 2009; Frumerie et al., 2010; Nivina et al., 2016). However, there are a few nucleotides conserved in the *attC* sequence, namely at the cleavage site (Frumerie et al., 2010) and at the level of the extrahelical bases (EHBs), and these were shown to have major roles in the recombination reaction. For example the EHBs determine the recombinogenic strand in the site, the bottom strand, and serve as stabilizers of the synaptic complex, establishing contacts with protein monomers across the synapse (Bouvier et al., 2009; MacDonald et al., 2006). However, the location of the bottom strand of an *attC* site on the leading strand template, where limited ssDNA is available during DNA replication, disfavours its folding (Loot et al., 2010). Interestingly, inversion of the superintegron is deleterious in conditions of integrase expression (Vit and Loot, unpublished). Another example relies on the single-stranded CTX phage involved in *V. cholerae* virulence. In the lysogenic phase, it integrates *V. cholerae* Chr1 or Chr2 at their respectives *dif1* and *dif2* sites. CTX enters the infected cells as ssDNA, and the single-stranded form is integrated directly into one of the chromosomes (Val et al., 2005). The folding of the CTX *attP* region into a double-forked hairpin unmasks a Xer recombination site, which is recognized by the host XerCD protein complex that catalyzes the strand exchange between *attP* and the *dif* site (Val et al., 2005).

The possibility that the genetic information required for proper Chr2 activation is not entirely encoded in the *crtS* primary sequence, but also determined by specific features of *crtS* secondary structure, adds a new layer of information and regulation in the Chr2 replication control. This would represent a novel mechanism regulating DNA replication in bacteria.

How can we better differentiate chromids from iteron-plasmids?

Secondary chromosomes or chromids are generally defined by being large replicons that have plasmid-type maintenance and replication systems; a nucleotide composition close to that of the chromosome; and encode core genes that are found on the chromosome in other species (Harrison et al., 2010). According to this definition the main difference between chromids and megaplasmids is based solely on presence/absence of essential genes. However, this has some limitations and does not seem enough to distinguish a secondary domesticated chromosome from megaplasmids. For example, large portions of the genome can be moved from one replicon to another. Similarly, the size of the replicon cannot be used as a criterion because of the existence of large mega-plasmids. This is the case of *Deinococcus deserti* VCD115, whose chromid is smaller than either of the two accompanying plasmids (Harrison et al., 2010). The knowledge we acquired by studying the *V. cholerae* Chr2 can provide us more objective criteria to differentiate chromids/secondary chromosomes from megaplasmids.

V. cholerae Chr2 harbours many features of the primary chromosome. For instance, it exploits the replication/segregation regulatory systems of Chr1. This is illustrated by common mechanisms acting on both chromosomes. For instance, Dam methylation prevents the over-initiation of Chr1 and Chr2 replication (Demarre and Chattoraj, 2010) and the final stages of Chr1 and Chr2 segregation depend on the same FtsK/XerCD machinery (Val et al., 2008).

In terms of Chr2 replication control it appears it has evolved from a plasmid-like system, however, it is considerably more complex. Chr2 acquired additional layers of control allowing the timing of replication to switch from random to cell cycle regulated. This include the modification of initiator-origin interactions by allowing initiator dimer binding to iterons as an additional inhibitory mechanism and by separating initiator binding sites involved in promoting iterons and in inhibiting (39-mer) initiation. Indeed, the inhibitory role of the 39-mers can be compared to the *E. coli datA* locus, as they both contribute to initiator titration. On Chr2 there is also the involvement of a Par protein (ParB2) in the regulation of replication, which mediates a cross-talk between chromosome replication and segregation. Additionally, here we have demonstrated a new layer of control where Chr1 and Chr2 communicate to coordinate their replication (Val et al., 2016). This is achieved by the replication of the *crtS* site on Chr1. We have shown that *crtS*

replication not only triggers Chr2 replication but it also controls its copy number (de Lemos Martins, in preparation). The presence of this site on Chr1 shows that Chr2 evolved to take advantage of the well-regulated replication of the main chromosome to be integrated in the cell cycle.

Another difference between Chr2 and the iteron-plasmids relies on the initiator protein. Despite the structural similarities between RctB domains 2 and 3 and the Rep proteins of the iteron-plasmids, RctB is considerably larger, possessing two additional domains (domain 1 and 4) (Orlova et al., 2016). Although it was not experimentally demonstrated, we can hypothesize that the presence of additional domains on RctB compared to its plasmid counterparts may indicate their involvement in regulatory processes not required in plasmid replication.

The fact that *V. cholerae* Chr2 adopted new layers of control not observed in related plasmids, allowing it to behave like a *bona fide* chromosome, reinforces the idea that the distinction between megaplasmids and chromids/secondary chromosomes cannot be based solely on descriptive criteria, such as replicon size and presence of essential genes. A functional analysis seems to be required to fully understand if secondary replicons can be considered chromids/secondary chromosomes. Based on our observations, this involves the study of their replication and segregation mechanisms to understand if these events are cell-cycle coordinated.

CONCLUSIONS AND PERSPECTIVES

Overall, the results obtained during this work show that *crtS* needs to be replicated to trigger Chr2 replication and that it controls Chr2 copy number. Our data suggest that this can be either mediated by a gene dosage effect, i. e., by duplication of the number of *crtS* sites during DNA replication, or by the formation of single stranded DNA during replication.

Our *crtS* targeted mutagenesis analysis has revealed that mutations affecting the putative hairpin structure inactivate *crtS*. These preliminary results suggested that *crtS* might adopt a stem loop conformation during DNA replication, which could be somehow responsible for the Chr2 replication initiation. Since the moment I started to write my thesis manuscript advances were made in the lab to test the hairpin hypothesis as the possible signal triggering Chr2 replication. *In vivo* replication slippage assays confirmed that *crtS* is able to form a stem loop in *E. coli*. In addition, *in vitro* RctB binding to single stranded DNA *crtS* has revealed that RctB binds preferentially the top strand (lagging strand template). Altogether, these results strongly suggest that the formation of a stem loop is somehow implicated in the Chr2 replication triggering in *V. cholerae*. However, a recent study has shown that Chr2 replication is triggered by the doubling of *crtS* gene dosage. The authors of the study claim that the presence of two unreplicated *crtS* sites is sufficient to license Chr2 replication and exclude the involvement of any DNA replication associated process. Our data do not allow us to exclude a gene dosage effect, however in some circumstances we have obtained results that left us sceptical about this hypothesis. For instance, when we insert two *crtS* copies very close to each other (approximately 1 kb away from each other) in the chromosome it behaves like a single site (data not shown). This observation together with our last results led us to hypothesize that the formation of the hairpin is an essential step to activate Chr2 replication. Nonetheless, to clarify this question we plan to generate a strain carrying two *crtS* sites located on the Chr2 of *V. cholerae*. If two unreplicated *crtS* sites are sufficient to activate Chr2 replication we would expect this strain to be functional and to replicate Chr2 normally.

In order to further confirm and test the importance of *crtS* folding in the activation of Chr2 replication it would be interesting to restore the stem loop structure on the *crtS* mutants where it has been destabilized and Chr2 replication impaired. This would allow us to clarify the RctB binding specificity to *crtS*. In addition, in the case of a stem loop formation, the *crtS* orientation regarding the passage of the replication fork would be relevant. Indeed, *crtS* orientation is conserved among Vibrio, being always found on the template for the lagging strand synthesis. During lagging strand synthesis large amounts of single stranded DNA are formed, allowing the formation of secondary structures.

Thus, by changing the orientation of *crtS* on the chromosome, i. e., by flipping it to the leading strand template, we expect less ssDNA to be available at the level of crtS, which can impact Chr2 replication.

Despite our data suggesting the formation of a stem loop, we still do not know exactly how it could trigger Chr2 replication. We have demonstrated that RctB binds to double-stranded *crtS* and by quantifying the RctB binding to ssDNA *crtS* we have observed a preferential binding to the top strand. An attractive and very intuitive model would be that *crtS* could work as a titration site for RctB and once the replication fork passes through it, it would release the bound RctB and it would be available to bind *ori2* and initiate Chr2 replication. However, this does not seem to be the case. The supply of extra *crtS* copies enhances Chr2 replication and in its absence we observe an impairment instead of an enhancement of Chr2 replication. A previous study has shown that *crtS* reduces RctB binding to the 39-mers, suggesting that *crtS* remodels RctB, in such a way that its affinity to the 39-mer sites is decreased. We can thus imagine that right before Chr2 replication initiation RctB is bound to all its binding sites (iterons, 39-mers and *crtS*). The binding to 39-mers has a negative regulatory role and inhibits Chr2 replication by handcuffing. Thus, upon *crtS* replication and consequent stem loop formation RctB would bind to this site differently. This could induce a rearrangement of the initiator molecules in such a way that certain domains could be exposed or masked, which would ultimately affect *ori2*-bound RctB molecules and promote Chr2 replication. RctB binds four different sites, (iterons, 39-mers, double-stranded *crtS* and single-straded *crtS*) with no sequence conservation among them. The determination of the RctB structure bound to these different binding sites is then essential to understand precisely how it can recognize such different sites and the mechanism behind the *crtS*-mediated Chr2 replication activation. The DNA-bound RctB structure determination would allow us to visualize the conformation of the initiator bound to the DNA and to understand how the different domains interact with each binding site. Since the DnaK/J chaperones are involved in RctB remodelling and monomerization it would also be interesting to test their effect on the structure of the DNA-bound RctB.

We have observed important differences between *E. coli* and *V. cholerae* in the *crtS*-mediated control of *ori2* copy number. While the supply of additional *crtS* copies in *E. coli* increases the copy number of an *ori2*-based plasmid exponentially, in *V. cholerae* the increase in Chr2 copy number seems to be restricted, increasing in a logarithmic manner. One possible explanation for this difference could be attributed to the fact that Chr2 carries a locus that negatively regulates replication at *ori2*. This locus spans 74 kb and contains five iterons and one 39-mer. It would be interesting to test if a sequence carrying these regulatory sites would restrain the *ori2*-based plasmid copy number in *E. coli* as it does in *V. cholerae*. However the differences between *E. coli* and *V. cholerae* do not reside solely on this regulatory locus. The DnaK/J chaperones also differ slightly

between these two organisms. The C-terminal extremities of DnaK of *E. coli* and *V. cholerae* only share 62% identity, while the N-terminal regions share 87% identity. Thus, in the future, it would be interesting to test the effect of *V. cholerae* DnaK/J chaperones in the *ori2*-based system that we reconstituted in *E. coli*. In addition to help us to understand the variances between the two bacteria at the level of *ori2* replication control, this could allow us to develop a more accurate *ori2*-based system in *E. coli*, which presents interesting potentials for biotechnological applications.

In general, these additional experiments would definitely increase our understanding regarding the control of Chr2 replication and would provide us important insights about how *crtS* replication activates RctB and consequently replication initiation at *ori2*.

MATERIAL AND METHODS

Bacterial strains and plasmids

All bacterial strains and plasmids used in this study are listed on tables 2 and 3, respectively.

Growth conditions

Bacteria were routinely grown at 37ºC in LB broth (Lennox) or Mueller Hinton broth with shaking or on agar plates. Growth of strains carrying temperature-sensitive plasmids (Ts) was performed at 30ºC, and these plasmids where cured by switching the temperature to 42ºC. When needed, antibiotics where used at the following concentrations: carbenicillin, 100 ug/mL; chloramphenicol, 25 ug/mL for E. coli and 5 ug/mL for V. cholerae; kanamycin, 25 ug/mL; spectinomycin, 100 ug/mL, rifampicin, 1 ug/mL. Diaminopimelic acid was used at 0,3 mM, thymidine (dT) at 10 ug/mL, glucose at 1% and arabinose at 0,2 % (w/v).

General DNA manipulation and purification

DNA fragments were amplified by PCR using the DreamTaq Green PCR Master Mix (Thermo Scientific) or the Phusion High-Fidelity PCR Master Mix (Thermo Scientific) when high fidelity PCR products were required. PCR amplifications were carried out in accordance to the manufacturer instructions in a standard thermocycler. The amplification products was analysed by electrophoresis in agarose gels running in 0,5X Tris-Acetate-EDTA (TAE) as electrophoresis buffer. After an ethidium bromide bath the gels were analysed under ultraviolet light and pictures were acquired using Gel Doc EZ Imager system (BIO-RAD).

Purification of DNA fragments obtained from PCR amplification or enzymatic restriction was performed using the GeneJET PCR Purification Kit (Thermo Scientific). Plasmid DNA purification was carried out using the GeneJET Plasmid Miniprep Kit (Thermo Scientific, Lafayette, CO, USA) according to the protocol recommended by the manufacturer. DNA was eluted in a minimal volume of sterile distilled water and stored at 4ºC or -20ºC. Restriction enzymes (FastDigest, Thermo Scientific) and T4 DNA ligase (New England Biolabs) were used according to supplier's instructions.

When necessary, DNA concentration was determined by spectrophotometry using NanoDrop® ND-1100 Spectrophotometer (Thermo Scientific). Samples purity was evaluated based on $A_{260/A280}$ ratio.

Construction of *E. coli* strains carrying multiple *crtS* sites

E. coli strains carrying 1, 2, 3 and 4 *crtS* sites are derivatives of *E. coli* MG1655. These strains were constructed by homologous recombination using the suicide plasmid pMP7. In all cases the *crtS* site was designed to be inserted in intergenic zones of inversely oriented ORFs to avoid gene or operon interruption (Fig. 28). PCR products carrying the *crtS* site and the two flanking 1 kb homology regions were generated by two-step PCR and cloned in pMP7 by Gibson Assembly. The mixture was then transformed into the Π3813 cloning strain. After screening, the pMP7 derivatives carrying *crtS* they were introduced in the conjugative strain β3914.

The transfer and further integration of the pMP7 derivatives in the MG1655 strain was performed by conjugation. For the conjugation step, the donor (β3914) and the recipient (MG1655) strains were grown overnight with the corresponding antibiotics and other additives (Chloramphenicol, DAP and glucose for the donor strain). After the overnight growth the cultures were diluted 100-fold on the respective medium (DAP and glucose for the donor strain) and grown until an OD_{600} of 0,4 – 0,5. Then, 1 mL of donor and 1 mL of recipient cultures were mixed, centrifuged, and the pellet was spread on a 0,45 µm filter placed on a plate supplemented with DAP and glucose for an overnight conjugation. The filter was then resuspended in 5 mL of medium, after which serial 1:10 dilutions were spread on plates supplemented with chloramphenicol and glucose to select for integration events.

Integration of the pMP7 at the desired genomic positions of MG1655 was checked by PCR. In order to get rid of the plasmid backbone to generate a scarless insertion, the integrants were plated on arabinose-containing plates after growth on liquid medium supplemented with glucose. Arabinose induces the expression of the CcdB toxin, whose gene which is under the control of the P_{BAD} promoter, and only the cells that have lost the plasmid backbone will survive. The excision step either originates WT clones (revertants) or clones carrying the *crtS* site at the desired location. The correct insertion was verified by PCR and further sequencing of the insertion locus.

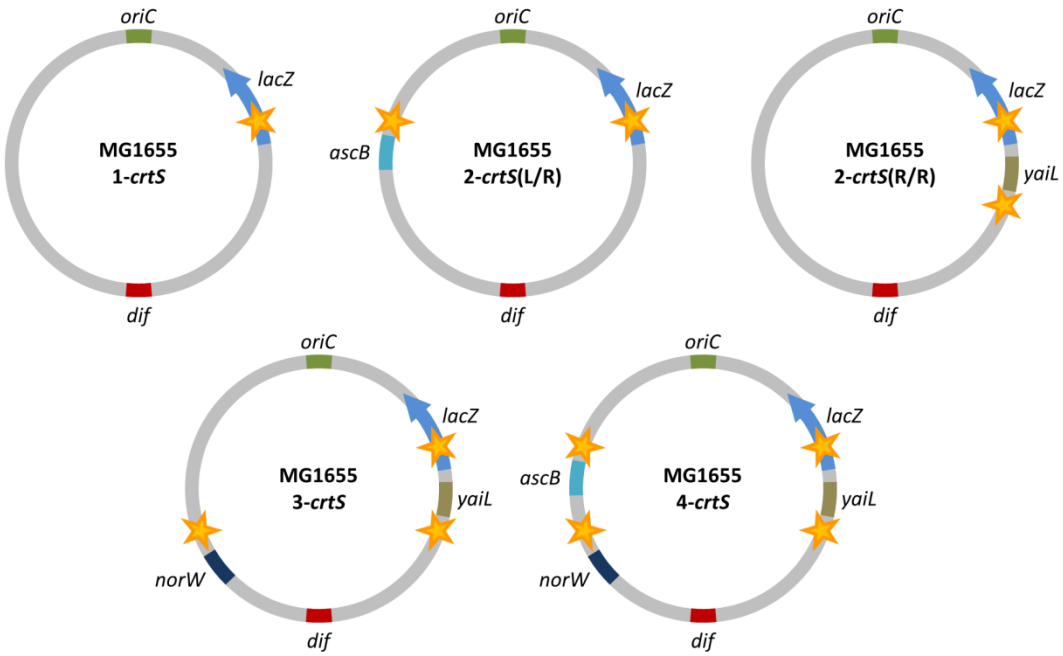

Figure 28. Chromosome map of the *E. coli* strains carrying multiple *crtS* sites. *crtS* is indicated by the yellow stars.

Construction of the *V. cholerae crtS* mutants

V. cholerae crtS mutants were constructed either using the co-transformation method (Dalia et al., 2014) or the Tn7 transposition system (McKenzie and Craig, 2006).

- Genome editing by co-transformation

To insert point mutations in *crtS*, chitin-induced *V. cholerae* competent cells were co-transformed with a PCR product carrying the mutation of interest and a PCR-generated antibiotic resistance cassette, both flanked by 3-kb homology arms. The antibiotic cassette was designed to be inserted in a neutral region of the genome, whereas the mutated *crtS* sequences replace the native *crtS* site by homologous recombination (Fig. 29A). The neutral locus targeted with the antibiotic cassette was the intergenic region between the convergent genes VC1902 and VC1903. We have previously observed that insertions at this region do not affect cell's physiology.

The preparation of chitin-induced competent cells and subsequent co-transformation was performed by adapting the procedure described in Dalia et al., 2014. After an overnight growth in LB at 30ºC, *V. cholerae* cultures were diluted in LB and grown at 30ºC with shaking. When the OD_{600} reached 0,4-1,0, 1 mL of the culture was washed in the same volume of IO (7 g/L Instant Ocean sea salts (Aquarium systems)) and resuspended to an OD_{600} of 1,0 in IO. Then, 100 µL of the cell suspension was mixed with 900 µL of chitin slurry (6 mg of chitin powder from shrimp cells (Sigma-Aldrich) per mL of IO) and incubated statically at 30ºC for 16 to 24h. After this period, 550 µL of supernatant were

removed without disturbing the settled chitin and the DNA was added. All the PCR products, i. e., the fragment carrying the *crtS* mutated site and the antibiotic-resistance cassette, were added to the transformation reaction at a final concentration of 3 µg/mL. The reaction mixtures were incubated at 30ºC for an additional 16 to 24 h in the presence of the DNA. After this, 1 mL of LB was added to the reaction and the cells were incubated at 30ºC with shaking for 2-5 h. This step allows the "resolution" and segregation of the mutations making sure that each colony will be clonal. The cell suspension was plated on media supplemented with spectinomycin and incubated at 30ºC overnight. Spectinomycin resistant clones were screened by PCR and point mutations on *crtS* were confirmed by sequencing of the insertion locus. Approximately 50% of the spectinomycin resistant clones carried the mutation of interest in *crtS*.

- Tn7 transposition

Previous Tn7 systems have been developed (McKenzie and Craig, 2006), however we have optimized this tool to increase its efficacy. For this we built a helper plasmid, pMVM1, carrying the TnsABCD transposases involved in the transposition event; and a shuttle plasmid, pMVM5, carrying the sequence to be transposed flanked by the terminal repeats of the Tn7 (Fig. 29B). The mutated *crtS* sites (*crtS**) were cloned between the Tn7 recombination sites contained in the pMVM5 shuttle vector. *crtS**-containing shuttle vectors were conjugated in the recipient strain (MV250) already harbouring the pMVM1 helper plasmid. For the conjugation, the donor (B3914) and the recipient (MV250::pMVM1) strains were grown overnight at 37ºC and 30ºC, respectively, with the corresponding antibiotics and other supplements (kanamycin, spectinomycin and DAP for the donor; and carbenicillin for the recipient). After the overnight growth, the cultures were diluted 100-fold on the same media without antibiotics and supplemented with arabinose for the recipient strain. When the cultures reached an OD600 of 0,4 – 0,5, 1 mL of the donor and 1 mL of the recipient cultures were mixed and centrifuged. The resultant pellet was spread on a 0,45 µm filter placed on a plate supplemented with DAP and arabinose for a 4h conjugation at 30ºC. The filter was then resuspended in 5 mL of LB and serial 1:10 dilutions were plated on spectinomycin-containing plates, which were incubated overnight at 42ºC. The temperature switch to 42ºC allows the loss of the pMVM1 helper plasmid. The spectinomycin-resistant clones were screened by PCR to check the *crtS** insertion at the *attTn7* site and *crtS* point mutations were verified by sequencing. Once the mutated *crtS* sites were inserted at the *attTn7* generating MV250-Tn7::*crtS** strain, the native *crtS* was excised by FLP-FRT recombination. For this, a Flipase-enconding plasmid, pMP108, was conjugated in the MV250-Tn7::*crtS** strain following a similar conjugation procedure as the one described above. After conjugation, the flipase expression was induced by growing the strains in the presence of arabinose.

Serial dilutions were then spread on plates without any antibiotic. The excision of the native *crtS* was checked by the loss of the rifampicin resistance and by PCR.

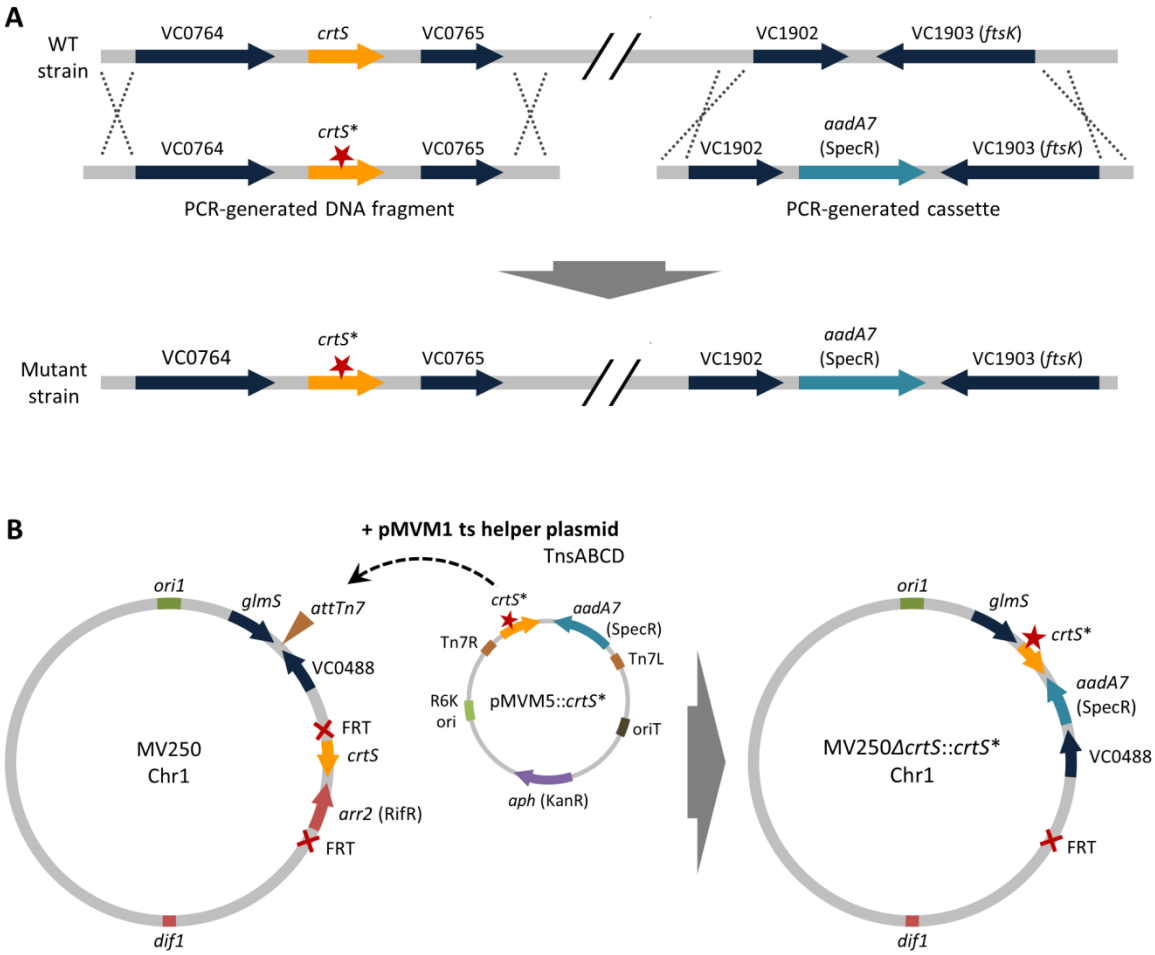

Figure 29. Construction of *crtS* mutants by targeted mutagenesis approaches. (A) Generation of *crtS* mutants by natural co-transformation. Briefly, a PCR fragment carrying each *crtS* mutation is co-transformed with a PCR-generated antibiotic resistance cassette into chitin-induced *V. cholerae* cells. After selection, approximately 50% of the spectinomycin resistant cells carry a mutation in *crtS*. (B) Insertion of *crtS* mutated sites at the *V. cholerae attTn7* site. The integration at the *attTn7* is mediated by the TnsABCD transposases carried in the thermo-sensitive helper plasmid pMVM1. The TnsABCD transposases recognize the Tn7 elements flanking *crtS*-aadA7* on the shuttle-plasmid pMVM5::*crtS** and promote its transposition into the chromosome of the recipient strain (MV250). The shuttle plasmid is not able to replicate in *V. cholerae*, being rapidly lost, while the helper plasmid is thermo-sensitive, being cured by switching the temperature to 42ºC. The red star/*crtS** refers to mutated *crtS* sequences.

Plasmid stability assays

Plasmid stability assays were performed by growing bacteria in MH at 37°C under agitation for 60 or 80 generations. For this, each culture was diluted in fresh medium every morning and every evening, allowing the cells to grow for 10 generations between dilutions. Based on the volume of the media in the tubes, we used a 1:1024 dilution factor to obtain growth for 10 generations (as Volume = 2n, with n = #of generations of bacteria). (We added 39,1 µL from the 10^{-1} dilution of the saturated culture to 4 mL of fresh medium). Every morning, serial dilutions (10^{-4}, 10^{-5}, 10^{-6}) of the saturated cultures were plated on non-selective media (MH). After an overnight incubation at 37ºC, 100 clones were streaked on MH and MH + chloramphenicol to determine the number of plasmid-containing bacteria. The plasmid kinetics was obtained by plotting the percentage of plasmid-containing cells at each time point against the number of generations.

Digital PCR quantification of DNA loci

E. coli and *V. cholerae* genomic DNA (gDNA) extraction was performed using the DNeasy® Tissue Kit (Qiagen) from 1 mL of a stationary phase culture (non-replicating). To measure the pORI2 copy number in *E. coli*, gDNA was digested with DraI before the PCR quantification. PCR reactions were done with 0,1 ng of gDNA using the PerfeCta Multiplex qPCR ToughMix (Quanta Biosciences) within Sapphire chips. Digital PCR was conducted on a Naica Geode (programmed to perform the sample partitioning step into droplets, followed by the thermal cycling program: 95ºC for 10 minutes, followed by 45 cycles of 95ºC for 10 seconds and 60ºC for 15 seconds). Image acquisition was performed using the Naica Prims3 reader. Images were then analysed using the Crystal Reader (total droplet enumeration and droplet quality control) and the Crystal Miner software (extracted fluorescence values for each droplet).

Table 2. Bacterial strains used in this study.

E. coli

Name	Relevant genotype/Feature	Source
Π3813	B462 *ΔthyA*::(*erm-pir116*)	Le Roux et al., 2007
B3914	B2163 *gyrA462 zei-298*::*Tn10*	Le Roux et al., 2007
MG1655	E. coli K-12 F-λ-ilvG-rfb-50 rph-1	Lab stock
MG1655-1-crtS	MG1655 *lacZ*::$crtS_{170bp}$	This study
MG1655-2-crtS(L/R)	MG1655 *lacZ*::$crtS_{170bp}$ – [*hycI-crtS-ascB*]	This study
MG1655-2-crtS(R/R)	MG1655 *lacZ*::$crtS_{170bp}$ – [*yaiL-crtS-frmB*]	This study
MG1655-3-crtS	MG1655 *lacZ*::$crtS_{170bp}$ – [*hycI-crtS-ascB*] – [*yaiL-crtS-frmB*]	This study
MG1655-4-crtS	MG1655 *lacZ*::$crtS_{170bp}$ – [*hycI-crtS-ascB*] – [*yaiL-crtS-frmB*] – [*hypF-crtS-ygbD*]	This study

V. cholerae

Name	Relevant genotype/Features	Source
WT	N16961rep: Vibrio cholerae serotype O1 biotype El Tor strain N16961 – repaired for *hapR*	Kühn et al., 2014
N16961 C*hapRΔlacZ*	N16961 C*hapRΔlacZ*	Val et al., 2012
C667	N16961 C*hapRΔlacZΔcrtS* with 2 separated chromosomes (before experimental evolution)	This study
C667-EV	C667 after ~200 generations (experimental evolution)	This study
C926	N16961 C*hapRΔlacZΔcrtS* with a single fused chromosome (before experimental evolution)	This study
C926-EV	C926 after ~200 generations (experimental evolution)	This study
WT-*aadA7*	WT-*aadA7*, spectinomycin resistance cassette used for natural co-transformation to co-select for point mutations elsewhere in the genome	This study
MV250	N16961 rep carrying *crtS* site flanked by FRT sites (*crtS* excision using Flippase)	This study
$crtS_{mut1}$	Point mutation in the GAA**TA**TGT motif to GAA**GG**TGT in *crtS* by co-transformation with *aadA7*	This study
$crtS_{mut2*}$	Point mutation in the ATA**TGT**AAC motif to ATA**AAA**AAC in *crtS* by Tn7 transposition	This study
$crtS_{mut3}$	Point mutation in the TGT**AA**CTT motif to TGT**CG**CTT in *crtS* by co-transformation with *aadA7*	This study
$crtS_{mut4}$	Point mutation in the CTT**ATG**CTT motif to CTT**CCC**CTT in *crtS* by co-transformation with *aadA7*	This study
$crtS_{mut5*}$	Point mutation in the TGC**TTT**CGG motif to TGC**GGG**CGG in *crtS* by Tn7 transposition	This study
$crtS_{mut6}$	Point mutation in the TGG**GTG**GTT motif to TGG**AAA**GTT in *crtS* by co-transformation with *aadA7*	This study
$crtS_{mut8}$	Point mutation in the AGT**TCT**TTT motif to AGT**GGG**TTT in *crtS* by co-transformation with *aadA7*	This study
$crtS_{mut9}$	Point mutation in the TTA**AAAT**TGA motif to TTA**GCCG**TGA in *crtS* by co-transformation with *aadA7*	This study
$crtS_{mut10}$	Point mutation in the GAT**TTTTAT**TCT motif to GAT**AAAATA**TCT in *crtS*	This study

	by co-transformation with *aadA7*	
crtS$_{mut11}$	Point mutation in the ATT**GAAA**TGC motif to ATT**CTTT**TGC in *crtS* by co-transformation with *aadA7*	This study
crtS$_{mut12}$	Point mutation in the AAT**GCA**GAA motif to AAT**CGT**GAA in *crtS* by co-transformation with *aadA7*	This study
crtS$_{mut13}$	Point mutation in the CAG**AA**TAT motif to CAG**TT**TAT in *crtS* by co-transformation with *aadA7*	This study
crtS$_{mut16}$	Point mutation in the AAT**T**GAA motif to AAT**C**GAA in *crtS* by co-transformation with *aadA7*	This study
crtS$_{mut17}$	Point mutation in the AAA**T**GCA motif to AAA**C**GCA in *crtS* by co-transformation with *aadA7*	This study
crtS$_{mut18}$	Point mutation in the GCA**G**AAT motif to GCA**A**AAT in *crtS* by co-transformation with *aadA7*	This study
crtS$_{mut19}$	Point mutation in the TAA**CT**TAT motif to TAA**AG**TAT in *crtS* by co-transformation with *aadA7*	This study
crtS$_{mut20}$	Point mutation in the ATG**C**TTT motif to ATG**A**TTT in *crtS* by co-transformation with *aadA7*	This study
crtS$_{mut21}$	Point mutation in the TTT**CGG**TGG motif to TTT**TAA**TGG in *crtS* by co-transformation with *aadA7*	This study
crtS$_{mut22}$	Point mutation in the CGG**TGG**GTG motif to CGG**ACA**GTG in *crtS* by co-transformation with *aadA7*	This study
crtS$_{mut25}$	Point mutation in the TAA**AAG**TTC motif to TAA**-CT**TTC in *crtS* by co-transformation with *aadA7*	This study
crtS$_{mut27}$	Point mutation in the TTG**TTTTT**AGA motif to TTG**GGGGG**AGA in *crtS* by co-transformation with *aadA7*	This study
crtS$_{mut28*}$	Point mutation in the TTT**AGAT**TTT motif to TTT**TCTA**TTT in *crtS* by Tn7 transposition	This study
crtS$_{mut29*}$	Point mutation in the TAT**TCTT**TTT motif to TAT**AGAA**TTT in *crtS* by Tn7 transposition	This study
crtS$_{mut30*}$	Point mutation in the CTT**TTTA**AAA motif to CTT**AAAT**AAA in *crtS* by Tn7 transposition	This study
crtS$_{mut31*}$	Point mutation in the TTA**A**AAT motif to TTA**T**AAT in *crtS* by Tn7 transposition	This study
crtS$_{mut32*}$	Point mutation in the AAA**T**GCA motif to AAA**-**GCA in *crtS* by Tn7 transposition	This study
crtS$_{mut33*}$	Point mutation in the ACT**T**ATG motif to ACT**A**ATG in *crtS* by Tn7 transposition	This study
crtS$_{mut33ΔT*}$	Point mutation in the ACT**T**ATG motif to ACT**-**ATG in *crtS* by Tn7 transposition	This study
crtS$_{mut34*}$	Point mutation in the CTT**A**TGC motif to CTT**C**TGC in *crtS* by Tn7 transposition	This study
crtS$_{mut35*}$	Point mutation in the TTT**C**GGT motif to TTT**G**GGT in *crtS* by Tn7 transposition	This study

Table 3. Plasmids used in this study.

Name	Relevant genotype/Features	Source
pMVM1	Tn7 helper – *ori*$_{pSC101}$ *repA*$_{ts}$ *oriT*RP4 *araC* P$_{BAD}$-*tnsABCD*; *bla*	This study
pMVM5	Tn7 shuttle – pSW29T::[Tn7R-*aadA7*-MCS-Tn7L]	This study
pMP108	*ori*$_{pSC101}$ *repA oriT*$_{RP4}$ *araC* P$_{BAD}$-*flp*; *bla*	This study
pUC18	*ori*$_{ColE1}$; *bla*	Lab stock
pFM1	pUC18::*crtS* flanked by 3 kb homology regions on each site	This study
pFM2	pUC18::*crtS*$_{mut1}$ flanked by 3 kb homology regions on each site	This study
pFM3	pUC18::*crtS*$_{mut3}$ flanked by 3 kb homology regions on each site	This study
pFM4	pUC18::*crtS*$_{mut4}$ flanked by 3 kb homology regions on each site	This study
pFM5	pUC18::*crtS*$_{mut6}$ flanked by 3 kb homology regions on each site	This study
pFM6	pUC18::*crtS*$_{mut8}$ flanked by 3 kb homology regions on each site	This study
pFM7	pUC18::*crtS*$_{mut9}$ flanked by 3 kb homology regions on each site	This study
pFM8	pUC18::*crtS*$_{mut10}$ flanked by 3 kb homology regions on each site	This study
pFM9	pUC18::*crtS*$_{mut11}$ flanked by 3 kb homology regions on each site	This study
pFM10	pUC18::*crtS*$_{mut12}$ flanked by 3 kb homology regions on each site	This study
pFM11	pUC18::*crtS*$_{mut13}$ flanked by 3 kb homology regions on each site	This study
pFM12	pUC18::*crtS*$_{mut16}$ flanked by 3 kb homology regions on each site	This study
pFM13	pUC18::*crtS*$_{mut17}$ flanked by 3 kb homology regions on each site	This study
pFM14	pUC18::*crtS*$_{mut18}$ flanked by 3 kb homology regions on each site	This study
pFM15	pUC18::*crtS*$_{mut19}$ flanked by 3 kb homology regions on each site	This study
pFM16	pUC18::*crtS*$_{mut20}$ flanked by 3 kb homology regions on each site	This study
pFM17	pUC18::*crtS*$_{mut21}$ flanked by 3 kb homology regions on each site	This study
pFM18	pUC18::*crtS*$_{mut22}$ flanked by 3 kb homology regions on each site	This study
pFM19	pUC18::*crtS*$_{mut25}$ flanked by 3 kb homology regions on each site	This study
pFM20	pUC18::*crtS*$_{mut27}$ flanked by 3 kb homology regions on each site	This study
pFM21	pMVM5::*crtS*$_{mut2}$	This study
pFM22	pMVM5::*crtS*$_{mut5}$	This study
pFM23	pMVM5::*crtS*$_{mut28}$	This study
pFM24	pMVM5::*crtS*$_{mut29}$	This study
pFM25	pMVM5::*crtS*$_{mut30}$	This study
pFM26	pMVM5::*crtS*$_{mut31}$	This study
pFM27	pMVM5::*crtS*$_{mut32}$	This study
pFM28	pMVM5::*crtS*$_{mut33}$	This study
pFM29	pMVM5::*crtS*$_{mut33\Delta T}$	This study
pFM30	pMVM5::*crtS*$_{mut34}$	This study
pFM31	pMVM5::*crtS*$_{mut35}$	This study

REFERENCES

Abe, Y., Jo, T., Matsuda, Y., Matsunaga, C., Katayama, T., and Ueda, T. (2007). Structure and Function of DnaA N-terminal Domains. J. Biol. Chem. *282*, 17816–17827.

Aiyar, S.E., Gaal, T., and Gourse, R.L. (2002). rRNA promoter activity in the fast-growing bacterium Vibrio natriegens. J. Bacteriol. *184*, 1349–1358.

Ausiannikava, D., Mitchell, L., Marriott, H., Smith, V., Hawkins, M., Makarova, K.S., Koonin, E. V, Nieduszynski, C.A., and Allers, T. (2018). Evolution of Genome Architecture in Archaea: Spontaneous Generation of a New Chromosome in Haloferax volcanii. Mol. Biol. Evol.

Bach, T., Krekling, M.A., and Skarstad, K. (2003). Excess SeqA prolongs sequestration of oriC and delays nucleoid segregation and cell division. EMBO J. *22*, 315–323.

Bae, S.-H., Cheong, H.-K., Cheong, C., Kang, S., Hwang, D.S., and Choi, B.-S. (2003). Structure and Dynamics of Hemimethylated GATC Sites. J. Biol. Chem. *278*, 45987–45993.

Baek, J.H., and Chattoraj, D.K. (2014). Chromosome I Controls Chromosome II Replication in Vibrio cholerae. PLoS Genet. *10*, e1004184.

Baker, T.A., and Kornberg, A. (1988). Transcriptional activation of initiation of replication from the E. coli chromosomal origin: an RNA-DNA hybrid near oriC. Cell *55*, 113–123.

Balakrishnan, L., and Bambara, R.A. (2013). Okazaki Fragment Metabolism. Cold Spring Harb. Perspect. Biol. *5*, a010173–a010173.

Barabas, O., Ronning, D.R., Guynet, C., Hickman, A.B., Ton-Hoang, B., Chandler, M., and Dyda, F. (2008). Mechanism of IS200/IS605 Family DNA Transposases: Activation and Transposon-Directed Target Site Selection. Cell *132*, 208–220.

Barnett, M.J., Toman, C.J., Fisher, R.F., and Long, S.R. (2004). A dual-genome Symbiosis Chip for coordinate study of signal exchange and development in a prokaryote-host interaction. Proc. Natl. Acad. Sci. U. S. A. *101*, 16636–16641.

Barry, E.R., and Bell, S.D. (2006). DNA replication in the archaea. Microbiol. Mol. Biol. Rev. *70*, 876–887.

Bartosik, D., Wlodarczyk, M., and Thomas, C.M. (1997). Complete Nucleotide Sequence of the Replicator Region ofParacoccus(Thiobacillus)versutuspTAV1 Plasmid and Its Correlation to Several Plasmids ofAgrobacteriumandRhizobiumSpecies. Plasmid *38*, 53–59.

Bartosik, D., Baj, J., and Wlodarczyk, M. (1998). Molecular and functional analysis of pTAV320, a repABC-type replicon of the Paracoccus versutus composite plasmid pTAV1. Microbiology *144*, 3149–3157.

Bates, D.B., Boye, E., Asai, T., and Kogoma, T. (1997). The absence of effect of gid or mioC transcription on the initiation of chromosomal replication in Escherichia coli. Proc. Natl. Acad. Sci. U. S. A. *94*, 12497–12502.

Bavishi, A., Lin, L., Schroeder, K., Peters, A., Cho, H., and Choudhary, M. (2010). The prevalence of gene duplications and their ancient origin in Rhodobacter sphaeroides 2.4.1. BMC Microbiol. *10*, 331.

Becker, A., Bergès, H., Krol, E., Bruand, C., Rüberg, S., Capela, D., Lauber, E., Meilhoc, E., Ampe, F., de Bruijn, F.J., et al. (2004). Global Changes in Gene Expression in *Sinorhizobium meliloti* 1021 under Microoxic and Symbiotic Conditions. Mol. Plant-Microbe Interact. *17*, 292–303.

Becskei, A., and Serrano, L. (2000). Engineering stability in gene networks by autoregulation. Nature *405*, 590–593.

Bell, S.P., and Kaguni, J.M. (2013). Helicase Loading at Chromosomal Origins of Replication. Cold Spring Harb. Perspect. Biol. *5*, a010124–a010124.

Bernhardt, T.G., and de Boer, P.A.J. (2005). SlmA, a nucleoid-associated, FtsZ binding protein required for blocking septal ring assembly over Chromosomes in E. coli. Mol. Cell *18*, 555–564.

Bikard, D., Loot, C., Baharoglu, Z., and Mazel, D. (2010). Folded DNA in Action: Hairpin Formation and Biological

Functions in Prokaryotes. Microbiol. Mol. Biol. Rev. *74*, 570–588.

Birch, O.M., Hewitson, K.S., Fuhrmann, M., Burgdorf, K., Baldwin, J.E., Roach, P.L., and Shaw, N.M. (2000). MioC Is an FMN-binding Protein That Is Essential for *Escherichia coli* Biotin Synthase Activity *in Vitro*. J. Biol. Chem. *275*, 32277–32280.

Blokesch, M. (2016). Natural competence for transformation. Curr. Biol. *26*, R1126–R1130.

de Boer, P.A., Crossley, R.E., Hand, A.R., and Rothfield, L.I. (1991). The MinD protein is a membrane ATPase required for the correct placement of the Escherichia coli division site. EMBO J. *10*, 4371–4380.

Bogan, J.A., and Helmstetter, C.E. (1997). DNA sequestration and transcription in the oriC region of Escherichia coli. Mol. Microbiol. *26*, 889–896.

Borgeaud, S., Metzger, L.C., Scrignari, T., and Blokesch, M. (2015). The type VI secretion system of Vibrio cholerae fosters horizontal gene transfer. Science *347*, 63–67.

Bouvier, M., Demarre, G., and Mazel, D. (2005). Integron cassette insertion: a recombination process involving a folded single strand substrate. EMBO J. *24*, 4356–4367.

Bouvier, M., Ducos-Galand, M., Loot, C., Bikard, D., and Mazel, D. (2009). Structural Features of Single-Stranded Integron Cassette attC Sites and Their Role in Strand Selection. PLoS Genet. *5*, e1000632.

Bowers, L.M., Krüger, R., and Filutowicz, M. (2007). Mechanism of Origin Activation by Monomers of R6K-encoded π Protein. J. Mol. Biol. *368*, 928–938.

Boye, E., Stokke, T., Kleckner, N., and Skarstad, K. (1996). Coordinating DNA replication initiation with cell growth: differential roles for DnaA and SeqA proteins. Proc. Natl. Acad. Sci. U. S. A. *93*, 12206–12211.

Bramhill, D., and Kornberg, A. (1988). Duplex opening by dnaA protein at novel sequences in initiation of replication at the origin of the E. coli chromosome. Cell *52*, 743–755.

Bregeon, D., Colot, V., Radman, M., and Taddei, F. (2001). Translational misreading: a tRNA modification counteracts a +2 ribosomal frameshift. Genes Dev. *15*, 2295–2306.

Brendler, T., Abeles, A., and Austin, S. (1991). Critical sequences in the core of the P1 plasmid replication origin. J. Bacteriol. *173*, 3935–3942.

Brendler, T., Abeles, A., and Austin, S. (1995). A protein that binds to the P1 origin core and the oriC 13mer region in a methylation-specific fashion is the product of the host seqA gene. EMBO J. *14*, 4083–4089.

Brézellec, P., Vallet-Gely, I., Possoz, C., Quevillon-Cheruel, S., and Ferat, J.-L. (2016). DciA is an ancestral replicative helicase operator essential for bacterial replication initiation. Nat. Commun. *7*, 13271.

Brilli, M., Fondi, M., Fani, R., Mengoni, A., Ferri, L., Bazzicalupo, M., and Biondi, E.G. (2010). The diversity and evolution of cell cycle regulation in alpha-proteobacteria: a comparative genomic analysis. BMC Syst. Biol. *4*, 52.

Bryant, J.A., Sellars, L.E., Busby, S.J.W., and Lee, D.J. (2014). Chromosome position effects on gene expression in Escherichia coli K-12. Nucleic Acids Res. *42*, 11383–11392.

Burgos, P.A., Velázquez, E., and Toro, N. (1996). Identification and distribution of plasmid-type A replicator region in rhizobia. Mol. Plant. Microbe. Interact. *9*, 843–849.

Camara, J.E., Breier, A.M., Brendler, T., Austin, S., Cozzarelli, N.R., and Crooke, E. (2005). Hda inactivation of DnaA is the predominant mechanism preventing hyperinitiation of Escherichia coli DNA replication. EMBO Rep. *6*, 736–741.

Campbell, J.L., and Kleckner, N. (1990). E. coli oriC and the dnaA gene promoter are sequestered from dam methyltransferase following the passage of the chromosomal replication fork. Cell *62*, 967–979.

Campbell, A., Mrázek, J., and Karlin, S. (1999). Genome signature comparisons among prokaryote, plasmid, and mitochondrial DNA. Proc. Natl. Acad. Sci. U. S. A. *96*, 9184–9189.

Campo, N., Dias, M.J., Daveran-Mingot, M.-L., Ritzenthaler, P., and Le Bourgeois, P. (2004). Chromosomal constraints in Gram-positive bacteria revealed by artificial inversions. Mol. Microbiol. *51*, 511–522.

Carbone, A., Zinovyev, A., and Kepes, F. (2003). Codon adaptation index as a measure of dominating codon

bias. Bioinformatics *19*, 2005–2015.

Cassler, M.R., Grimwade, J.E., and Leonard, A.C. (1995). Cell cycle-specific changes in nucleoprotein complexes at a chromosomal replication origin. EMBO J. *14*, 5833–5841.

Castillo-Ramírez, S., Vázquez-Castellanos, J.F., González, V., and Cevallos, M.A. (2009). Horizontal gene transfer and diverse functional constrains within a common replication-partitioning system in Alphaproteobacteria: the repABC operon. BMC Genomics *10*, 536.

Cervantes-Rivera, R., Romero-Lopez, C., Berzal-Herranz, A., and Cevallos, M.A. (2010). Analysis of the Mechanism of Action of the Antisense RNA That Controls the Replication of the repABC Plasmid p42d. J. Bacteriol. *192*, 3268–3278.

Cervantes-Rivera, R., Pedraza-López, F., Pérez-Segura, G., and Cevallos, M.A. (2011). The replication origin of a repABC plasmid. BMC Microbiol. *11*, 158.

Cevallos, M.A., Porta, H., Izquierdo, J., Tun-Garrido, C., García-de-los-Santos, A., Dávila, G., and Brom, S. (2002). Rhizobium etli CFN42 contains at least three plasmids of the repABC family: a structural and evolutionary analysis. Plasmid *48*, 104–116.

Cevallos, M.A., Cervantes-Rivera, R., and Gutiérrez-Ríos, R.M. (2008). The repABC plasmid family. Plasmid *60*, 19–37.

Chai, Y., and Winans, S.C. (2005a). A small antisense RNA downregulates expression of an essential replicase protein of an *Agrobacterium tumefaciens* Ti plasmid. Mol. Microbiol. *56*, 1574–1585.

Chai, Y., and Winans, S.C. (2005b). RepB protein of an *Agrobacterium tumefaciens* Ti plasmid binds to two adjacent sites between *repA* and *repB* for plasmid partitioning and autorepression. Mol. Microbiol. *58*, 1114–1129.

Chain, P.S.G., Comerci, D.J., Tolmasky, M.E., Larimer, F.W., Malfatti, S.A., Vergez, L.M., Aguero, F., Land, M.L., Ugalde, R.A., and Garcia, E. (2005). Whole-genome analyses of speciation events in pathogenic Brucellae. Infect. Immun. *73*, 8353–8361.

Chain, P.S.G., Denef, V.J., Konstantinidis, K.T., Vergez, L.M., Agulló, L., Reyes, V.L., Hauser, L., Córdova, M., Gómez, L., González, M., et al. (2006). Burkholderia xenovorans LB400 harbors a multi-replicon, 9.73-Mbp genome shaped for versatility. Proc. Natl. Acad. Sci. U. S. A. *103*, 15280–15287.

Chattoraj, D., Cordes, K., and Abeles, A. (1984). Plasmid P1 replication: negative control by repeated DNA sequences. Proc. Natl. Acad. Sci. U. S. A. *81*, 6456–6460.

Cho, H., McManus, H.R., Dove, S.L., and Bernhardt, T.G. (2011). Nucleoid occlusion factor SlmA is a DNA-activated FtsZ polymerization antagonist. Proc. Natl. Acad. Sci. U. S. A. *108*, 3773–3778.

Choudhary, M., Mackenzie, C., Nereng, K.S., Sodergren, E., Weinstock, G.M., and Kaplan, S. (1994). Multiple chromosomes in bacteria: structure and function of chromosome II of Rhodobacter sphaeroides 2.4.1T. J. Bacteriol. *176*, 7694–7702.

Choudhary, M., Mackenzie, C., Nereng, K., Sodergren, E., Weinstock, G.M., and Kaplan, S. (1997). Low-resolution sequencing of Rhodobacter sphaeroides 2.A.1T: chromosome II is a true chromosome. Microbiology *143*, 3085–3099.

Choudhary, M., Fu, Y.-X., Mackenzie, C., and Kaplan, S. (2004). DNA sequence duplication in Rhodobacter sphaeroides 2.4.1: evidence of an ancient partnership between chromosomes I and II. J. Bacteriol. *186*, 2019–2027.

Choudhary, M., Zanhua, X., Fu, Y.X., and Kaplan, S. (2007). Genome analyses of three strains of Rhodobacter sphaeroides: evidence of rapid evolution of chromosome II. J. Bacteriol. *189*, 1914–1921.

Choudhary, M., Cho, H., Bavishi, A., Trahan, C., and Myagmarjav, B.-E. (2012). Evolution of Multipartite Genomes in Prokaryotes. In Evolutionary Biology: Mechanisms and Trends, (Berlin, Heidelberg: Springer Berlin Heidelberg), pp. 301–323.

Clemens, J.D., Nair, G.B., Ahmed, T., Qadri, F., and Holmgren, J. (2017). Cholera. Lancet (London, England) *390*, 1539–1549.

Collins, M., and Myers, R.M. (1987). Alterations in DNA helix stability due to base modifications can be

evaluated using denaturing gradient gel electrophoresis. J. Mol. Biol. *198*, 737–744.

Dalia, A.B., McDonough, E., and Camilli, A. (2014). Multiplex genome editing by natural transformation. Proc. Natl. Acad. Sci. *111*, 8937–8942.

Dalrymple, B.P., Kongsuwan, K., Wijffels, G., Dixon, N.E., and Jennings, P.A. (2001). A universal protein-protein interaction motif in the eubacterial DNA replication and repair systems. Proc. Natl. Acad. Sci. *98*, 11627–11632.

Daubin, V., Lerat, E., and Perrière, G. (2003). The source of laterally transferred genes in bacterial genomes. Genome Biol. *4*, R57.

David, A., Demarre, G., Muresan, L., Paly, E., Barre, F.-X., and Possoz, C. (2014). The Two Cis-Acting Sites, parS1 and oriC1, Contribute to the Longitudinal Organisation of Vibrio cholerae Chromosome I. PLoS Genet. *10*, e1004448.

Deghelt, M., Mullier, C., Sternon, J.-F., Francis, N., Laloux, G., Dotreppe, D., Van der Henst, C., Jacobs-Wagner, C., Letesson, J.-J., and De Bolle, X. (2014). G1-arrested newborn cells are the predominant infectious form of the pathogen Brucella abortus. Nat. Commun. *5*, 4366.

DelVecchio, V.G., Kapatral, V., Redkar, R.J., Patra, G., Mujer, C., Los, T., Ivanova, N., Anderson, I., Bhattacharyya, A., Lykidis, A., et al. (2002). The genome sequence of the facultative intracellular pathogen Brucella melitensis. Proc. Natl. Acad. Sci. U. S. A. *99*, 443–448.

Demarre, G., and Chattoraj, D.K. (2010). DNA adenine methylation is required to replicate both Vibrio cholerae chromosomes once per cell cycle. PLoS Genet. *6*, e1000939.

Demarre, G., Galli, E., Muresan, L., Paly, E., David, A., Possoz, C., and Barre, F.-X. (2014). Differential Management of the Replication Terminus Regions of the Two Vibrio cholerae Chromosomes during Cell Division. PLoS Genet. *10*, e1004557.

diCenzo, G.C., and Finan, T.M. (2015). Genetic redundancy is prevalent within the 6.7 Mb Sinorhizobium meliloti genome. Mol. Genet. Genomics *290*, 1345–1356.

diCenzo, G.C., and Finan, T.M. (2017). The Divided Bacterial Genome: Structure, Function, and Evolution. Microbiol. Mol. Biol. Rev. *81*, e00019-17.

diCenzo, G., Milunovic, B., Cheng, J., and Finan, T.M. (2013). The tRNAarg gene and engA are essential genes on the 1.7-Mb pSymB megaplasmid of Sinorhizobium meliloti and were translocated together from the chromosome in an ancestral strain. J. Bacteriol. *195*, 202–212.

diCenzo, G.C., Zamani, M., Milunovic, B., and Finan, T.M. (2016). Genomic resources for identification of the minimal N_2-fixing symbiotic genome. Environ. Microbiol. *18*, 2534–2547.

Dillon, S.C., and Dorman, C.J. (2010). Bacterial nucleoid-associated proteins, nucleoid structure and gene expression. Nat. Rev. Microbiol. *8*, 185–195.

Díaz-López, T., Lages-Gonzalo, M., Serrano-López, A., Alfonso, C., Rivas, G., Díaz-Orejas, R., and Giraldo, R. (2003). Structural Changes in RepA, a Plasmid Replication Initiator, upon Binding to Origin DNA. J. Biol. Chem. *278*, 18606–18616.

Donachie, W.D., and Blakely, G.W. (2003). Coupling the initiation of chromosome replication to cell size in Escherichia coli. Curr. Opin. Microbiol. *6*, 146–150.

Doran, K.S., Konieczny, I., and Helinski, D.R. (1998). Replication origin of the broad host range plasmid RK2. Positioning of various motifs is critical for initiation of replication. J. Biol. Chem. *273*, 8447–8453.

Dryselius, R., Izutsu, K., Honda, T., and Iida, T. (2008). Differential replication dynamics for large and small Vibrio chromosomes affect gene dosage, expression and location. BMC Genomics *9*, 559.

Du, W.-L., Dubarry, N., Passot, F.M., Kamgoué, A., Murray, H., Lane, D., and Pasta, F. (2016). Orderly Replication and Segregation of the Four Replicons of Burkholderia cenocepacia J2315. PLoS Genet. *12*, e1006172.

Duderstadt, K.E., Chuang, K., and Berger, J.M. (2011). DNA stretching by bacterial initiators promotes replication origin opening. Nature *478*, 209–213.

Duggin, I.G., and Bell, S.D. (2009). Termination structures in the Escherichia coli chromosome replication fork trap. J. Mol. Biol. *387*, 532–539.

Duigou, S., Knudsen, K.G., Skovgaard, O., Egan, E.S., Løbner-Olesen, A., and Waldor, M.K. (2006). Independent control of replication initiation of the two Vibrio cholerae chromosomes by DnaA and RctB. J. Bacteriol. *188*, 6419–6424.

Duigou, S., Yamaichi, Y., and Waldor, M.K. (2008). ATP negatively regulates the initiator protein of Vibrio cholerae chromosome II replication. Proc. Natl. Acad. Sci. *105*, 10577–10582.

Dupaigne, P., Tonthat, N.K., Espéli, O., Whitfill, T., Boccard, F., and Schumacher, M.A. (2012). Molecular Basis for a Protein-Mediated DNA-Bridging Mechanism that Functions in Condensation of the E. coli Chromosome. Mol. Cell *48*, 560–571.

Egan, E.S., and Waldor, M.K. (2003). Distinct replication requirements for the two Vibrio cholerae chromosomes. Cell *114*, 521–530.

Egan, E.S., Fogel, M.A., and Waldor, M.K. (2005). MicroReview: Divided genomes: negotiating the cell cycle in prokaryotes with multiple chromosomes. Mol. Microbiol. *56*, 1129–1138.

Egan, E.S., Duigou, S., and Waldor, M.K. (2006). Autorepression of RctB, an Initiator of Vibrio cholerae Chromosome II Replication. J. Bacteriol. *188*, 789–793.

Esnault, E., Valens, M., Espéli, O., and Boccard, F. (2007). Chromosome structuring limits genome plasticity in Escherichia coli. PLoS Genet. *3*, e226.

Espéli, O., Borne, R., Dupaigne, P., Thiel, A., Gigant, E., Mercier, R., and Boccard, F. (2012). A MatP-divisome interaction coordinates chromosome segregation with cell division in *E. coli*. EMBO J. *31*, 3198–3211.

Espinosa, E., Barre, F.-X., and Galli, E. (2017). Coordination between replication, segregation and cell division in multi-chromosomal bacteria: lessons from Vibrio cholerae. Int. Microbiol. *20*, 121–129.

Fekete, R.A., Venkova-Canova, T., Park, K., and Chattoraj, D.K. (2006). IHF-dependent activation of P1 plasmid origin by DnaA. Mol. Microbiol. *62*, 1739–1751.

Fogel, M.A., and Waldor, M.K. (2006). A dynamic, mitotic-like mechanism for bacterial chromosome segregation. Genes Dev. *20*, 3269–3282.

Frage, B., Döhlemann, J., Robledo, M., Lucena, D., Sobetzko, P., Graumann, P.L., and Becker, A. (2016). Spatiotemporal choreography of chromosome and megaplasmids in the Sinorhizobium meliloti cell cycle. Mol. Microbiol. *100*, 808–823.

Francia, M. V., Fujimoto, S., Tille, P., Weaver, K.E., and Clewell, D.B. (2004). Replication of Enterococcus faecalis Pheromone-Responding Plasmid pAD1: Location of the Minimal Replicon and oriV Site and RepA Involvement in Initiation of Replication. J. Bacteriol. *186*, 5003–5016.

Fricke, W.F., Kusian, B., and Bowien, B. (2009). The Genome Organization of <i>Ralstonia eutropha</i> Strain H16 and Related Species of the <i>Burkholderiaceae</i> J. Mol. Microbiol. Biotechnol. *16*, 124–135.

Frimodt-Møller, J., Charbon, G., Krogfelt, K.A., and Løbner-Olesen, A. (2015). Control regions for chromosome replication are conserved with respect to sequence and location among Escherichia coli strains. Front. Microbiol. *6*, 1011.

Frimodt-Møller, J., Charbon, G., Krogfelt, K.A., and Løbner-Olesen, A. (2016). DNA Replication Control Is Linked to Genomic Positioning of Control Regions in Escherichia coli. PLOS Genet. *12*, e1006286.

Frimodt-Møller, J., Charbon, G., and Løbner-Olesen, A. (2017). Control of bacterial chromosome replication by non-coding regions outside the origin. Curr. Genet. *63*, 607–611.

Frumerie, C., Ducos-Galand, M., Gopaul, D.N., and Mazel, D. (2010). The relaxed requirements of the integron cleavage site allow predictable changes in integron target specificity. Nucleic Acids Res. *38*, 559–569.

Fujikawa, N., Kurumizaka, H., Nureki, O., Tanaka, Y., Yamazoe, M., Hiraga, S., and Yokoyama, S. (2004). Structural and biochemical analyses of hemimethylated DNA binding by the SeqA protein. Nucleic Acids Res. *32*, 82–92.

Fujimitsu, K., Senriuchi, T., and Katayama, T. (2009). Specific genomic sequences of E. coli promote replicational initiation by directly reactivating ADP-DnaA. Genes Dev. *23*, 1221–1233.

Fuller, R.S., Funnell, B.E., and Kornberg, A. (1984). The dnaA protein complex with the E. coli chromosomal replication origin (oriC) and other DNA sites. Cell *38*, 889–900.

Galibert, F., Finan, T.M., Long, S.R., Puhler, A., Abola, P., Ampe, F., Barloy-Hubler, F., Barnett, M.J., Becker, A., Boistard, P., et al. (2001). The composite genome of the legume symbiont Sinorhizobium meliloti. Science *293*, 668–672.

Galli, E., Poidevin, M., Le Bars, R., Desfontaines, J.-M., Muresan, L., Paly, E., Yamaichi, Y., and Barre, F.-X. (2016). Cell division licensing in the multi-chromosomal Vibrio cholerae bacterium. Nat. Microbiol. *1*, 16094.

Galli, E., Paly, E., and Barre, F.-X. (2017). Late assembly of the Vibrio cholerae cell division machinery postpones septation to the last 10% of the cell cycle. Sci. Rep. *7*, 44505.

García de Viedma, D., Serrano-López, A., and Díaz-Orejas, R. (1995). Specific binding of the replication protein of plasmid pPS10 to direct and inverted repeats is mediated by an HTH motif. Nucleic Acids Res. *23*, 5048–5054.

Georgescu, R.E., Kim, S.-S., Yurieva, O., Kuriyan, J., Kong, X.-P., and O'Donnell, M. (2008). Structure of a Sliding Clamp on DNA. Cell *132*, 43–54.

Gerding, M.A., Chao, M.C., Davis, B.M., and Waldor, M.K. (2015). Molecular Dissection of the Essential Features of the Origin of Replication of the Second *Vibrio cholerae* Chromosome. MBio *6*, e00973-15.

Gering, M., Götz, F., and Brückner, R. (1996). Sequence and analysis of the replication region of the Staphylococcus xylosus plasmid pSX267. Gene *182*, 117–122.

Gille, H., and Messer, W. (1991). Localized DNA melting and structural pertubations in the origin of replication, oriC, of Escherichia coli in vitro and in vivo. EMBO J. *10*, 1579–1584.

Gille, H., Egan, J.B., Roth, A., and Messer, W. (1991). The FIS protein binds and bends the origin of chromosomal DNA replication, oriC, of Escherichia coli. Nucleic Acids Res. *19*, 4167–4172.

Giraldo, R., Fernández-Tornero, C., Evans, P.R., Díaz-Orejas, R., and Romero, A. (2003). A conformational switch between transcriptional repression and replication initiation in the RepA dimerization domain. Nat. Struct. Mol. Biol. *10*, 565–571.

Gonzalez-Perez, B., Lucas, M., Cooke, L.A., Vyle, J.S., de la Cruz, F., and Moncalián, G. (2007). Analysis of DNA processing reactions in bacterial conjugation by using suicide oligonucleotides. EMBO J. *26*, 3847–3857.

Goodman, M.F., and Woodgate, R. (2013). Translesion DNA Polymerases. Cold Spring Harb. Perspect. Biol. *5*, a010363–a010363.

Goodner, B., Hinkle, G., Gattung, S., Miller, N., Blanchard, M., Qurollo, B., Goldman, B.S., Cao, Y., Askenazi, M., Halling, C., et al. (2001). Genome sequence of the plant pathogen and biotechnology agent Agrobacterium tumefaciens C58. Science *294*, 2323–2328.

Grantham, R., Gautier, C., and Gouy, M. (1980). Codon frequencies in 119 individual genes confirm corsistent choices of degenerate bases according to genome type. Nucleic Acids Res. *8*, 1893–1912.

Grimwade, J.E., Ryan, V.T., and Leonard, A.C. (2000). IHF redistributes bound initiator protein, DnaA, on supercoiled oriC of Escherichia coli. Mol. Microbiol. *35*, 835–844.

Guarné, A., Zhao, Q., Ghirlando, R., and Yang, W. (2002). Insights into negative modulation of E. coli replication initiation from the structure of SeqA–hemimethylated DNA complex. Nat. Struct. Biol. *9*, 839–843.

Guijo, M.I., Patte, J., del Mar Campos, M., Louarn, J.M., and Rebollo, J.E. (2001). Localized remodeling of the Escherichia coli chromosome: the patchwork of segments refractory and tolerant to inversion near the replication terminus. Genetics *157*, 1413–1423.

Guo, Q., Lu, M., and Kallenbach, N.R. (1995). Effect of hemimethylation and methylation of adenine on the structure and stability of model DNA duplexes. Biochemistry *34*, 16359–16364.

Guo, X., Flores, M., Mavingui, P., Fuentes, S.I., Hernández, G., Dávila, G., and Palacios, R. (2003). Natural genomic design in Sinorhizobium meliloti: novel genomic architectures. Genome Res. *13*, 1810–1817.

Hansen, F.G., Christensen, B.B., and Atlung, T. The initiator titration model: computer simulation of chromosome and minichromosome control. Res. Microbiol. *142*, 161–167.

Hansen, F.G., Atlung, T., Braun, R.E., Wright, A., Hughes, P., and Kohiyama, M. (1991). Initiator (DnaA) protein concentration as a function of growth rate in Escherichia coli and Salmonella typhimurium. J. Bacteriol. *173*, 5194–5199.

Hansen, F.G., Christensen, B.B., and Atlung, T. (2007). Sequence Characteristics Required for Cooperative Binding and Efficient in Vivo Titration of the Replication Initiator Protein DnaA in E. coli. J. Mol. Biol. *367*, 942–952.

Harrison, P.W., Lower, R.P.J., Kim, N.K.D., and Young, J.P.W. (2010). Introducing the bacterial "chromid": Not a chromosome, not a plasmid. Trends Microbiol. *18*, 141–148.

Hedglin, M., Kumar, R., and Benkovic, S.J. (2013). Replication Clamps and Clamp Loaders. Cold Spring Harb. Perspect. Biol. *5*, a010165–a010165.

Heidelberg, J.F., Elsen, J.A., Nelson, W.C., Clayton, R.A., Gwinn, M.L., Dodson, R.J., Haft, D.H., Hickey, E.K., Peterson, J.D., Umayam, L., et al. (2000). DNA sequence of both chromosomes of the cholera pathogen Vibrio cholerae. Nature *406*, 477–483.

Helmstetter, C.E., and Leonard, A.C. (1987). Coordinate initiation of chromosome and minichromosome replication in Escherichia coli. J. Bacteriol. *169*, 3489–3494.

Hiasa, H., and Marians, K.J. (1994). Fis cannot support oriC DNA replication in vitro. J. Biol. Chem. *269*, 24999–25003.

Hill, C.W., and Gray, J.A. (1988). Effects of chromosomal inversion on cell fitness in Escherichia coli K-12. Genetics *119*, 771–778.

Hill, T.M., Henson, J.M., and Kuempel, P.L. (1987). The terminus region of the Escherichia coli chromosome contains two separate loci that exhibit polar inhibition of replication. Proc. Natl. Acad. Sci. U. S. A. *84*, 1754–1758.

Horwitz, M.S., and Loeb, L.A. (1988). An E. coli promoter that regulates transcription by DNA superhelix-induced cruciform extrusion. Science *241*, 703–705.

Huq, A., Small, E.B., West, P.A., Huq, M.I., Rahman, R., and Colwell, R.R. (1983). Ecological relationships between Vibrio cholerae and planktonic crustacean copepods. Appl. Environ. Microbiol. *45*, 275–283.

Hwang, D.S., and Kornberg, A. (1992). Opening of the replication origin of Escherichia coli by DnaA protein with protein HU or IHF. J. Biol. Chem. *267*, 23083–23086.

Ingmer, H., and Cohen, S.N. (1993). Excess intracellular concentration of the pSC101 RepA protein interferes with both plasmid DNA replication and partitioning. J. Bacteriol. *175*, 7834–7841.

Inoue, Y., Tanaka, H., Kasho, K., Fujimitsu, K., Oshima, T., and Katayama, T. (2016). Chromosomal location of the DnaA-reactivating sequence *DARS2* is important to regulate timely initiation of DNA replication in *Escherichia coli*. Genes to Cells *21*, 1015–1023.

Ishiai, M., Wada, C., Kawasaki, Y., and Yura, T. (1994). Replication initiator protein RepE of mini-F plasmid: functional differentiation between monomers (initiator) and dimers (autogenous repressor). Proc. Natl. Acad. Sci. U. S. A. *91*, 3839–3843.

Itaya, M., and Tanaka, T. (1997). Experimental surgery to create subgenomes of Bacillus subtilis 168. Proc. Natl. Acad. Sci. U. S. A. *94*, 5378–5382.

Izquierdo, J., Venkova-Canova, T., Ramírez-Romero, M.A., Téllez-Sosa, J., Hernández-Lucas, I., Sanjuan, J., and Cevallos, M.A. (2005). An antisense RNA plays a central role in the replication control of a repC plasmid. Plasmid *54*, 259–277.

Jha, J.K., Demarre, G., Venkova-Canova, T., and Chattoraj, D.K. (2012). Replication regulation of Vibrio cholerae chromosome II involves initiator binding to the origin both as monomer and as dimer. Nucleic Acids Res. *40*, 6026–6038.

Jha, J.K., Li, M., Ghirlando, R., Miller Jenkins, L.M., Wlodawer, A., and Chattoraj, D. (2017). The DnaK Chaperone Uses Different Mechanisms To Promote and Inhibit Replication of *Vibrio cholerae* Chromosome 2. MBio *8*, e00427-17.

Jumas-Bilak, E., Michaux-Charachon, S., Bourg, G., O'Callaghan, D., and Ramuz, M. (1998). Differences in

chromosome number and genome rearrangements in the genus *Brucella*. Mol. Microbiol. *27*, 99–106.

Junier, I. (2014). Conserved patterns in bacterial genomes: A conundrum physically tailored by evolutionary tinkering. Comput. Biol. Chem. *53*, 125–133.

Kang, S., Han, J.S., Park, J.H., Skarstad, K., and Hwang, D.S. (2003). SeqA Protein Stimulates the Relaxing and Decatenating Activities of Topoisomerase IV. J. Biol. Chem. *278*, 48779–48785.

Kasho, K., and Katayama, T. (2013). DnaA binding locus datA promotes DnaA-ATP hydrolysis to enable cell cycle-coordinated replication initiation. Proc. Natl. Acad. Sci. *110*, 936–941.

Kasho, K., Fujimitsu, K., Matoba, T., Oshima, T., and Katayama, T. (2014). Timely binding of IHF and Fis to DARS2 regulates ATP-DnaA production and replication initiation. Nucleic Acids Res. *42*, 13134–13149.

Kasho, K., Tanaka, H., Sakai, R., and Katayama, T. (2017). Cooperative DnaA Binding to the Negatively Supercoiled *datA* Locus Stimulates DnaA-ATP Hydrolysis. J. Biol. Chem. *292*, 1251–1266.

Katayama, T., Kubota, T., Kurokawa, K., Crooke, E., and Sekimizu, K. (1998). The initiator function of DnaA protein is negatively regulated by the sliding clamp of the E. coli chromosomal replicase. Cell *94*, 61–71.

Katayama, T., Ozaki, S., Keyamura, K., and Fujimitsu, K. (2010). Regulation of the replication cycle: conserved and diverse regulatory systems for DnaA and oriC. Nat. Rev. Microbiol. *8*, 163–170.

Kato, J. -i., and Katayama, T. (2001). Hda, a novel DnaA-related protein, regulates the replication cycle in Escherichia coli. EMBO J. *20*, 4253–4262.

Kawakami, H., Keyamura, K., and Katayama, T. (2005). Formation of an ATP-DnaA-specific Initiation Complex Requires DnaA Arginine 285, a Conserved Motif in the AAA+ Protein Family. J. Biol. Chem. *280*, 27420–27430.

Kawasaki, Y., Wada, C., and Yura, T. (1990). Roles of Escherichia coli heat shock proteins DnaK, DnaJ and GrpE in mini-F plasmid replication. Mol. Gen. Genet. *220*, 277–282.

Kemter, F.S., Messerschmidt, S.J., Schallopp, N., Sobetzko, P., Lang, E., Bunk, B., Spröer, C., Teschler, J.K., Yildiz, F.H., Overmann, J., et al. (2018). Synchronous termination of replication of the two chromosomes is an evolutionary selected feature in Vibrionaceae. PLOS Genet. *14*, e1007251.

Kennedy, S.P., Chevalier, F., and Barre, F.-X. (2008). Delayed activation of Xer recombination at dif by FtsK during septum assembly in Escherichia coli. Mol. Microbiol. *68*, 1018–1028.

Keyamura, K., Fujikawa, N., Ishida, T., Ozaki, S., Su'etsugu, M., Fujimitsu, K., Kagawa, W., Yokoyama, S., Kurumizaka, H., and Katayama, T. (2007). The interaction of DiaA and DnaA regulates the replication cycle in E. coli by directly promoting ATP DnaA-specific initiation complexes. Genes & Dev. *21*, 2083–2099.

Keyamura, K., Abe, Y., Higashi, M., Ueda, T., and Katayama, T. (2009). DiaA Dynamics Are Coupled with Changes in Initial Origin Complexes Leading to Helicase Loading. J. Biol. Chem. *284*, 25038–25050.

Kitagawa, R., Mitsuki, H., Okazaki, T., and Ogawa, T. (1996). A novel DnaA protein-binding site at 94.7 min on the Escherichia coli chromosome. Mol. Microbiol. *19*, 1137–1147.

Kitagawa, R., Ozaki, T., Moriya, S., and Ogawa, T. (1998). Negative control of replication initiation by a novel chromosomal locus exhibiting exceptional affinity for Escherichia coli DnaA protein. Genes Dev. *12*, 3032–3043.

Koch, B., Ma, X., and Løbner-Olesen, A. (2010). Replication of Vibrio cholerae chromosome I in Escherichia coli: dependence on dam methylation. J. Bacteriol. *192*, 3903–3914.

Koch, B., Ma, X., and Løbner-Olesen, A. (2012). rctB mutations that increase copy number of Vibrio cholerae oriCII in Escherichia coli. Plasmid *68*, 159–169.

Kontur, W.S., Schackwitz, W.S., Ivanova, N., Martin, J., Labutti, K., Deshpande, S., Tice, H.N., Pennacchio, C., Sodergren, E., Weinstock, G.M., et al. (2012). Revised sequence and annotation of the Rhodobacter sphaeroides 2.4.1 genome. J. Bacteriol. *194*, 7016–7017.

Kowalski, D., and Eddy, M.J. (1989). The DNA unwinding element: a novel, cis-acting component that facilitates opening of the Escherichia coli replication origin. EMBO J. *8*, 4335–4344.

Kühn, J., Finger, F., Bertuzzo, E., Borgeaud, S., Gatto, M., Rinaldo, A., and Blokesch, M. (2014). Glucose- but not rice-based oral rehydration therapy enhances the production of virulence determinants in the human pathogen Vibrio cholerae. PLoS Negl. Trop. Dis. *8*, e3347.

Kurokawa, K., Nishida, S., Emoto, A., Sekimizu, K., and Katayama, T. (1999). Replication cycle-coordinated change of the adenine nucleotide-bound forms of DnaA protein in Escherichia coli. EMBO J. *18*, 6642–6652.

Kurz, M., Dalrymple, B., Wijffels, G., and Kongsuwan, K. (2004). Interaction of the Sliding Clamp -Subunit and Hda, a DnaA-Related Protein. J. Bacteriol. *186*, 3508–3515.

Kwong, S.M., Skurray, R.A., and Firth, N. (2004). Staphylococcus aureus multiresistance plasmid pSK41: analysis of the replication region, initiator protein binding and antisense RNA regulation. Mol. Microbiol. *51*, 497–509.

Lawrence, J.G. (2003). Gene Organization: Selection, Selfishness, and Serendipity. Annu. Rev. Microbiol. *57*, 419–440.

Lawrence, J.G., and Ochman, H. (1997). Amelioration of bacterial genomes: rates of change and exchange. J. Mol. Evol. *44*, 383–397.

Leach, D.R.F. (1994). Long DNA palindromes, cruciform structures, genetic instability and secondary structure repair. BioEssays *16*, 893–900.

Leonard, A.C., and Grimwade, J.E. (2004). Building a bacterial orisome: emergence of new regulatory features for replication origin unwinding. Mol. Microbiol. *55*, 978–985.

Leonard, A.C., and Grimwade, J.E. (2009). Initiating chromosome replication in E. coli: it makes sense to recycle. Genes Dev. *23*, 1145–1150.

Leonard, A.C., and Grimwade, J.E. (2011). Regulation of DnaA Assembly and Activity: Taking Directions from the Genome. Annu. Rev. Microbiol. *65*, 19–35.

Leonard, A.C., and Mechali, M. (2013). DNA Replication Origins. Cold Spring Harb. Perspect. Biol. *5*, a010116–a010116.

Lesterlin, C., Barre, F.-X., and Cornet, F. (2004). Genetic recombination and the cell cycle: what we have learned from chromosome dimers. Mol. Microbiol. *54*, 1151–1160.

Lesterlin, C., Mercier, R., Boccard, F., Barre, F.-X., and Cornet, F. (2005). Roles for replichores and macrodomains in segregation of the Escherichia coli chromosome. EMBO Rep. *6*, 557–562.

Liang, X., Baek, C.-H., and Katzen, F. (2013). *Escherichia coli* with Two Linear Chromosomes. ACS Synth. Biol. *2*, 734–740.

Liu, G.-R., Liu, W.-Q., Johnston, R.N., Sanderson, K.E., Li, S.-X., and Liu, S.-L. (2006). Genome plasticity and ori-ter rebalancing in Salmonella typhi. Mol. Biol. Evol. *23*, 365–371.

Lobner-Olesen, A. (1999). Distribution of minichromosomes in individual Escherichia coli cells: implications for replication control. EMBO J. *18*, 1712–1721.

Løbner-Olesen, A., Hansen, F.G., Rasmussen, K. V, Martin, B., and Kuempel, P.L. (1994). The initiation cascade for chromosome replication in wild-type and Dam methyltransferase deficient Escherichia coli cells. EMBO J. *13*, 1856–1862.

Loot, C., Bikard, D., Rachlin, A., and Mazel, D. (2010). Cellular pathways controlling integron cassette site folding. EMBO J. *29*, 2623–2634.

López-Guerrero, M.G., Ormeño-Orrillo, E., Acosta, J.L., Mendoza-Vargas, A., Rogel, M.A., Ramírez, M.A., Rosenblueth, M., Martínez-Romero, J., and Martínez-Romero, E. (2012). Rhizobial extrachromosomal replicon variability, stability and expression in natural niches. Plasmid *68*, 149–158.

Louarn, J.M., Bouché, J.P., Legendre, F., Louarn, J., and Patte, J. (1985). Characterization and properties of very large inversions of the E. coli chromosome along the origin-to-terminus axis. Mol. Gen. Genet. *201*, 467–476.

Lu, M., Campbell, J.L., Boye, E., and Kleckner, N. (1994). SeqA: a negative modulator of replication initiation in E. coli. Cell *77*, 413–426.

Lutkenhaus, J. (2007). Assembly dynamics of the bacterial MinCDE system and spatial regulation of the Z ring. Annu. Rev. Biochem. *76*, 539–562.

MacAlpine, D.M., and Almouzni, G. (2013). Chromatin and DNA Replication. Cold Spring Harb. Perspect. Biol. *5*, a010207–a010207.

MacDonald, D., Demarre, G., Bouvier, M., Mazel, D., and Gopaul, D.N. (2006). Structural basis for broad DNA-specificity in integron recombination. Nature *440*, 1157–1162.

Mackenzie, C., Choudhary, M., Larimer, F.W., Predki, P.F., Stilwagen, S., Armitage, J.P., Barber, R.D., Donohue, T.J., Hosler, J.P., Newman, J.E., et al. (2001). The home stretch, a first analysis of the nearly completed genome of Rhodobacter sphaeroides 2.4.1. Photosynth. Res. *70*, 19–41.

MacLellan, S.R., Smallbone, L.A., Sibley, C.D., and Finan, T.M. (2004). The expression of a novel antisense gene mediates incompatibility within the large repABC family of α-proteobacterial plasmids. Mol. Microbiol. *55*, 611–623.

Maida, I., Fondi, M., Orlandini, V., Emiliani, G., Papaleo, M.C., Perrin, E., and Fani, R. (2014). Origin, duplication and reshuffling of plasmid genes: Insights from Burkholderia vietnamiensis G4 genome. Genomics *103*, 229–238.

Margulies, C., and Kaguni, J.M. (1996). Ordered and sequential binding of DnaA protein to oriC, the chromosomal origin of Escherichia coli. J. Biol. Chem. *271*, 17035–17040.

Margulies, C., and Kaguni, J.M. (1998). The FIS protein fails to block the binding of DnaA protein to oriC, the Escherichia coli chromosomal origin. Nucleic Acids Res. *26*, 5170–5175.

Marszalek, J., and Kaguni, J.M. (1994). DnaA protein directs the binding of DnaB protein in initiation of DNA replication in Escherichia coli. J. Biol. Chem. *269*, 4883–4890.

Marszalek, J., Zhang, W., Hupp, T.R., Margulies, C., Carr, K.M., Cherry, S., and Kaguni, J.M. (1996). Domains of DnaA protein involved in interaction with DnaB protein, and in unwinding the Escherichia coli chromosomal origin. J. Biol. Chem. *271*, 18535–18542.

Masai, H., and Arai, K. (1997). Frpo: a novel single-stranded DNA promoter for transcription and for primer RNA synthesis of DNA replication. Cell *89*, 897–907.

Mazel, D. (2006). Integrons: agents of bacterial evolution. Nat. Rev. Microbiol. *4*, 608–620.

Mazel, D., Dychinco, B., Webb, V.A., and Davies, J. (1998). A distinctive class of integron in the Vibrio cholerae genome. Science *280*, 605–608.

McDonough, E., Kamp, H., and Camilli, A. (2016). Vibrio cholerae phosphatases required for the utilization of nucleotides and extracellular DNA as phosphate sources. Mol. Microbiol. *99*, 453–469.

McEachern, M.J., Bott, M.A., Tooker, P.A., and Helinski, D.R. (1989). Negative control of plasmid R6K replication: possible role of intermolecular coupling of replication origins. Proc. Natl. Acad. Sci. U. S. A. *86*, 7942–7946.

McGarry, K.C., Ryan, V.T., Grimwade, J.E., and Leonard, A.C. (2004). Two discriminatory binding sites in the Escherichia coli replication origin are required for DNA strand opening by initiator DnaA-ATP. Proc. Natl. Acad. Sci. U. S. A. *101*, 2811–2816.

McKenzie, G.J., and Craig, N.L. (2006). Fast, easy and efficient: site-specific insertion of transgenes into enterobacterial chromosomes using Tn7 without need for selection of the insertion event. BMC Microbiol. *6*, 39.

Meibom, K.L., Blokesch, M., Dolganov, N.A., Wu, C.-Y., and Schoolnik, G.K. (2005). Chitin Induces Natural Competence in Vibrio cholerae. Science (80-.). *310*, 1824–1827.

Mercado-Blanco, J., and Olivares, J. (1994). The Large Nonsymbiotic Plasmid pRmeGR4a of Rhizobium meliloti GR4 Encodes a Protein Involved in Replication That Has Homology with the RepC Protein of Agrobacterium Plasmids. Plasmid *32*, 75–79.

Mercier, R., Petit, M.-A., Schbath, S., Robin, S., El Karoui, M., Boccard, F., and Espéli, O. (2008). The MatP/matS site-specific system organizes the terminus region of the E. coli chromosome into a macrodomain. Cell *135*, 475–485.

Messer, W. (2002). The bacterial replication initiator DnaA. DnaA and oriC, the bacterial mode to initiate DNA replication. FEMS Microbiol. Rev. *26*, 355–374.

Messer, W., and Weigel, C. (1997). DnaA initiator-also a transcription factor. Mol. Microbiol. *24*, 1–6.

Miesel, L., Segall, A., and Roth, J.R. (1994). Construction of chromosomal rearrangements in Salmonella by transduction: inversions of non-permissive segments are not lethal. Genetics *137*, 919–932.

Moreno, E. (1998). Genome evolution within the alpha *Proteobacteria* : why do some bacteria not possess plasmids and others exhibit more than one different chromosome?: Figure 1. FEMS Microbiol. Rev. *22*, 255–275.

Morigen, Løbner-Olesen, A., and Skarstad, K. (2003). Titration of the Escherichia coli DnaA protein to excess datA sites causes destabilization of replication forks, delayed replication initiation and delayed cell division. Mol. Microbiol. *50*, 349–362.

Morigen, Molina, F., and Skarstad, K. (2005). Deletion of the datA Site Does Not Affect Once-per-Cell-Cycle Timing but Induces Rifampin-Resistant Replication. J. Bacteriol. *187*, 3913–3920.

Moukadiri, I., Prado, S., Piera, J., Velázquez-Campoy, A., Björk, G.R., and Armengod, M.-E. (2009). Evolutionarily conserved proteins MnmE and GidA catalyze the formation of two methyluridine derivatives at tRNA wobble positions. Nucleic Acids Res. *37*, 7177–7193.

Nakamura, A., Wada, C., and Miki, K. (2007). Structural basis for regulation of bifunctional roles in replication initiator protein. Proc. Natl. Acad. Sci. *104*, 18484–18489.

Natrajan, G., Noirot-Gros, M.F., Zawilak-Pawlik, A., Kapp, U., and Terradot, L. (2009). The structure of a DnaA/HobA complex from *Helicobacter pylori* provides insight into regulation of DNA replication in bacteria. Proc. Natl. Acad. Sci. *106*, 21115–21120.

Nereng, K.S., and Kaplan, S. (1999). Genomic complexity among strains of the facultative photoheterotrophic bacterium Rhodobacter sphaeroides. J. Bacteriol. *181*, 1684–1688.

Ng, W. V, Ciufo, S.A., Smith, T.M., Bumgarner, R.E., Baskin, D., Faust, J., Hall, B., Loretz, C., Seto, J., Slagel, J., et al. (1998). Snapshot of a large dynamic replicon in a halophilic archaeon: megaplasmid or minichromosome? Genome Res. *8*, 1131–1141.

Nievera, C., Torgue, J.J.-C., Grimwade, J.E., and Leonard, A.C. (2006). SeqA Blocking of DnaA-oriC Interactions Ensures Staged Assembly of the E. coli Pre-RC. Mol. Cell *24*, 581–592.

Nishida, S., Fujimitsu, K., Sekimizu, K., Ohmura, T., Ueda, T., and Katayama, T. (2002). A Nucleotide Switch in the *Escherichia coli* DnaA Protein Initiates Chromosomal Replication. J. Biol. Chem. *277*, 14986–14995.

Nivina, A., Escudero, J.A., Vit, C., Mazel, D., and Loot, C. (2016). Efficiency of integron cassette insertion in correct orientation is ensured by the interplay of the three unpaired features of *attC* recombination sites. Nucleic Acids Res. *44*, 7792–7803.

Nozaki, S., Yamada, Y., and Ogawa, T. (2009). Initiator titration complex formed at *datA* with the aid of IHF regulates replication timing in *Escherichia coli*. Genes to Cells *14*, 329–341.

O'Donnell, M. (2006). Replisome Architecture and Dynamics in *Escherichia coli*. J. Biol. Chem. *281*, 10653–10656.

Ochman, H. (2002). Bacterial evolution: chromosome arithmetic and geometry. Curr. Biol. *12*, R427-8.

Ogawa, T., and Okazaki, T. (1994). Cell cycle-dependent transcription from the gid and mioC promoters of Escherichia coli. J. Bacteriol. *176*, 1609–1615.

Ogawa, T., Yamada, Y., Kuroda, T., Kishi, T., and Moriya, S. (2002). The datA locus predominantly contributes to the initiator titration mechanism in the control of replication initiation in Escherichia coli. Mol. Microbiol. *44*, 1367–1375.

Orlova, N., Gerding, M., Ivashkiv, O., Olinares, P.D.B., Chait, B.T., Waldor, M.K., and Jeruzalmi, D. (2016). The replication initiator of the cholera pathogen's second chromosome shows structural similarity to plasmid initiators. Nucleic Acids Res. *45*, gkw1288.

Österman, J., Marsh, J., Laine, P.K., Zeng, Z., Alatalo, E., Sullivan, J.T., Young, J.P.W., Thomas-Oates, J., Paulin, L., and Lindström, K. (2014). Genome sequencing of two Neorhizobium galegae strains reveals a noeT gene responsible for the unusual acetylation of the nodulation factors. BMC Genomics *15*, 500.

Ozaki, S., and Katayama, T. (2012). Highly organized DnaA– oriC complexes recruit the single-stranded DNA for replication initiation. Nucleic Acids Res. *40*, 1648–1665.

Pal, S.K., and Chattoraj, D.K. (1988). P1 plasmid replication: initiator sequestration is inadequate to explain control by initiator-binding sites. J. Bacteriol. *170*, 3554–3560.

Pal, D., Venkova-Canova, T., Srivastava, P., and Chattoraj, D.K. (2005). Multipartite Regulation of rctB, the Replication Initiator Gene of Vibrio cholerae Chromosome II. J. Bacteriol. *187*, 7167–7175.

Palmer, K.M., Turner, S.L., and Young, J.P.W. (2000). Sequence Diversity of the Plasmid Replication Gene repC in the Rhizobiaceae. Plasmid *44*, 209–219.

Pappas, K.M. (2008). Cell–cell signaling and the Agrobacterium tumefaciens Ti plasmid copy number fluctuations. Plasmid *60*, 89–107.

Pappas, K.M., and Winans, S.C. (2003a). A LuxR-type regulator from Agrobacterium tumefaciens elevates Ti plasmid copy number by activating transcription of plasmid replication genes. Mol. Microbiol. *48*, 1059–1073.

Pappas, K.M., and Winans, S.C. (2003b). The RepA and RepB autorepressors and TraR play opposing roles in the regulation of a Ti plasmid repABC operon. Mol. Microbiol. *49*, 441–455.

Park, K., Han, E., Paulsson, J., and Chattoraj, D.K. (2001). Origin pairing (handcuffing') as a mode of negative control of P1 plasmid copy number. EMBO J. *20*, 7323–7332.

van Passel, M.W.J., Bart, A., Luyf, A.C.M., van Kampen, A.H.C., and van der Ende, A. (2006). Compositional discordance between prokaryotic plasmids and host chromosomes. BMC Genomics *7*, 26.

Paulsson, J., and Chattoraj, D.K. (2006). Origin inactivation in bacterial DNA replication control. Mol. Microbiol. *61*, 9–15.

Perri, S., and Helinski, D.R. (1993). DNA sequence requirements for interaction of the RK2 replication initiation protein with plasmid origin repeats. J. Biol. Chem. *268*, 3662–3669.

Petersen, J., Brinkmann, H., and Pradella, S. (2009). Diversity and evolution of *repABC* type plasmids in *Rhodobacterales*. Environ. Microbiol. *11*, 2627–2638.

Pinto, U.M., Flores-Mireles, A.L., Costa, E.D., and Winans, S.C. (2011). RepC protein of the octopine-type Ti plasmid binds to the probable origin of replication within repC and functions only in cis. Mol. Microbiol. *81*, 1593–1606.

Pinto, U.M., Pappas, K.M., and Winans, S.C. (2012). The ABCs of plasmid replication and segregation. Nat. Rev. Microbiol. *10*, 755–765.

Pratt, J.T., Ismail, A.M., and Camilli, A. (2010). PhoB regulates both environmental and virulence gene expression in Vibrio cholerae. Mol. Microbiol. *77*, 1595–1605.

Prozorov, A.A. (2008). Additional chromosomes in bacteria: Properties and origin. Microbiology *77*, 385–394.

Rajewska, M., Kowalczyk, L., Konopa, G., and Konieczny, I. (2008). Specific mutations within the AT-rich region of a plasmid replication origin affect either origin opening or helicase loading. Proc. Natl. Acad. Sci. *105*, 11134–11139.

Rajewska, M., Wegrzyn, K., and Konieczny, I. (2012). AT-rich region and repeated sequences – the essential elements of replication origins of bacterial replicons. FEMS Microbiol. Rev. *36*, 408–434.

Ramachandran, R., Jha, J., Paulsson, J., and Chattoraj, D. (2017). Random versus Cell Cycle-Regulated Replication Initiation in Bacteria : Insights. Microbiol. Mol. Biol. Rev. *81*, 1–18.

Ramachandran, V.K., East, A.K., Karunakaran, R., Downie, J.A., and Poole, P.S. (2011). Adaptation of Rhizobium leguminosarum to pea, alfalfa and sugar beet rhizospheres investigated by comparative transcriptomics. Genome Biol. *12*, R106.

Ramírez-Romero, M.A., Téllez-Sosa, J., Barrios, H., Pérez-Oseguera, A., Rosas, V., and Cevallos, M.A. (2001). RepA negatively autoregulates the transcription of the repABC operon of the Rhizobium etli symbiotic plasmid basic replicon. Mol. Microbiol. *42*, 195–204.

Rasmussen, T., Jensen, R.B., and Skovgaard, O. (2007). The two chromosomes of Vibrio cholerae are initiated at different time points in the cell cycle. EMBO J. *26*, 3124–3131.

Ravin, N. V, Kuprianov, V. V, Gilcrease, E.B., and Casjens, S.R. (2003). Bidirectional replication from an internal ori site of the linear N15 plasmid prophage. Nucleic Acids Res. *31*, 6552–6560.

Reen, F.J., Almagro-Moreno, S., Ussery, D., and Boyd, E.F. (2006). The genomic code: inferring Vibrionaceae niche specialization. Nat. Rev. Microbiol. *4*, 697–704.

Reyes-Lamothe, R., Nicolas, E., and Sherratt, D.J. (2012). Chromosome Replication and Segregation in Bacteria. Annu. Rev. Genet. *46*, 121–143.

Riber, L., and Lobner-Olesen, A. (2005). Coordinated Replication and Sequestration of oriC and dnaA Are Required for Maintaining Controlled Once-per-Cell-Cycle Initiation in Escherichia coli. J. Bacteriol. *187*, 5605–5613.

Riber, L., Fujimitsu, K., Katayama, T., and Løbner-Olesen, A. (2009). Loss of Hda activity stimulates replication initiation from I-box, but not R4 mutant origins in *Escherichia coli*. Mol. Microbiol. *71*, 107–122.

Rocha, E.P.C. (2004). The replication-related organization of bacterial genomes. Microbiology *150*, 1609–1627.

Rocha, E.P.C. (2008). The Organization of the Bacterial Genome. Annu. Rev. Genet. *42*, 211–233.

Rocha, E.P.C., and Danchin, A. (2002). Base composition bias might result from competition for metabolic resources. Trends Genet. *18*, 291–294.

Rosenberg, C., Boistard, P., Dénarié, J., and Casse-Delbart, F. (1981). Genes controlling early and late functions in symbiosis are located on a megaplasmid in Rhizobium meliloti. Mol. Gen. Genet. MGG *184*, 326–333.

Roth, A., and Messer, W. (1998). High-affinity binding sites for the initiator protein DnaA on the chromosome of Escherichia coli. Mol. Microbiol. *28*, 395–401.

Le Roux, F., Binesse, J., Saulnier, D., and Mazel, D. (2007). Construction of a Vibrio splendidus mutant lacking the metalloprotease gene vsm by use of a novel counterselectable suicide vector. Appl. Environ. Microbiol. *73*, 777–784.

Rowe-Magnus, D.A., Guerout, A.M., Ploncard, P., Dychinco, B., Davies, J., and Mazel, D. (2001). The evolutionary history of chromosomal super-integrons provides an ancestry for multiresistant integrons. Proc. Natl. Acad. Sci. U. S. A. *98*, 652–657.

Rowe-Magnus, D.A., Guerout, A.-M., and Mazel, D. (2002). Bacterial resistance evolution by recruitment of super-integron gene cassettes. Mol. Microbiol. *43*, 1657–1669.

Rowe-Magnus, D.A., Guerout, A.-M., Biskri, L., Bouige, P., and Mazel, D. (2003). Comparative analysis of superintegrons: engineering extensive genetic diversity in the Vibrionaceae. Genome Res. *13*, 428–442.

Rozgaja, T.A., Grimwade, J.E., Iqbal, M., Czerwonka, C., Vora, M., and Leonard, A.C. (2011). Two oppositely oriented arrays of low-affinity recognition sites in oriC guide progressive binding of DnaA during Escherichia coli pre-RC assembly. Mol. Microbiol. *82*, 475–488.

Ryan, V.T., Grimwade, J.E., Nievera, C.J., and Leonard, A.C. (2002). IHF and HU stimulate assembly of pre-replication complexes at Escherichia coli oriC by two different mechanisms. Mol. Microbiol. *46*, 113–124.

Ryan, V.T., Grimwade, J.E., Camara, J.E., Crooke, E., and Leonard, A.C. (2004). Escherichia coli prereplication complex assembly is regulated by dynamic interplay among Fis, IHF and DnaA. Mol. Microbiol. *51*, 1347–1359.

Sack, D.A., Sack, R.B., Nair, G.B., and Siddique, A.K. (2004). Cholera. Lancet (London, England) *363*, 223–233.

Schaper, S., and Messer, W. (1995). Interaction of the initiator protein DnaA of Escherichia coli with its DNA target. J. Biol. Chem. *270*, 17622–17626.

Segall, A., Mahan, M.J., and Roth, J.R. (1988). Rearrangement of the bacterial chromosome: forbidden inversions. Science *241*, 1314–1318.

Sekimizu, K., Bramhill, D., and Kornberg, A. (1987). ATP activates dnaA protein in initiating replication of plasmids bearing the origin of the E. coli chromosome. Cell *50*, 259–265.

Simpson, M.L., Cox, C.D., and Sayler, G.S. (2003). Frequency domain analysis of noise in autoregulated gene circuits. Proc. Natl. Acad. Sci. *100*, 4551–4556.

Skarstad, K., and Løbner-Olesen, A. (2003). Stable co-existence of separate replicons in Escherichia coli is dependent on once-per-cell-cycle initiation. EMBO J. *22*, 140–150.

Skarstad, K., Baker, T.A., and Kornberg, A. (1990). Strand separation required for initiation of replication at the

chromosomal origin of E.coli is facilitated by a distant RNA--DNA hybrid. EMBO J. *9*, 2341–2348.

Slater, S., Wold, S., Lu, M., Boye, E., Skarstad, K., and Kleckner, N. (1995). E. coli SeqA protein binds oriC in two different methyl-modulated reactions appropriate to its roles in DNA replication initiation and origin sequestration. Cell *82*, 927–936.

Slater, S.C., Goldman, B.S., Goodner, B., Setubal, J.C., Farrand, S.K., Nester, E.W., Burr, T.J., Banta, L., Dickerman, A.W., Paulsen, I., et al. (2009). Genome sequences of three agrobacterium biovars help elucidate the evolution of multichromosome genomes in bacteria. J. Bacteriol. *191*, 2501–2511.

del Solar, G., Giraldo, R., Ruiz-Echevarría, M.J., Espinosa, M., and Díaz-Orejas, R. (1998). Replication and control of circular bacterial plasmids. Microbiol. Mol. Biol. Rev. *62*, 434–464.

Soler-Bistué, A., Mondotte, J.A., Bland, M.J., Val, M.-E., Saleh, M.-C., and Mazel, D. (2015). Genomic Location of the Major Ribosomal Protein Gene Locus Determines Vibrio cholerae Global Growth and Infectivity. PLOS Genet. *11*, e1005156.

Speck, C., and Messer, W. (2001). Mechanism of origin unwinding: sequential binding of DnaA to double- and single-stranded DNA. EMBO J. *20*, 1469–1476.

Speck, C., Weigel, C., and Messer, W. (1999). ATP- and ADP-DnaA protein, a molecular switch in gene regulation. EMBO J. *18*, 6169–6176.

Srivastava, P., and Chattoraj, D.K. (2007). Selective chromosome amplification in Vibrio cholerae. Mol. Microbiol. *66*, 1016–1028.

Stokes, H.W., and Hall, R.M. (1989). A novel family of potentially mobile DNA elements encoding site-specific gene-integration functions: integrons. Mol. Microbiol. *3*, 1669–1683.

Su'etsugu, M., Emoto, A., Fujimitsu, K., Keyamura, K., and Katayama, T. (2003). Transcriptional control for initiation of chromosomal replication in Escherichia coli: fluctuation of the level of origin transcription ensures timely initiation. Genes Cells *8*, 731–745.

Su'etsugu, M., Takata, M., Kubota, T., Matsuda, Y., and Katayama, T. (2004). Molecular mechanism of DNA replication-coupled inactivation of the initiator protein in Escherichia coli: interaction of DnaA with the sliding clamp-loaded DNA and the sliding clamp-Hda complex. Genes to Cells *9*, 509–522.

Su'etsugu, M., Shimuta, T., Ishida, T., Kawakami, H., and Katayama, T. (2005). Protein Associations in DnaA-ATP Hydrolysis Mediated by the Hda-Replicase Clamp Complex. J. Biol. Chem. *280*, 6528–6536.

Su'etsugu, M., Nakamura, K., Keyamura, K., Kudo, Y., and Katayama, T. (2008). Hda Monomerization by ADP Binding Promotes Replicase Clamp-mediated DnaA-ATP Hydrolysis. J. Biol. Chem. *283*, 36118–36131.

Sun, S., Guo, H., and Xu, J. (2006). Multiple gene genealogical analyses reveal both common and distinct population genetic patterns among replicons in the nitrogen-fixing bacterium Sinorhizobium meliloti. Microbiology *152*, 3245–3259.

Tamplin, M.L., Gauzens, A.L., Huq, A., Sack, D.A., and Colwell, R.R. (1990). Attachment of Vibrio cholerae serogroup O1 to zooplankton and phytoplankton of Bangladesh waters. Appl. Environ. Microbiol. *56*, 1977–1980.

Tanaka, T., Ishida, H., and Maehara, T. (2005). Characterization of the Replication Region of Plasmid pLS32 from the Natto Strain of Bacillus subtilis. J. Bacteriol. *187*, 4315–4326.

Theisen, P.W., Grimwade, J.E., Leonard, A.C., Bogan, J.A., and Helmstetter, C.E. (1993). Correlation of gene transcription with the time of initiation of chromosome replication in Escherichia coli. Mol. Microbiol. *10*, 575–584.

Tolun, A., and Helinski, D.R. (1981). Direct repeats of the F plasmid incC region express F incompatibility. Cell *24*, 687–694.

Tonthat, N.K., Arold, S.T., Pickering, B.F., Van Dyke, M.W., Liang, S., Lu, Y., Beuria, T.K., Margolin, W., and Schumacher, M.A. (2011). Molecular mechanism by which the nucleoid occlusion factor, SlmA, keeps cytokinesis in check. EMBO J. *30*, 154–164.

Torheim, N.K., and Skarstad, K. (1999). Escherichia coli SeqA protein affects DNA topology and inhibits open complex formation at oriC. EMBO J. *18*, 4882–4888.

Toukdarian, A.E., Helinski, D.R., and Perri, S. (1996). The plasmid RK2 initiation protein binds to the origin of replication as a monomer. J. Biol. Chem. *271*, 7072–7078.

Trucksis, M., Michalski, J., Deng, Y.K., and Kaper, J.B. (1998). The Vibrio cholerae genome contains two unique circular chromosomes. Proc. Natl. Acad. Sci. U. S. A. *95*, 14464–14469.

Tsutsui, H., Fujiyama, A., Murotsu, T., and Matsubara, K. (1983). Role of nine repeating sequences of the mini-F genome for expression of F-specific incompatibility phenotype and copy number control. J. Bacteriol. *155*, 337–344.

Val, M.-E., Bouvier, M., Campos, J., Sherratt, D., Cornet, F., Mazel, D., and Barre, F.-X. (2005). The Single-Stranded Genome of Phage CTX Is the Form Used for Integration into the Genome of Vibrio cholerae. Mol. Cell *19*, 559–566.

Val, M.-E., Kennedy, S.P., El Karoui, M., Bonné, L., Chevalier, F., and Barre, F.-X. (2008). FtsK-Dependent Dimer Resolution on Multiple Chromosomes in the Pathogen Vibrio cholerae. PLoS Genet. *4*, e1000201.

Val, M.-E., Skovgaard, O., Ducos-Galand, M., Bland, M.J., and Mazel, D. (2012). Genome engineering in Vibrio cholerae: a feasible approach to address biological issues. PLoS Genet. *8*, e1002472.

Val, M.-E., Kennedy, S.P., Soler-Bistué, A.J., Barbe, V., Bouchier, C., Ducos-Galand, M., Skovgaard, O., and Mazel, D. (2014a). Fuse or die: how to survive the loss of Dam in *V ibrio cholerae*. Mol. Microbiol. *91*, 665–678.

Val, M.-E., Soler-Bistué, A., Bland, M.J., and Mazel, D. (2014b). Management of multipartite genomes: the Vibrio cholerae model. Curr. Opin. Microbiol. *22*, 120–126.

Val, M.-E., Marbouty, M., de Lemos Martins, F., Kennedy, S.P., Kemble, H., Bland, M.J., Possoz, C., Koszul, R., Skovgaard, O., and Mazel, D. (2016). A checkpoint control orchestrates the replication of the two chromosomes of Vibrio cholerae. Sci. Adv. *2*, e1501914.

Venkova-Canova, T., and Chattoraj, D.K. (2011). Transition from a plasmid to a chromosomal mode of replication entails additional regulators. Proc. Natl. Acad. Sci. *108*, 6199–6204.

Venkova-Canova, T., Soberón, N.E., Ramírez-Romero, M.A., and Cevallos, M.A. (2004). Two discrete elements are required for the replication of a repABC plasmid: an antisense RNA and a stem-loop structure. Mol. Microbiol. *54*, 1431–1444.

Venkova-Canova, T., Srivastava, P., and Chattoraj, D.K. (2006). Transcriptional inactivation of a regulatory site for replication of Vibrio cholerae chromosome II. Proc. Natl. Acad. Sci. U. S. A. *103*, 12051–12056.

Venkova-Canova, T., Saha, A., and Chattoraj, D.K. (2012). A 29-mer site regulates transcription of the initiator gene as well as function of the replication origin of Vibrio cholerae chromosome II. Plasmid *67*, 102–110.

Venkova-Canova, T., Baek, J.H., Fitzgerald, P.C., Blokesch, M., and Chattoraj, D.K. (2013). Evidence for two different regulatory mechanisms linking replication and segregation of vibrio cholerae chromosome II. PLoS Genet. *9*, e1003579.

Wake, R.G. (1997). Replication fork arrest and termination of chromosome replication in Bacillus subtilis. FEMS Microbiol. Lett. *153*, 247–254.

Waldminghaus, T., and Skarstad, K. (2009). The Escherichia coli SeqA protein. Plasmid *61*, 141–150.

Waldor, M.K., and Mekalanos, J.J. (1996). Lysogenic conversion by a filamentous phage encoding cholera toxin. Science *272*, 1910–1914.

Wang, J.D., and Levin, P.A. (2009). Metabolism, cell growth and the bacterial cell cycle. Nat. Rev. Microbiol. *7*, 822–827.

Wang, X., and Rudner, D.Z. (2014). Spatial organization of bacterial chromosomes. Curr. Opin. Microbiol. *22*, 66–72.

Weng, X., and Xiao, J. (2014). Spatial organization of transcription in bacterial cells. Trends Genet. *30*, 287–297.

Wickner, S., Hoskins, J., and McKenney, K. (1991). Monomerization of RepA dimers by heat shock proteins activates binding to DNA replication origin. Proc. Natl. Acad. Sci. U. S. A. *88*, 7903–7907.

Wold, S., Crooke, E., and Skarstad, K. (1996). The Escherichia coli Fis protein prevents initiation of DNA replication from oriC in vitro. Nucleic Acids Res. *24*, 3527–3532.

Wong, K., and Golding, G.B. (2003). A phylogenetic analysis of the pSymB replicon from the *Sinorhizobium meliloti* genome reveals a complex evolutionary history. Can. J. Microbiol. *49*, 269–280.

Wong, K., Finan, T., and Golding, B. (2002). Dinucleotide compositional analysis of Sinorhizobium meliloti using the genome signature: distinguishing chromosomes and plasmids. Funct. Integr. Genomics *2*, 274–281.

Wu, L.J., and Errington, J. (2004). Coordination of Cell Division and Chromosome Segregation by a Nucleoid Occlusion Protein in Bacillus subtilis. Cell *117*, 915–925.

Wu, Z., Liu, J., Yang, H., and Xiang, H. (2014). DNA replication origins in archaea. Front. Microbiol. *5*, 179.

Xu, Q., Dziejman, M., and Mekalanos, J.J. (2003). Determination of the transcriptome of Vibrio cholerae during intraintestinal growth and midexponential phase in vitro. Proc. Natl. Acad. Sci. *100*, 1286–1291.

Xu, Q., McMullan, D., Abdubek, P., Astakhova, T., Carlton, D., Chen, C., Chiu, H.-J., Clayton, T., Das, D., Deller, M.C., et al. (2009). A Structural Basis for the Regulatory Inactivation of DnaA. J. Mol. Biol. *385*, 368–380.

Yamaichi, Y., Iida, T., Park, K.S., Yamamoto, K., and Honda, T. (1999). Physical and genetic map of the genome of Vibrio parahaemolyticus: presence of two chromosomes in Vibrio species. Mol. Microbiol. *31*, 1513–1521.

Yamaichi, Y., Fogel, M.A., and Waldor, M.K. (2007). par genes and the pathology of chromosome loss in Vibrio cholerae. Proc. Natl. Acad. Sci. U. S. A. *104*, 630–635.

Yamaichi, Y., Gerding, M.A., Davis, B.M., and Waldor, M.K. (2011). Regulatory Cross-Talk Links Vibrio cholerae Chromosome II Replication and Segregation. PLoS Genet. *7*, e1002189.

Yamaichi, Y., Bruckner, R., Ringgaard, S., Möll, A., Cameron, D.E., Briegel, A., Jensen, G.J., Davis, B.M., and Waldor, M.K. (2012). A multidomain hub anchors the chromosome segregation and chemotactic machinery to the bacterial pole. Genes Dev. *26*, 2348–2360.

Yoder-Himes, D.R., Konstantinidis, K.T., and Tiedje, J.M. (2010). Identification of Potential Therapeutic Targets for Burkholderia cenocepacia by Comparative Transcriptomics. PLoS One *5*, e8724.

York, D., and Filutowicz, M. (1993). Autoregulation-deficient mutant of the plasmid R6K-encoded pi protein distinguishes between palindromic and nonpalindromic binding sites. J. Biol. Chem. *268*, 21854–21861.

Yoshikawa, H., O'Sullivan, A., and Sueoka, N. (1964). SEQUENTIAL REPLICATION OF THE BACILLUS SUBTILIS CHROMOSOME, III. REGULATION OF INITIATION. Proc. Natl. Acad. Sci. U. S. A. *52*, 973–980.

Yu, X.C., and Margolin, W. (1999). FtsZ ring clusters in min and partition mutants: role of both the Min system and the nucleoid in regulating FtsZ ring localization. Mol. Microbiol. *32*, 315–326.

Yuzhakov, A., Turner, J., and O'Donnell, M. (1996). Replisome assembly reveals the basis for asymmetric function in leading and lagging strand replication. Cell *86*, 877–886.

Zawilak-Pawlik, A., Donczew, R., Szafrański, S., Mackiewicz, P., Terradot, L., and Zakrzewska-Czerwińska, J. (2011). DiaA/HobA and DnaA: A Pair of Proteins Co-evolved to Cooperate During Bacterial Orisome Assembly. J. Mol. Biol. *408*, 238–251.

Zheng, J., Guan, Z., Cao, S., Peng, D., Ruan, L., Jiang, D., and Sun, M. (2015). Plasmids are vectors for redundant chromosomal genes in the Bacillus cereus group. BMC Genomics *16*, 6.

Zorman, S., Seitz, H., Sclavi, B., and Strick, T.R. (2012). Topological characterization of the DnaA–oriC complex using single-molecule nanomanipuation. Nucleic Acids Res. *40*, 7375–7383.

Zzaman, S., and Bastia, D. (2005). Oligomeric Initiator Protein-Mediated DNA Looping Negatively Regulates Plasmid Replication In Vitro by Preventing Origin Melting. Mol. Cell *20*, 833–843.